PHD

Approaches to new DNA-repair inhibitors for applications in cancer therapy

Dhami, Archana

Award date:
2008

Awarding institution:
University of Bath

Approaches to new DNA-repair inhibitors for applications in cancer therapy

submitted by

Archana Dhami

for the degree of PhD

of the University of Bath

2008

The research work in this thesis has been carried out in the Department of Pharmacy and Pharmacology, under the supervision of Dr Michael D. Threadgill and Dr Matthew D. Lloyd.

……

……

Abstract

Poly(ADP-ribose) polymerase-1 (PARP-1) is a nuclear enzyme that catalyses the synthesis of ADP-ribose polymers from NAD^+, in response to DNA strand breaks. PARP-1 is implicated in the pathogenesis of many diseases and plays a major role in controlling the repair of damaged DNA. Inhibitors of PARP-1 are of use in the treatment of cancer, as potentiators of radiotherapy and chemotherapy. 5-Aminoisoquinolin--1(*2H*)-one hydrochloride (5-AIQ.HCl) is a potent, water-soluble PARP-1 inhibitor that exhibits outstanding activity in a wide range of disease models *in vivo*. The aim of this project is the design and synthesis of derivatives with substituents at the 4-position of 5-AIQ.

The modes of cyclisation of methyl 2-(substituted)alkynyl-3-nitrobenzoates with different electrophiles (ICl, PhSeCl, $HgSO_4$) were studied. The exclusive formation of isocoumarins demonstrates the influence of the nitro group in directing electrophile-driven cyclisations towards the 6-*endo*-dig mode. The crystal structure of 5-nitro-3-phenyl-4-phenylselenylisocoumarin showed intermolecular and intramolecular π-stacking. Attempted synthesis of 4-benzyl-5-nitroisoquinolin-1-one by selective reduction of the nitrile of methyl 2-(1-cyano-2-phenylethyl)-3-nitrobenzamide failed; approach of DIBAL-H to the nitrile was sterically obstructed, leading to reduction of the ester to give 2-(2-formyl-6-nitrophenyl)-3-phenylpropanenitrile. Bromination of 5-nitro-isoquinolin-1-one gave 4-bromo-5-nitroisoquinolin-1-one but Pd(0)-catalysed cross-couplings (Stille, Sonogashira, Suzuki-Miyaura) of this and of 4-bromo-5-AIQ failed. An alternative approach was Pd-catalysed cyclisation of N-(2-alkenyl)-2-iodo-3-nitrobenzamides. Reaction of N,N-diallyl-2-iodo-3-nitrobenzamide with $Pd(PPh_3)_4$ gave 2-allyl-4-methyl-5-nitroisoquinolin-1-one and 2-allyl-4-methylene-5-nitro-3,4-dihydro-isoquinolin-1-one. N-Benzhydryl-N-cinnamyl-2-iodo-3-nitrobenzamide gave 2-benz-hydryl-4-benzyl-5-nitroisoquinolin-1-one and 2-benzhydryl-4-benzylidene-5-nitro-3,4-dihydroisoquinolin-1-one. These products are not interconvertible. The secondary amides N-allyl-2-iodo-3-nitrobenzamide and N N-((substituted)-cinnamyl)-2-iodo-3-nitrobenzamide gave good yields of the required 4-methyl- and 4-((substituted)-benzyl)-5-nitroisoquinolin-1-ones, respectively, under optimised conditions ($Pd(PPh_3)_4$, Et_3N, Bu_4NCl, 150°C, rapid heating). Hydrogenation gave 4-methyl- and 4-benzyl-5-amino-isoquinolin-1-ones. The 4-substituted 5-AIQs were evaluated for inhibition of recombinant human PARP-1 activity. Three were more potent than 5-AIQ; 5-amino-4-methylisoquinolin-1-one (IC_{50} = 0.25 μM), 5-amino-4-benzylisoquinolin-1-one (IC_{50} = 0.5 μM) and 5-amino-4-bromoisoquinolin-1-one (IC_{50} = 1.0 μM).

Acknowledgements

I consider this as an opportunity to express my gratitude to all the people who have been involved directly or indirectly with the successful completion of this thesis.

Firstly, I would like to thank my supervisors, Dr Mike Threadgill and Dr Matthew Lloyd, for their valuable guidance, patience, encouragement and enthusiasm throughout the period of study.

I would also like to thank Dr Steve Black and Dr Tim Woodman for their NMR services, Mr Chris Cryer, Mr James Amato and Dr Anneke Lubben for the provision of Mass Spectra, Dr Mary Mahon for X-ray crystallography.

I thank overseas research studentship scheme (ORS) for their funding.

My deepest appreciation and thanks to the postdoctoral and postgraduate colleagues I have worked with in 3.5/3.7: Anna, Annika, Christian, Dan, Joey, Pete, Sabela, Vanja and Victoria, for their advice support and friendship.

I wish to express my deepest gratitude to my family and friends, for their love and support throughout the course of my PhD. Finally, I would like to dedicate this thesis with love to my beloved husband Manjit. Thank you, for believing in me and making me believe in myself.

Contents

List of Figures, Schemes and Tables

Figures

Schemes

Tables

Abbreviations

3-AB	3-aminobenzamide
A/C	adenine/cytosine
Ac	acetyl
AcOH	acetic acid
ADP	adenosine diphosphate
AIF	apoptosis inducing factor
5-AIQ	5-aminoisoquinolin-1(2*H*)-one
ANK	ankyrin
Aq.	aqueous
Arg	arginine
Asp	aspartic acid
ATP	adenosine triphosphate
BER	base excision repair
Boc	*tert*-butoxycarbonyl
BRCA	breast cancer gene
BRCT	breast cancer susceptibility protein, BRCA1, C-terminus
CF	catalytic fragment
C/C	cytosine/cytosine
Calcd	calculated
COSY	correlation spectroscopy
C/G	cytosine/guanine
COX	cyclooxygenase
C_q	quaternary carbon
Cys	cysteine
d	day(s)
Da	Daltons
dba	dibenzylideneacetone
DBD	DNA binding domain
DCM	dichloromethane
DIPA	diisopropylamine
DIBAL-H	diisobutylaluminium hydride
DLB-CL	diffuse large B-cell lymphomas
DMSO	dimethyl sulphoxide

DMAP	4-(dimethylamino)pyridine
DMF	*N,N*-dimethylformamide
DNA	deoxyribonucleic acid
DNMT	DNA methyltransferase-1
DSB	double strand breaks
DSBR	double strand break repair
ES	electrospray
Equiv	equivalent(s)
EtOAc	ethyl acetate
EtOH	ethanol
FAB	fast atom bombardment
FGI	functional group interconversion
g	gram(s)
GIT	gastrointestinal tract
Glu	glutamic acid
Gly	glycine
G/T	guanine/thymine
h	hour(s)
Hz	Hertz
His	histidine
HIV	human immunodeficiency virus
HMBC	heteronuclear multiple bond correlation
HMQC	heteronuclear multiple quantum coherence
HPLC	high pressure liquid chromatography
HR	homologous recombination
HRMS	high resolution mass spectrometry
I/R	ischaemia reperfusion
IC_{50}	concentration required for 50% inhibition of activity
ICAM-1	intracellular adhesion molecule-1
IR	infrared
iNOS	inducible nitric oxide synthase
J	coupling constant
K_i	inhibition constant
Lit.	literature
LHMDS	lithium hexamethyldisilazide
LPS	lipopolysaccharides
Lys	lysine

M	molar
MGMT	O^6-methylguanine DNA methyltransferase
Me	methyl
MeCN	acetonitrile
MeOH	methanol
min	minute(s)
mL	millilitre(s)
MM2	molecular mechanics 2
MMR	mismatch repair
mol	mole(s)
mp	melting point
MS	mass spectrometry
m/z	mass to charge ratio (mass spectrometry)
NAD^+	nicotinamide adenine dinucleotide
NADPH	reduced nicotinamide adenine dinucleotide phosphate
NER	nucleotide excision repair
NF	nuclear factor
NHEJ	non-homologous end-joining
NBS	*N*-bromosuccinimide
NIS	*N*-iodosuccinimide
NLS	nuclear localisation signal
NMDA	*N*-methyl-D-aspartate
NMP	*N*-methylpyrrolidinone
NMR	nuclear magnetic resonance
NoLS	nucleolar localisation signal
nM	nanomolar
NOESY	Nuclear overhauser effect
PARG	poly(ADP-ribose) glycohydrolase
PARP	poly(ADP-ribose) polymerase
PBS	phosphate-buffered saline
Pet.ether	Petroleum ether
Ph	phenyl
ppm	parts per million
Pro	proline
R_f	retention factor
RNA	ribonucleic acid
SAM	sterile alpha motif

SAR	structure activity relationship
SEM	standard error of the mean
Ser	serine
siRNA	small inhibitory ribonucleic acid
S_N2	bimolecular nucleophilic substitution
SSB	single strand breaks
Strep-HRP	streptavidin horseradish peroxidase
TANK	tankyrase
TBAF	tetrabutylammonium fluoride
tert	tertiary
TFA	trifluoroacetic acid
THF	tetrahydrofuran
TLC	thin layer chromatography
TMS	trimethylsilyl
TMSA	trimethylsilyl acetylene
TMZ	temozolomide
TRF	telomere repeat-binding factor
TEF-1	transcription enhancer factor-1
TNF	tumour necrosis factor
UV	ultraviolet
vPARP	vault poly(ADP-ribose) polymerase
XRCC	X-ray cross-complementing

1. Introduction

Advanced cancer is one of the leading causes of death in the Western world. Chemotherapy and radiotherapy are the two main treatment modalities currently available. However, lack of selectivity, treatment-related toxicity and the emergence of resistance limit their effectiveness. Efficient repair of DNA in the cancer cell is an important reason for therapeutic resistance and this repair of tumour cell DNA that has been damaged by radiation and chemotherapeutic agents has been identified as a major obstacle in the path of effective treatment of cancer. Targeting DNA repair pathways has been identified as one of the novel strategies for effective DNA repair inhibition in cancer therapy. Inhibition of DNA repair has the potential to enhance the effectiveness of currently available DNA damaging agents.[1]

1.1 DNA repair

The integrity and survival of a cell is critically dependent on the stability of the gene. Cellular DNA is repeatedly exposed to exogenous and endogenous toxins, such as oxygen free radicals, ionising radiation, UV light and various chemical agents. Cells have highly conserved DNA-damage sensor mechanisms in response to such cytotoxic exposures.[2] These include:

1. Initiation of DNA repair, removal of DNA damage and restoration of the continuity of the DNA duplex.
2. Activation of the DNA-damage checkpoint, which stops cell cycle progression to allow for repair and prevention of the transmission of damaged chromosomes.
3. Transcriptional responses cause changes in the transcriptional profile that are beneficial to the cell.
4. Apoptosis to eliminate heavily damaged or seriously deregulated cells.
5. Tolerance of damage

These responses determine survival of the cell (with mutated gene) or initiation of programmed cell death. DNA repair is the most effective defence system and comprises six major DNA repair pathways.

1. Base excision repair (BER)
2. Nucleotide excision repair (NER)
3. Mismatch repair (MMR)
4. Double-strand break repair (DSBR)

5. Reversion repair (Direct repair)
6. Cross-link repair

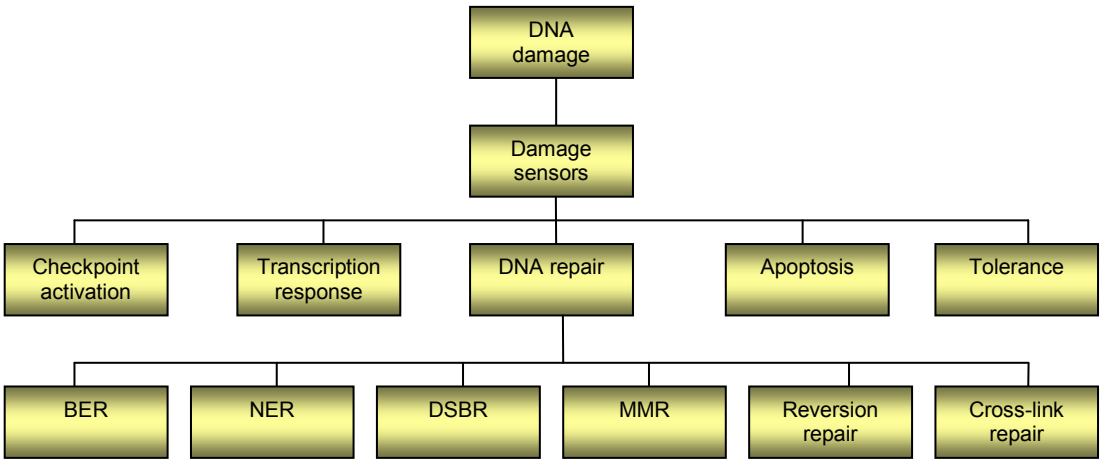

Figure 1. DNA damage responses in mammalian cells.[1]

NER is the major repair system for removing bulky DNA lesions formed by exposure to UV radiation or chemicals, or by addition of protein to DNA. The damaged bases are removed by excision nuclease which makes dual incisions bracketing the lesion in the damaged strand.[3] MMR removes nucleotides mispaired by DNA polymerases and insertion/deletion loops that result from slippage during replication or during recombination. The main targets of MMR are base mismatches such as G/T, C/G, A/C and C/C. The four principal steps in MMR are:

1. Recognition of mismatch
2. Recruitment of additional MMR factors
3. Strand discrimination
4. Resynthesis of excised strand

Double-strand breaks are produced by reactive oxygen species, X-rays or ionising radiation and during replication of single strand breaks (SSB). DNA double-strand breaks are repaired either by homologous recombination (HR) or non-homologous end-joining (NHEJ) mechanisms. When, after replication, a second identical DNA copy is available, homologous recombination is preferred; otherwise cells rely on end-joining, which is error-prone.

Treatment of cells with alkylating agents gives rise to *N*-alkylated and *O*-alkylated purines and pyrimidines. One of the critical *O*-alkylated lesions is O^6-alkylguanine. Some single repair proteins can directly revert these lesions. In human cells, removal

of the O^6-methyl group from O^6-methylguanine in DNA is accomplished by O^6-methylguanine DNA methyltransferase (MGMT). Another protein involved in the DNA damage reversion is photolyase which binds to DNA damage induced by UV light and causes photoreversal of UV-induced pyrimidine dimers.[4] Many bifunctional agents such as cisplatin, nitrogen mustard, and mitomycin D induce interstrand DNA cross-links and DNA-protein cross-links. XPF-ERCC1 nuclease plays a special role in cross-link repair.

Base excision repair is the main guardian against damage due to cellular metabolism, including that resulting from oxygen species, methylation, deamination and hydroxylation. BER is mainly responsible for removing damaged bases, which can be recognised by specific enzymes, the DNA glycosylases. Lesions removed from DNA by BER include N-alkylated purines (7-methylguanine, 3-methyladenine, 3-methylguanine), 8-oxo-7,8-dihydroguanine (8-OxoG) and thymine glycol. The major oxidised purine, 8-OxoG is highly mutagenic because of mispairing with adenine. N-Alkylpurines are hydrolysed at the N-glycosylic bond, giving rise to apurinic/apyrimidinic (AP) sites, which are one of the most frequent and potent lethal lesions. Both modified bases and AP sites are repaired by BER.[4,5] Depending on the initial events in base removal, the repair patch may be single nucleotide (short patch) or 2-10 nucleotides (long patch). Short-patch BER involves removal of the incorrect or damaged base by a DNA glycosylase which generates an AP site, which in turn is cleaved by an AP endonuclease/3´phosphodiesterase leaving a single-strand break. Replacement of the damaged base and religation of the DNA involves binding of PARP-1 and / or PARP-2, followed by recruitment of a complex including DNA polymerase β, DNA ligase I or III/XRCC I (X-ray repair cross-complementing) protein. Long-patch repair is involved in the repair of oxidised or reduced AP sites.[6]

In response to DNA damage, the progression of the cell cycle into S phase is delayed by the G1 cell cycle checkpoint control, whereas progression into M phase is halted by the G2 checkpoint. Prolongation of the G1 and G2 phases functions to permit more effective repair of DNA, and thus avoids DNA synthesis and mitosis in the presence of excessive DNA damage.

Some DNA lesions often persist through replication of the genome, in which case cells have evolved damage tolerance systems to allow complete replication in the presence of DNA damage. This response tolerates, rather than removes, DNA damage and consists of two mechanisms: a) template switching and b) lesion bypass. Template switching involves synthesis of DNA on the undamaged template only. Lesion bypass

utilises the damaged template by nucleotide incorporation opposite the lesion, followed by extension of DNA synthesis.[7]

1.2 DNA repair inhibition

Use of pseudosubstrates of MGMT as DNA repair inhibitors is a promising strategy to increase the efficacy of therapies based on alkylating agents. O^6-Benzylguanine (O^6-BG) is a non-toxic inhibitor of MGMT. It reacts with MGMT by covalent transfer of the benzyl group to the active site cysteine and, hence, leads to inactivation of MGMT. O^6-(4-bromothenyl)guanine (O^6-BTG) is an orally bioavailable inhibitor of MGMT, which is ten-fold more potent than O^6-BG. One strategy for disabling BER is to target the DNA repair enzyme APE I which processes the AP site. Methoxyamine is a small molecule which specifically targets BER by binding directly to AP sites and preventing their processing by APE I. This leads to an accumulation of these potentially cytotoxic sites.

Human protein kinases ATM (ataxia-telangiectasia, mutated) and ATR (ATM-Rad3-related) are potential sensors of DNA damage. ATM responds to the presence of DNA double-strand breaks (DSBs) and initiate signaling cascades leading to a DNA damage checkpoint. Wortmannin is an irreversible inhibitor of ATM. and hence rejoining of double strand breaks (DSBs). 3-Cyano-6-hydrazonomethyl-5-(4-pyridyl)pyrid-(1*H*)-2-one (OK-1035) and NU7026 (2-(morpholin-4-yl)-benzo[h]chromen-4-one) are potent and specific inhibitors of DNA-PK. KU-0055933 (2-morpholin-4-yl-6-thianthren-1-yl-pyran-4-one) is a small-molecule ATP competitive inhibitor of ATM kinase. Use of small inhibitory RNA molecules (siRNAs) to inhibit specific protein expression has highlighted their potential as therapeutic agents. Peptide co-therapy is another strategy that can be used to specifically inhibit protein function. Pentamidine is a potent inhibitor of the enzyme endo-exonuclease which plays a role in double strand break repair and recombination. PARP-targeting inhibitors have structural similarity to the natural substrate NAD^+, and thus act as competitive inhibitors.[8]

1.3 Poly(ADP-ribose) polymerase-1

NAD^+ **(1)** is a versatile biomolecule, which functions as a coenzyme in many oxidation-reduction reactions. Poly(ADP-ribosyl)ation is a post-translational modification of proteins catalysed by poly(ADP-ribose) polymerases (PARPs) and is involved in the regulation of DNA repair, gene transcription, cell-cycle progression, cell death, chromatin function, genomic stability and cell adhesion.[9] Poly(ADP-ribose)polymerase-

1 (PARP-1, EC 2.4.2.30) is the most abundant, founder member of the PARP family and has been the most extensively studied. PARP-1 is also known as poly(ADP-ribose) synthetase (PARS) and poly(ADP-ribose) transferase (PADPRT). It is a nuclear enzyme present in eukaryotes. PARP-1, upon activation by DNA damage, catalyses poly(ADP-ribosyl)ation by transferring ADP-ribose units from its substrate NAD^+ to a variety of acceptor proteins.

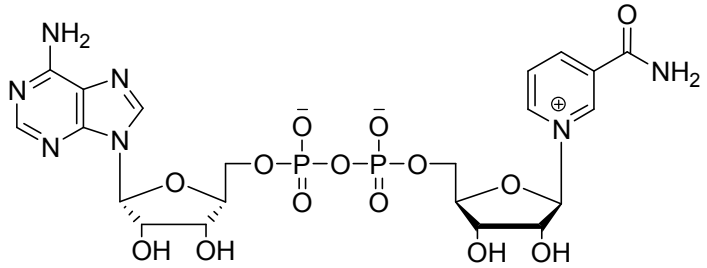

Nicotinamide Adenine Dinucleotide (NAD^+) **(1)**

1.3.1 The PARP super family

Recently identification of some novel putative PARP homologues increased the number of PARP family members to seventeen. The main members of the family are categorised into five groups.[9]

- DNA-damage dependent PARPs consisting of PARP-1 and PARP-2
- Tankyrases consisting of tankyrase-1 and tankyrase-2
- CCCH-type zinc finger PARPs consisting of tiPARP, PARP-12 and PARP-13
- Macro-PARPS such as PARP-9, PARP-14, and PARP-15
- Other PARPs including PARP-3, vPARP, PARP-10, PARP-6, PARP-8, PARP-11 and PARP-16

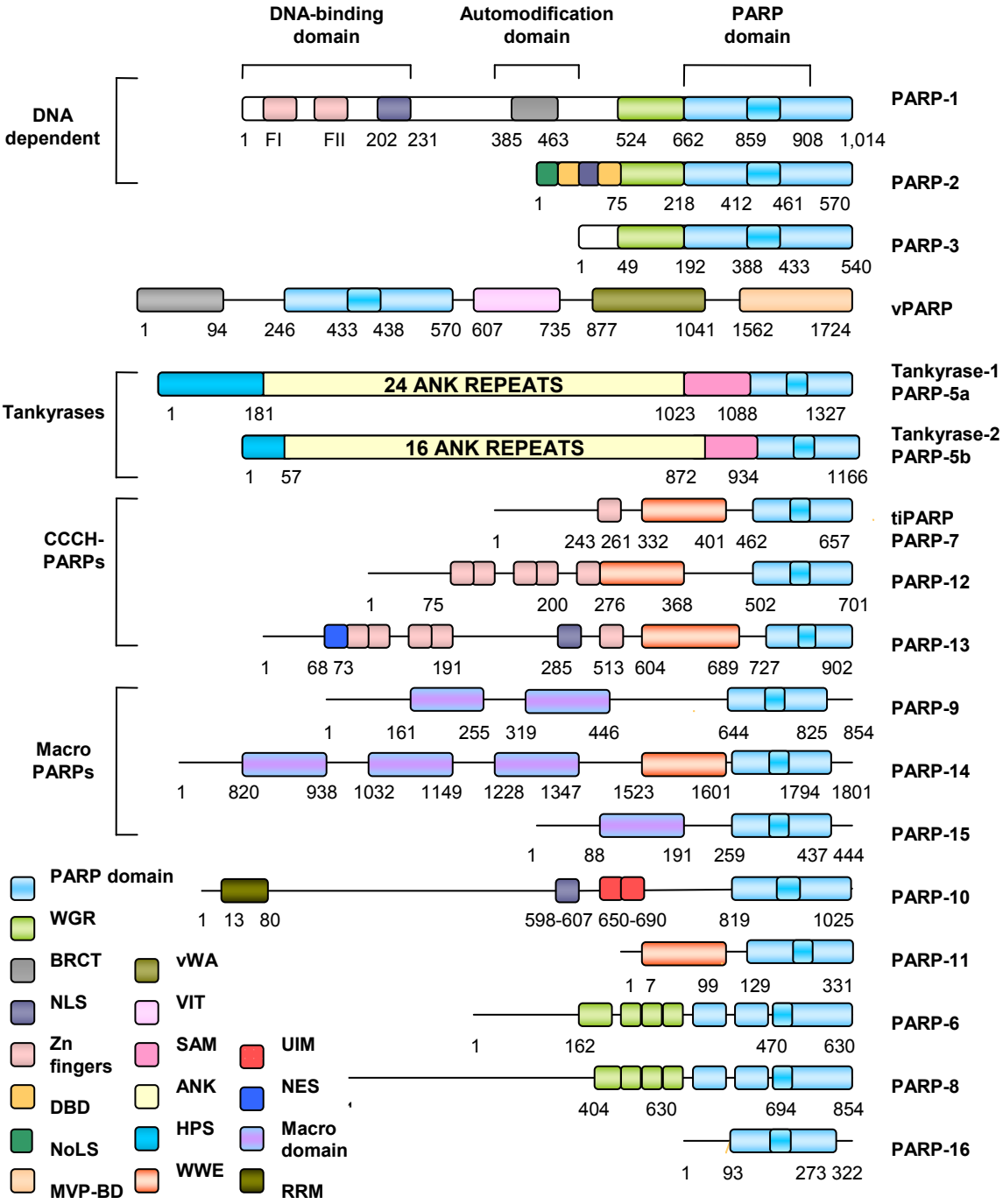

BRCT Breast Cancer Susceptibility protein C terminus; NLS Nuclear Localisation Signal; DBD DNA-Binding Domain; NoLS Nucleolar Localisation Signal; MVP-BD Major Vault Protein Binding Domain; vWA von Willebrand factor type A domain; VIT Vault Inter-α-trypsin; SAM Sterile α-motif; ANK Ankyrin; HPS Histidine-, proline-, serine-rich region; NES Nuclear Export Signal; UIM Ubiquitin Interacting Motif; RRM RNA Recognition Motif; WGR domain is defined by conserved Trp, Gly, and Arg residues.

Figure 2. Schematic representation of the domain structures of the PARP superfamily.[9]

1.3.2 Modular organisation of PARP-1

PARP-1 molecular sensor of DNA breaks, is a 113 KDa protein composed of 1014 amino acid residues, predominantly localised in the cell nucleus. Three main functional elements were identified in the PARP molecule following partial proteolysis.[10]

- The amino terminal fragment of 46 KDa contains the DNA-binding domain, which includes two zinc-finger motifs and a nuclear localisation signal (NLS).[11] Zinc fingers (FI and FII) are loops (residues 2-97 and 106-207) in the polypeptide chain formed as a result of a zinc-ion-coordinating cysteine and histidine residues.[12] These zinc fingers of PARP-1 recognize single and double-stranded DNA breaks and trigger activation of the enzyme. FII plays an important role in the binding of DNA containing single stranded breaks, whereas enzymatic activity is totally abolished in FI mutants, whatever the nature of the DNA breaks.[13] Bipartite NLS ensures efficient translocation to the nucleus.
- The central 22 KDa fragment, the automodification domain, contains 15 conserved glutamate residues, which are presumed targets for auto-poly(ADP-ribosyl)ation. Through the breast cancer susceptibility protein C terminus (BRCT) motif PARP-1 participates in various protein-protein interactions. A leucine zipper motif, characteristic of protein-protein associations, is also present in this domain.
- The C-terminal catalytic domain (46 KDa) contains a block of 50 amino acids (residues 859-908) that are highly conserved among vertebrates and is known as the 'PARP signature'.[13] It catalyses NAD^+ hydrolysis, initiation, elongation, branching and termination of ADP-ribose polymer synthesis. This also contains Glu988 which is directly involved in the catalysis of the ADP-ribose transfer reaction. The structure of catalytically competent PARP-CF (40 KDa polypeptide) has been reported by Ruf *et al*.[14]

1.3.3 Other members

PARP-2 is a 62 KDa protein of 570 amino acids. PARP-2 bears the strongest resemblance to PARP-1 and is also activated by DNA strand interruptions. PARP-2 contributes to the residual PARP activity observed in PARP-$1^{(-/-)}$ cells after treatment with DNA damaging agents. DNA binding domain of PARP-2 is distinct from PARP-1 and PARP-2 lacks the central automodification domain. Even though PARP-2 is devoid of zinc fingers, DNA binding is facilitated by the high ratio of basic amino acids in DBD.[15]

PARP-3 is a 67 KDa polypeptide comprising 540 amino acid residues. The N-terminal region is short (54 amino acid residues) and contains a targeting motif which localises the enzyme in the centrosome. PARP-3 functions in the maturation of the daughter centriole until the G1-S restriction point. hPARP-3 appears to be the first known marker of the daughter centriole.[16]

PARP-4/vPARP is the catalytic component of vault particles, which are barrel-shaped ribonucleoprotein complexes involved in multidrug resistance of human tumours. As shown in Figure 2, vPARP contains a BRCT domain, a region homologous to the catalytic domain of PARP, a region similar to the inter-α-trypsin inhibitor protein, von Willebrand factor type A domain and major vault protein interacting domain. vPARP is involved in mitosis by ADP-ribosylation of the major vault protein.[17]

Tankyrases were identified as components of the human telomeric complex. Telomeres are essential for chromosome maintenance and stability and are maintained by telomerase, a specialised reverse transcriptase. Besides the PARP catalytic domain, tankyrase-1 (PARP-5a) has a sterile α motif, ANK domain containing 24 ankyrin repeats and histidine-, proline-, serine-rich region (HPS) that mediates protein-protein interactions. Tankyrase-1 poly(ADP-ribosyl)ates telomere repeat binding factor 1 (TRF1), thereby causing the latter to be released from telomeres, allowing access of telomerase, that restores telomeric sequences lost during cell division. In this way, Tankyrase-1 acts as a positive regulator for telomere length. Tankyrase-2 (PARP-5b) differs from tankyrase-1 in that it lacks the N-terminal HPS domain, but it probably shares some overlapping functions with tankyrase-1. Knocking down human tankyrase-1 gene expression with small interfering RNA (siRNA) showed that it has an essential regulatory function in mitotic segregation.[18,19]

The CCCH-type PARP subfamily contains tiPARP (PARP-7), PARP-12 and PARP-13. These members share a similar domain organisation comprising $CX_8CX_5CX_3$-like zinc fingers, a WWE domain and a PARP catalytic domain. The WWE domain is a putative protein–protein interaction motif that contains two conserved Trp residues and one Glu residue. PARP-13, identified as ZAP, is a rat protein that confers resistance to retroviral infection.[20] ZAP binds to viral RNA via the CCCH zinc fingers and inhibits the accumulation of viral RNA.

PARP-9, PARP-14 and PARP-15 belong to the subfamily of macro-PARPs, which link 1–3 macro domains to a PARP domain. All three are localised within the same 3q21

chromosomal region. PARP-9 was found to be overexpressed in aggressive diffuse large B-cell lymphomas (DLB-CL) and might promote the dissemination of malignant B cells in high-risk DLB-CL. Macro domains in macro PARPs have a phosphoesterase activity that functions on poly(ADP-ribose). Such macro-PARPs could generate polymer ends that could not be elongated by a PARP, which would provide a way for macro PARPs to control polymer size. [21,22]

PARP-10 contains an RNA recognition motif (RRM) and a Gly-rich domain. PARP-10 shuttles between the cytoplasm and the nucleus and accumulates within the nucleolus where it acquires a CDK2-dependent phosphorylation during late-G1–S phase and during prometaphase to cytokinesis.[23] PARP-10 is potent inhibitor of the cell transformation that is mediated by c-Myc in the presence of Ha-Ras.

1.4 Mechanism of action of PARP-1

Poly(ADP-ribosyl)ation occurs in almost all nucleated cells of mammals, plants and lower eukaryotes but is absent in yeast.[24] The activation of PARP-1, followed by poly(ADP-ribosyl)ation, is one of the earliest cellular responses to DNA damage. In the absence of DNA damage, PARP-1 displays negligible activity. However, binding of PARP-1 to DNA breaks increases enzyme activity up to 500-fold.[25] Poly(ADP-ribosyl)ation comprises of very complex regulatory mechanisms and consists of three main reactions: initiation, elongation and branching.

1.4.1 Initiation

During initiation, substrate NAD^+ binds to the catalytic site of PARP-1. Tight hydrogen bonding with Gly863 and Ser904 mechanically stretches and weakens the C-N glycosidic bond (nicotinamide-ribose). This cleavage results in generation of the intermediate cyclic oxonium ion and leaving of nicotinamide **(2)**. This is followed by the transfer of the resulting ADP-ribosyl moiety (electrophile) to the nucleophilic centre of an appropriate protein acceptor. The protein acceptors may be nuclear proteins including histones (H1 and H2B), p53 and DNA ligases, DNA polymerases, DNA topoisomerases, high mobility group proteins (HMG) and DNA-dependent protein kinases. Poly(ADP-ribosyl)ation of these nuclear proteins is referred to as heteromodification. However, the main protein to be poly(ADP-ribosyl)ated is PARP-1 itself in a process known as automodification. Glutamate, aspartate or carboxy terminal lysine (Glu, Asp, or COOH-Lys) residues of acceptor proteins are then covalently

modified by the addition of an ADP-ribose subunit, *via* formation of an ester bond between the protein and the ADP-ribose residue.[26]

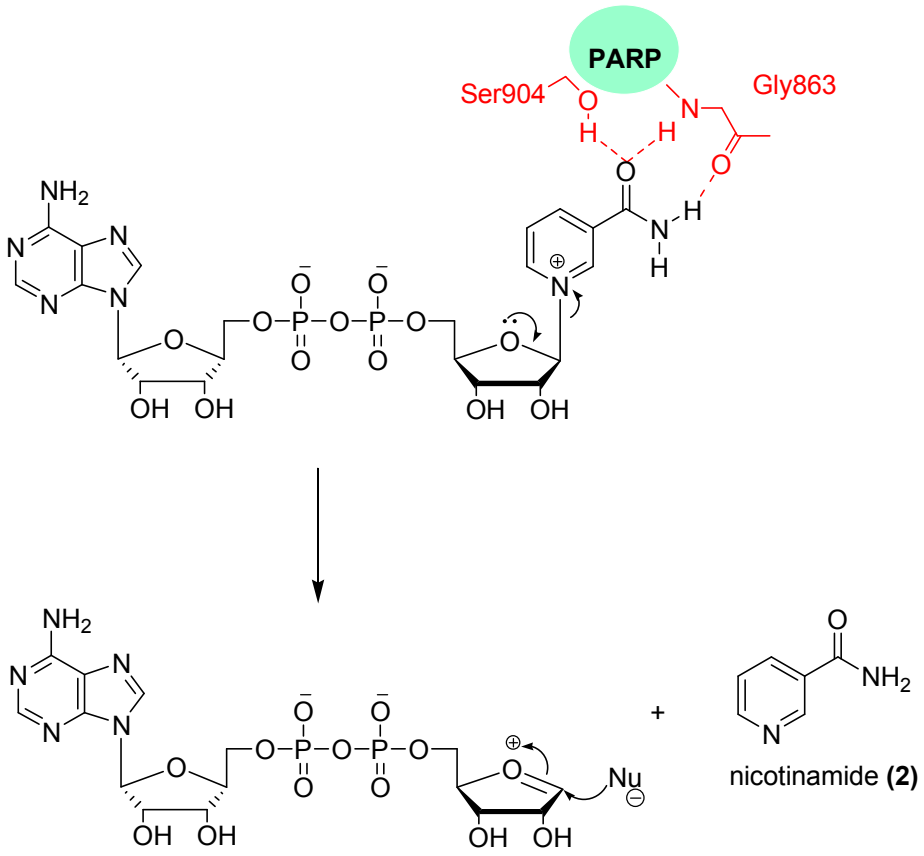

Scheme 1. The proposed mechanism of NAD^+ cleavage by PARP-1.

1.4.2 Elongation

Polymer elongation involves the formation of an α(1''→2') glycosidic bond between C-1'' of nicotinamide ribose and the 2'-OH of the adenine ribose. This results in formation of linear polyanionic polymers with chain lengths of up to 200 ADP-ribose units.[27,28]

1.4.3 Branching

Polymer branching occurs when the C-1 of the nicotinamide ribose is joined with the 2-OH of the nicotinamide ribose of another ADP-ribose polymer *via* a 1'''→2'' glycosidic bond. Polymer branching occurs on average after 20 ADP-ribose units.

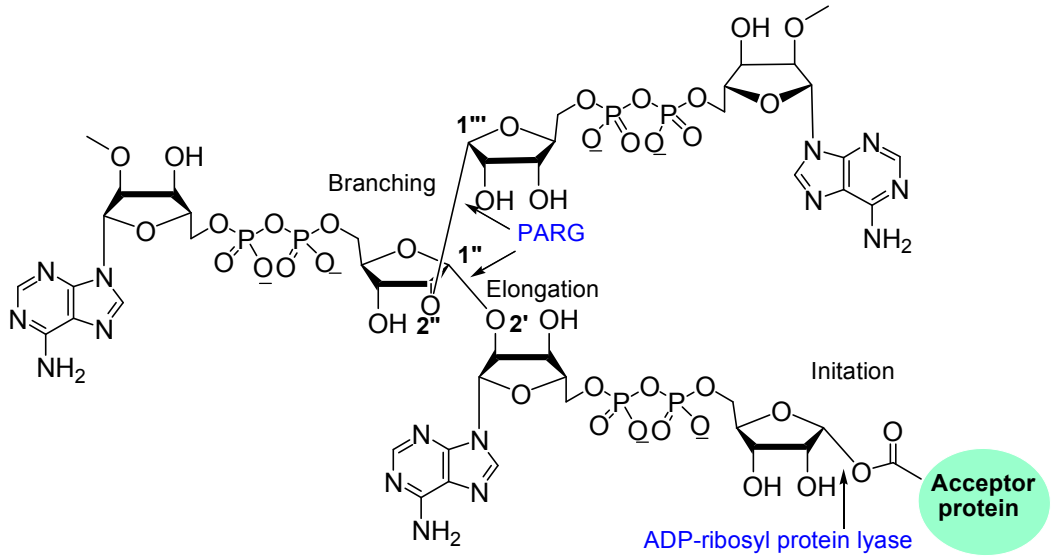

Figure 3. Formation of linear and branched poly(ADP-ribose) polymer.

1.4.4 Termination

The synthesis of long negatively charged polymers on histones causes an electrostatic repulsion of the nuclear protein from DNA. The strong affinity of histones for poly(ADP-ribose) compared to DNA, results in temporary dissociation of histones from damaged DNA and their transient electrostatic binding to poly(ADP-ribose). This results in relaxation of the chromatin at the site of the nick allowing access of repair enzymes.[29] Reassembly of the histone-DNA complex is triggered by poly(ADP-ribose)glycohydrolase (see below).[30]

During automodification, PARP-1 acts as a catalytic dimer. The introduction of a SSB in the DNA duplex induces flexibility at the nicked site. PARP-1 binds specifically through the second zinc finger to the centre of the characteristic V-shape in the DNA molecule and the enzyme covers seven base-pairs symmetrically on each side of the break.[13] This, in turn, leads to the recruitment of a second PARP-1 molecule through the leucine zipper motif in the automodification domain.[31] The second PARP-1 molecule serves as a polymer acceptor during subsequent ADP-ribose polymer synthesis by the first PARP-1 molecule.[32]

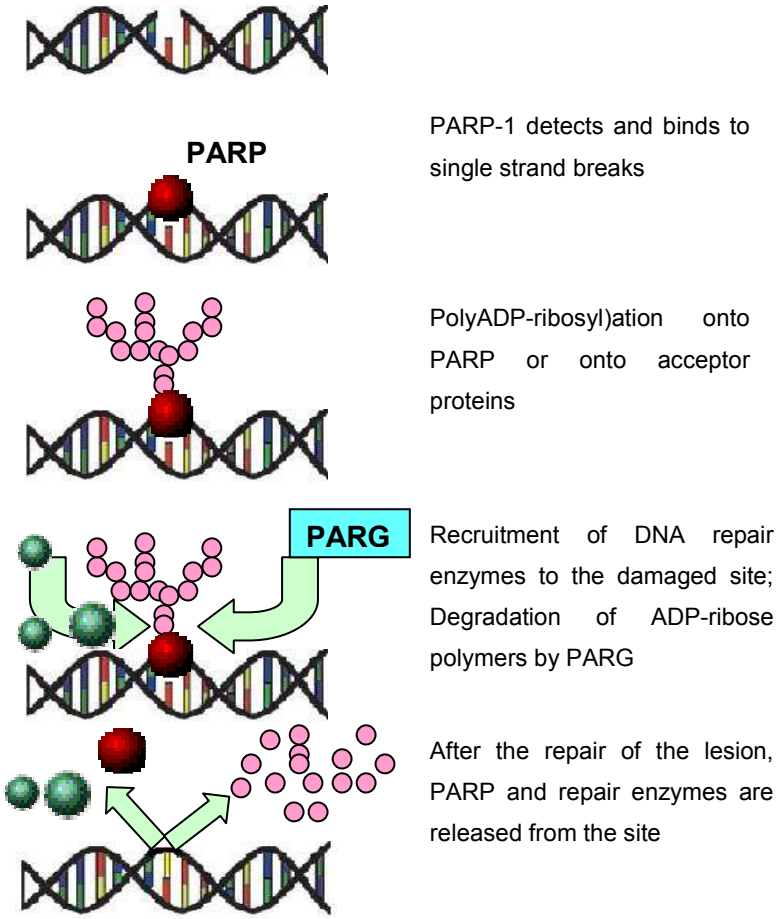

Figure 4. Mechanism of action of PARP-1.[33]

1.4.5. Catabolism of ADP-ribose polymers

Poly(ADP-ribosyl)ation is a dynamic process with a short a half-life (<1 min) of the polymer *in vivo*. The transient nature of the polymer is due to its degradation by a major catabolic enzyme poly(ADP-ribose)glycohydrolase (PARG). Once the ADP-ribose polymer is synthesised by PARP-1, it is immediately hydrolysed by the constitutively active PARG, which cleaves the ribose-ribose linkage in the linear (1''→2' glycosidic bond) and branched (1'''→2'' glycosidic bond) portions of the polymer to produce ADP-ribose monomers.[34] PARG is known to catalyse hydrolysis both of terminal ADP-ribose units from poly(ADP-ribose) polymers *via* exoglycosidic activity and to remove larger oligo(ADP-ribose) fragments through endoglycosidic cleavage.[35] The K_m value of PARG is lower for larger ADP-ribose polymers than for smaller ones, indicating that the enzyme probably removes and catabolises bigger fragments first, then switches to remove ADP-ribose units one by one. The proximal ADP-ribose moiety is removed from the acceptor proteins by ADP-ribosyl protein lyase.[36] It was shown to liberate a

dehydrated form of ADP-ribose (5'-ADP-3"-deoxypent-2"-enofuranose) from the acceptor protein. The degradation of ADP-ribose polymers represents a major regulatory mechanism for PARP-1, resulting in the down regulation of the enzyme and frees the site for further polymer synthesis.

1.5 PARP-1: Biological Roles

1.5.1 PARP-1 and DNA repair

PARP-1 has been implicated in DNA repair and the maintenance of genomic integrity. This 'guardian angel' function of PARP-1 is supported by delayed DNA base-excision repair (BER) and the high frequency of sister chromatid exchange in PARP-1-deficient cells after exposure to ionizing radiation or alkylating agents.[37] PARP-1 interacts with multiple nuclear components of the single-strand break repair (SSBR) and BER pathways, including the nick sensor DNA ligase III, the adaptor factor XRCC1 and DNA repair enzymes such as DNA polymerase-β and DNA ligase III.[38] The following steps are found to be involved in the process:

- Identification of the DNA break
- Translation and amplification of the damage signal, the poly(ADP-ribosyl)ation of PARP-1 itself and of histones H1 and H2B, the triggering of chromatin structure relaxation thereby increasing the access of DNA repair enzymes to the break
- Recruitment of XRCC1 to the damaged site followed by the assembly of the SSBR complex
- End processing, whereby polynucleotide kinase that is stimulated by XRCC1 converts the DNA ends to 5′-phosphate and 3′-hydroxyl moieties
- Gap filling by DNA polymerase
- Ligation step catalysed by DNA ligase III.

Another role of PARP-1 in DNA repair is regulation of the topological state of DNA, *i.e*. activity of DNA topoisomerase I. This enzyme plays an important role in controlling the level of DNA supercoiling and relieving the torsional stress that is generated during replication, transcription, recombination and chromatin remodelling. During this process, topoisomerase I can get trapped in a covalent complex with nicked DNA through the 3′-phosphate terminus, which inhibits its DNA-ligase activity. If unrepaired, this can lead to genomic instability or apoptosis. ADP-ribose polymers target specific domains of topoisomerase I and induce the enzyme to remove itself from cleaved DNA

and close the resulting gap.[39] The poly(ADP-ribose)polymer can also serve as an emergency source of energy used by base-excision machinery to synthesise ATP.[40]

1.5.2 PARP-1 in the regulation of gene expression

PARP-1 regulates the expression of various proteins at the transcriptional level. Three principal mechanisms are found to be involved: first, the regulation of chromatin structure and function; second, the regulation of DNA methylation by PARP-1; and third, the participation of PARP-1 in enhancer/promoter-binding complexes. In the first, poly(ADP-ribosyl)ation confers negative charge to histones, resulting in electrostatic repulsion between DNA and histones. Loosening histone-DNA interactions renders various genes accessible to the transcriptional machinery. In the second mechanism, PARP-1 binds to DNA methyltransferase-1 (DNMT), which is a key enzyme in DNA methylation and a global regulator of gene expression, and thereby inhibits its catalytic function.[41] Thirdly, regulation of transcription is associated with functional interactions of PARP-1 and various non-histone proteins. PARP-1 acts as a coactivator in nuclear factor-κB (NF-κB)-mediated transcription.[42] NF-κB is a key transcription factor regulating the expression of several elements of inflammation such as cytokines, chemokines, adhesion molecules (ICAM-1), and inflammatory mediators like inducible nitric oxide synthase (iNOS) and inducible form of cyclooxygenase (COX-2). It has been shown that inhibition of PARP-1 activity (5-AIQ) reduces NF-κB-mediated transcription suggesting that catalytic activity of the enzyme is required.[43-45] Studies have also showed that PARP-1 deficient cells were defective in NF-κB-dependent transcription activation in response to tumour necrosis factor (TNF). Treating mice with bacterial lipopolysaccharide (LPS), an endotoxin, resulted in the rapid activation of NF-κB in macrophages from PARP-1 competent mice but not from PARP-1 knockout mice. In fact, PARP-1-deficient mice were extremely resistant to LPS-induced endotoxic shock.[46] Although NF-κB-dependent transcriptional activation is promoted by PARP-1, sometimes expression of NF-κB-target genes is silenced by PARP-1.[47] PARP-1 is also required for the activation of other inflammation-related transcription factors, such as activator protein-1 (AP1), AP2, transcription enhancer factor-1 (TEF-1), *trans*-acting transcription factor-1 (SP1), octamer-binding transcription factor-1 (Oct1), yin-yang-1 (YY1) and signal transducer and activator of transcription-1 (STAT1).[48]

1.5.3 PARP-1 in DNA replication and cellular differentiation

Poly(ADP-ribosyl)ation plays an active role during the process of DNA replication and differentiation. The involvement of PARP-1 in the regulation of replication is supported by observations that poly(ADP-ribose) metabolism is accelerated in the nuclei of proliferating cells. The fact that PARP-1 copurifies with DNA polymerase α and δ, DNA primase, DNA helicase, DNA ligase, topoisomerases I and II, and key components of the multiprotein replication complex (MRC) suggests that PARP-1 is part of the MRC. Poly(ADP-ribosylation) of histones was proposed to facilitate the assembly and deposition of histone complexes on DNA during replication. Various experimental models using PARP-1-knockout cells and pharmacological inhibition have demonstrated an inhibition of DNA replication and cell proliferation, thus suggesting a possible role of PARP-1 in regulating these two processes.[28]

Replication and differentiation are closely coupled processes and this may provide a rationale for the differentiation-modifying effect of PARP-1. To function as specialised building blocks of tissues, cells need to undergo a series of proliferative steps during which they gain new functions and lose others. This process requires concerted gene activation and results in differentiation into specialised cells such as hepatocytes, neurons and renal tubular cells. The idea that PARP-1 interferes with differentiation is supported by the findings that PARP-1 inhibitors were found to inhibit differentiation of human granulocyte-macrophage progenitor cells to the macrophage lineage. Overexpression of PARP-1 also arrests NB4 cells and blocks all *trans*-retinoic acid-induced terminal neutrophilic differentiation.[40]

1.5.4 PARP-1 in cell death

Despite the 'guardian angel' functions of PARP-1, its over-activation has been proposed to represent a cell-elimination pathway through which severely damaged cells are removed from tissues. This suggests that the PARP-1-directed DNA repair process is a highly inefficient and energy-consuming process.

1.5.4.1 Cellular energy dynamics

PARP-1 is a very abundant enzyme with up to one PARP molecule for each 1000 bp of DNA. With the formation of each ADP-ribose polymer, PARP-1 consumes up to 200 molecules of NAD^+. In addition, the rate of turnover of nuclear NAD^+ in a normal intact

cell is estimated to be at least 100-fold less than in the DNA-damaged poly(ADP ribosyl)ating cell.[25] Over-activation of PARP-1 can affect cellular energy levels by depleting the cellular stores of substrate NAD^+.

NAD^+ is an essential cofactor in energy metabolism. It is an important respiratory coenzyme that regulates an array of vital cellular processes, such as glycolysis and mitochondria respiration, thereby providing ATP for most cellular processes. NAD^+ also serves as the precursor for nicotinamide adenine dinucleotide phosphate (NADP), which acts as a cofactor for the pentose shunt and for bioreductive synthetic pathways, and is involved in the maintenance of reduced glutathione pools.[49] The level of poly(ADP-ribosyl)ation in cells is the most important factor for the maintenance of NAD^+ levels. DNA-damage-induced NAD^+ depletion results in ATP depletion because NAD^+ resynthesis requires at least two molecules of ATP per molecule. The result of massive NAD^+ usage is a decline in the rate of all vital processes, leading to cellular dysfunction and, ultimately, cell death. Moreover, under these precarious conditions, phosphoribosyl pyrophosphate synthetase and nicotinamide mononucleotide adenylyl transferase consume ATP in an effort to replenish the cellular NAD^+ store, further worsening the energy shortage and leading to a pronounced reduction of energy-dependent processes, such as DNA, RNA and protein synthesis.[25]

1.5.4.2 The "suicide hypothesis"

PARP-1 carries out two seemingly contradictory activities, DNA repair that enables the cell to survive and NAD^+ depletion to kill the cell. Based on this observation, Berger[50] proposed a "suicide concept" postulating that the activation of PARP-1 by massive DNA damage is actually a suicide response, since it causes rapid depletion of NAD^+ and ATP depletion and leads to cell death before there is an opportunity to repair the DNA. This cell death is presumably Nature's way of preventing gravely damaged cells from attempting to repair themselves. Such a suicide mechanism limits the possibility that massively damaged cells will try to repair and survive with a high mutation frequency and a potentially malignant transformation. This activation of PARP-1 by DNA damage may provide a safety mechanism whereby massively damaged cells are removed from the population, thereby decreasing the likelihood of preserving cells with highly mutant phenotypes. When a cell is damaged, the partial energy depletion provided by PARP-1 activation may prevent the cell from overexerting itself until DNA repair is completed.

1.5.4.3 The "molecular switch hypothesis"

The "suicide hypothesis" is controversial because it was never established whether an extensively damaged cell dies because of a depleted NAD^+/ ATP pool or from the DNA damage itself. The two sides of the argument viewed PARP-1 either as an indispensable cellular survival factor or as an active mediator of cell death. However, it is currently accepted that PARP-1 has been implicated in both apoptosis and necrosis, the actual mode of cell death being determined chiefly by the level of NAD^+ and ATP. It was therefore plausible to hypothesise that PARP-1 serves as a molecular switch between apoptosis and necrosis.[51] Virág and Szabó[40] proposed a unifying concept according to which, cells that are exposed to DNA-damaging agents can enter three pathways based on the intensity of the stimulus (severity of DNA damage) (FIG. 5).

- PARP-1 activated by mild to moderate genotoxic stimuli facilitates DNA repair, by signalling cell-cycle arrest and by interacting with DNA-repair enzymes such as XRCC1 and DNA-dependent protein kinase (DNA-PK). As a result, DNA damage is repaired and cells survive without the risk of passing on mutated genes.
- In the second pathway, more severe DNA damage induces apoptotic cell death, with caspases, the main executor enzymes (caspase 7 and caspase 3) of the apoptotic process, inactivating PARP-1 by cleaving it into two fragments (p89 and p24) at the DEVD motif in the nuclear localization signal of PARP-1.[52] Cleavage at this site separates the DNA binding domain from the catalytic domain, which inactivates the enzyme. PARP-1 cleavage is viewed as a marker of apoptosis, rather than an executor of the process. This pathway allows cells with irreparable DNA damage to be eliminated in a safe way *i.e. via* ingestion by macrophages. In fact, PARP-1 cleavage prevents the overactivation and thereby maintains cellular energy for certain ATP-sensitive steps of apoptosis.[53] Cleavage of PARP-1 is believed to aim at promoting apoptosis by preventing DNA repair-induced survival and by blocking energy depletion-induced necrosis.
- The third pathway, necrotic cell death, is induced by extensive DNA breakage caused by oxidative or nitrosative stress (hydroxyl radical, peroxynitrite, nitroxyl anion). The overactivation of PARP-1 depletes the cellular stores of its substrate NAD^+ and, consequently, ATP level. The severely compromised cellular energetic state inhibits the apoptotic cell death process to proceed because many steps of apoptosis are known to depend on ATP. Under these conditions, pharmacological PARP inhibition or the absence of PARP in PARP-

deficient mice preserves cellular ATP and NAD^+ pools in oxidatively stressed cells and thereby allows them to either function normally or die by apoptosis instead of necrosis.[40] In addition to numerous biochemical and morphological similarities and differences between apoptosis and necrosis, a distinctive feature of necrosis is the disintegration of the plasma membrane (as opposed to the compaction of apoptotic cells, which is followed by elimination). Consequent leakage of cellular content from necrotic cells into the surrounding tissue exacerbates the inflammatory responses.

According to Figure 5, depending on the intensity of the stimulus, PARP-1 regulates three different pathways. In the case of mild DNA damage, poly(ADP-ribosyl)ation facilitates DNA repair and, therefore, survival (route 1). More severe genotoxic stimuli activate an apoptotic pathway that eliminates cells with damaged DNA (route 2). The most severe DNA damage can cause excessive PARP activation, which depletes cellular NAD^+/ATP stores. NAD^+/ATP depletion blocks apoptosis and results in necrosis (route 3). The inhibition of PARP-1 in cells entering route 1 suppresses repair and, therefore, diverts cells to route 2 (dashed arrow on the left). The inhibition of PARP in cells that are entering route 3 preserves ATP and cellular energy stores, and either prevents cell death or enables it to occur through apoptosis instead of necrosis (dashed arrow on the right).

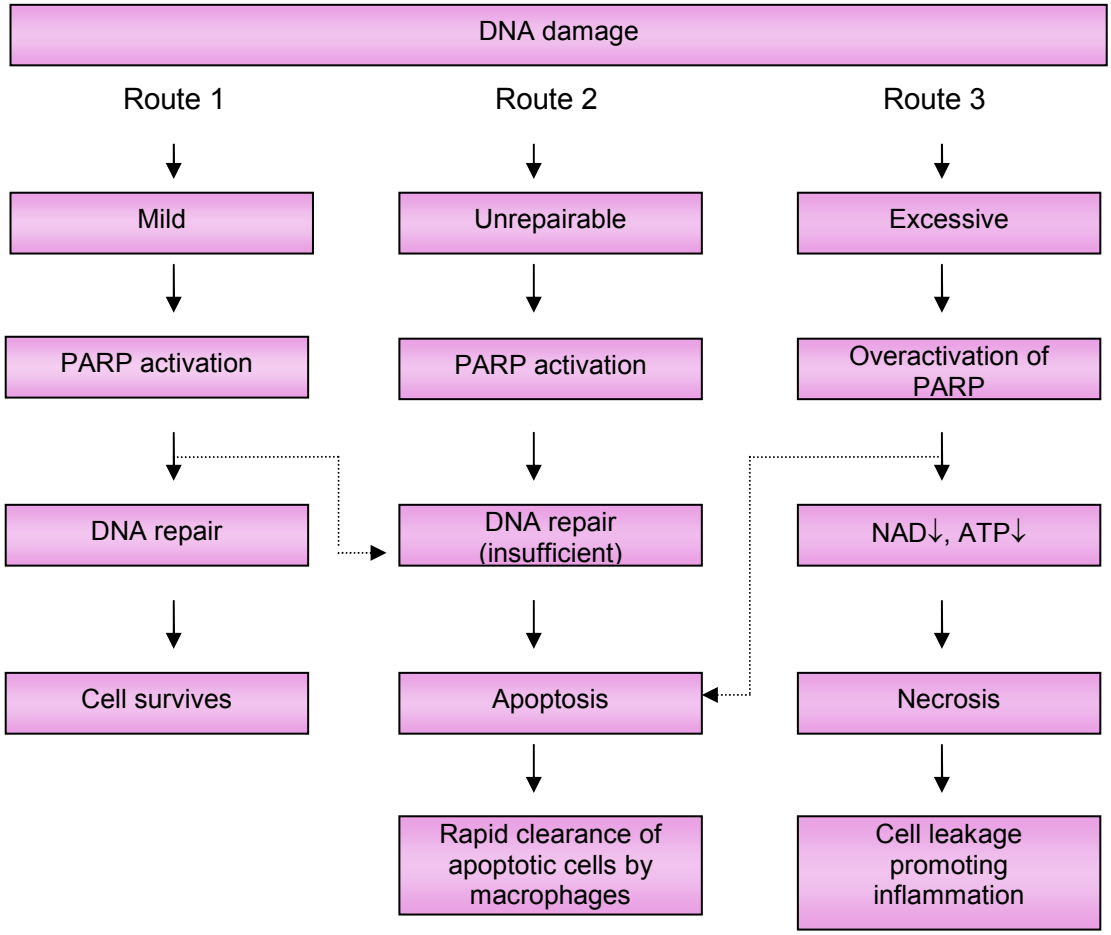

Figure 5. Intensity of DNA-damaging stimuli determines the fate of cells: survival, apoptosis or necrosis.[40]

A great variety of human diseases, such as cancer, ischaemia-reperfusion injury, inflammatory disorders and neurodegenerative diseases involve damage to DNA as a crucial element to their pathogenesis. Most of these damages are caused by oxidative stress where PARP-1 is very much involved as the final mediator of cellular injury and death. PARP-1 inhibition, therefore, is an attractive method for studying the significance of this enzyme in biological systems and may prove useful for the therapy of these diseases. PARP-1 has been extensively investigated as a target of novel compounds, capable of inhibiting its catalytic activity, which may be used in a broad spectrum of diseases to counteract PARP mediated cell death or to enhance the efficacy of chemotherapy and radiotherapy.

1.6 Therapeutic potential of PARP-1 inhibition

1.6.1 PARP-1 inhibition in cancer therapy

Radiotherapy and many chemotherapeutic approaches to cancer therapy act by inducing DNA damage. Since PARP-1 is a controlling enzyme in the repair of damage to DNA, it is unsurprising that the first proposed application of PARP-1 inhibition was in radiopotentiation and chemopotentiation. DNA repair processes mediated by PARP-1 can lead to resistance to chemotherapy and radiotherapy. Therefore inhibition of DNA repair may be therapeutically beneficial in the treatment of cancer. The rationale for the use of PARP-1 inhibitors as chemo- and radio-sensitisers comes from the observation that PARP-1 is important for DNA base-excision repair and its inhibition caused a significant delay in the DNA repair processes.

1.6.1.1 Chemopotentiation

Co-administration of a PARP-1 inhibitor with cytotoxic drugs that cause single- and double-strand DNA breaks potentiates the activity of these agents and causes persistent DNA single-strand breaks. A potential role of PARP-1 inhibitors as resistance modifiers when used in combination with the methylating agent temozolomide (TMZ) were evaluated.[54] The methylating agent temozolomide (TMZ) is used in the therapy of various central nervous system (CNS) tumours. TMZ resistance develops frequently and diminishes the clinical response. This phenomenon is often the result of the efficient repair of methyl adducts at the O^6-position of guanine mediated by MGMT. The combination of PARP inhibitors with TMZ interferes with the repair of methylpurines. When PARP is inhibited, the recruitment-promoting functions of XRCC1 are impaired, which hampers strand rejoining; this leads to the generation of permanent single-strand breaks that trigger the apoptotic process. It is in combination with this cytotoxic agent that PARP-1 inhibitors were introduced into the clinic for cancer patients in 2003. Tentori *et al*.[55] demonstrated that the antitumour activity of TMZ against brain lymphoma is enhanced by the use of an intracerebral injection of the PARP-1 inhibitor NU1025 (8-hydroxy-2-methylquinazolin-4(*3H*)-one). Systemic administration of GPI15427 enhanced the efficacy of TMZ against metastatic melanoma, glioblastoma multiforme and lymphoma growing in the brain. These drug combinations enhanced the survival of lymphoma-bearing mice with respect to treatment with TMZ only. AG14361 increased the activity of temozolomide and topotecan, and the activity of radiation therapy *in vitro.*[56] AG014699 is a potent tricyclic

indole PARP inhibitor that has completed both Phase I and II studies in combination with temozolomide. Clinical trials are also in progress for INO-1001 in combination with temozolomide in patients with malignant glioma.[6]

PARP inhibitors have also been shown to enhance the cytotoxicity of the camptothecin-derived DNA topoisomerase I poisons irinotecan and topotecan.[57] Camptothecins act through the stabilisation of topoisomerase I-cleavage complexes. Poly(ADP-ribosyl)ated PARP-1 and PARP-2 counteract the action of camptothecin by facilitating the resealing of DNA-strand breaks. Therefore, it is conceivable that the enhancement of camptothecin cytotoxicity induced by PARP inhibitors may be due to the impairment of the strand break re-joining mediated by topoisomerase I itself.[58]

Non-toxic concentrations of 5-methylnicotinamide dramatically potentiated the cytotoxicity of N-methyl-N-nitrosourea and of γ-radiation.[59] The PARP inhibitor 4-amino-1,8-naphthalimide has been shown to sensitize p53-deficient breast cancer cell lines to apoptosis induced by doxorubicin, an anticancer drug commonly used for adjuvant therapy of breast cancer. The combination of doxorubicin and PARP inhibitor PJ34 is effective in reducing cardiac toxicity induced by the former.[60] Cisplatin and its analogue carboplatin, which generate platinum DNA adducts, are used for the treatment of germ cell tumours, gynaecologic cancers, lung, bladder and head/neck cancer, whereas oxaliplatin is used for the treatment of colon cancer. Oral administration of BGP-15 shortly before cisplatin treatment prevented drug induced renal failure without reducing the antitumor efficacy of the chemotherapeutic agent.[61]

1.6.1.2 Radiopotentiation

An intriguing area of use of PARP-1 inhibitors is in the potentiation of radiotherapy. Treatment with ionising radiation is the most widely used anticancer intervention after surgery. Radiotherapy damages cells by causing both single- and double-strand breaks and inducing apoptotic cell death. DNA repair mechanisms within cancer cells attempt to minimise this damage and then resistance emerges. *In vivo* efficacy of PARP inhibition for radiosensitisation has been recently demonstrated by a preclinical study showing that intraperitoneal administration of the PARP inhibitor AG14361 significantly enhances sensitivity of colon carcinoma subcutaneous xenografts to radiation therapy.[56] AG14361 also inhibited the recovery of growth-arrested cells from potentially lethal irradiation damage. This sensitisation of growth-arrested cells is important for tumour radiation therapy because experimental and clinical evidence indicate that the

growth-arrested cell fraction within a tumour is radiation-resistant and capable of re-entering the cell proliferation cycle and thereby re-populating the tumour after radiation therapy. The PARP inhibitor INO-1001 has also demonstrated radiosensitising effects *in vitro* and *in vivo*. 6(*5H*)-Phenanthridinone, a PARP-1 inhibitor, also enhanced cytotoxicity induced by ionising radiation.[62]

1.6.1.3 PARP-1 inhibitors as single agents in DNA repair-deficient tumours

PARP inhibitors might be beneficial in cancer treatment as a single agent. This would certainly have an advantage in terms of toxicity, as one of the concerns of chemotherapy combination studies is systemic toxicity caused by the use of PARP inhibitors as enhancers of cancer therapy. BRCA1 and BRCA2 are essential for the repair of double strand DNA breaks (DSBs) by the process of homologous recombination (HR). BRCA1-deficient and BRCA2-deficient cells, when compared with matched wild-type cells, were profoundly sensitive to inhibitors of PARP-1 In some cases, BRCA-deficient cells were more than 1000 times more sensitive to nanomolar concentrations of PARP inhibitor, suggesting the possibility of a highly selective therapy.[63] PARP-1 is crucial for the repair of single-strand DNA breaks (SSBs) and PARP inhibitors cause an increase in persistent SSBs by targeting the HR deficiency in BRCA-deficient cells. Germ-line mutations in BRCA1 and BRCA2 indicate high risk for breast, ovarian, and other malignancies. In these cells, PARP inhibition results in cell cycle arrest and apoptosis. This suggests a role for PARP inhibitors as single agents in cancers exhibiting BRCA1 and BRCA2 mutations. Evaluation of KU0058948 suggested that the sensitivity of BRCA1- and BRCA2-deficient cells to PARP inhibition seems to be dependent on the potency and/or specificity of the PARP inhibitor. A Phase I study is ongoing with the KuDOS orally available PARP-1 inhibitor (KU-00559436) as a single anti-cancer agent. In addition, a Phase II study of AG014699 in metastatic breast and ovarian cancer in proven carriers of a BRCA-1 or BRCA-2 mutation is in progress.[64]

1.6.2 PARP-1 inhibition in reperfusion injury

Clinically, when there is a reduced blood supply to the tissues, the cells are said to be ischaemic. Ischaemia is a common condition during surgery and in many diseases, such as myocardial infarction, stroke and haemorrhage. Early reperfusion is an absolute prerequisite for the survival of ischaemic tissues. However, reperfusion has often been observed to exacerbate the injury sustained by the ischaemic tissues and lethally damage the organs (ischaemia-reperfusion injury). The damage, which occurs

during the early minutes of reperfusion, is far greater than would have occurred if the ischaemia had been maintained.[65]

It is well established that oxygen-derived free radicals and oxidants play a role in the pathogenesis of ischaemia–reperfusion. Recent studies confirmed this "oxygen paradox" and suggested that reperfusion could trigger sudden metabolic and physiological changes, most notably, an outburst of oxidants and free radical production, in particular, hydrogen peroxide, hydroxyl radical, superoxide anion, nitric oxide and peroxynitrite.[66-68] These are capable of exerting cytotoxic effects independently or synergistically, *via* a number of mechanisms; both hydroxyl radical and peroxynitrite (a highly reactive oxidant produced from the reaction between nitric oxide and superoxide) can also trigger massive DNA single strand break, leading to PARP-1 over-activation.[66] In stroke, heart attack and other forms of reperfusion injury, the main steps of the process are as follows.[48]

- The occlusion of a blood vessel prevents blood flow to the organ.
- Restoration of the blood flow (spontaneously or in conjunction with a medical intervention, such as thrombolysis or angioplasty) triggers the generation of various oxidants and free radicals.
- These species (hydrogen peroxide, hydroxyl radical and peroxynitrite) induce a range of oxidative and nitrosative injuries to the cells, including protein and lipid modifications, mitochondrial dysfunction and DNA damage (base modifications and DNA-strand breakage).
- PARP-1 senses the DNA breaks and becomes activated.
- This process leads to the consumption of NAD^+, initially mainly from the cytosolic pool.
- The cell attempts to regenerate NAD^+ from nicotinamide, which is converted to nicotinamide mononucleotide by phosphoribosyl transferase using phosphoribosyl pyrophosphate obtained from ATP.
- PARP-activation-induced depletion of the cellular pyridine nucleotide pool impairs important NAD^+-dependent cellular pathways, including glycolysis and mitochondrial respiration. NAD^+ deficiency allows only the ATP-consuming part of anaerobic glycolysis to take place, thereby decreasing the synthesis of pyruvate and the mitochondrial formation of NADH. NADH-deficient mitochondria undergo depolarisation, which converts the ATP synthase into an ATPase.
- Finally, the ensuing cellular energetic starvation leads to the shutdown of energy-requiring processes which leads to a breakdown of membrane potential

and leakage of the membrane. These events promote futile cycles that, ultimately, lead to cell death through the necrotic route.

It has been proposed that inhibition of PARP-1 should alleviate depletion of NAD^+ and protect organs from damage following ischaemia and reperfusion. Table 1 summarises some of the diseases in which PARP inhibition or deficiency provides therapeutic benefit *in vivo*. Two organs in which PARP-mediated reperfusion injury has been intensively investigated are the brain and heart. Pharmacological inhibition of PARP-1 with 3-aminobenzamide (3-AB) significantly improved the outcome of myocardial dysfunction, as evidenced by a reduction in creatine phosphokinase levels, reduced infarct size, and preserved ATP pools.[69-72] 5-Aminoisoquinolin-1-one (5-AIQ) also proved to be a potent inhibitor of poly(ADP-ribose)polymerase activity in cardiac myoblasts and reduces myocardial infarct size *in vivo*.[73] Neuronal damage following stroke and other neurodegenerative processes is thought to stem from over-excitation attributable to a massive release of the excitatory neurotransmitter glutamate acting on the *N*-methyl-D-aspartate (NMDA) receptor and other subtype receptors.[74] Stimulation of NMDA activates the production of nitric oxide by neuronal nitric oxide synthase (nNOS), which ultimately accounts for reperfusion injury in the central nervous system. In PARP-1 knockout mice, a markedly reduced infarct volume is observed after transient middle cerebral artery occlusion.[75] Several PARP-1 inhibitors have also been shown to reduce infarct size and improve neurological status in cerebral ischaemia-reperfusion.[75-77]

Table 1. PARP inhibition in animal models of inflammation, reperfusion, degenerative and vascular diseases.[48]

3-AB, 3-aminobenzamide; ISQ, 5-hydroxyisoquinolin-1-one; DPQ, 3,4-dihydro-5-[4-1(1-piperidinyl)butoxy]1(2H)-isoquinolinone; G-PH, aza-5[H]-phenanthridin-6-one derivative; PHT, 6(5H)-phenanthridinone; INH2B, 5-iodo-6-amino-1,2-benzopyrone; GPI-6150, 1,11b-dihydro-[2H]benzopyrano[4,3,2-de]isoquinolin-3-one; PJ-34, N-(6-oxo-5,6-dihydro-phenanthridin-2-yl)-N,N-dimethylacetamide; INO-1001, Inotek's indenoisoquinolinone derivative; 5-AIQ, 5-aminoisoquinolin-one; ONO-1924H, N-[3-(4-Oxo-3,4-dihydro-phthalazin-1-yl)phenyl]-4-(morpholin-4-yl)butanamide methanesulfonate monohydrate; DR2313, 2-methyl-3,5,7,8-tetrahydrothipyrano[4,3-d]pyrimidine-4-one; AIF, apoptosis-inducing factor; F-Q, 2,8-disubstituted quinazolin-4(*3H*)-one **(43d)**; NA, nicotinamide; 4-OHQ, 4-hydroxyquinazoline; I/R, ischaemia/reperfusion; NMDA, N-methyl-D-aspartate.

Organ/Disease model	PARP inhibitors	Effects of PARP-1 inhibition
Brain		
Stroke	3-AB, ISQ, DPQ, G-PH, PHT, INH2BP, GPI-6150, PJ-34[76], INO-1001, ONO-1924H,	Reduction in necrosis of the neurons, improvement in neurological status, protection against white-matter damage and AIF translocation
Traumatic brain injury	3-AB[44], GPI-6150, PJ-34, INO-1001	Improved neurological status
Hypoglycaemia	ISQ	Improved survival and behavioural status
Meningitis	3-AB	Improved survival, neurological status and reduced inflammatory mediator production
Parkinson's disease	GPI-6150, ISQ, F-Q	Improved neurological outcome and dopamine loss
Heart		
Myocardial infarction	3-AB,[71,72] NA, ISQ, 5-AIQ,[73] PJ-34, INO-1001, GPI-6150	Reduced myocardial necrosis, reduced infarct size, improved myocardial contractility, and reduced neutrophil infiltration
Transplantation	3-AB[84], PJ-34, INO-1001	Improved myocardial contractility, reduced inflammatory mediator production, extension of transplant survival
Ischaemic cardiomyopathy	PJ-34, INO-1001	Improved myocardial contractility, improved survival
Diabetic cardiomyopathy	PJ-34, INO-1001	Improved myocardial contractility
Ageing-associated heart failure	PJ-34, INO-1001	Prevention or reversal of diabetic endothelial dysfunction
Vasculature		
Diabetic endothelial dysfunction	PJ-34, INO-1001	Prevention or reversal of diabetic endothelial dysfunction
Ageing, Hypertension	PJ-34, INO-1001	Protection against the development of endothelial dysfunction
Lung		
Acute respiratory distress syndrome	Benzamide, PJ-34, 5-AIQ[95]	PARP inhibition suppresses endotoxin induced pulmonary damage, reduces inflammatory mediator production and NMDA mediator production and lung oedema formation

Organ/Disease model	PARP inhibitors	Effects of PARP-1 inhibition
Ovalbumin-induced asthma	3-AB, 5-AIQ, PJ-34	Reduced inflammatory mediator production and improved pulmonary function
Endocrine/pancreas		
Diabetes	NA, 3-AB, INH2BP	Protection against necrosis of islets and reduction in the degree of hyperglycaemia
Joint/Arthritis	NA, 3-AB, PJ-34	Reduced arthritis severity and incidence
Skeletal muscle I/R	3-AB[70]	Reduction in reperfusion injury necrosis markers
Liver		
I/R injury	PJ-34, 5-AIQ[80,81]	Improved survival, reduced hepatic necrosis and protection against hepatic leukostasis
Kidney I/R	Benzamide, 3-AB, 5-AIQ,[82] PJ-34	PARP inhibitors accelerate the recovery of normal renal function after I/R injury
Transplantation	PJ-34	No effect on the function of the transplanted kidney
GI tract		
Colitis	3-AB[78], NA, INH2B, PJ-34, 5-AIQ[92], GPI-6150,[79] INO-1001, ISQ	Improved survival, protection against gut shortening, lipid peroxidation, nitrosative damage and ICAM1 expression
Mesenteric I/R injury	3-AB, NA, GPI-6150,	Protection against histological damage, neutrophil infiltration and mucosal barrier failure
Eye		
Uveitis	PJ-34	Protection from leukocyte migration
Diabetic retinopathy	PJ-34	Inhibition of the development of acellular capillaries and reduced leukostasis
Retinal I/R	3-AB[83]	Reduced I/R damage to the retina
Ear		
Cochlear I/R injury	3-AB	Improvement of cochlear function
Skin		
Sulphur mustard induced vesication	3-AB, NA	Protection against NAD+ depletion and microvesicle formation
Peripheral nerve		
Diabetic neuropathy	ISQ, PJ-34	Protection against loss of motor and sensory nerve conductance
Cavernous nerve injury	INO-1001	Improved erectile function

Organ/Disease model	PARP inhibitors	Effects of PARP-1 inhibition
Many organs		
Haemorrhagic, endotoxic and septic shock	3-AB, NA, PJ-34, INH2BP, GPI-6150, 4-OHQ, 5-AIQ[86]	Protection against haemodynamic decompensation, improved survival, protection against gut hyperpermeability and myocardial, vascular, hepatic and renal failure
Thoracoabdominal I/R	PJ-34	Improved survival and neurological status
HIV	Benzamides, benzopyrones, INH2BP	PARP deficiency reduces viral replication and integration

Protection against organ damage by PARP-1 inhibitors are also reported in reperfused organs such as gut,[78,79] skeletal muscle,[70] liver,[80,81] kidney[82] and retina.[83] It also improves the outcome of heart transplantation[84] and protects against multiple organ damage secondary to haemorrhagic shock.[85-87]

1.6.3 PARP-1 inhibition in inflammatory diseases

Over-activation of PARP-1 also induces the expression of a number of genes that are essential for inflammatory responses (overviewed in section 1.5.2). PARP-1 acts as co activator of NF-κB resulting in expression of NF-κB-dependent inflammatory elements, such as cytokines, chemokines, *i*NOS, ICAM-1 and TNF. Both cytokines and chemokines can trigger free-radical formation through many different pathways, for example by stimulating xanthine oxidase activity and by recruiting activated neutrophils. In addition, the level of production of nitric oxide is increased due to *de novo* iNOS expression. These events further worsen the oxidant stress, producing even greater PARP-1 activation and cell dysfunction. The earliest implication of PARP-1 in the pathophysiology of inflammatory diseases was related to pancreatic islet cell injury and diabetes. In streptozotocin-induced pancreatic islet cell injury and diabetes, inhibition of PARP-1 with 3-AB prevented NAD^+ depletion and the suppression of proinsulin synthesis without modifying the extent of DNA damage. Subsequent experiments *in vivo* demonstrated that such inhibition delays the onset of streptozotocin- and alloxan-induced diabetes.[88,89]

The role of PARP-1 activation and the protective effects of PARP inhibitors have also been demonstrated in various experimental models of inflammation, including acute inflammatory diseases (such as endotoxic shock), as well as chronic inflammation of the gut, joints and various other organs. (Table 1) For instance, PARP inhibitors and/or PARP deficiency is effective in arthritis,[90] colitis,[91,92] and pulmonary inflammation.[93-95]

Systemic inflammatory diseases (circulatory shock) are associated with a reduced responsiveness of blood vessels to vasoconstrictor agents (a result of nitric oxide and peroxynitrite production), myocardial dysfunction and impaired intracellular energetic processes, culminating in multiple organ failure. The severity of these inflammatory diseases is suppressed by PARP inhibitors and the production of multiple pro-inflammatory mediators is down-regulated. It was also demonstrated that treatment of mice for tissue injury associated with stroke and neurotrauma with PARP inhibitors 3-AB and 5-AIQ reduced the degree of spinal cord inflammation, tissue injury, neutrophil infiltration and apotopsis.[96]

1.6.4 PARP-1 inhibition in cardiovascular diseases

PARP-1 activation also has a pathogenic role in hypertension, atherosclerosis and diabetic cardiovascular complications. In these diseases, the dysfunction of the vascular endothelium (that is, a reduction in the ability of the endothelial cell to produce nitric oxide and other cytoprotective mediators) is diminished. The oxidant-mediated endothelial cell injury is dependent on PARP-1 and can be attenuated by pharmacological inhibitors or genetic PARP-1 deficiency.[97] For instance elevated extracellular glucose levels (as in diabetes) trigger PARP-1 activation through the mitochondrial release of oxidants, which is followed by DNA-strand breakage. In hypertension, angiotensin II acts on its endothelial receptors and up regulates NADPH oxidases. The subsequent generation of superoxide and peroxynitrite triggers DNA-strand breakage and PARP activation.[98] *In vivo* studies show that PARP-1 inhibition improves endothelium-dependent relaxations in hypertensive and diabetic animals.[99] PARP-1 activation is also involved in the early functional changes that are associated with atherosclerosis and vascular injury. The preservation of vascular function might underlie the protective effect of PARP inhibitors against diabetic neuropathy and retinopathy.[100,101]

1.6.5 PARP-1 inhibition in HIV-1 infection

There is an increasing body of evidence suggesting the involvement of PARP-1 in HIV-1 infection. During the life cycle of the HIV-1 virus within the infected cell, the RNA genome of the virus is reverse-transcribed into double-stranded DNA by reverse transcriptase.[102] The proviral DNA, in turn, enters the nucleus, where the virion-associated viral enzyme, integrase, catalyses the integration of the viral double-stranded DNA into the host genome. This process requires nicking of both DNA strands and may therefore lead to PARP-1 activation. At present, it seems that PARP-1

regulates HIV infection at two levels: integration and transcription and PARP-1 inhibition may be a viable strategy in controlling HIV-1 infection. Studies show that benzopyrone derivatives, benzamides and nicotinamide possess potent antiviral effects in HIV-infected cells.[103]

1.6.6 Other diseases

A large number of studies have been published providing experimental evidence that suggests other clinical indications of PARP-1 inhibitors. PARP-1 inhibitors provided beneficial effects in a variety of disease conditions including Parkinson's disease,[104] Alzheimer's disease,[105] acetaminophen-induced hepatotoxicity[106] and UV radiation-induced dermal necrosis.[107] PARP-1 inhibition by 5-AIQ prevents experimental asthma-like conditions in guinea pigs[108] and PJ34 protects against allergic encephalomyelitis in an animal model.[109] Malfunction of the immune systems often follows profound stress and this immunocompromise is alleviated by inhibition of PARP-1 activity.[110]

1.7 Development of PARP-1 inhibitors

Intensive research over the last decade has yielded multiple classes of PARP-1 inhibitors, the vast majority of which bind to the nicotinamide-binding domain of the enzyme and act as competitive, reversible inhibitors with respect to NAD^+, the natural substrate for PARP-1.

1.7.1 Classical PARP inhibitors

Nicotinamide **(2)** and its 5-methyl derivative **(3)** were shown to be competitive inhibitors of PARP-1, at millimolar concentrations (IC_{50} 210 μM). Being a natural compound, nicotinamide also acts as a substrate for NAD^+ biosynthesis.[111] Although reasonably soluble, it is a weak inhibitor of the enzyme and lacks specificity. Moreover, nicotinamide administered to cells is not always inhibitory but is often stimulatory to ADP-ribosylation. It has also been shown to act as a radical scavenger in certain experimental models. Benzamide **(4)** (IC_{50} 22 μM), a close structural analogue of nicotinamide first shown by Shall[111] to be an effective inhibitor, lacks the ring nitrogen and cannot undergo metabolism by NAD-biosynthetic enzymes analogously to nicotinamide. However, this compound had limited solubility in water, given the hydrophobic nature of its structure. In an attempt to improve the aqueous solubility of benzamide, Purnell and Whish[112] introduced polar substituents on the 3-position of the

aromatic ring of benzamide. 3-Amino- **(5)**, 3-hydroxy- **(6)** and 3-methoxy-benzamide **(7)** were found to maintain inhibitory activity with improved water solubility. They were found to be competitive inhibitors and two of them, 3-amino- and 3-methoxy benzamide, (K_i < 2 μM) have become the benchmark PARP inhibitors against which novel compounds have been compared.

1.7.2 Structure-activity relationships of PARP-1 inhibitors

The emergence of 3-substituted benzamides as prototype PARP-1 inhibitors has stimulated considerable interest in the structure-activity relationship (SAR) of this class of compounds and a number of very detailed investigations by research groups working independently have been undertaken. Sims *et al*[113] provided new information concerning SARs for nicotinamide analogues. The presence of an unsubstituted carbamoyl group was found to be essentially a prerequisite for significant activity. Picolinamide **(8)** and isonicotinamide **(9)** both exhibited activity comparable to nicotinamide. Introduction of additional ring nitrogens was also tolerated and pyrazinamide **(10)** was only marginally less potent than nicotinamide. Upon alkylation of the ring nitrogen **(11)** or reduction of the aromatic ring **(12)** activity was abolished, or markedly lowered.

Sestili and coworkers investigated the enzyme-inhibitory activity and *in vitro* potentiation of alkylating agent cytotoxiclty of a series of benzamide analogues modified with respect to the nature of the aromatic ring, the carboxamide function and aryl substituents.[114,115] Replacement of amide group with a carboxylate **(13)**, alkylamide **(14)**, sulphonamide **(15)** and thioamide **(16)** resulted in dramatic loss of activity. Reduction of the aryl ring to furnish cyclohexanecarboxamide **(17)** abolished activity. Replacement of the benzene ring with a thiophene ring in thiophene-3-carboxamide **(18a)** reduced the activity. In contrast to earlier reports which showed that replacement of the benzene ring with a thiophene ring in thiophene-3-carboxamide reduced the inhibitory potency, an investigation by Shinkwin *et al*[116] demonstrated that the isomeric thiophene-2-carboxamide **(18b)** displayed good PARP-1 inhibition, with potency of the same order of magnitude as benzamide. This confirmed that the heterocyclic thiophene ring can substitute for the benzene ring in simple PARP inhibitors without significant loss in potency. Alkylation of the amino group of 3-aminobenzamide had little effect, acylation of this substituent significantly enhanced potency, with 3-acetamido- and 3-propanamidobenzamide **(19)** and **(20)** proving to be potent PARP-1 inhibitors.

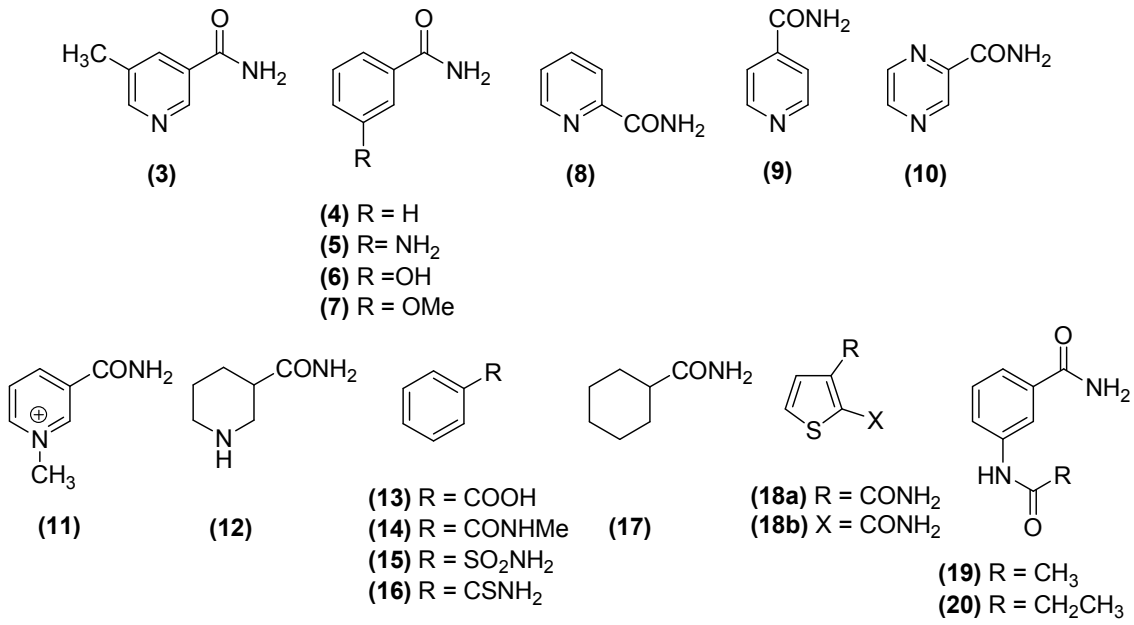

Figure 6: SARs for nicotinamide and benzamide analogues.

Banasik *et al*[117] conducted one of the most comprehensive investigations to date, where they evaluated more than 170 compounds of diverse structures for their ability to inhibit PARP-1 and mono(ADP-ribosyl)transferases using standardised assay methods. These wide ranges of compounds led to the identification of new templates for the design of novel PARP inhibitors. All highly potent inhibitors were polyaromatic heterocycles. The studies showed that the compounds that had the carboxamide group incorporated within the ring system displayed very potent PARP-1 inhibitory activity. The strategy of cyclising an open benzamide structure or creating a further ring system on the existing cyclic amide was one of the best approaches to designing new PARP-1 inhibitors. The compounds include the 1,8-naphthalimide derivatives **(21)** and **(22)**, 5-hydroxyisoquinolin-1-one **(23)**, phenanthridinone **(24)** and the quinazolinone **(25)**. Compound **(23)** was over 100-fold more potent than benzamide and 3-aminobenzamide.

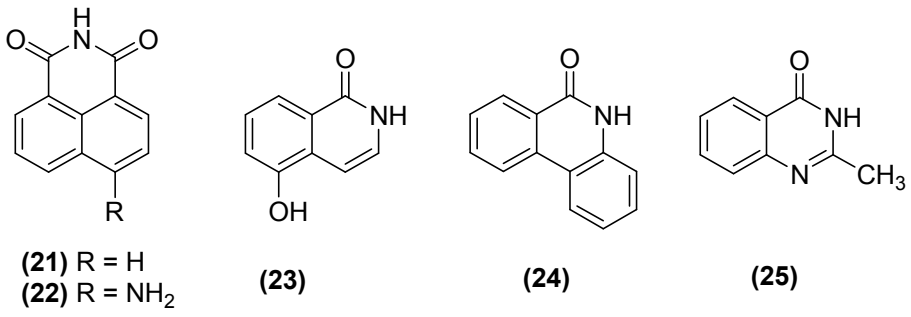

Figure 7: Potent polyaromatic heterocyclic inhibitors according to Banasik's study.[117]

On the basis of the above structural requirements Griffin *et al*[29] proposed a hypothesis for the interaction of inhibitors with the enzyme active-site. According to this hypothesis:

- Benzamides occupy the nicotinamide binding site of PARP-1, with the 3-substituent accommodated within the ribose nucleoside-binding domain. In contrast to the substrate NAD^+, inhibitors were incapable of undergoing C-N bond cleavage and instead serve as competitive inhibitors.
- The orientation and electronic properties of the carboxamide group were important factors in the binding of inhibitors.
- Molecular orbital calculations of benzamide derivatives indicated that the ability of the carbonyl oxygen to donate π electrons correlates positively with inhibitory activity. Hence the carbonyl substituent should be a good hydrogen-bond donor to a putative amino acid acceptor within the NAD^+-binding domain.
- Conjugation to an electron-rich aromatic ring improves the donor properties of the carbonyl group.
- The fact that PARP-1 inhibition is good in compounds with an unsubstituted carboxamide in the benzamide series explored the possibility of important hydrogen-bond interactions this group can have with amino acid donor in the enzyme active site.

The preferred conformation of the carboxamide group of NAD^+ within the active site of the enzyme also has important implications for inhibitor design. *Ab initio* energy calculations performed on the nicotinamide ring of NAD^+ indicate that when enzyme bound the cofactor adopts the *anti*-orientation *(i.e.* carbonyl *anti* to the 1,2-bond of the ring).

Suto *et al* designed a series of rigid benzamide analogues, the 5-substituted dihydroisoquinolin-1-ones and isoquinolin-1-ones, by closing the amide nitrogen upon the benzene ring with an ethane bridge to constrain the orientation of the carboxamide group into either the *anti-* or *syn-confor*mation.[118] This was achieved *via* two strategies. The first was cyclising an open benzamide structure which gave two compounds, depending on the direction of closure: 1) 7-substituted 3,4-dihydroisoquinolin-1-ones and 2) 5-substituted 3,4-dihydroisoquinolin-1-ones. The second approach involved inserting substituents at the 2-position of 3-hydroxybenzamides, providing a series of 2,3-disubstituted benzamides. The 5-substituted 3,4-dihydroisoquinolin-1-ones **(25a-d)**, where the carboxamide is in the biologically-active *anti*-orientation, were 50-to 75-fold more potent than the 7-substituted *syn*-analogues **(26a-d)**. The positioning of the

substituents on the benzene ring was also found to be critical for optimal activity. When the substituent in 5-substituted 3,4-dihydroisoquinolin-1-ones was moved to the -6, -7 or -8 position (which corresponds to position 4, 5 and 6 of benzamides respectively), activity was decreased. It was believed that substituents at the 5-position (or 3-position of benzamides) were accommodated within the ribose-nucleoside binding domain. In contrast to the substrate NAD^+, these compounds are incapable of undergoing C-N bond cleavage, thus serving as competitive inhibitors.

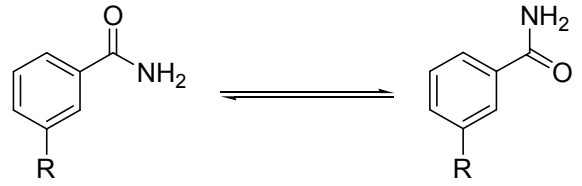

Active *anti*-conformation Inactive *syn*-conformation

Figure 8. Schematic representation of the *anti*- or *syn*- conformation of the carboxamide group.

Dihydroisoquinolinone derivatives **2,3-Disubstituted benzamides**

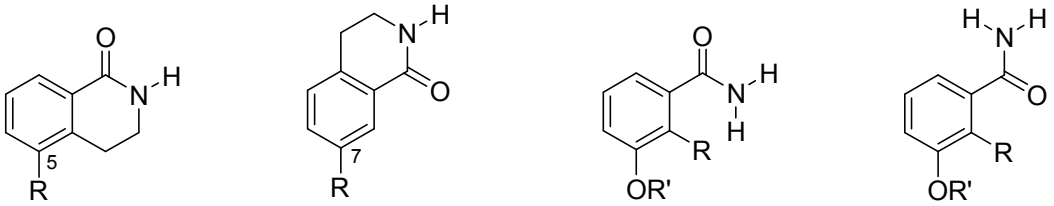

'anti' **(25)** *'syn'* **(26)** *'anti'* **(27)** *'syn'* **(28)**

R = H, Me, Et, propyl
R^1 = H or Me

Code	R	IC_{50} (μM)
25a	NO_2	3.2
26a	NO_2	13
25b	OMe	0.42
26b	OMe	120
25c	NH_2	0.41
26c	NH_2	8.0
25d	OH	0.10
26d	OH	9.5

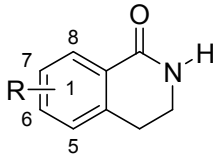

R	IC_{50} (μM)
5-OH **(25d)**	0.10
6-OH	2.0
7-OH	9.5
8-OH	11
5-OMe **(25b)**	0.42
6-OMe	39
7-OMe	120

Table 2. PARP-1 inhibitory activity of conformationally restricted dihydroisoquinolinones and benzamide PARP-1 inhibitors.[29,118]

Interestingly, the 2,3-disubstituted benzamide analogues were almost completely devoid of activity except for 3-hydroxy-2-methylbenzamide which has only very weak activity (IC_{50} 590 μM). Energy calculations revealed that the presence of a 2-substituent restricts the rotation of the amides, causing them to exist predominantly in the less hindered, inactive *syn*-conformation.

Structures of representative classes of PARP-1 inhibitors derived from the classical PARP scaffolds (benzamide or cyclic lactams) have the benzamide pharmacophore in all core structures (Figure 8). This constrained arylamide motif was identified as a consensus pharmacophore. In this amide the N-H is held *cis* to the amide carbonyl either by incorporation into a covalent five-membered ring (isoindolones), in covalent six-membered rings (isoquinolin-1-ones, 3,4-dihydro-isoquinolin-1-ones, quinazolin-4-ones, phthalazin-1-ones, thienoisoquinolinones, phenanthridinones, and naphthalimides) and covalent seven-membered rings (tricyclic inhibitors of the Newcastle group). Intramolecular hydrogen bonds have also been used by this group to maintain the required planar benzamide conformation in their potent benzoxazole-4-carboxamides and benzimidazole-4-carboxamides.[119] General understanding of the SARs of these benzamide pharmacophore-based PARP inhibitors has led to the synthesis of highly potent novel inhibitors.

From the above referenced studies, it became apparent that the following features are essential for the competitive inhibition of PARP-1. (Figure 9)

1. An unsubstituted aromatic or polyaromatic ring system
2. A carboxamide group restricted into the *anti*-conformation
3. At least one proton on the amide nitrogen.
4. A non-cleavable bond in the 3-position relative to the carboxamide group.

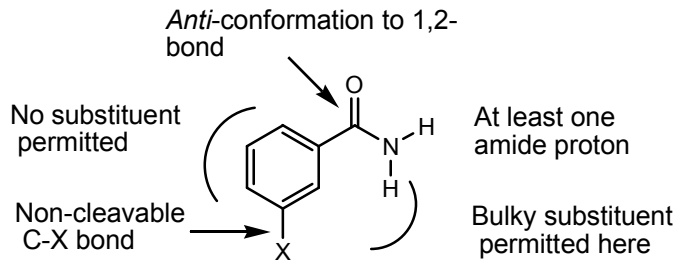

Figure 9. The consensus pharmacophore for PARP-1 inhibition.

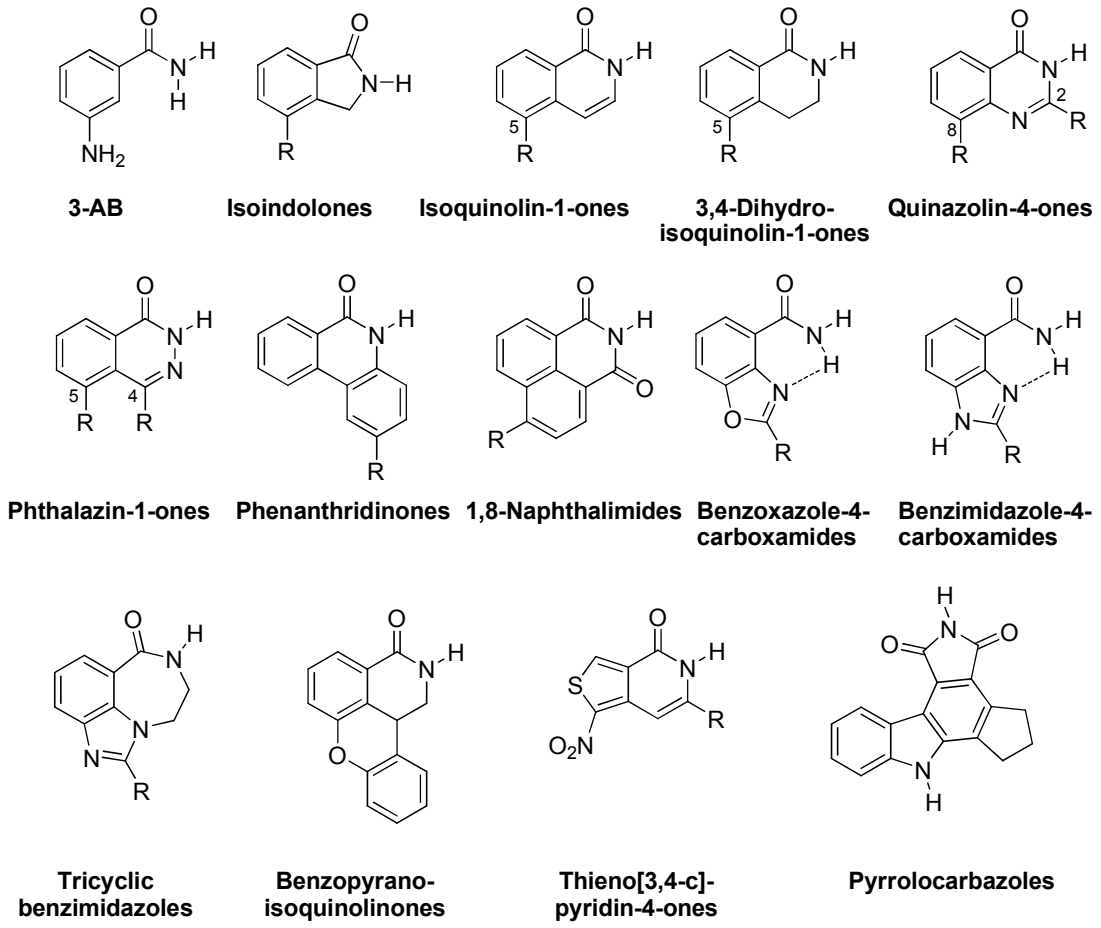

Figure 10. Structures of examples of potent inhibitors of PARP activity.

1.7.3 PARP-1 enzyme inhibitor interaction studies

X-ray crystallographic structures of the catalytic fragment of chicken PARP-1 and those crystallised with competitive inhibitors, such as PD128763 **(25e)**, NU1025 **(41d)**, 3-methoxybenzamide **(7)** and 4-amino-1,8-naphthalimide **(22)** have helped to confirm the above SAR scheme.[14,120] Costantino *et al* have discussed the modelling of PARP-1 inhibitors bound to the enzyme and the consequent SARs.[121] It was found that, in all the above PARP-1-inhibitor crystal structures, the position of binding is similar *i.e.* in the nicotinamide sub-site of the NAD^+-binding domain of PARP-1. Analysis of the co-crystal structure for PD128763 (Figure 11) showed that the carboxamide group invariably forms three important hydrogen bonds. The carbonyl oxygen of the inhibitor accepts two hydrogen bonds, one from the side-chain OH of Ser904, the other from Gly863 polypeptide amide NH. The third hydrogen bond is formed between the carboxamide NH and Gly863 carbonyl oxygen. The carboxamide must be in an *anti* conformation in order for these interactions to occur with the active site. This supports the fact that compounds, in which the amide is constrained in this conformation, are

significantly more potent than those with a free amide group. The presence of a planar electron-rich aromatic ring is needed to enhance the ability of the carbonyl group to participate in hydrogen bonding within the active site. The aromatic ring presumably interacts through π-π interactions with Tyr907 and, to some degree, Tyr896, which lines the other face of the pocket and provides further binding energy forming a "π-electron sandwich". This contributes to the increased potency for the larger, planar fused ring molecule.

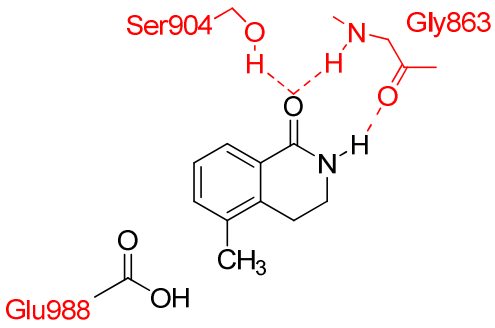

Figure 11. Enzyme-inhibitor (conserved) interactions between PARP-1 catalytic fragment and PD128763 **(25e)**[14]

'Non-conserved interactions' are strictly dependent on the structural diversity of docked inhibitors. For instance, the carboxylate group of Glu-988 is at a distance of only 4 Å to the C9 atom of PD128763 **(25e)** that is structurally equivalent to the anomeric C1N atom of the nicotinamide ribose of NAD^{+}[14]. At this location, Glu-988 could either function as a general base activating the acceptor protein for nucleophilic attack at the C-1 of the nicotinamide ribose or by stabilising the intermediate oxocarbenium ion formed from the cleavage of the ribose-nicotinamide bond of NAD^{+}. DPQ **(25f)** forms a salt-bridge interaction with Asp766, the amino group of 4-amino-1,8-naphthalimide **(22)** forms additional hydrogen bonds with Glu988, and the nitro group of 8-methyl-2-(4-nitrophenyl)quinazolin-4-one **(42i)** forms hydrogen bonds with the side chain of Asn767.[121]

In some cases, inhibitors induce structural changes to the active site of human PARP-1. Fujisawa published the crystal structure of the catalytic domain of human recombinant PARP-1 complexed with the inhibitor FR257517 **(43e)**.[122] The quinazolinone part of the compound binds tightly to the nicotinamide–ribose binding site. The hydrophobic 4-fluorophenyl ring of the inhibitor induces a significant conformational change in the active site of PARP-1 by displacing the side chain of Arg878, which forms the bottom of the active site. X-ray crystallography and molecular modelling results for the quinazolinedione-based PARP-1 inhibitor **(44)**[123] also showed

that the nitrogen atom of the tetrahydropyridine ring directly binds to the COOH of Asp766 and, similar to FR257517, the tetrahydropyridine moiety of this compound induces a conformational change. The terminal phenyl ring lies in a deep pocket and interacts *via* van der Waals interactions with the protein.

Modelling studies of 5-AIQ docked into the nicotinamide-binding site of PARP-1 (chicken) also showed putative water-mediated hydrogen-bond interactions between Glu988 of the active site and the amino group similar to 4-amino-1,8-naphthalimide **(22)** (Figure 12).

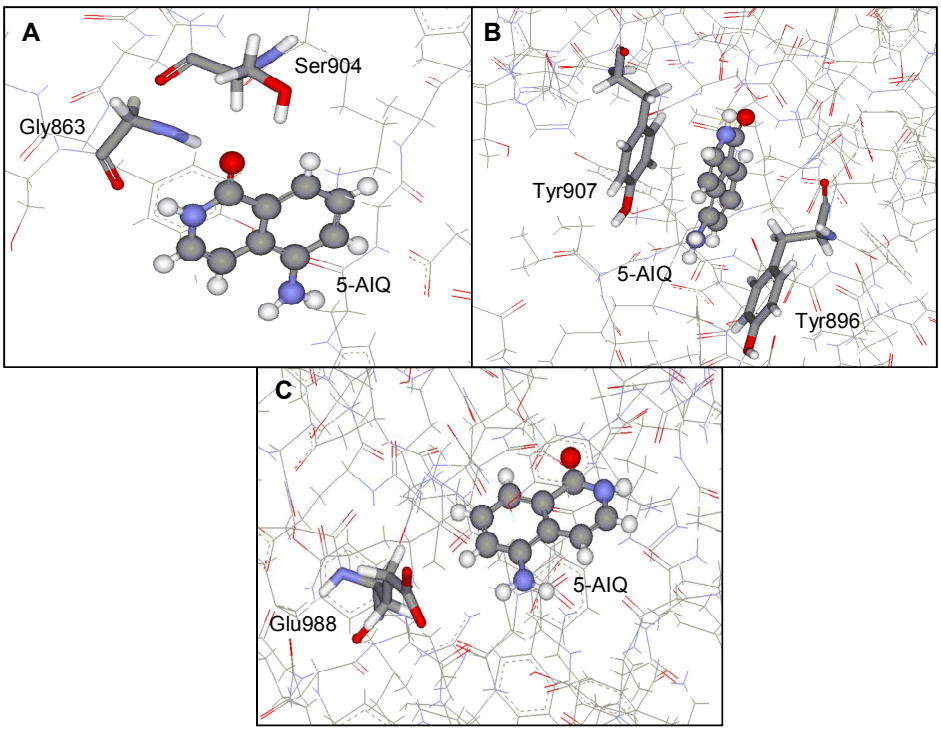

Figure 12. Molecular modelling study of 5-AIQ docked into PARP-1 binding site. A: View showing hydrogen bonds from secondary amide to Gly863 and Ser904. B: View showing the π-electron sandwich with 5-AIQ between Tyr896 and Tyr907. C: View showing proximity of 5-NH_2 group of 5-AIQ to the Glu988 carboxylate.

1.7.4 New PARP-1 inhibitors

During the past decade, structure-based drug design and an increased understanding of the molecular details of the active site of PARP-1 have facilitated the discovery of highly potent new PARP inhibitors.

1.7.4.1 Dihydroisoquinolinones and isoquinolinones

On the basis of Suto's studies, numerous structural modifications have been made to the parent dihydroisoquinolinone and isoquinolinone, giving rise to a great number of highly potent and selective PARP-1 inhibitors. 5-hydroxy-3,4-dihydroisoquinolin-1-one (**25d**) was shown to be a potent neuroprotective agent against NMDA-NO mediated neurotoxicity in brain cortical cultures.[124]

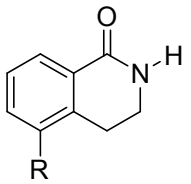

(25)

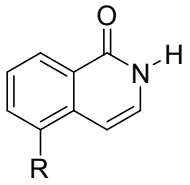

(29)

Code	R	IC_{50} (μM)
25(d)	OH	0.10
25(e) (PD128763)	Me	0.14
25(f) (DPQ)	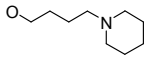	0.04

Code	R	IC_{50} (μM)
29(a)	H	6.2
29(b)	NO_2	3.2
29(c)	OMe	0.58
29(d) (5-AIQ)	NH_2	0.24
29(e) ISQ	OH	0.14

Table 3. PARP-1 inhibitory activity of various 5-substituted dihydroisoquinolinones and isoquinolinones.[118]

PD128763 (3,4-dihydro-5-methyl-1(*2H*)-isoquinolinone, **(25e)** as a chemopotentiating agent, sensitises cells to ionising radiation and reduces DNA repair.[125] PD128763 was found to be 60-fold more potent a PARP-1 inhibitor than 3-AB. DPQ **(25f)** (3,4-dihydro-5-(4-(1-piperidinyl)butoxyl)-1(*2H*)-isoquinolinone) patented by Guilford Pharmaceuticals, has been shown to exert neuroprotective effects in cultured cells *in vitro* and stroke models *in vivo*. It was believed that the structurally flexible butoxypiperidine side chain at the 5-position of DPQ favours its insertion into the

hydrophobic pocket within the active site, thereby increasing its potency tremendously. The effectiveness of 5-substituted isoquinolinones was comparable to that of the corresponding 3,4-dihydro series. 5-Hydroxyisoquinolin-1-one **(ISQ**, **29e)** was found to exert PARP inhibitory and cardioprotective effects in ischemic reperfused heart preparations *in vitro*.[70] 5-AIQ **(29d)** was found to exhibit tremendous therapeutic benefits in a wide range of disease models *in vivo*, including animal models of myocardial infarction, ischaemia-reperfusion of the liver and kidney and acute lung inflammation.[73,80,81,82,86,92,95,96]

1.7.4.2 Isoquinolin-1-one-related compounds

The isoquinolin-1-one core is also present in various tricyclic compounds. 1,8-Naphthalimide **(21)** (IC_{50} = 1.4μM) exerts protective effects in oxidatively stressed endothelial cells *in vitro*. The 4-amino derivative **(22)** (IC_{50} = 0.18μM) has been found to reduce ischaemia-reperfusion injury in the heart, liver and skeletal muscle.[70] It also exerts radio- and chemo-sensitising effects *in vitro*. The benzopyrano(4,3,2-*de*)isoquinolinones are a related class of tetracyclic lactams of which GPI-6150 **(30)** (1,11b-dihydro-(2H)benzopyrano(4,3,2-*de*)isoquinolin-3-one) has been studied intensively. GPI-6150 is cytoprotective *in vitro* and exerts significant protective effects in experimental models of stroke, traumatic brain injury, neurodegeneration, circulatory shock, diabetes mellitus and various inflammatory conditions (including colitis and gouty arthritis).[79,126]

6(*5H*)-Phenanthridinone **(24)** was first identified as a potent PARP inhibitor *in vitro* by Banasik *et al.*[118] This compound, insoluble in water and commonly dissolved in DMSO, enhances the cytotoxicity of nitrogen mustards and ionising radiation on lymphoma cells in culture. Substituents at the 2- or 3- and 8- positions of the core skeleton were preferred attachment points for good PARP-1 inhibition. By incorporation of suitable acidic or basic residues onto the ring system, water solubility and improvements of potency *in vitro* were observed. Compound **(24e)** was found to have 52-fold greater inhibition activity as compared to **(24)** (Table 4). The electron-withdrawing 2-nitro compound **(24b)** and electron-donating 2-amino **(24c)** and 2,3-diamino **(24g)** compounds showed values of IC_{50} at *ca.* 0.17 μM and about 3-fold better than **(24)**.[127] The phenanthridinone derivative PJ-34 **(24h)** is cytoprotective *in vitro* and suppresses pro-inflammatory cytokine and chemokine production in immunostimulated macrophages.[128] In *in vivo* models, PJ-34 improves the functional outcome in stroke, myocardial infarction and reperfusion injury, circulatory shock, diabetes and its vascular

complications, colitis, arthritis and uveitis. PJ-34 also protects in chronic heart failure and improves the endothelium dependent vascular relaxant function in various disease models.[60,76,94,109,]

Phenanthridinones (24)

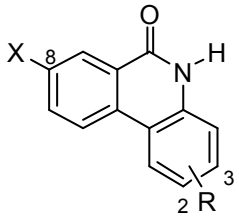

Code	X	R	IC_{50}(μM)
24	H	H	0.52
24(a)	H	3-COOMe	0.18
24(b)	H	2-NO_2	0.15
24(c)	H	2-NH_2	0.18
24(d)	F	3-COOMe	0.04
24(e)	F	3-SO_3H	0.01
24(f)	Cl	3-Cl	0.24
24(g)	H	2- NH_2 & 3-NH_2	0.18
24(h) (PJ34)	H	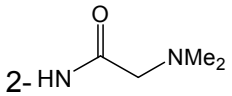	0.04

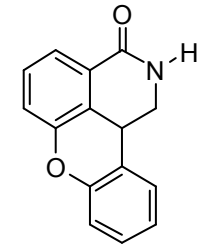

(30)

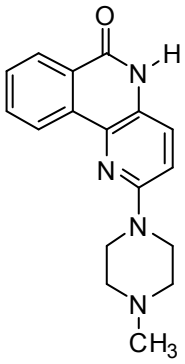

(31)

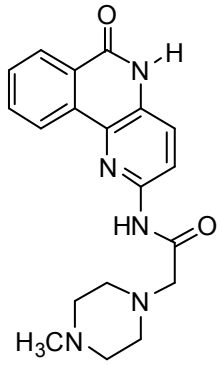

(32)

Thieno(2,3-c)isoquinolin-1-ones (33)

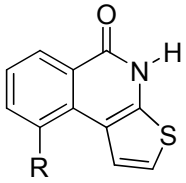

Thieno[3,4-c]pyridin-4(*5H*)-ones (34)

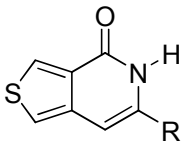

Code	R	IC_{50}(μM)
33(a)	H	0.30
33(b)	OMe	0.30
33(c)	OH	0.10
33(d)	NH_2	0.05
34(a)	Me	9.7
34(b)	Ph	9.9

Table 4. PARP-1 inhibitory activity of isoquinolin-1-one-related compounds.

Guilford reported a new series of compounds that contain aza-5(H)-phenanthridin-6-one and partially saturated aza-5(H)phenanthridin 6-one scaffolds.[129,130] Two such compounds **(31)** and **(32)** were evaluated in the transient and permanent stroke models

and provided a 30–40% reduction in infarct volume. SmithKline Beecham reported thieno(2,3-c)isoquinolin-1-ones **(33)**, in which the thieno ring is fused to the isoquinolinone scaffold, the most potent being (**33d)**. (**33a)** was neuroprotective in models of brain ischaemia.[131,132] Shinkwin *et al*[116] reported the synthesis of thienopyridinones **(34)** inhibiting PARP-1 activity at *ca*.10 μM.

1.7.4.3 Benzoxazoles and benzimidazoles

Researchers at the University of Newcastle-upon-Tyne designed a series of benzoxazole-4-carboxamides[119] **(35)** and benzimidazole-4-carboxamides[133] **(36)** that elegantly favoured the active *anti*-conformation by means of an intramolecular hydrogen bond between the amide proton and the cyclic nitrogen. The benzimidazole analogues are a few times more potent than the corresponding benzoxazoles. These compounds exhibit potencies superior to those usually shown by monocyclic carboxamides. Compounds with substituted phenyl groups at the 2-position, such as **(37b)**, **(37d)** and **(37g)** are the most potent examples in these classes of inhibitors. NU1085 **(37d)** has been adopted as a benchmark inhibitor of PARP-1 due to its potency and good solubility in water. It increased the potency of the cytotoxic agents topotecan and temozolomide by up to 3-fold.[133]

Benzoxazole-4-carboxamides (35)

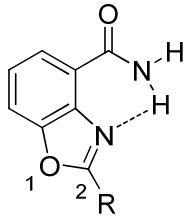

Benzimidazole-4-carboxamides (36)

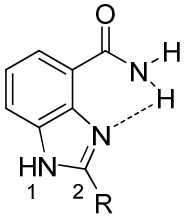

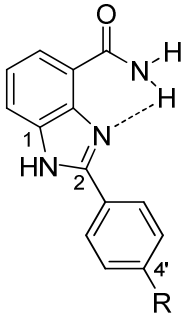

(37)

Code	R	IC_{50} (μM)
35(a)	Me	9.5
35(b)	Ph	2.1

Code	R	K_i (nM)	Code	R	K_i (nM)
36(a)	H	95	**37(c)**	NO_2	8
36(b) [NU1064]	Me	99	**37(d) [NU1085]**	OH	6
36(c)	Ph	15	**37(e)**	CN	4
37(a)	OMe	6.8	**37(f)**	Cl	3
37(b)	CF_3	1.2	**37(g)**	CH_2OH	1.6

Table 5. PARP-1 inhibitory activity of benzoxazole-4-carboxamides and benzimidazole-4-carboxamides.

1.7.4.4 Benzimidazole-related compounds

A natural extension of the benzimidazole class of compounds is to replace the hydrogen bond that encourages the molecule to adopt the *anti*-conformation with a covalent bond. Skalitzky *et al*[134] synthesised a series of tricyclic benzimidazoles **(38)** of which **(38b)**, **(38f)** and **(38g)** were found to be strong potentiators of the cytotoxic activities of temozolomide and topotecan. AG14361 **(38f)** increased the delay of LoVo xenograft growth induced by irinotecan, irradiation or temozolomide by two- to three fold. A combination of AG14361 and temozolomide caused the complete regression of SW620 xenograft tumours.[46] A potent new class of tricyclic lactam indole PARP-1 inhibitors have been designed, represented by **(39)** and **(40)**. Compounds **(40a)**, (**40c)** and **(40d)** displays potent *in vitro* PARP-1 enzymatic inhibition and enhancement of cellular growth inhibition.[135]

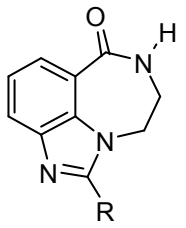

(38)

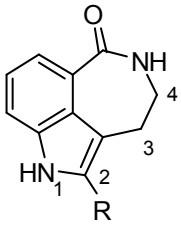

(39)

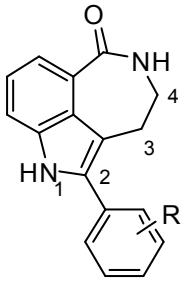

(40)

Code	R	K_i (nM)
(a)	Ph	4.1
(b)	4-Cl-Ph	5.7
(c)	2-Cl-Ph	7.7
(d)	1-naphthyl	4.9
(e)	4-PhCH_2OH	4.2
(f) AG14361	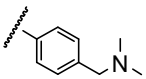	6.3
(g)	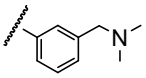	5.8

Code	R	K_i (nM)
39(a)	H	38
(b)	CN	11
(c)	1-naphthyl	5
40(a)	H	6
(b)	4-CF_3	5
(c)	4-CH_2NMe_2	5
(d)	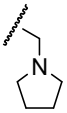	6

Table 6. PARP-1 inhibitory activity of benzimidazole-related compounds.

1.7.4.5 Quinazolin-4-ones

During initial synthetic studies with benzoxazole-4-carboxamides, an unexpected rearrangement occurred to afford the 8-hydroxyquinazolin-4(3*H*)-one NU1025 **(41d)**.[119] A series of 2-alkyl- and 2-aryl substituted 8-hydroxy-, 8-methyl -, and 8-methoxy quinazolin-4(3*H*)-ones were synthesized and evaluated for PARP inhibitory activity.[136] 2-Phenylquinazolinones **(42)** were marginally less potent than the corresponding 2-methylquinazolinones **(41)**, but the introduction of an electron-withdrawing or electron-donating 4-substituent on the 2-aryl ring invariably increased potency. The 8-methylquinazolinone series (IC_{50} values 0.13-0.27 μM), were found to be the most potent PARP-1 inhibitors. NU1025 **(41d)** potentiated the cytotoxicity of the monomethylating agent 5-(3-methyltriazen-1-yl)imidazole-4-carboxamide (MTIC) and of γ-radiation 3.5-and 1.4-fold, respectively.[136]

Fujisawa synthesised several highly potent quinazolin-4(*3H*)-one derivatives **(43)** that are modified at the 2,5- and 2,8-positions.[137,138] Compound **(43b)** FR247304 exerts its neuroprotective efficacy in *in vitro* and *in vivo* experimental models of cerebral ischaemia *via* potent PARP-1 inhibition.[139] The 2,8-disubstituted derivative **(43d)** has a three-methylene unit and 4-(4-fluorophenyl)tetrahydropyridine substitution at the quinazolinone-2-position. This compound shows strong PARP-1 inhibition and *in vivo* neuroprotective activity. In a mouse model of Parkinson's disease, this compound prevented the depletion of striatal dopamine and metabolites of dihydroxyphenylacetic acid and homovanillic acid.

Quinazolinedione-based PARP inhibitor **(44)** linked with large substitution exhibits strong potency against PARP-1 with an IC_{50} of 60 nM.[137] Quinoxaline derivatives **(45)** were identified as potent and selective PARP-2 inhibitors in PARP enzyme assays using recombinant PARP-1 and PARP-2.[137] Compound **(45b) (FR261529)** (2-(4-chlorophenyl)-5- quinoxalinecarboxamide) was about 5-fold more potent for PARP-2 (IC_{50} = 7 nM) than PARP-1 (IC_{50} = 33 nM) and protects against both ROS-induced cell injury *in vitro* and METH-induced dopaminergic neuronal damage in an *in vivo* Parkinson's disease (PD) model.[140]

Quinazolin-4-ones (41)

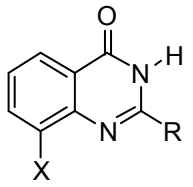

Code	X	R	IC_{50} (μM)
41(a)	H	H	9.50
(b)	OMe	Me	0.78
(c)	Me	Me	0.39
(d) [NU1025]	OH	Me	0.40

2-Phenyl substituted quinazolin-4-ones (42)

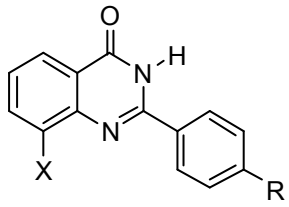

Code	X	R	IC_{50} (μM)
42(a)	OH	H	1.06
(b)	OH	NO_2	0.23
(c)	OH	OH	0.29
(d)	OH	NH_2	0.52
(e)	Me	H	0.87
(f)	Me	OH	0.22
(g)	Me	NH_2	0.44
(h)	Me	CN	0.27
(i)	Me	NO_2	0.13
(j)	Me	OMe	0.19
(k)	OMe	H	4.2
(l)	OMe	OMe	2.0
(m)	OMe	NO_2	0.85

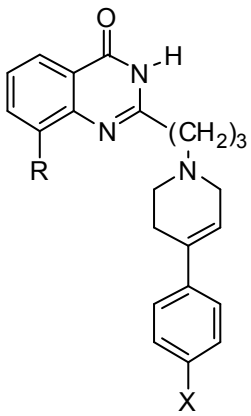

(43)

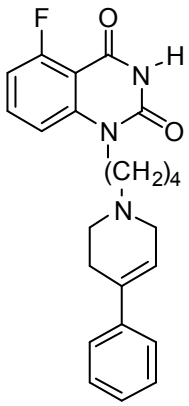

(44)

Code	R	X	IC_{50} (nM)
43(a)	H	H	21
(b)	Cl **FR247304**	H	23
(c)	Cl	CN	3
(d)	Cl	F	13
(e)	Me **FR257517**	F	16

Quinoxalines (45)

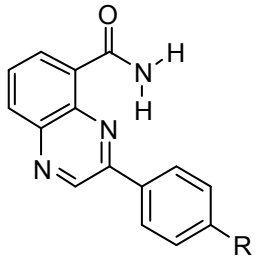

Code	R	PARP-1 IC_{50}(nM)	PARP-2 IC_{50}(nM)
45(a)	H	131	14
(b)	Cl **FR261529**	33	7
(c)	CN	101	8
(d)	CF_3	118	11
(e)	OMe	71	8
(f)	NH_2	87	9

Table 7. PARP-1 inhibitory activity of quinazolin-4-ones and quinoxalines.

1.7.4.6 Quinazolinone-related compounds

Iconix claimed that **(46a)** showed selectivity for PARP-1 over PARP-2 with IC_{50} values of 5.5 and 41 μM, respectively. Of the thieno(3,4-d)pyrimidin-4(3)ones, **(47a)** and **(47b)** give 81% and 42% inhibition of PARP-1 (mouse) at a concentration of 10.8 and 8.8 μM respectively.[116] Meiji Seika Kaisha reported the neuroprotective effects of DR2313 **(48)** in *in vivo* models of permanent and transient stroke in rats.[141] DR2313 also showed excellent profiles in terms of water-solubility and CNS penetration. Pyrimidinones fused to a saturated heterocycle with additional keto group **(49)** were also reported.[142] Uracil derivatives iodouracil **(50a)** and iodouridine **(50b)** reported by Banasik *et al*[117] have weak inhibitory effects on PARP-1.

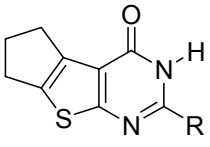

(46)

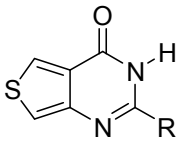

(47)

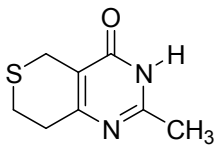

(48)

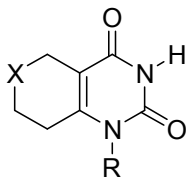

(49)

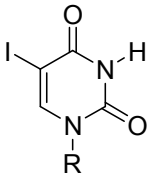

(50)

Code	R	IC_{50}(μM)
46(a)	H	5.5
47(a)	Me	10.8
47(b)	Ph	8.8
50(a)	H	70
50(b)	ribofuran	43

Table 8. PARP-1 inhibitory activity of quinazolinone-related compounds.

1.7.4.7 Phthalazinones

KuDOS Pharmaceuticals, in collaboration with Maybridge, have identified a series of 4-aryl-2*H*-phthalazinones as sub-micromolar PARP-1 inhibitors.[143] Early SAR studies, suggested that structural elaboration around the *meta* position of the benzyl moiety could be potency enhancing. The enhancement of potency *via* the fluoro substituent *ortho* to the imide ring appeared quite general for this series as exemplified by compounds **51e-g**. The substituted homopiperazine based amides **(51i)** were found to be most promising lead compounds.[144] Further introduction of fluorine at the *para* position of the pendant benzene ring, aiming to block possible metabolism at this

position and extend half-life, resulted in a class of potent inhibitors with excellent cellular activity as indicated by **(52e-j)**.

Kamanaka *et al* reported the neuroprotective effects of the phthalazinone-based PARP inhibitor ONO-1924H **(53)**. In a rat stroke model, ONO-1924H reduced the stroke volume and attenuated the development of neurological deficits. Structurally, ONO-1924H is a 2*H*-phthalazin-1-one substituted in the 4-position with phenyl groups, and bearing amine-containing side chains to improve water solubility.[145] Further variations include a series of tetracyclic benzopyrano(4,3,2-*de*)phthalazinones **(54)** and indeno(1,2,3-*de*) phthalazinones **(55).** Here the 4-phenyl group is held rigid by linking to the 5-position either *via* an oxygen or directly.

1.7.4.8 Isoindolinones

Isoindolinones are another class of PARP-1 inhibitors, which incorporate the requisite lactam in a 5-membered ring. The simple 5-substituted derivatives **(56)** have only poor potency (IC_{50} > 10 μM) but more elaborate side-chains improve activity. Guilford claimed the tetracyclic isoindolinones **(57)** for use in peripheral neuropathy caused by stroke trauma, spinal cord damage, ischaemia, reperfusion injury and neurodegeneration.[142] Novartis patented a series of substituted derivatives of indoloquinazolinones as PARP inhibitors. The tetrazole-substituted compound **(58)** has an *in vitro* IC_{50} value of 12 nM and dose-dependently reduced infarct size by up to 60% in a rabbit myocardial infarction model.[48] A series of novel pyrrolocarbazoles was synthesized as potential PARP-1 inhibitors. When an additional keto group is adjacent to the ring nitrogen to give the imide, the potency is enhanced. Pyrrolocarbazole **(59c)** was identified as a potent PARP-1 inhibitor.[146,147] Cephalon evaluated the chemo-potentiating capacity of CEP-6800 **(59d)**, the novel 3-aminomethyl carbazole imide, in combination with three chemotherapeutic agents (temozolomide, irinotecan and cisplatin) against U251MG, glioblastoma, HT29 colon carcinoma, and Calu-6 non-small cell lung carcinoma xenografts and cell lines. This is an inhibitor of both PARP-1 and PARP-2, and has an inhibition constant (K_i) of 5 nM.[148] Compound **(60)** was reported to have an IC_{50} of 2 nM.

Phthalazinones (51)

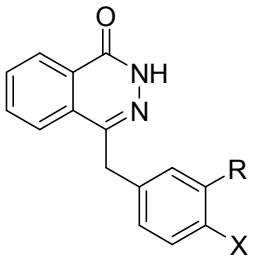

Code	R	X	IC_{50} (nM)
51(a)	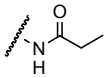	H	20
(b)	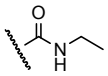	H	50
(c)	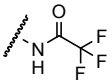	H	13
(d)		H	13
(e)		F	5
(f)	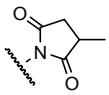	F	3.8
(g)	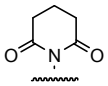	F	4.1
(h)	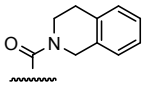	H	8
(i)	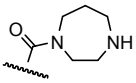	H	9

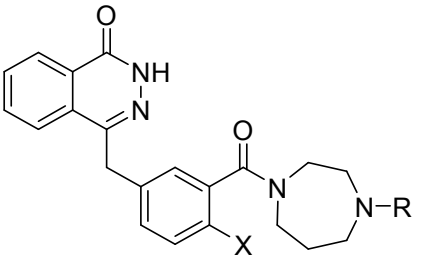

(52)

Code	R	X	IC_{50} (nM)
52(a)	Me	H	23
(b)	Et	H	15
(c)	nPr	H	10
(d)		H	6
(e)	H	F	7
(f)	Me	F	9
(g)	Et	F	7
(h)	nPr	F	5
(i)		F	5
(j)		F	5

Code	R	IC_{50} (nM)
54(a)	H	80
54(b)	NHCOMe	37
55(a)	H	140
55(b)	NHCOMe	69

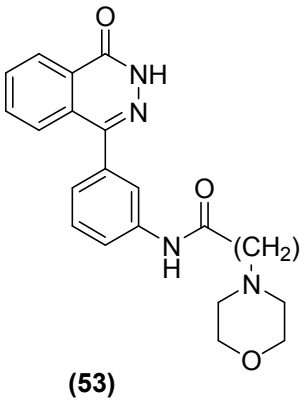

(53)

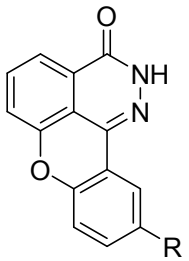

(54)

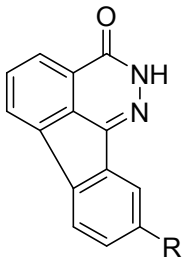

(55)

Table 9. PARP-1 inhibitory activity of phthalazinones.

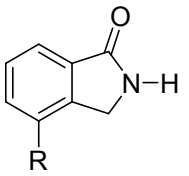

(56)

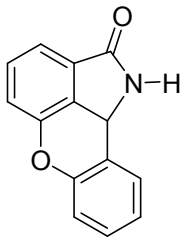

(57)

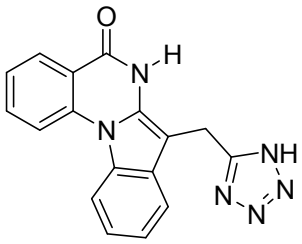

(58)

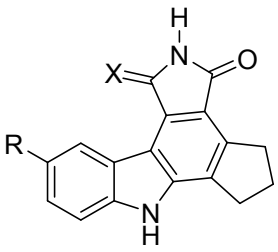

(59)

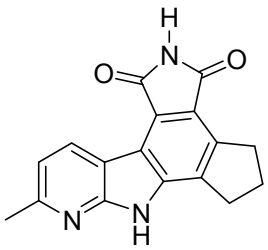

(60)

Code	X	R	IC_{50} (nM)
59(a)	H	H	56
(b)	H	CN	18
(c)	O	H	36
(d) CEP-6800	O	CH_2NH_2	5

Table 10. PARP-1 inhibitory activity of isoindolinones, indoloquinazolinones and pyrrolocarbazoles.

1.7.4.9 Miscellaneous classes of compounds

While much development has centered on the lactam/carboxamide pharmacophore, there are several groups of compounds that do not possess this functionality. Most of these are inhibitors of moderate potency compared to those discussed above and they have very different modes of action. For instance, 1,2-benzopyrone **(61a)** was reported as a non-competitive inhibitor of PARP and 6-nitrosobenzopyrone **(61b)** inhibits PARP by interacting with the DNA-binding Zn finger in the N-terminal domain of PARP.[149] 5-Iodo-6-amino-1,2-benzopyrone (INH2B) **(61c)** inhibits PARP-1 by uniquely oxidising one of its two zinc fingers, resulting in zinc ion ejection and a concomitant inactivation of its activity. It has been shown to protect oxidatively damaged cells *in vitro* and exert beneficial effects in stroke, circulatory shock and autoimmune diabetes.[149] Other examples include aryl carboxylic acids linked to a 4-*t*-butylbenzene-1,2-diol fragment **(62)** and coumalic acid derivatives **(63)**.[142]

The O-(3-piperidino-2-hydroxy-1-propyl)nicotinic amidoxime (BGP-15) **(64)** belongs to the class of unsaturated hydroximic acid derivatives which are claimed to be PARP-1 inhibitors, and protects the isolated heart from ischaemia–reperfusion injury, with an IC_{50} value of 120 μM.[61]

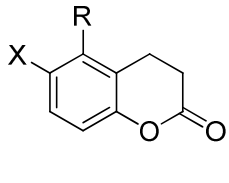

(61)

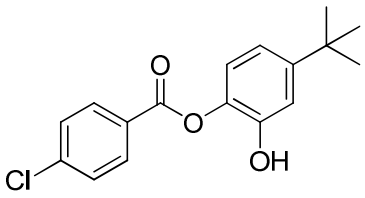

(62)

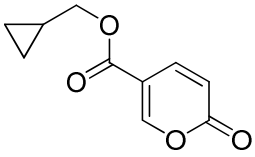

(63)

Code	X	R	IC_{50}(μM)
61(a)	H	H	-
(b)	NO	H	-
(c)	NH_2	I	10
62	-	-	2.2
63	-	-	<10

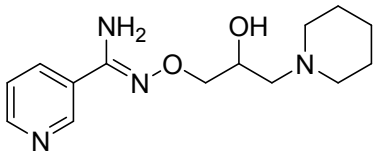

(64)

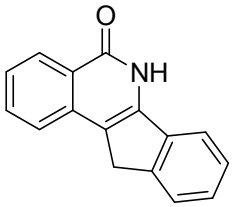

(65)

Table 11. PARP-1 inhibitory activity of miscellaneous classes of compounds.

Inotek has developed a series of PARP inhibitors derived from compound **(65)**. The potent parenteral inhibitor, INO-1001 has an *in vitro* IC_{50} value of 1 nM and protective effects in stroke, myocardial infarction and chronic heart failure. This drug is now in clinical trials for the treatment of reperfusion injury induced by myocardial infarction, cardiopulmonary bypass and thoraco-abdominal aortic aneurysm surgery.[48]

1.7.5 Bioreductive prodrugs of PARP-1 inhibitors

Tissue selectivity is important for PARP-1 inhibitors to sensitise cancer cells towards chemotherapy and radiotherapy. Since PARP-1 inhibitors lack selectivity for cancer cells, the DNA repair process for rapidly dividing normal cells exposed to cytotoxic agents will also be impaired along with those of the tumour cells. This limits the effectiveness of inhibitors and gives rise to severe side effects. Use of a prodrug, which, in itself, is biologically inactive but could be selectively unmasked or activated by the tissues on which it is intended to act, could improve selectivity. Such systems make use of biochemical or physiological differences between the normal and tumour cells such as bioreductive prodrugs. It was observed that many disease states where PARP-1 inhibition is therapeutically beneficial, such as cancer, inflammatory disorders and ischaemia-reperfusion injuries, are marked by acute or chronic tissue hypoxia. This physiological difference in the concentration of oxygen between normal and hypoxic tissues was exploited through the design of biologically inactive prodrug systems which, upon selective bioreduction in hypoxic tissue, would release PARP-1 inhibitors only in that tissue. Four different types of redox-sensitive triggers were designed and

the proposed mechanism for bioreductive release of PARP-1 inhibitors (DRUG) from nitroheterocyclylmethyl- and 4,7-dioxoindole-3-methyl- types are illustrated in schemes 2 and 3, respectively.[150-152]

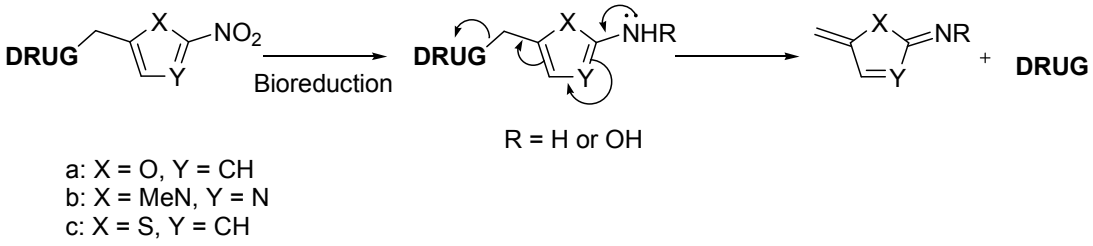

a: X = O, Y = CH
b: X = MeN, Y = N
c: X = S, Y = CH

Scheme 2. Demonstration of reductively triggered release of drugs from (a) 5-nitrofuran-2-ylmethyl, (b) 1-methyl-2-nitroimidazole-5-ylmethyl and (c) 5-nitrothien-2-ylmethoxy prodrugs.[150, 151]

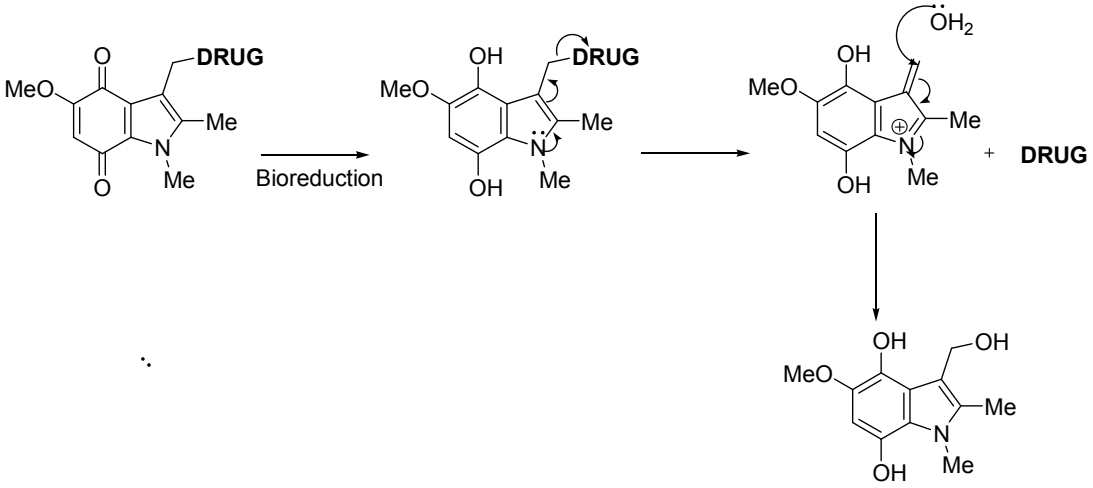

Scheme 3. Proposed mechanism of reductively triggered release of drugs from 4,7-dioxoindole-3-methyl prodrugs.[152]

The prodrug designed was made of a Trigger (a substrate for the endogenous or exogenous activating enzyme) and an Effector (the active drug to be released), joined by a Linker which releases the Effector in response to the Trigger.[153] 5-Iodo- and 5-bromoisoquinolin-1(2*H*)-one were chosen as the DRUG for linkage to the Triggers.[154] Since the PARP-1 inhibitory activity of isoquinolin-1(2*H*)-ones depends critically on the carboxamide group, masking of the pharmacophore was achieved either by attaching the Trigger at oxygen (giving 1-alkoxyisoquinolinones) or at nitrogen (giving 2-alkylisoquinolin-1-ones) as shown below.[155]

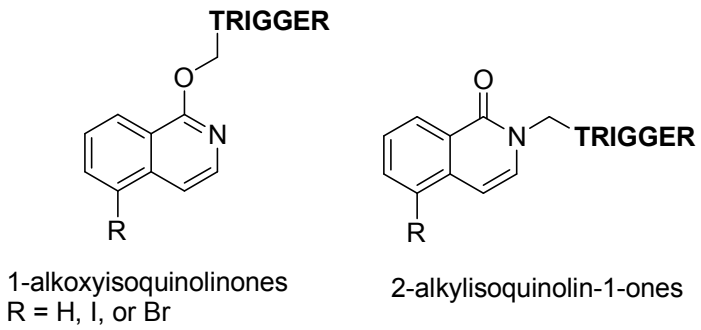

Figure 13. Representation of 1-alkoxyisoquinolinones and 2-alkylisoquinolin-1-ones triggers.

In each case, the release of the isoquinolin-1-one Effector was initiated by chemical reduction of the Trigger, designed to mimic bioreduction in hypoxic tissues. Their release studies, resulted in a successful expulsion of 5-substituted isoquinolin-1-ones from 1-(5-nitrothien-2-ylmethoxy)isoquinolines and 2-(5-nitrofuran-2-ylmethyl) isoquinolines upon reductive triggering with a sodium borohydride / palladium / aqueous propan-2-ol system. Isoquinolin-1-ones were also found to be rapidly and quantitatively released from their 2-(1-methyl-2-nitroimidazole-5-ylmethyl)- and 1-(4,7-dioxoindole-3-methoxy) derivatives by treatment with zinc / ammonium chloride and tin(II) chloride, respectively. It was also observed that reductively triggered release of the isoquinolin-1-ones only occurred from the O-linked prodrugs and not from N-linked ones.[152] Another successful prodrug 4-iodo-3-nitrobenzamide was selectively retained and reduced to highly reactive and tumouricidal nitroso-compound, INOBA, in the presence of nitroreductase activity in malignant cells.[156] In view of the preliminary success achieved *in vitro* with these prodrug systems, it is evident that use of tissue-selective prodrugs would reduce their potential toxicity on normal tissues and reduce the dosage required for therapy.

1.8 PARP Inhibitors in clinical trials

Five PARP inhibitors are currently known to be in oncology clinical trials and two more are expected to enter clinical trials shortly; their current status is summarized in Table 12.

AG-014699 was the first PARP inhibitor to be evaluated in humans for cancer therapy. Preclinical data of this agent indicated that the combination of AG-014699 with irinotecan and with radiotherapy delayed xenograft tumor growth, and caused xenograft tumour regression with temozolomide. The Phase 1 study combined i.v. AG014699 with temozolomide in solid tumors, initially evaluating PARP activity in

peripheral blood lymphocytes with reduced doses of temozolomide until PARP inhibition was observed, and then increasing temozolomide to standard doses (200 mg/m^2) at a fixed AG-014699 dose. The recommended dose for the Phase 2 trial was 12 mg/m^2 AG-014699 with 200 mg/m^2 temozolomide. In the Phase 2 trial, there was enhancement of temozolomide-related myelosuppression.

Product	Company	Clinical status	Indication
INO-1001	Inotek/Genentech	Phase 2 Phase 1b	Cardiovascular indications Malignant melanoma
AGO14699	Pfizer	Phase 2	Advanced solid tumours in combination with temozolomide Metastatic malignant melanoma
BS-201	BiPar Sciences	Phase 1	Cancer
BS-401	BiPar Sciences	Preclinical	Pancreatic cancer
AZD2281	AstraZeneca	Phase 1	Breast cancer
KU59436	AstraZeneca/KuDOS	Phase 2	Advanced solid tumors BRCA1/2 mutant cancers In combination with DSB agents in HRD tumours
MGI Pharma	n/a	Preclinical	Radiation/chemotherapy sensitizer
ABT-888	Abbott Laboratories	Preclinical	Refractory solid tumours and lymphoid malignancies

Table 12. PARP-1 inhibitors in cancer therapy.[157,33]

KU-0059436 is currently being evaluated in a Phase 1 trial in patients with advanced tumours. This study began with daily and twice a day dosing of the oral inhibitor for 14 days of a 21-day cycle, and is now evaluating continuous twice a day dosing. Minimal toxicity has been reported. Pharmacodynamic studies showed dose-dependent inhibition of PARP activity in peripheral blood mononuclear cells.

ABT-888 is an oral PARP inhibitor that is the first oncology agent to be studied in a Phase 0 clinical trial. In the Phase 0 study, participants with biopsiable tumour are given a single dose of ABT-888 to determine the dose range at which PARP is effectively inhibited in peripheral blood mononuclear cells and tumour cells. The study also aims to assess the pharmacokinetic characteristics of the agent and the time

course of PARP inhibition. Phase 1 combination studies will be with temozolomide, irinotecan, cyclophosphamide, and carboplatin.

BiPAR Science's lead compound BSI-201 is being tested as i.v. monotherapy in solid tumours, with the objective to determine a maximum tolerated dose and a pharmacokinetic profile. BiPAR also currently has another PARP inhibitor, BSI-401, in clinical oncology trials.

Inotek's INO-1001, an indenoisoquinolinone-based PARP inhibitor, is currently in Phase 2 trials for cardiovascular indications. It is also being studied in combination therapy in metastatic melanoma and glioma and as a single agent in cancer for BRCA1- and BRCA2-deficient tumours. A preliminary analysis of a Phase 1 trial evaluated INO-1001 in combination with temozolomide in unresectable stage III/IV melanoma. The investigators found that non-haematologic toxicities were mild and mostly related to temozolomide.

MGI Pharma is developing GPI-21016, an orally available inhibitor of PARP-1 with a K_i of 50 nmol/L. Interestingly, GP-21016 ameliorated cisplatin induced neuropathy at the same time that antitumour efficacy was enhanced.

AstraZeneca's AZD2281 was studied in a range of tumour types in Phase I studies. Results showed that treatment with AZD2281 led to inhibition of PARP functional activity in both surrogate and tumour tissue and they have reported that strong signals were detected in hereditary ovarian cancer.

1.9 Water-soluble PARP-1 inhibitors

Most of the PARP-1 inhibitors reported to date are structurally based on the benzamide planar ring system, and are poorly water soluble. As a result, many potent inhibitors such as 5-hydroxydihydroisoquinolin-1-one **(25d)**, DPQ **(25f)**, PND **(24),** GPI-6150 **(30)** and INH2B **(61c)** suffer from poor water-solubility and this gives rise to poor pharmaceutical properties. Good water-solubility is a highly desirable property since it causes faster dissolution of the drug and thus, better bioavailability. DMSO is often used in place of water as a biocompatible vehicle for *in vivo* administration. However, it is a potent scavenger of hydroxyl radicals, and thus is able to reduce the organ injury and dysfunction in situations where the production of hydroxyl radicals is observed, such as haemorrhagic and endotoxic shock.[158] In addition, it also inhibits PARP-1

activity weakly.[159] This causes a great amount of ambiguity in the determination of the actual PARP-1 inhibitory activity.

Our laboratory optimised a synthetic route for the known PARP-1 inhibitor 5-AIQ **(29d)** and then converted it to its highly water-soluble hydrochloride salt, 5-AIQHCl. (IC_{50} 0.24 μM).[86] Investigation of pharmacological effects of 5-AIQ in a wide range of diseases, including animal models of myocardial infarction,[73] ischaemia-reperfusion of the liver[80,81] and kidney,[82] heart transplantation[84] and acute lung inflammation[95] showed tremendous therapeutic potential. It also demonstrated protective effects on ischaemia-reperfusion injury caused by severe haemorrhage and resuscitation in anaesthetized rats by abolishing multiple organ injury and dysfunction.[86] Compared to the benchmark inhibitor 3-AB **(5)** (10 mg Kg^{-1} i.v.) only a remarkably low i.v. dose of 30 μg Kg^{-1} is required to confer similar protection. It is evident that 5-AIQ.HCl gains much of its advantage over other PARP-1 inhibitors through its excellent water-solubility, which conferred favourable pharmacokinetics, such as good absorption and biodistribution.

Following the success of 5-AIQ our laboratory decided to build upon this lead and synthesised a series of 3-substituted 5-aminoisoquinolin-1-ones. In general, besides having a very good water-solubility profile, most of the 3-substituted isoquinolin-1(2*H*)-ones exhibited excellent PARP-1 inhibitory potency with IC_{50} values in the low micromolar range (Table 13). It appeared that alkyl substituents confer slightly greater enhancement in PARP-1 inhibitory activities than an aryl moiety. This is especially evident with compounds 5-amino-3-methylisoquinolin-1-one **(66a)** and 5-amino-3-pentylisoquinolin-1-one **(66c)** which are about 5- and 3-fold, respectively, more potent than the 3-phenyl substituted compound **(67a)** making them among the most potent members in this series. The presence of a *para*-substituent in the phenyl ring seemed to increase the activity, with inductive electron-withdrawing functionalities, such as trifluoromethyl **(67d)** and chloro **(67e)**, appearing to confer slightly greater improvement in activity. It is also interesting to note that the introduction of a thiophene ring **(66e)** and a benzyl group **(66f)** at the 3-position resulted in a drastic loss of potency. 5-AIQ substituted, at the *N*5-position with an amidine group resulted in a 2.5-fold reduction in activity **(68) (**IC_{50} 4.04 μM).

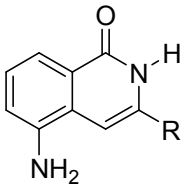

(66)

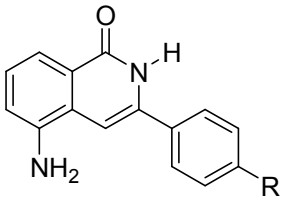

(67)

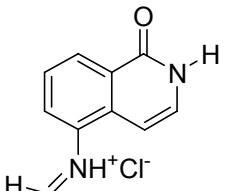

(68)

Code	R	IC_{50} (μM)
5-AIQ 29(d)	H	1.60
66(a)	Me	0.23
66(b)	Et	0.49
66(c)	Pentyl	0.32
66(d)	isobutyl	1.17
66(e)	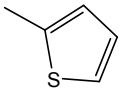	5.61
66(f)	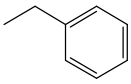	5.14

Code	R	IC_{50} (μM)
67(a)	H	1.07
67(b)	OMe	0.90
67(c)	Me	0.88
67(d)	CF_3	0.33
67(e)	Cl	0.57

Table 13. PARP-1 inhibitory activity of 3-substituted 5-aminoisoquinolin-1-ones.

The strategy of building upon 5-AIQ could potentially be extended to the synthesis of another class of potential PARP-1 inhibitors, the 4-substituted isoquinolin-1(2*H*)-ones, and 3- and 4-substituted 5-aminoisoquinolin-1(2*H*)-ones.

2. Aims and Objectives

2.1 Aim

The aim of this research is to design, synthesise and evaluate potent and water-soluble DNA-repair (PARP-1) inhibitors using currently established SAR.

2.2 Research proposal

Following the success of 5-AIQ.HCl **(29d)** with highly encouraging activity *in vivo*, enzyme selectivity and very good water solubility, our laboratory decided to build upon this lead. Previous studies on the 5-substituted 3,4-dihydroisoquinolin-1-one and 5-substituted isoquinolin-1-one classes of PARP-1 inhibitors centred around modifications at the 5, 6, 7 or 8-positions.[118,154] Following the successful synthesis and demonstration of inhibitory activity of a series of 3-substituted 5-aminoisoquinolin-1(2*H*)-ones,[160] attention was directed to the synthesis of the 4-substituted 5-aminoisoquinolin-1(2*H*)-ones. These were also of considerable interest as potential PARP-1 inhibitors, since an examination of the PARP-1 active site indicated that there is a relatively large binding pocket in the region corresponding to the 4-position of the isoquinolin-1(2*H*)-one ring which could potentially be exploited to enhance PARP-1 inhibitory potency.

X-Ray crystallographic data on the PARP-1 structure with quinazolinones[136] and phthalazinones[121] bound seemed to suggest that benzyl groups were well tolerated in that region and that they generally improve inhibitory activity by binding to hydrophobic pockets.[118] Identification of a novel series of *meta*-substituted 4-benzyl-*2H*-phthalazin-1-ones as PARP-1 inhibitors with IC_{50} in the low nanomolar range also supported 4-substitution.[143,144] We therefore hypothesised that substitution in the four position of 5-AIQ with lipophilic substituents may further improve its potency through an increased interaction with the active site. There is evidence to suggest putative water-mediated hydrogen-bond interactions between Glu988 of the active site and the amino group of 4-amino-1,8-naphthalimide (**22)**.[121] This amino group corresponds, approximately, to the 5-position of 5-AIQ. The 5-amino group enables 5-AIQ to be easily converted into the water-soluble hydrochloride salt, consequently giving it excellent *in vivo* potency, and this will be retained in the design. This has, therefore, led to the investigation of a series of 4-substituted isoquinolin-1(*2H*)-one hydrochlorides.

The specific objectives are:

1. To introduce small alkyl substituents, such as methyl and ethyl to the 4-position of 5-AIQ.
2. To introduce bulkier groups like benzyl, 4-methylbenzyl 4-methoxybenzyl and 3-succinimidobenzyl- to the 4-position of 5-AIQ.
3. To study the modes of cyclisation of methyl 2-(substituted)alkynyl-3-nitrobenzoates with different electrophiles (ICl, PhSeCl, $HgSO_4$) to form 3-substituted-5-nitroisocoumarins.
4. To test these novel target compounds for their water solubility and *in vitro* PARP-1 inhibitory potency.

3.1 3-Substituted 5-aminoisoquinolin-1(2*H*)-ones

3.1.1 Retrosynthetic analysis

The first targets for chemical synthesis were 3-substituted 5-aminoisoquinolin-1-ones, which should be accessible through the corresponding 3-substituted-5-nitroisocoumarins. A retrosynthetic analysis for the 3-substituted target is illustrated in Scheme 4. The retrosynthetic approach involved two functional group interconversions (FGI) on the target molecule. Both the conversions, *i.e.* reduction of the nitro group to amine (*e.g. via* catalytic hydrogenation or acid/metal reduction) and the conversion of isocoumarin to isoquinolin-1(2*H*)-one (*e.g. via* boiling with ammonia-saturated 2-methoxyethanol), are reasonable and well-established reactions.

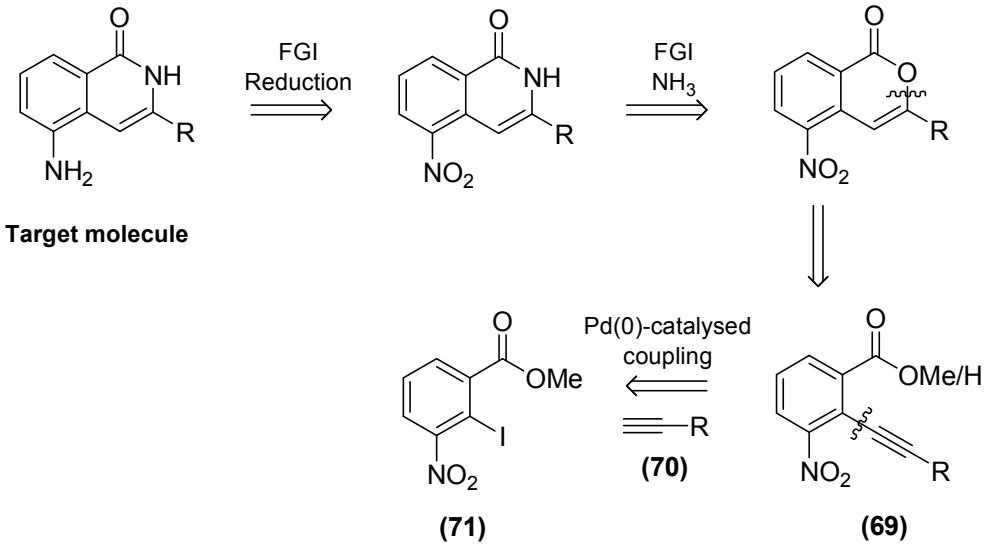

Scheme 4. Retrosynthetic analysis of the 3- substituted 5-aminoisoquinolin-1-ones.

Disconnection at the C-O bond of the isocoumarin leads to 2-alkynylbenzoates **(69)** as starting materials. Synthesis of aryl alkynes is most reliably and conveniently achieved using organometallic approaches. A number of aryl-alkyne coupling methods have been developed over the past few decades. The Castro-Stephens reaction involves direct introduction of sp^2 carbon to alkynes by the reaction of Cu acetylides with aryl and alkenyl halides to form arylalkynes and alkenylalkynes.[161] Heck and Cassar reported direct coupling of terminal alkynes catalysed by a phosphine-Pd(0) complex in the presence of amines.[162,163] Sonogashira coupling uses copper iodide as co-catalyst *i.e.* Pd(0)-CuI-catalysed reaction.[164,165] Coupling reactions with metallated alkynes such

as zinc and tin acetylides, under palladium catalysis are known as Negishi and Stille reactions, respectively. Among this wide array of coupling reactions, the Sonogashira coupling reaction was chosen for the synthesis of the aryl alkyne, since it has been used in the synthesis of a wide range of heterocyclic compounds and is generally considered to be superior to other currently known protocols. It is also highly versatile, has great tolerance for nearly all types of functional groups and mild conditions are usually employed.[166] The Sonogashira reaction cross-couples an aryl or vinyl halide (electrophile) with a terminal alkyne (nucleophile) under palladium catalysis. This catalytic process requires the use of a palladium(0) complex, and is performed in the presence of an aliphatic amine (base) and copper(I) iodide as a co-catalyst. (Scheme 5)

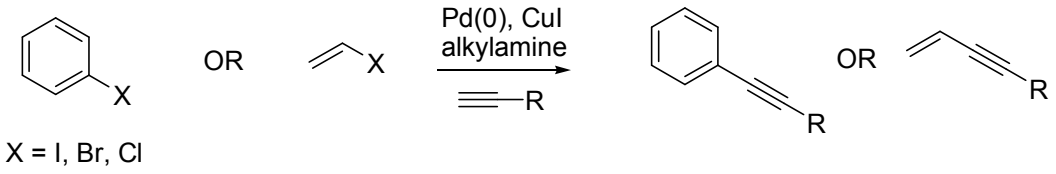

Scheme 5. Reaction conditions for the Sonogashira coupling reaction.

The general order of reactivity of the organic halide is in line with the reactivity of the leaving group. Hence an iodoarene generally affords shorter reaction times and higher yield compared to its bromo or chloro counterparts.[166] Based on these observations, a C-C disconnection of **(69)** (Scheme 4) led back to two starting materials: methyl 2-iodo-3-nitrobenzoate **(71)** and the substituted ethyne **(70)**. Sonogashira coupling suffers from two serious competitive side-reactions, namely homocoupling and decomposition of alkynes.[166] The most direct route to the synthesis of arylalkyne **(69)** is to cross-couple the iodo-ester **(71)** with ethyne gas. However, the product **(72)**, would be more acidic than ethyne itself, thus competing for coupling reaction with halide **(71)** and ultimately leading to the formation of 1,2-disubstituted alkyne **(73)** (Scheme 6). To overcome this difficulty, an indirect route involving protection and deprotection of the ethynyl group is, therefore, necessary. The trimethylsilyl (TMS) group is commonly used for this purpose. CuI and Pd(0) also catalyse oxidative homocoupling of terminal alkynes in an O_2 atmosphere (Glaser reaction). Hence, carrying out the reaction in an atmosphere of N_2 or argon is necessary.

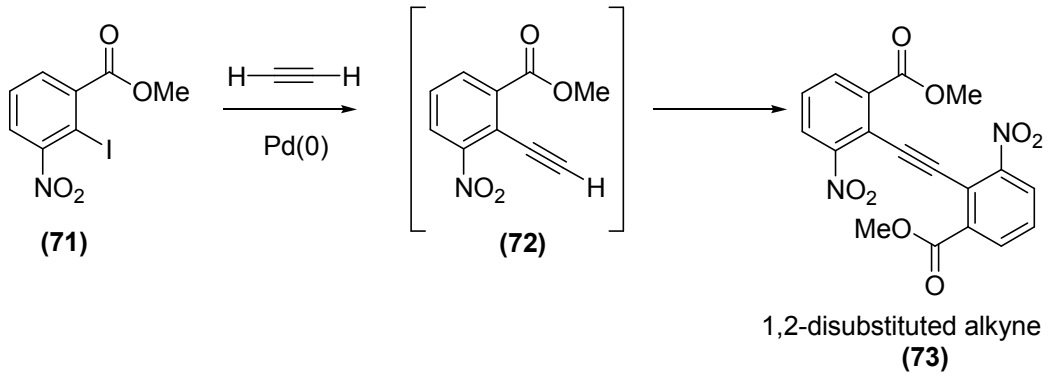

Scheme 6. Potential Formation of 1,2-disubstituted alkyne from Sonogashira homocoupling reaction.

3.1.2 Synthesis of methyl 2-iodo-3-nitrobenzoate

The iodo-ester methyl 2-iodo-3-nitrobenzoate **(71)**, starting material for the preparation of the target compounds, is not commercially available and the synthesis as shown in Scheme 7 is now well established. Culhane *et al*[167] first described the synthesis of 2-iodo-3-nitrobenzoic acid **(76)** by the decarboxylative iodination of 3-nitrophthalic acid. The starting material 3-nitrophthalic acid **(74)** has both the required carboxylic acid (1-position) and nitro functions (3-position) positioned *meta* to each other. The first stage in the synthesis was to decarboxylate 3-nitrophthalic acid with mercury(II) acetate, followed by electrophilic iodination with a mixture of iodine and potassium iodide. Interestingly, only the desired 2-iodo-acid **(76)** was formed without any of the possible by-products arising from iodination at the 1-position suggesting that mercuration has occurred regiospecifically at the 2-position. Presumably the reaction proceeded through a free radical mechanism *via* an aryl-mercury intermediate, 2-hydroxymercuri-3-nitrobenzoic acid **(75)**. The second stage involved H_2SO_4-catalysed esterification of the iodo-acid and this reaction proceeded smoothly affording the methyl ester **(71)** in excellent yield (95%). This compound serves as an important precursor for the Sonogashira coupling reaction.

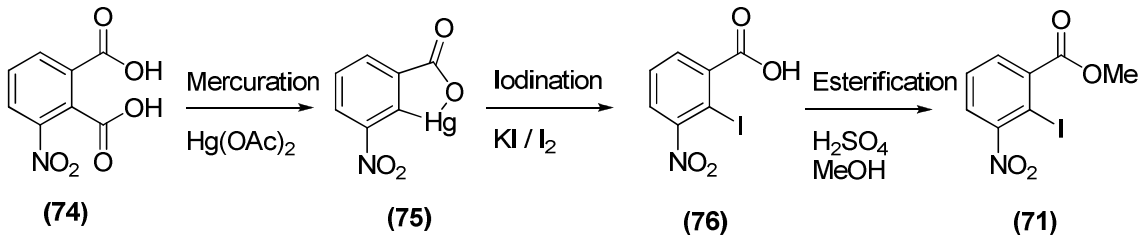

Scheme 7. Synthesis of methyl 2-iodo-3-nitrobenzoate.

3.1.3 Sonogashira coupling reaction

Sonogashira coupling was performed between methyl 2-iodo-3-nitrobenzoate **(71)** and trimethylsilylacetylene (TMSA) **(77)**, in the presence of a catalytic amount of bis(triphenylphosphine)palladium(II) chloride [$(Ph_3P)_2PdCl_2$] **(78)** and copper(I) iodide in diisopropylamine (DIPA) and dry THF. The mixture was stirred at 45 ^oC for 72 h under argon. The catalyst, used in this reaction, $(Ph_3P)_2PdCl_2$, was prepared separately by heating a mixture of palladium(II) chloride and two equivalents of triphenylphosphine in DMF at 80 ^oC for 24 h (Scheme 10). Although the coordinatively unsaturated Pd(0) is the catalytically active species, it is often more convenient to use Pd(II) derivatives, such as palladium(II) acetate [$Pd(OAc)_2$] and bis(acetonitrile)palladium(II) chloride [$(MeCN)_2PdCl_2$]. Palladium(II) complexes are generally more stable than their palladium(0) counterparts. They are also generally more soluble in organic solvents. The copper(I) salt functions as an important co-catalyst that facilitates the substitution reaction. Coupling catalysed by Pd(0) and CuI proceeds *via in situ* generation of Cu acetylides. The aliphatic amine diisopropylamine serves as a reducing agent to generate Pd(0) from the Pd(II) precatalyst and is sometimes used as a solvent.[166]

The reaction mechanism as proposed by Sonogashira[166] suggests that the substitution reaction occurs *via* a catalytic cycle which consists of three main steps (Scheme 8):

1. Oxidative addition
2. Transmetallation
3. Elimination

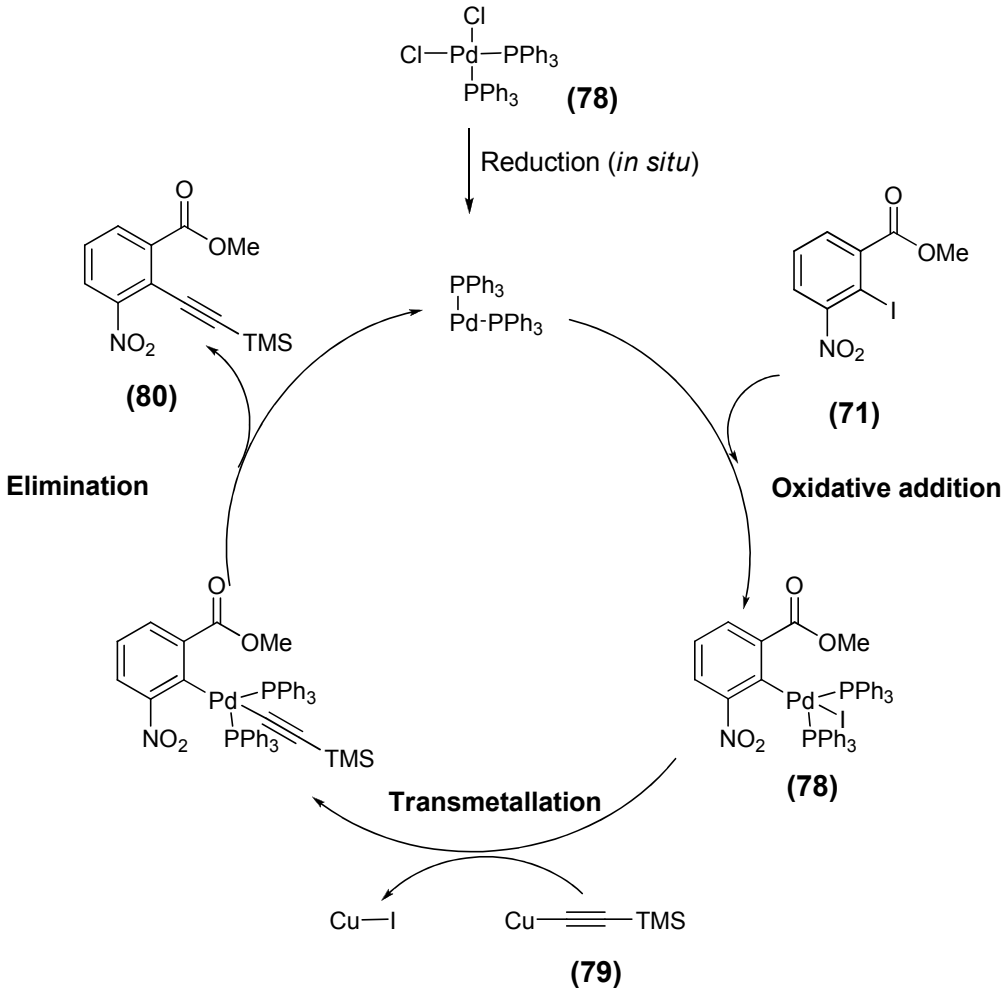

Scheme 8. Proposed mechanism for Sonogashira coupling between methyl 2-iodo-3-nitrobenzoate **(71)** and trimethylsilylacetylene.

Under the reaction conditions, $(Ph_3P)_2PdCl_2$ was rapidly reduced *in situ* to give the catalytic species $(Ph_3P)_2Pd(0)$. Oxidative addition of this Pd(0) complex with the methyl 2-iodo-3-nitrobenzoate **(71)** gives a Pd(II) intermediate **(78).** It is speculated that an alkynylcopper species **(79)**, is generated as a result of a π-alkyne-copper complex formed *in situ* from a reaction between TMSA and the copper(I) iodide, thus making the alkyne proton more acidic for easier abstraction (Scheme 9). Finally coupling of the two organic ligands and reductive elimination gave the desired methyl 3-nitro-2-(2-trimethylsilylethynyl) benzoate **(80)** in 28% yield. The reaction also gave methyl 3-nitrobenzoate **(81)** as a dehalogenated side product (14% yield). This was formed from decomposition of the intermediate arylpalladium, which had failed to couple with the alkyne, *i.e.* replacement of iodine with hydrogen during the coupling process.

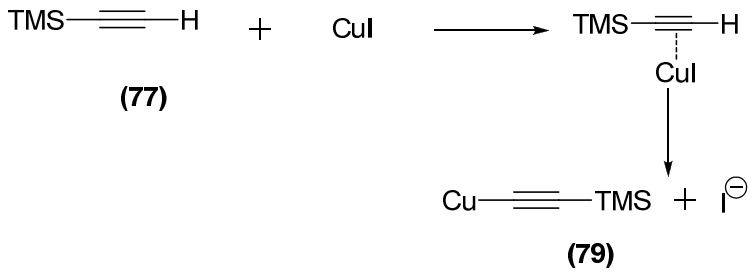

Scheme 9. Formation of alkynyl copper species.

The long reaction time (72 h), modest yield of the desired alkyne **(80)** (28%) and side product **(81)** (14%) could be associated with the use of sterically hindered halides **(71)** where both *ortho* positions were substituted with bulky groups.

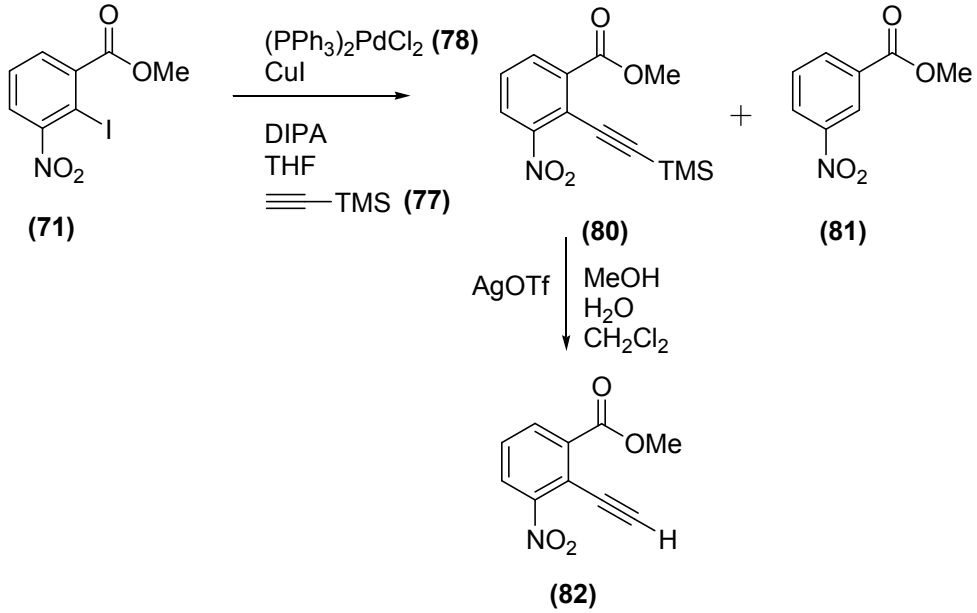

Scheme 10. Sonogashira coupling of methyl 2-iodo-3-nitrobenzoate with TMSA and subsequent desilylation of methyl 3-nitro-2-(2-trimethylsilylethynyl)benzoate.

Attempted desilylation of methyl 3-nitro-2-(2-trimethylsilylethynyl)benzoate **(80)** under a variety of basic conditions (*e.g.*, potassium carbonate/methanol) caused extensive decomposition.[160] The classical tetrabutylammonium fluoride (TBAF) ion-mediated desilylation gave only a maximum yield of 9% of desilylated product.[160] Removal of trimethylsilyl protection from alkynes with silver(I) nitrate is widely reported to be efficient if cyanide ion is added to break up the initially formed alkynylsilver(I).[168,169] Orsini *et al*[170] have recently developed a selective desilylation of 1-trimethylsilyl-2-alkylalkynes with silver(I) triflate in a biphasic solvent system at room temperature.

Adapting this method to desilylate **(80)**, prolonged heating with silver(I) triflate in a mixture of methanol, water and dichloromethane gave good yields (>70%) of the required alkyne **(82)**. We attribute the need for the higher temperature and much longer reaction times to the highly electron-deficient nature of the starting trimethylsilylalkyne.

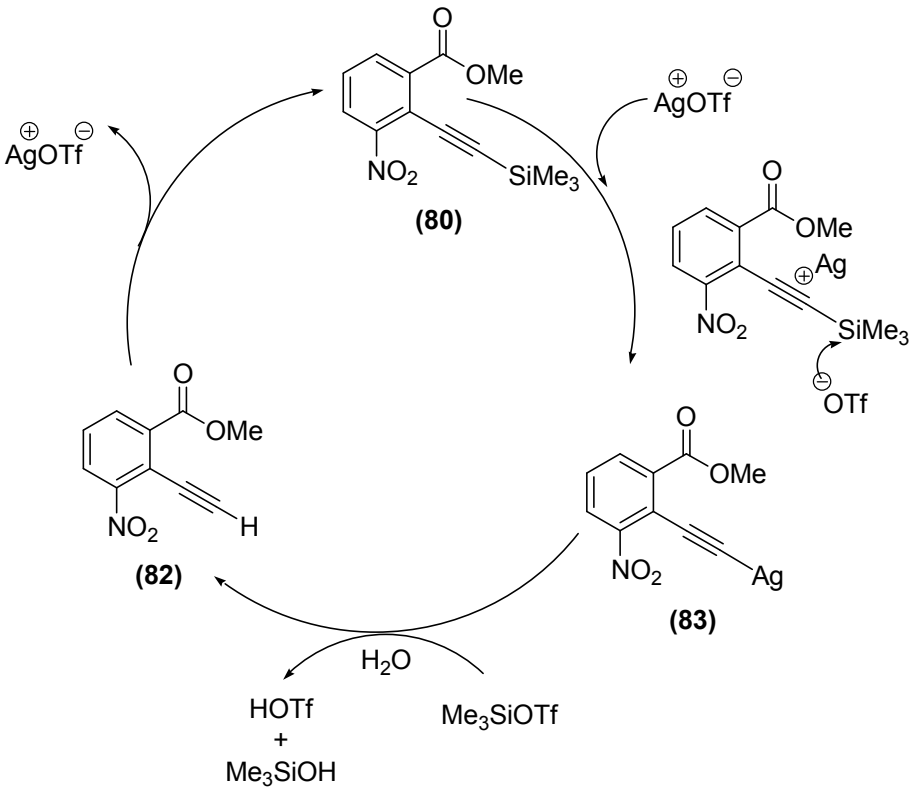

Scheme 11. Desilylation of methyl 3-nitro-2-(2-trimethylsilylethynyl)benzoate with silver(I) triflate.

The first step in the mechanism is the formation of a π-complex between the silver triflate and **(80)**.[171] This coordination activates the TMS group towards nucleophilic attack by either the counterion ($^{-}$OTf) or a nucleophilic solvent which leads to cleavage of the C–Si bond and *in situ* formation of silver acetylide and a silyl-triflate species. In protic solvents, the latter is hydrolysed leading to a better proton source (HOTf), strong enough to hydrolyse the alkynyl silver species **(83)**. Silver ion released completes the catalytic cycle (Scheme 11).

Having successfully coupled TMSA to the iodo-ester, the corresponding reaction with phenylacetylene was investigated. The Sonogashira coupling reaction between **(71)** and phenylacetylene **(84)** (the least expensive and exceptionally reactive alkyne) under the same reaction conditions as with TMSA gave the coupling product, methyl 3-nitro-2-(2-phenylethynyl)benzoate **(85)**, in very good yield (51%) and the reaction

was completed in a much shorter period of time (48 h). As in the previous reaction, the dehalogenated side product **(81)** was also isolated (38%) (Scheme 12). The reaction also gave 1,4-diphenylbutadiyne **(86)** as a by-product, the product of Glaser-like homodimerisation of the starting alkyne.

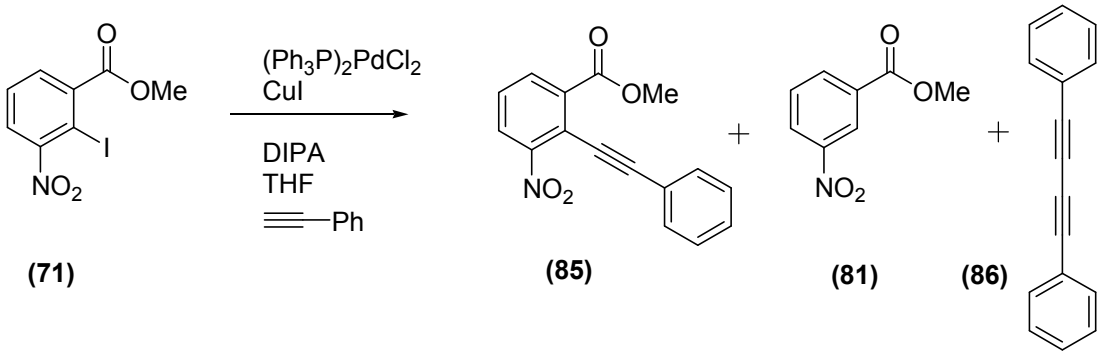

Scheme 12. Sonogashira coupling of methyl 2-iodo-3-nitrobenzoate with phenylacetylene.

3.1.4 Study of the modes of cyclisation of methyl 2-alkynyl-3-nitrobenzoates

Several groups have reported the cyclisation of 2-alkynylbenzoic acids and 2-alkynylbenzoate esters under electrophilic conditions, although no examples have a substituent at the 3-position of the benzoate. There is debate about whether the reaction goes 5-*exo*-dig (giving ylidenephthalides **88**) or 6-*endo*-dig (giving isocoumarins **89**), as shown in Scheme 13 (R^3 = H); both are favoured under Baldwin's Guidelines.[172]

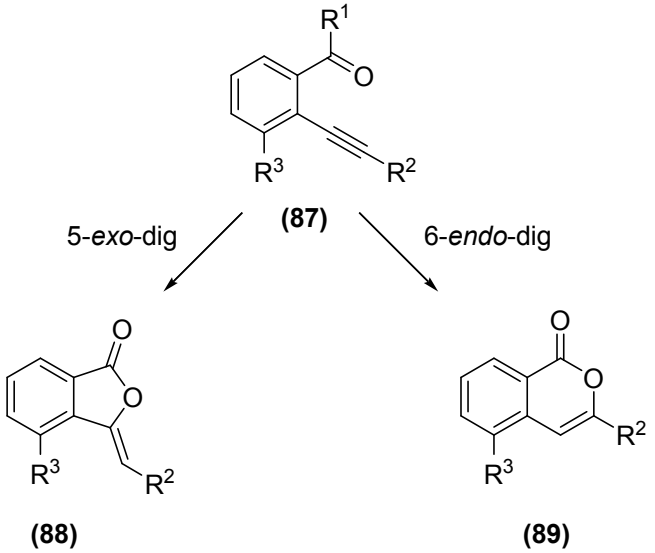

Scheme 13. Possible alternative cyclisation modes of 2-alkynylbenzoic acids **(87)** (R^1 = OH) and 2-alkynylbenzoate esters (R^1 = OMe) *via* 5-*exo*-dig (giving **88**) and 6-*endo*-dig (giving **89**) routes. R^2 = alkyl, aryl. R^3 = H.

Treatment of methyl 2-arylethynylbenzoates with Hg(II) under acidic conditions is reported to give intermediate mercurials, from which 3-arylisocoumarins can be isolated by reduction with $NaBH_4$.[173,174] Similarly, reaction of the same starting materials with hydrogen iodide, electrophilic iodine reagents, bromine, sulfenyl chlorides and selenyl chlorides gave 3-arylisocoumarins and their 4-iodo, 4-bromo, 4-arylthio and 4-arylselenyl derivatives, respectively.[175-178] Dihydrofuroisocoumarins have also been synthesised by Ag(I)-promoted 6-*endo*-dig cyclisation of the corresponding arylalkynylbenzoate esters.[179] In contrast, methyl 2-ethynylbenzoate undergoes 5-*exo*-dig cyclisation with iodine[178] and Ag(I)-mediated cyclisation of 2-alkynylbenzoic acids affords the corresponding ylidinephthalides.[180] Under basic conditions (LiOH), methyl 2-(pent-1-ynyl)benzoate undergoes exclusive 6-endo-dig cyclisation whereas methyl 2-(3-hydroxypent-1-ynyl)benzoate gives a mixture of products from both cyclisation modes.[181] Cherry *et al*.[182] have shown very recently that treatment of 2-iodobenzoic acid with allenylstannanes under Pd-catalysed Stille conditions also gives isocoumarins, through 6-*endo*-dig cyclisation of the intermediate 2-(3-substituted-allenyl)benzoic acids.

3.1.5 Castro-Stephens coupling reaction

Stephens and Castro,[161] during the synthesis of arylalkynes from iodoarenes and Cu^{I}-acetylides, claimed that treatment of 2-iodobenzoic acid **(90)** with Cu-C≡C-Ph gave 3-phenylisocoumarin **(91)** by Cu-catalysed 6-*endo*-dig cyclisation of the intermediate 2-phenylethynylbenzoic acid (Scheme 14). However this claim was later withdrawn[184] with the correction of the characterisation of the product to be the benzylidenephthalide **(92)** resulting from 5-*exo*-dig cyclisation.

Woon *et al*[160] carried out the reaction of 2-iodo-3-nitrobenzoic acid **(76)** with copper(I) phenylacetylide in boiling pyridine under nitrogen and characterised the only cyclisation product to be 5-nitro-3-phenylisocoumarin **(93)** (Scheme 15). It was firmly established that Cu-catalysed cyclisation of the 2-(arylalkynyl)-3-nitrobenzoic acids **(76)** followed 6-*endo*-dig mode of cyclisation as **(93)** was the only product formed. It may be significant that the presence of a highly electron-withdrawing nitro group in the 2-iodo-3-nitrobenzoic acid **(76)** might favour the formation of isocoumarin **(93)** rather than phthalide **(94)**.

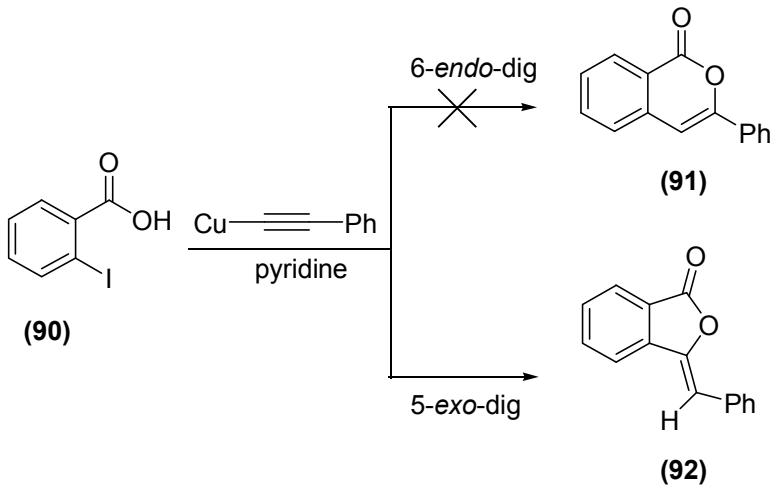

(90) **(91)** **(92)**

Scheme 14: Reaction of 2-iodobenzoic acid with copper(I)phenylacetylide to yield 3-benzylidene phthalide instead of the isomeric 3-phenylisocoumarin.[161,183]

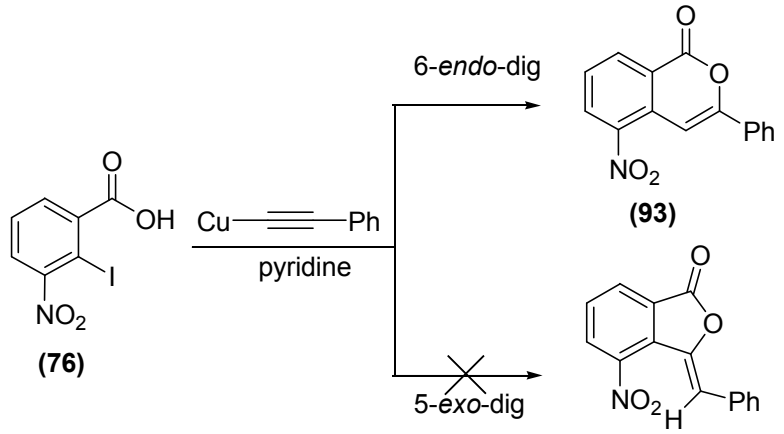

(76) **(93)** **(94)**

Scheme 15: Reaction of 2-iodo-3-nitrobenzoic acid with copper(I) phenylacetylide to yield 5-nitro-3-phenylisocoumarin instead of 3-benzylidene-4-nitrophthalide.[160]

3.1.6 Investigations into electrophile driven cyclisations of methyl 2-alkynyl–3-nitrobenzoates

Given the dichotomy of reports of the outcome of the cyclisations, in the Castro-Stephens tandem version, we initiated a short study on whether the mode of cyclisation would be influenced by the presence of the nitro group *ortho* to the alkyne. This strongly electron-withdrawing group should influence the electron distribution in the alkyne and was predicted to favour 6-*endo*-dig cyclisation by making the alkyne carbon further from the nitroarene more electrophilic (Figure

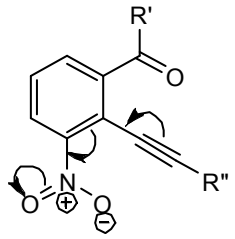

Figure 14: Proposed influence of the *ortho* nitro group on the electron-distribution in the alkyne in 2-alkynyl-3-nitro benzoic acids and 2-alkynyl-3-nitrobenzoate esters. R' = H or alkyl, R" = H, silyl, alkyl, aryl.

14). Each of the three methyl 2-alkynyl-3-nitrobenzoates **(85)**, **(80)** and **(82)** (carrying the diverse substituents Ph, $SiMe_3$ and H, respectively) was treated with three different electrophiles ($HgSO_4/H_2SO_4$, ICl and PhSeCl), to investigate whether or not cyclisation would occur and whether such cyclisation would be 5-*exo* or 6-*endo* (Scheme 18).

3.1.6.1 Hg(II)-mediated cyclisations

It was reported earlier that treatment of **(85)** with mercury(II) sulfate under acidic conditions afforded an almost quantitative yield of a single product, the isocoumarin **(93)**, which was identical to the material prepared by the Castro–Stephens one-pot method.[160] (Scheme 16)

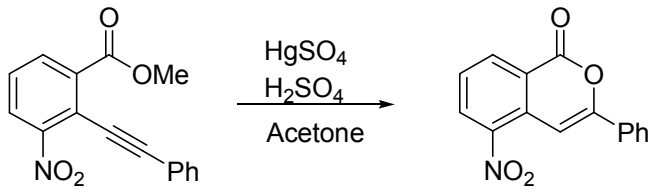

(85) **(93)**

Scheme 16: Mercury-mediated ring-closure of methyl 3-nitro-2-(2-phenylethynyl)benzoate.

Similar treatment of the analogous trimethylsilylalkyne **(80)**, however, gave only methyl 2-acetyl-3-nitrobenzoate **(95)**, in modest yield after chromatography. The same ketone was also isolated from the reaction of **(82)** with mercury(II) sulfate and acid; the NMR spectrum also indicated the presence of a trace of the isomeric pseudoester **(96)**.[184]

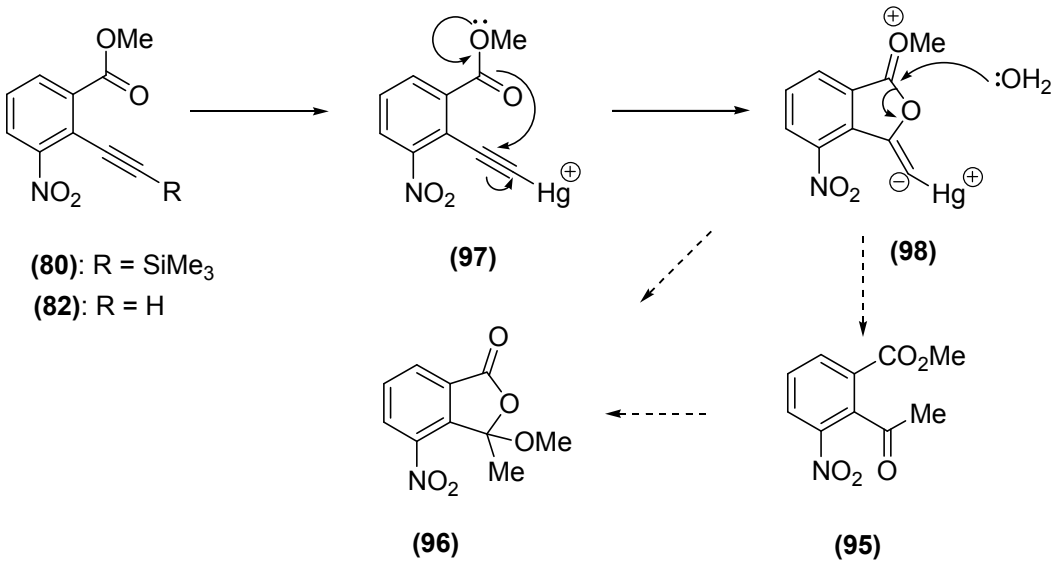

Scheme 17: Proposed routes for the formation of **(95)** and **(96)** through 5-*exo* attack of the neighbouring ester carbonyl oxygen.

The mechanism of the reaction involves the formation of 2-acetyl-3-nitrobenzoate **(95)** from both **(80)** and **(82)**. This is achieved by attack of an oxygen nucleophile on the alkyne carbon nearest to the benzene ring, in contrast to the formation of 5-nitro-3-phenylisocoumarin **(93)** from **(85)**, which must arise from 6-*endo* attack of the ester carbonyl oxygen on the carbon remote from the substituted ring. The alkyne here is polarised in the opposite sense. Scheme 17 shows a mechanism for this change in reactivity. By analogy with the mechanism of the silver(I)-mediated desilylations,[170,171] we propose that transmetallation of **(80)** occurs to form an alkynylmercury species, such as **(97)**. This intermediate could also be formed by direct metallation of **(82)**. In intermediate **(97)** the polarisation of the alkyne is caused by coordination to mercury. It is likely that this is more than the opposite polarisation induced by the two ortho-electron-withdrawing substituents (nitro, carbonyl) on the benzene ring. The ester carbonyl oxygen is located on the same side for 5-*exo* nucleophilic attack, giving intermediate **(98)**. Hydrolysis would then afford the major product, the ketone **(95)**. It is not clear whether the minor side-product **(96)** is formed from **(95)** or directly from intermediate **(98)**.

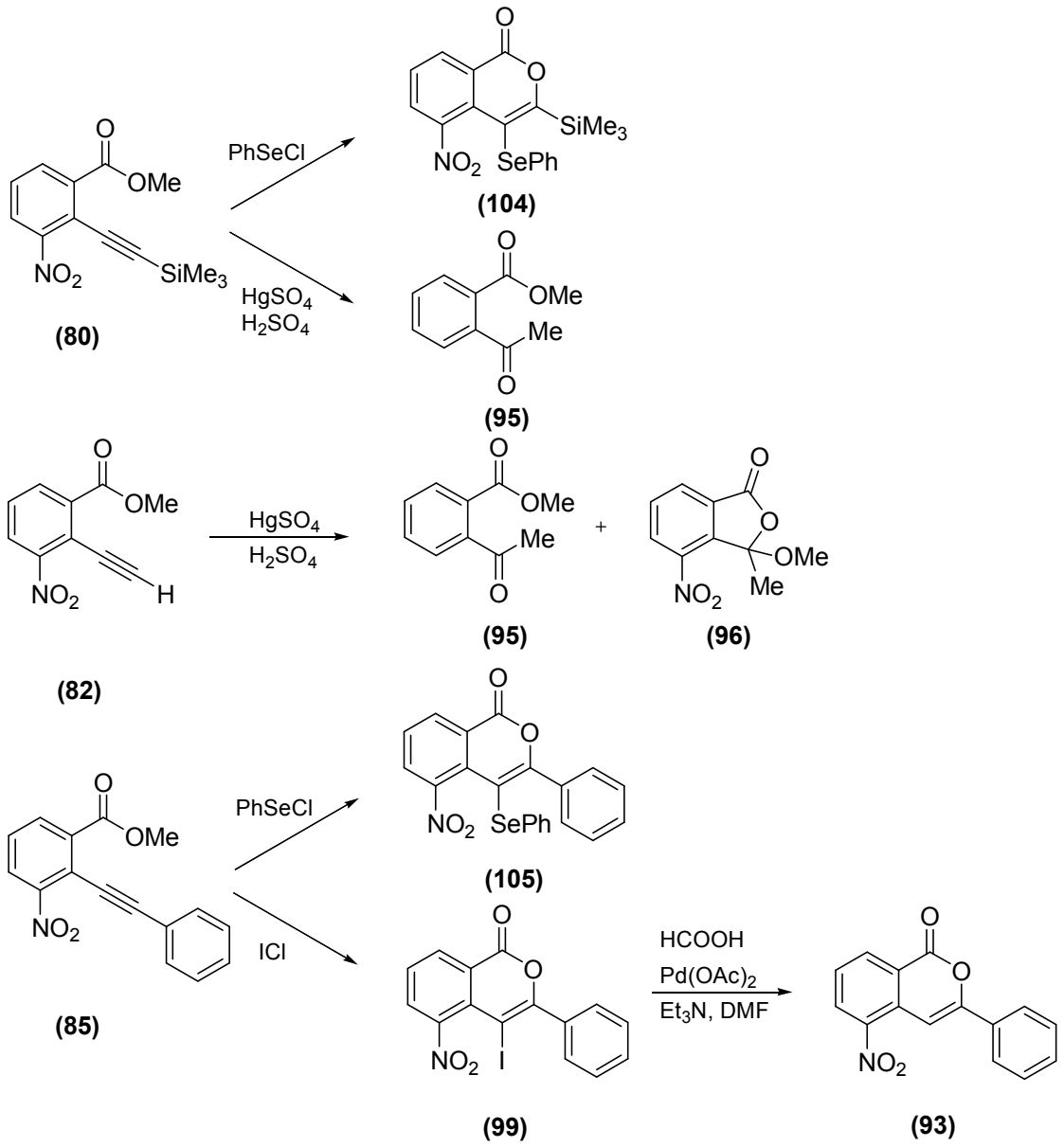

Scheme 18: Electrophile-driven cyclisations of methyl 2-alkynyl-3-nitrobenzoates.

3.1.6.2 ICl- mediated cyclisations

The set of three alkynes **(80), (82)** and **(85)** was also treated with the electrophilic iodine reagent iodine monochloride at ambient temperature in dichloromethane. Only the phenylalkyne **(85)** gave an identifiable product, affording 4-iodo-5-nitro-3-phenylisocoumarin **(99)** in good yield (81%) (Scheme 18).

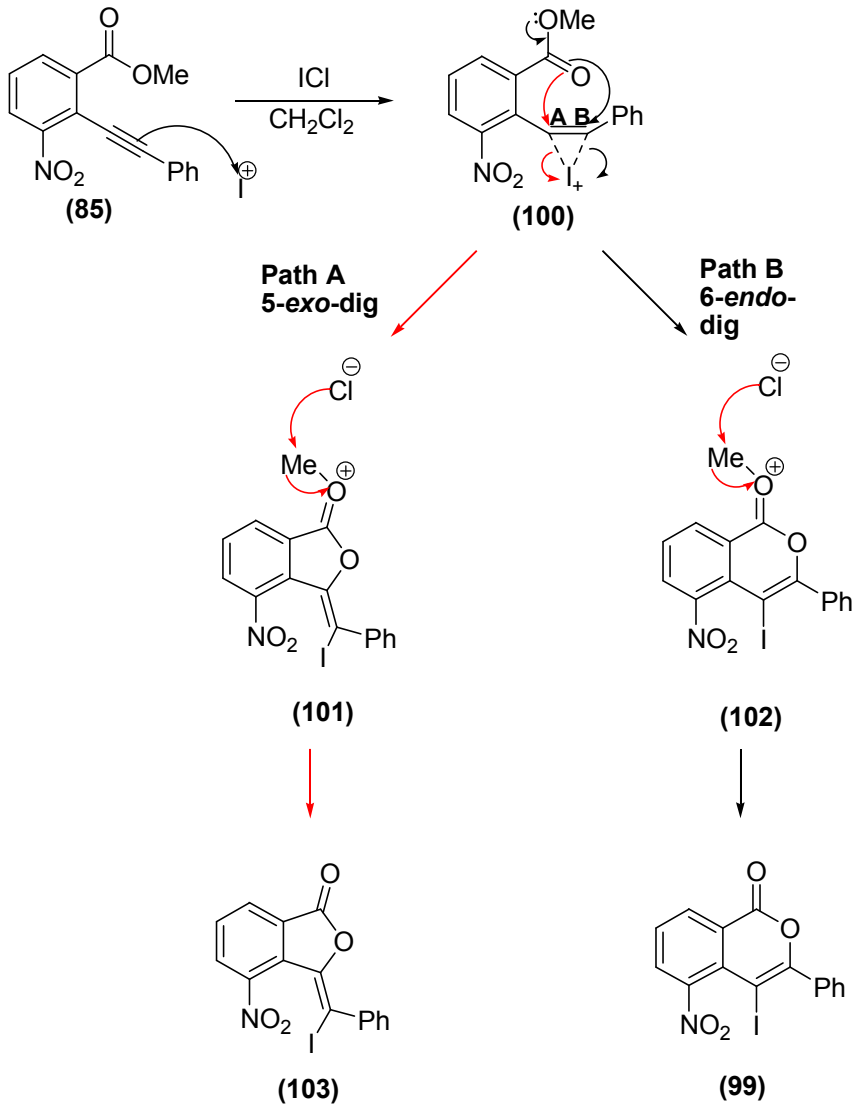

Scheme 19. Proposed mechanism for the putative formation of phthalide **(103)** and 4-iodo-5-nitro-3-phenylisocoumarin **(99)**.

It was believed that heteroannulation proceeded *via* the mechanism outlined in Scheme 19. The first step presumably involves the formation of the bridged iodonium complex **(100)** *via* electrophilic addition of I^+ to the alkyne. This was followed by nucleophilic attack by the oxygen of the carbonyl group. Finally facile removal of the methyl group via S_N2 displacement by the chloride anion present in the reaction mixture generates the 4-iodo-5-nitro-3-phenylisocoumarin **(99)** and one molecule of MeCl. Theoretically, there are two possible ways in which cyclisation can occur. The carbonyl oxygen may either attack in a 5-*exo*-dig manner (Path A) to give a 5-membered side product, 3-(iodo(phenyl)methylene)-4-nitrophthalide **(103)**, or it may undergo 6-*endo*-dig ring closure (Path B) to give the desired 4-iodo-5-nitro-3-phenylisocoumarin **(99).** According to Baldwin's guidelines for ring closure,[172]

both reactions are favourable because both carbons of the acetylene have two π^* orbitals, one of which must always lie in the plane of the new ring, making it very easy for the lone pair on the carbonyl oxygen to overlap with. Hence a mixture of phthalide and isocoumarin was expected from the reaction.

Only isocoumarin **(99)** was obtained from this iodocyclisation. No benzofuranone product was observed to arise by this process. Obviously, 6-*endo* cyclisation is more facile than 5-*exo* cyclisation. The presence of a neighbouring powerfully electron-withdrawing nitro group possibly made carbon B more electron deficient compared to carbon A, thus greatly favouring 6-*endo*-dig over 5-*exo*-dig ring closure, and accounting for the lack of formation of any 5-membered phthalide product **(103)**. The structure of **(99)** was confirmed as being the isocoumarin product of 6-*endo* cyclisation by two methods.

- Firstly, the IR spectrum showed absorption at 1732 cm^{-1}, which lies in the range 1730–1750 cm^{-1} for six-membered ring lactones but not in the corresponding range for five-membered ring lactones (1760–1780 cm^{-1}).
- Secondly, palladium-catalysed reductive deiodination of **(99)** with triethyl ammonium formate (by the general method of Rossi et al.[178]) gave an excellent yield of 5-nitro-3-phenylisocoumarin **(93)**, identical to samples prepared by the one-pot Castro–Stephens method and the Hg(II)-mediated cyclisation of **(85)**.

No isocoumarins or isobenzofuranones were identified in the NMR spectra of the crude mixtures of products formed from the treatment of ICl with trimethylsilylalkyne **(80)** or from the monosubstituted alkyne **(82)**. An interesting feature of the iodocyclisation reaction is the fact that the iodoisocoumarins generated could be further elaborated by using various palladium-catalysed processes (Sonogashira, Heck or Suzuki coupling reactions) to introduce substituents at the 4-position of the isocoumarin. Hence this reaction could prove a useful tool for the synthesis of 3,4-disubstituted 5-aminoisoquinolin-1(2*H*)-ones.

3.1.6.3 PhSeCl-mediated cyclisations

The reactions of the electrophile phenylselenyl chloride with the alkynes (**80), (82)** and **(85)** were investigated (Scheme 18). The monosubstituted alkyne **(82)** did not undergo cyclisation as no isocoumarins or isobenzofuranones could be identified as products of the reaction. However, the disubstituted alkynes **(80)** and **(85)** formed the corresponding 4-phenylselenylisocoumarins **(104)** and **(105)** in moderate-to-good

yields, through 6-*endo* cyclisation. Again, the IR spectra indicated 6-membered ring lactones, with bands at 1733 cm^{-1} for both isocoumarins. Since suitable methods for reductive removal of phenylselenyl group were lacking, we could not carry out the comparison with **(93)** synthesised previously by three independent routes. An X-ray crystal structure determination was carried out for 5-nitro-3-phenyl-4-phenylselenylisocoumarin **(105)**. Large bright orange-red crystals were formed from ethyl acetate. The structure and X-ray crystallographic numbering scheme are shown in Figure 15.

The most striking observation in this crystal structure is the intermolecular and intramolecular π-stacking of all three benzene rings in the molecule. Figure A shows four molecules in two parallel stacks, viewed from the axis of the stacking. The nature of the stacking is shown in the side view in Figure B, with the C–Ph and SePh rings stacked intramolecularly; these then stack intermolecularly with the carbocyclic ring of the isocoumarins. This isocoumarin also displays interesting conformational features within the molecule, as shown in Figure 16.

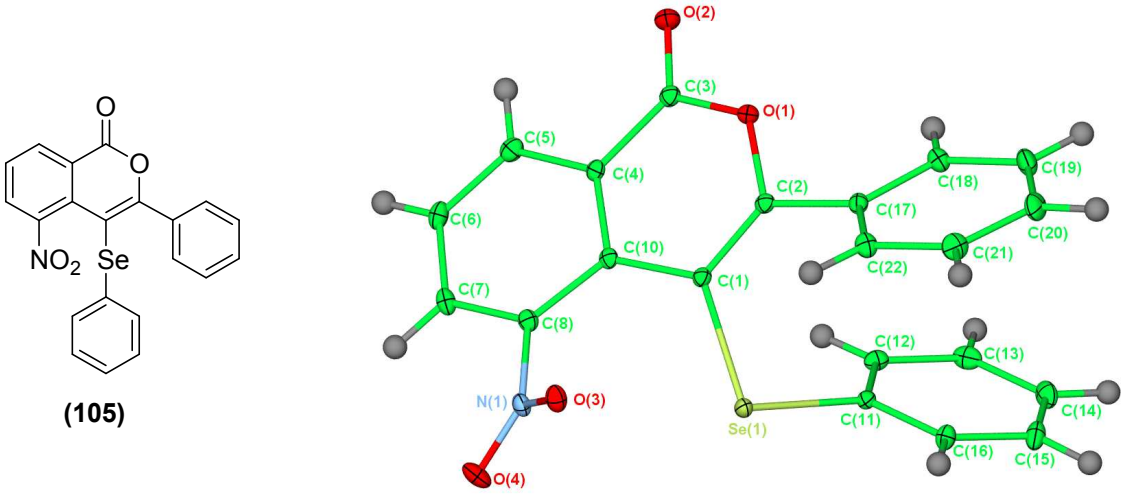

Figure 15. The structure and X-ray crystal structure of 5-nitro-3-phenyl-4-phenylselenylisocoumarin **(105)** with crystallographic numbering.

The three adjacent substituents, phenyl, phenylselenyl and nitro, at the 3-, 4- and 5-positions, respectively, occupy very crowded regions of space. In particular, there is a severe peri interaction between the nitro and phenylselenyl groups. The nitro group is twisted out of the plane–plane subtended by atoms C2–C8 and C10 of the isocoumarin, by 36.9 °. Because of the severe steric crowding the pyranone ring of the isocoumarin is forced out of the plane described above, such that C-1 lies some 0.19 Å above same. This effect is demonstrated even more clearly by the position of the

selenium atom at 0.93 Å above this mean plane, as depicted in Figure C (wherein the structure is viewed from the plane of the benzene ring) and in Figure D (in which the structure is viewed along the Se–C bond vector). The 3-phenyl substituent is twisted out of the isocoumarin mean plane by 36.5°. The presence of the adjacent bulky phenylselenyl is presumably responsible for this greater lack of coplanarity.

The gross structure is dominated by interdigitating intra- and intermolecular stacking of the aromatic rings. The intermolecular centroid–centroid distance between the aromatic rings is 3.8 Å, while the comparable intermolecular aromatic–aromatic distances average 4.1 Å. This latter value reflects the fact that the π-stacking is offset in the intermolecular case.

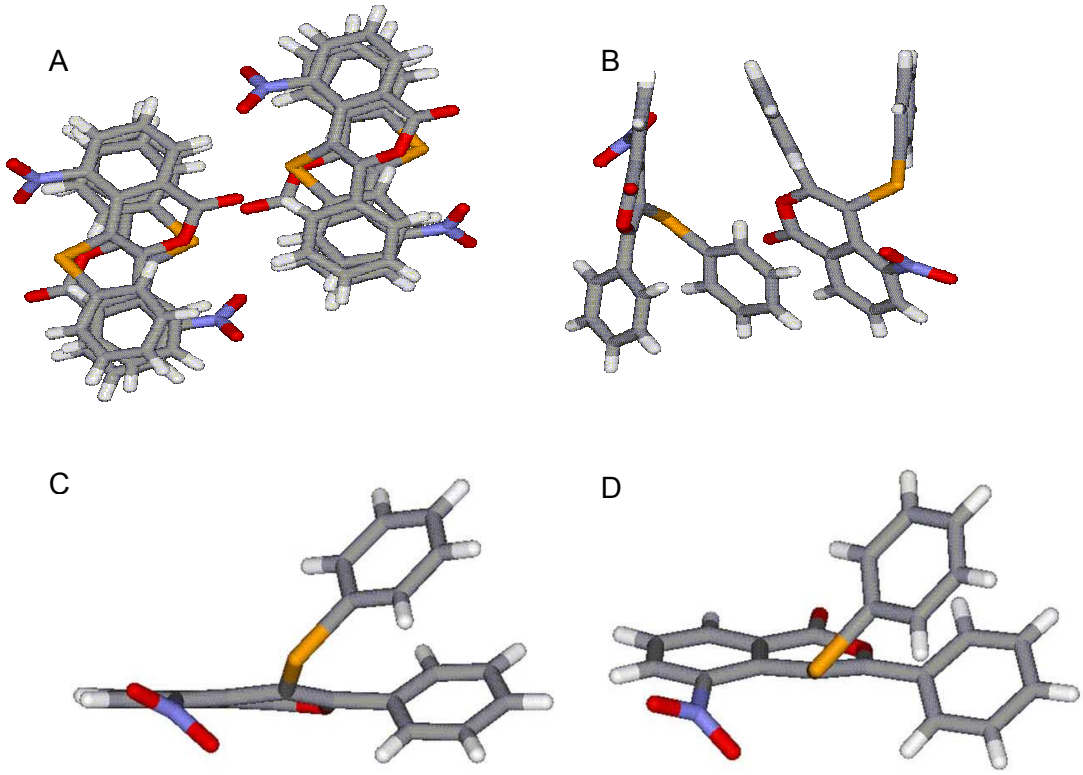

Figure 16 A: Axial view of intermolecular and intramolecular π-stacking in the crystal of **(105)**. **B**: Side view of intermolecular and intramolecular π-stacking of two molecules. **C**: View of single molecule of **(105)** in the plane of the isocoumarin carbocyclic ring. **D**: View of single molecule of **(105)** along the Se–C bond. Grey = C, white = H, blue = N, red = O and orange = Se.

3.1.7 Conclusions

Cyclisations of methyl 2-alkynyl-3-nitrobenzoates with various electrophiles were studied. Cyclisations of methyl 3-nitro-2-phenylethynylbenzoate **(85)** with iodine monochloride and with phenylselenyl chloride followed the 6-*endo* route to give the isocoumarins **(99)** and **(105)**, respectively, as did cyclisation of methyl 3-nitro-2-trimethylsilylethynylbenzoate **(80)** with phenylselenyl chloride, affording the isocoumarins **(104)**. This change in regiochemistry of cyclisation is presumably due to the nitro group inducing polarisation of the alkyne, making the remote sp-carbon more electrophilic (Figure 14). Similarly, Hg(II)-catalysed cyclisation of methyl 2-phenylalkynyl-3-nitrobenzoate **(85)** was reported to proceed in the 6-*endo* mode to give 2-nitro-3-phenylisocoumarin **(93)**. This too demonstrates the directing influence of the electron-withdrawing nitro group on the electrophilicity of the alkyne. Thus the regiochemistry of these cyclisations is also likely to be under the control of the nitro group. In contrast, the formation of methyl 2-acetyl-3-nitrobenzoate **(95)** by treatment of **(80)** and **(82)** with Hg(II) suggests that a 5-*exo* cyclisation may have been driven by the change in electron-distribution caused by the formation of an intermediate alkynylmercury complex.

These studies extend the understanding of electrophile-driven cyclisations of 2-alkynylbenzoic acids and 2-alkynylbenzoate esters to the previously unreported cases where a powerful electron-withdrawing group is present, influencing the electron-distribution of the alkyne. This understanding will be useful in predicting modes of cyclisation in the synthesis of more complex isocoumarins.

3.2 Route I: 4-Substituted 5-aminoisoquinolin-1(2*H*)-ones by reductive cyclisation of Phenylacetonitrile

3.2.1 Retrosynthetic analysis

The first series of target compounds investigated were the 4-substituted 5-aminoisoquinolin-1(2*H*)-ones. In designing our synthetic strategies, efforts were made to ensure sufficient versatility to allow for a great variety of substituents (alkyl and aryl substituents of various electronic and steric nature) to be attached at the 4-position *via* a common synthetic route. Ideally; diversification should occur at a late stage of synthesis to avoid inefficient repetition of synthetic steps.

Retrosynthetic analysis for the 4-substituted targets is illustrated in Scheme 20. We approached our retrosynthesis by first performing functional group interconversion (FGI) on the target molecule **(106)**. Reduction of the nitro group to an amine *via* catalytic hydrogenation or acid/metal reduction is a highly efficient and reliable reaction. Though the nitro group, being highly electron-withdrawing, is likely to reduce the reactivity of the carbocyclic ring towards electrophilic attack and should, in most cases, be disconnected first, we reasoned that incorporation of nitro group at the beginning of synthesis will avoid the need for subsequent regioselective nitration of the 4-substituted isocoumarin or isoquinolin-1(2*H*)-one ring. Disconnection at the C-N bond of the ring of **(107)** focusses on the cyclisation between an imine and an ester. DIBAL-H, well known for its selectivity for reducing nitriles, is used to reduce the nitrile function to imine.[185,186]

Disconnection at the C-C bond of **(108)** led to methyl 2-cyanomethyl-3-nitrobenzoate **(109)**. At this point, the desired substituents could be introduced *via* alkylation of the methylene carbon of compound **(109)**. This could be achieved quite simply, for instance *via* initial deprotonation with a hindered base such as lithium hexamethyldisilazide (LHMDS), followed by reaction with an appropriate alkylating agent such as iodomethane. The alkylation process is considered as a reliable and standard process to introduce appropriate substituents. Synthesis of **(109)** from **(110)** requires a functional group interconversion (FGI) and is achieved by nucleophilic substitution with tetraethylammonium cyanide. The precursor is formed from radical bromination of the ester **(111)** which, in turn, could be synthesised *via* acid-catalysed esterification of the carboxylic acid **(112)**.

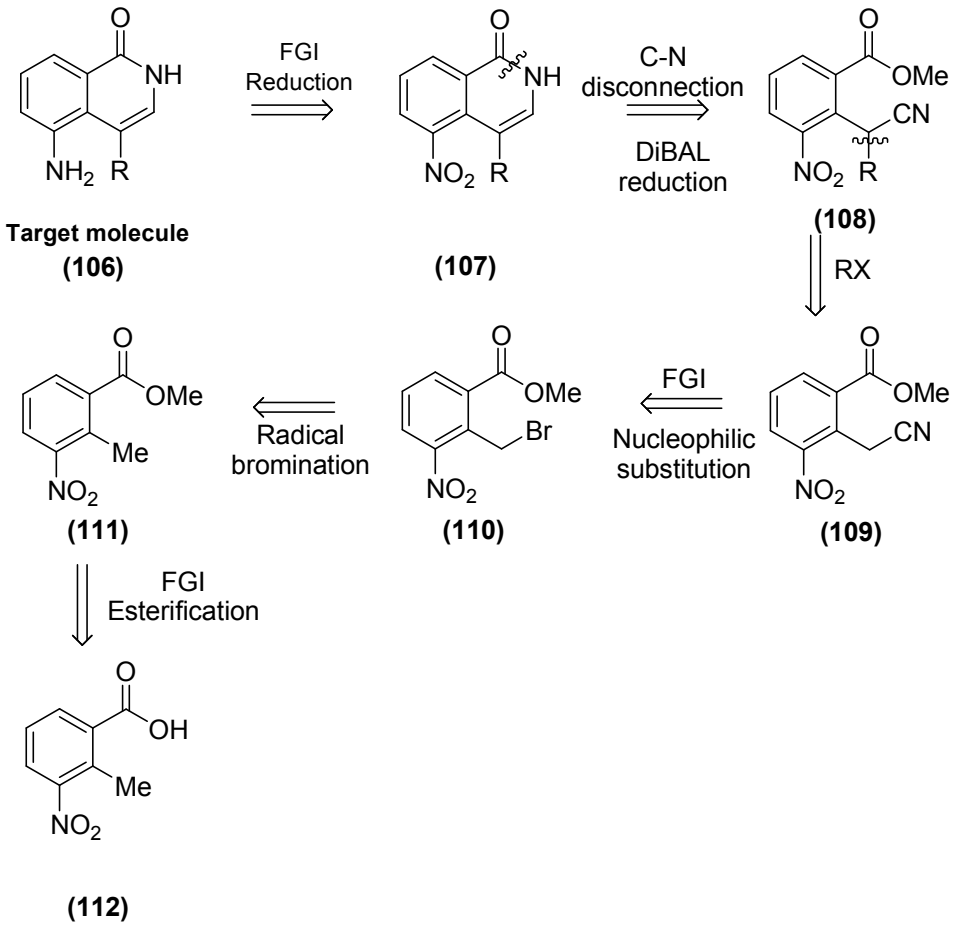

Scheme 20. Retrosynthetic analysis of the 4-substituted 5-aminoisoquinolin-1-ones *via* reduction of a phenylacetonitrile.

In the project on PARP-1 inhibitors, new synthetic approaches to 5-aminoisoquinolin-1-ones were investigated.[160] In one of the synthetic routes to 5-aminoisoquinolin-1-one the 2-N and 3-C were introduced at a higher oxidation level, as a cyanide group.[187] This route not only provides a novel, reliable and simple route for the preparation of 5-AIQ (Scheme 21) but also represents a promising synthetic strategy for the synthesis of the 4-substituted 5-aminoisoquinolin-1-ones. This could be achieved by introducing the desired substituents *via* alkylation of the methylene carbon of compound **(109)** and subsequent ring closure of **(108)** with DIBAL-H to form the 4-substituted 5-nitroisoquinolin-1(2*H*)-ones.

2-Methyl 3-nitrobenzoic acid **(112)** was used as the precursor. The first step was esterification of the acid *via* an acid-catalysed esterification process. Radical bromination of the aryl methyl was achieved with bromine and dibenzoyl peroxide in boiling carbon tetrachloride under irradiation with a tungsten lamp. This gave the monobrominated product, methyl 2-bromomethyl-3-nitrobenzoate **(110)**, in good yield.

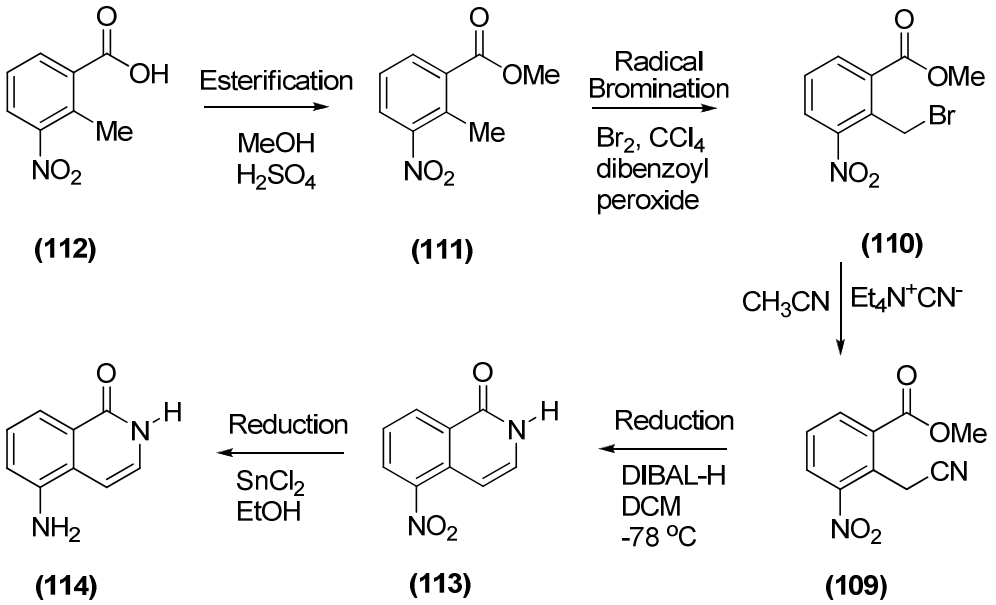

Scheme 21. Synthesis of 5-aminoisoquinolin-1(*2H*)-one.

Displacement of the bromo group with cyanide was carried out by nucleophilic substitution with $Et_4N^+CN^-$ in acetonitrile at room temperature affording the nitrile **(109)** in good yield. The nitrile was then reduced selectively with DIBAL-H at -78°C, generating the intermediate imine **(115)** which cyclised to give 5-nitroisoquinolin-1-one **(113)** in moderate yield. Presumably, during aqueous acid work-up, the transitional imine (or the tautomeric enamine) underwent rapid intramolecular cyclisation to **(113)** before reduction of the neighbouring methyl ester could occur (Scheme 22).

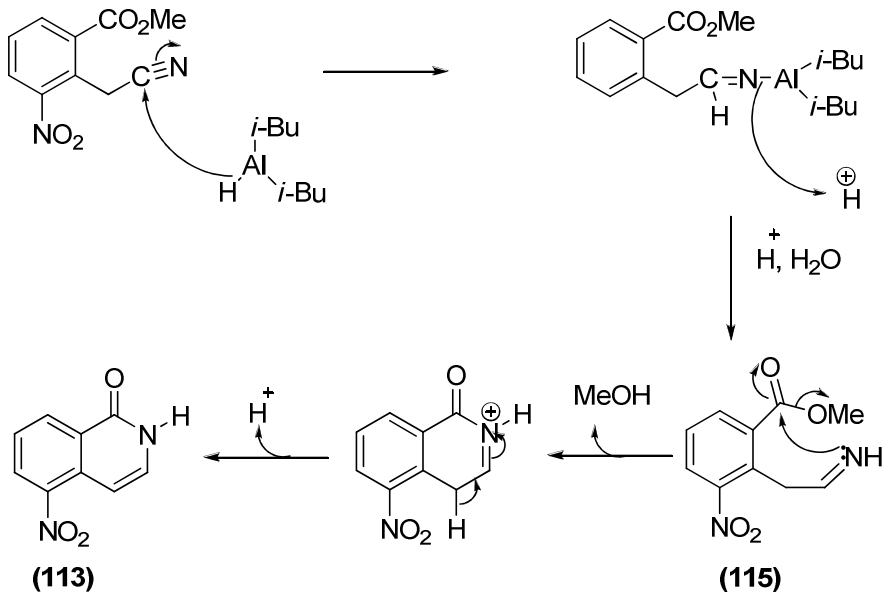

Scheme 22. Proposed mechanism for the reductive cyclisation of methyl 2-cyanomethyl-3-nitrobenzoate **(109)**.

3.2.2 Investigations into reductive cyclisations catalysed by DIBAL-H

The DIBAL-H reductions of two analogues of **(114)** with bulky substituents at either the ester or methylene position were studied to explore the generality of this route. The benzyl group was chosen to increase the steric bulk at the methylene position while an isopropyl ester was used instead of a methyl ester. The acidity of methylene protons adjacent to the nitrile group allowed introduction of the benzyl group. As these methylene protons were adjacent to the two electron-withdrawing groups, one of them could be removed using the non-nucleophilic base lithium hexamethyldisilazide (LHMDS). This, on quenching with benzyl bromide, afforded **(116)** (Scheme 23). Reduction with DIBAL-H at -78 °C, did not form 5-nitro-4-benzylisoquinolin-1(*2H*)-one **(118)** as predicted but afforded only the aldehyde 2-(2-formyl-6-nitrophenyl)-3-phenylpropanenitrile **(117)**, arising from reduction of the ester while leaving the nitrile unaltered. To form the desired product **(118)** DIBAL-H has to reduce the nitrile function first to an imine, which on subsequent intramolecular nucleophilic attack of the ester undergoes cyclisation.

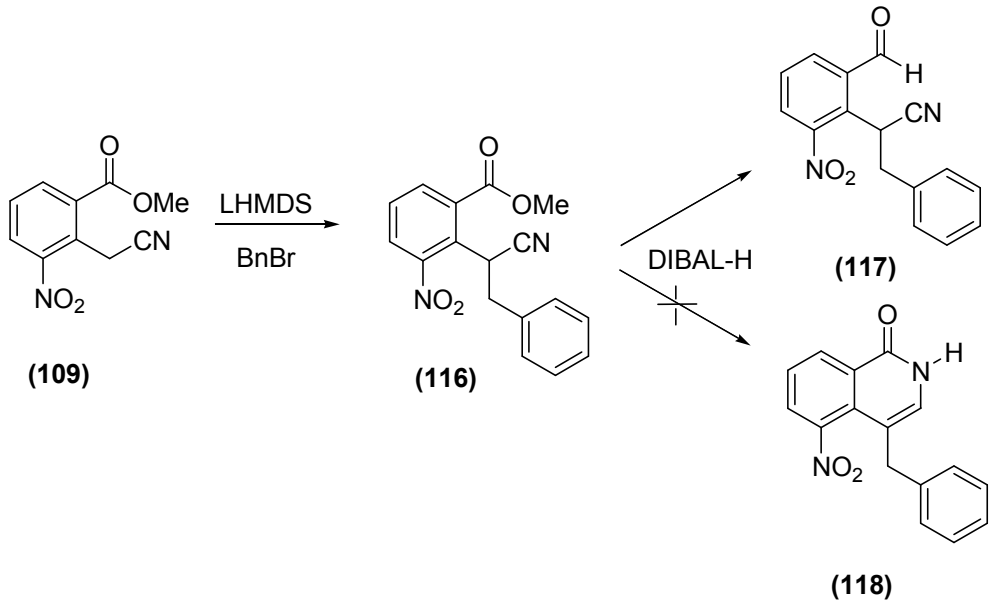

Scheme 23. Formation of 2-(2-formyl-6-nitrophenyl)-3-phenylpropanenitrile **(117)**.

In compound **(116)** approach of the DIBAL-H to the nitrile is obstructed by the adjacent benzyl group, leading to reduction at the ester only, giving **(117)** *via* formation of the tetrahedral intermediate **(119)** which is stable even at -70°C (Scheme 24). This intermediate collapses to the aldehyde on aqueous work-up.

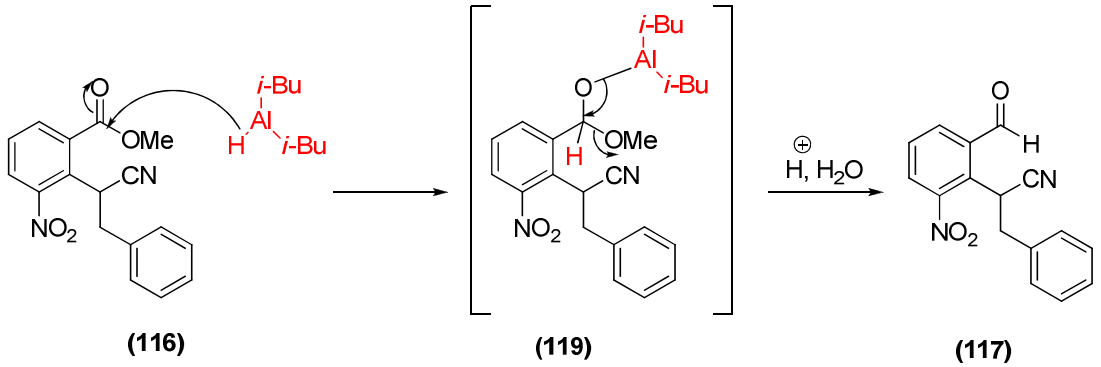

Scheme 24. Proposed mechanism for formation of 2-(2-formyl-6-nitrophenyl)-3-phenylpropanenitrile **(117)**.

Studies using the isopropyl ester to increase steric bulk at the ester were conducted earlier in our laboratory.[187] It was expected that steric bulk at the ester would slow down reduction of the ester, allowing the nitrile more time to react. The isopropyl ester[188] was brominated and converted to the nitrile **(120)**. Reduction with DIBAL-H, however, gave the isoquinoline **(123)** as the sole identifiable product, formed from reduction of both the ester and the nitrile. This indicates, surprisingly, that increasing the steric bulk of the ester makes it more prone to reduction. Careful examination of the mechanism reveals that for **(120)**, step **1** is fast, giving **(121)** but approach of the nucleophile in step **2** is slowed by the steric bulk of the Pr^i, allowing time for reduction of the ester (step **3**), leading to aldehyde (**122)** and cyclisation to 5-nitroisoquinoline **(123)** (scheme 25).

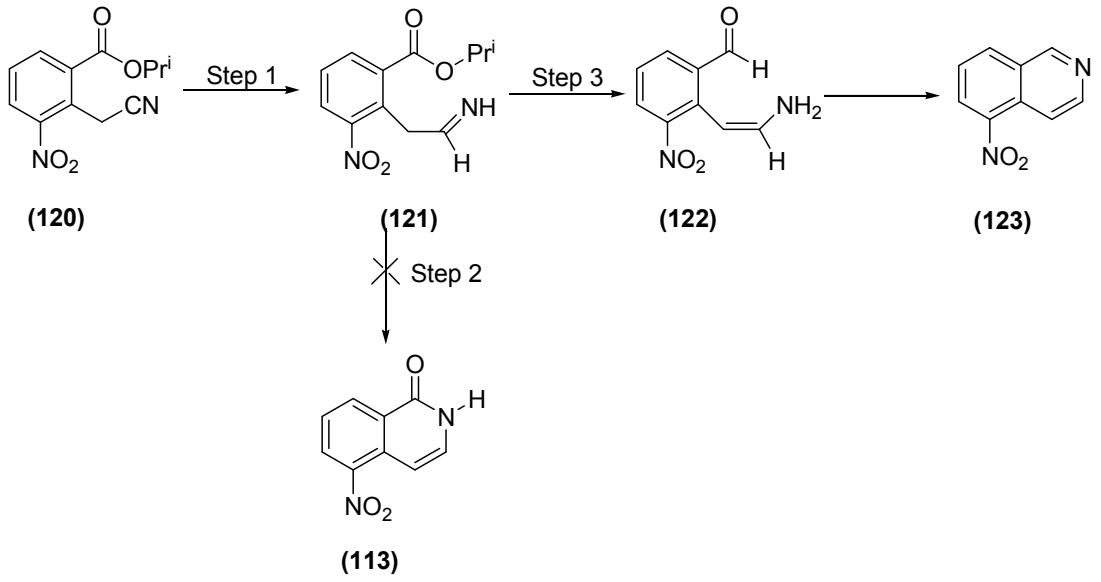

Scheme 25. Proposed route for the formation of 5-nitroisoqunioline (**123**).[187]

This route could thus only be used for the synthesis of 5-AIQ **(114)** (scheme 21). The severe effects of steric bulk mitigate against the general utility of this reductive cyclisation using DIBAL-H. Since reductive cyclisation of nitrile is the most critical step in the proposed route, difficulties in this step called for alternative routes to be developed.

3.3 Route II: 4-Substituted 5-aminoisoquinolin-1(2*H*)-ones *via* Pd-catalysed couplings of 4-bromoisoquinolin-1-ones

3.3.1 Retrosynthetic analysis

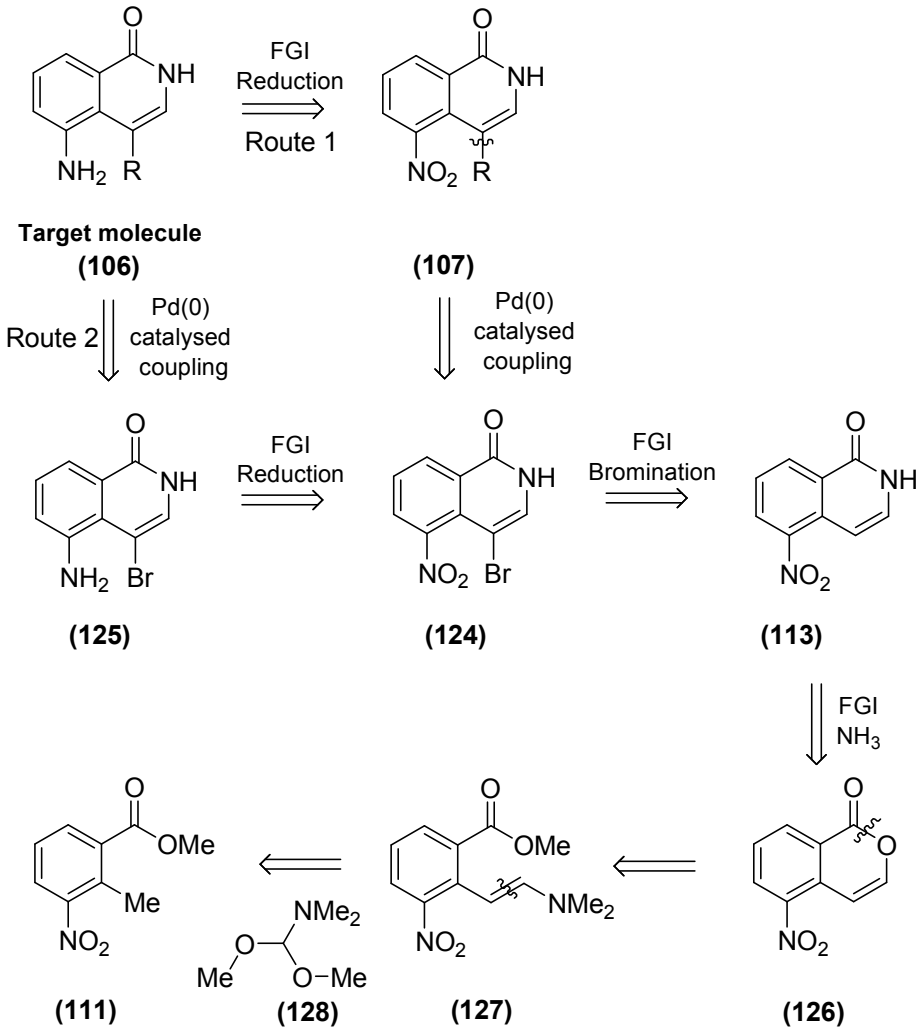

Scheme 26. Retrosynthetic analysis of the 4-substituted 5-aminoisoquinolin-1-ones *via* Pd-catalysed couplings of 4-bromoisoquinolin-1-ones.

Retrosynthetic analysis of our 4-substituted target **(106)** gave the pathway illustrated in Scheme 26. The target molecule could be synthesised by two routes. Route 1 requires the formation of 4-substituted 5-nitroisoquinolin-1-ones **(107)** achieved using organometallic approaches on 4-bromo-5-nitroisoquinolin-1-one **(124)**. Route 2 suggested synthesis of the target molecule directly by organometallic approaches using Pd(0) coupling reactions on 5-amino-4-bromoisoquinolin-1-one **(125)**, followed by functional group interconversion to 4-bromo-5-nitroisoquinolin-1-one **(124)**. In Route 2 reduction of the nitro group to amine (*via* hydrogenolysis or acid/metal reduction) is

performed prior to Pd(0)-catalysed coupling reactions. This is done in order to minimise any steric hindrance that may be arising from sterically bulky groups like bromo and nitro placed adjacent to each other. The 4-bromo group is of great value in organometallic synthesis as a means through which a diverse range of substituents may be introduced at the 4-position *via* appropriate organometallic reagents, such as organoboranes (**Suzuki coupling reaction)**, organostannanes (**Stille coupling reaction**) or organoacetylenes (**Sonogashira coupling reaction**). We believe that a series of 4-substituted targets are synthetically accessible through these pathways.

Both the Routes (1 and 2) converge at this stage to 4-bromo-5-nitroisoquinolin-1-one **(124)**, synthesis of which could be achieved by bromination of 5-nitroisoquinolin-1-one **(113)**. Synthesis of the latter requires functional group interconversion of isocoumarin to isoquinolin-1(2*H*)-one (*e.g.* by treatment with boiling ammonia-saturated 2-methoxyethanol). This is well-established reaction that is highly reliable and efficient. The challenge, then, was to devise a synthetic strategy for the construction of the isocoumarin **(126)**. Disconnection at the C-O bond of the isocoumarin as shown, *i.e.* ring opening is rational because the reverse lactonisation process is a very fast reaction, easily accomplished, for instance, through the use of an acid catalyst. The synthesis of 5-nitroisocoumarin **(126)** (Scheme 27) is now well established,[86] through condensation of methyl 2-methyl-3-nitrobenzoate **(111)** with dimethylformamide dimethylacetal **(128)**, followed by hydrolysis of the intermediate methyl *E*-2-(2-dimethylaminoethenyl)-3-nitrobenzoate **(127)** and cyclisation catalysed by wet silica.

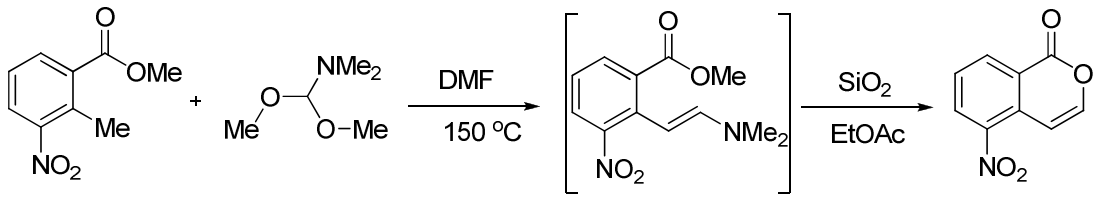

(111) **(128)** **(127)** **(126)**

Scheme 27. Chemical synthesis of 5-nitroisocoumarin *via* condensation of compound **(111)** with DMFDMA.

It was reported earlier that condensation of methyl 2-methyl-3-nitrobenzoate with, DMFDMA at high temperature (150 °C) gave the enamine methyl E-2-(2-dimethylaminoethenyl)-3-nitrobenzoate **(127)** (Scheme 27).[86] Immediate passage of this crude enamine through undried silica gel (column chromatography) not only provides sufficient acid catalysis to hydrolyse the enamine and to cyclise the

intermediate enol to 5-nitroisocoumarin, but also purifies the product, all in one elegant step. Alternatively (route 2) the enamine is hydrolysed to the aldehyde which later displaces the methoxy group to form **(126)**.

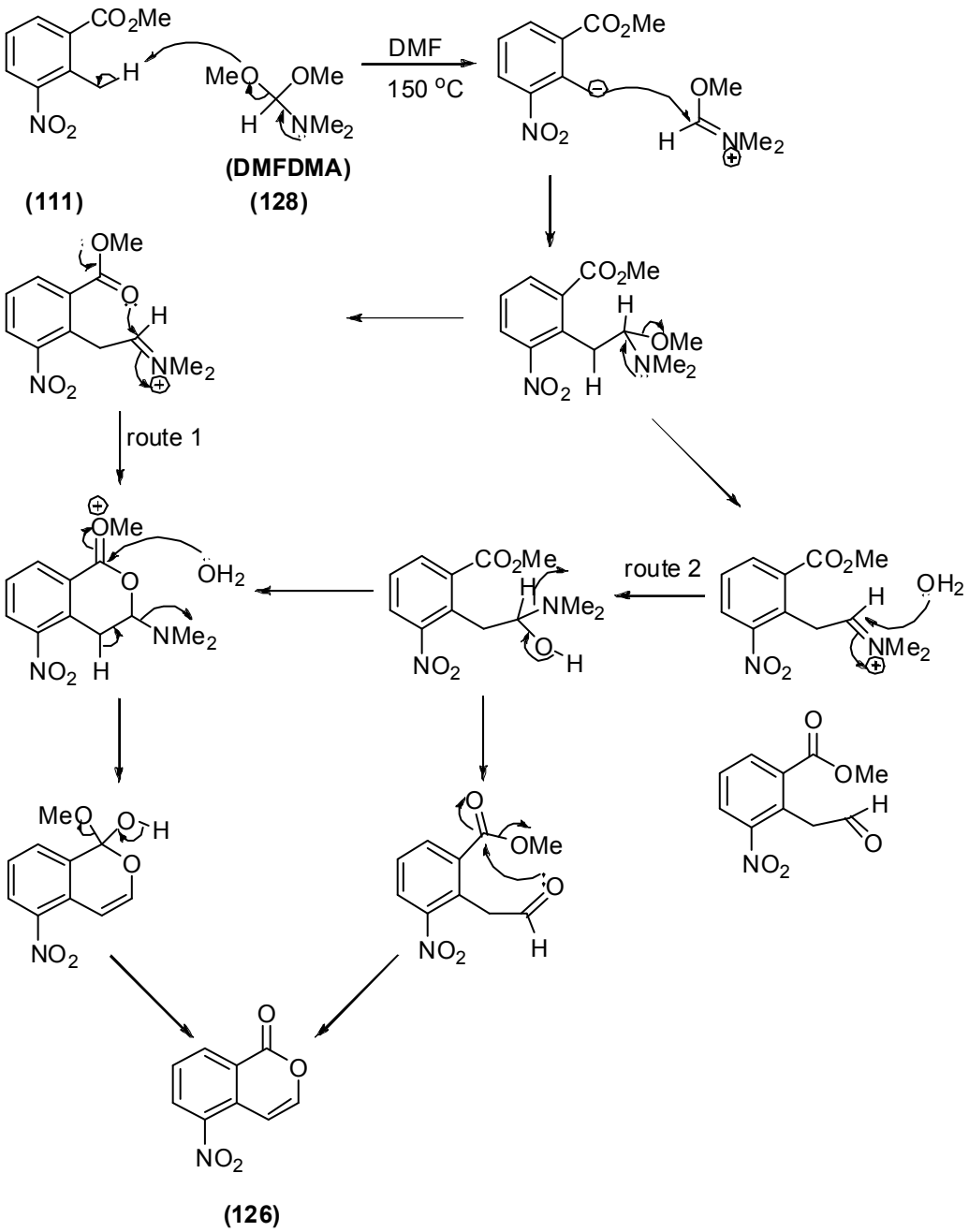

Scheme 28. Proposed mechanism for the condensation reaction between methyl 2-methyl-3-nitrobenzoate **(111)** and DMFDMA **(128)**.

Heating with ammonia at high temperature[154,150] is one of the simplest procedures reported in the literature for the conversion of isocoumarins to isoquinolin-1-ones. Thus

5-nitroisocoumarin **(126)** was treated with boiling ammonia-saturated 2-methoxyethanol and this afforded 5-nitroisoquinolin-1-one **(113)** in good yield (89%).

3.3.2 Iodination / bromination at 4-position of 5-nitroisoquinolin-1-one

The 4-position of 5-nitroisoquinolin-1-one **(113)** is believed to be more nucleophilic, compared to the 3-position, due to a mesomeric electron-donating effect of the ring nitrogen. Such a difference in nucleophilicity, and thus reactivity, towards electrophiles between the 3- and 4-position can be exploited to attach an electrophile selectively, such as iodine or bromine, at the 4-position. Alternatively, the pyridine ring of isoquinolin-1-one also act as N-acyl enamine thus contributing to the nucleophilicity of 4-position (Figure 17).

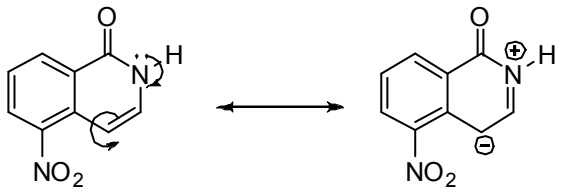

Figure 17: Pyridine ring of 4-nitroisoquinolin-1-one as tautomeric enamine

The iodination of 5-nitroisoquinolin-1-one **(113)** with a solution of iodine in acetic acid was undertaken. However, the reaction mixture remained unchanged even after stirring for 24 h with heating to 100 ^{o}C. Employment of more electrophilic conditions, such as *N*-iodosuccinimide in acetic acid, also failed to effect halogenation. Treatment of 5-nitroisoquinolin-1-one **(113)** with iodine in the presence of silver trifluoroacetate in Et_2O/THF/$CHCl_3$ also gave the starting material unchanged.[189,190] A switch to the use of brominating reagents (bromine being more reactive compared to iodine) was therefore considered. Bromination of 5-nitroisoquinolin-1-one **(113)** with *N*-bromosuccinimide in glacial acetic acid furnished a mixture of 4-bromo-5-nitroisoquinolin-1-one **(124)** and 4-bromo-5-nitro-1-oxo-1,2,3,4-tetrahydroisoquinolin-3-yl acetate **(129)**. The latter when heated to melt gave a mixture of 4-brominated **(124)** and debrominated **(113)** compounds in the ratio of 2:3. However, the low yield (30%) and lack of reproducibility of the reaction discouraged further attempts of bromination with *N*-bromosuccinimide.

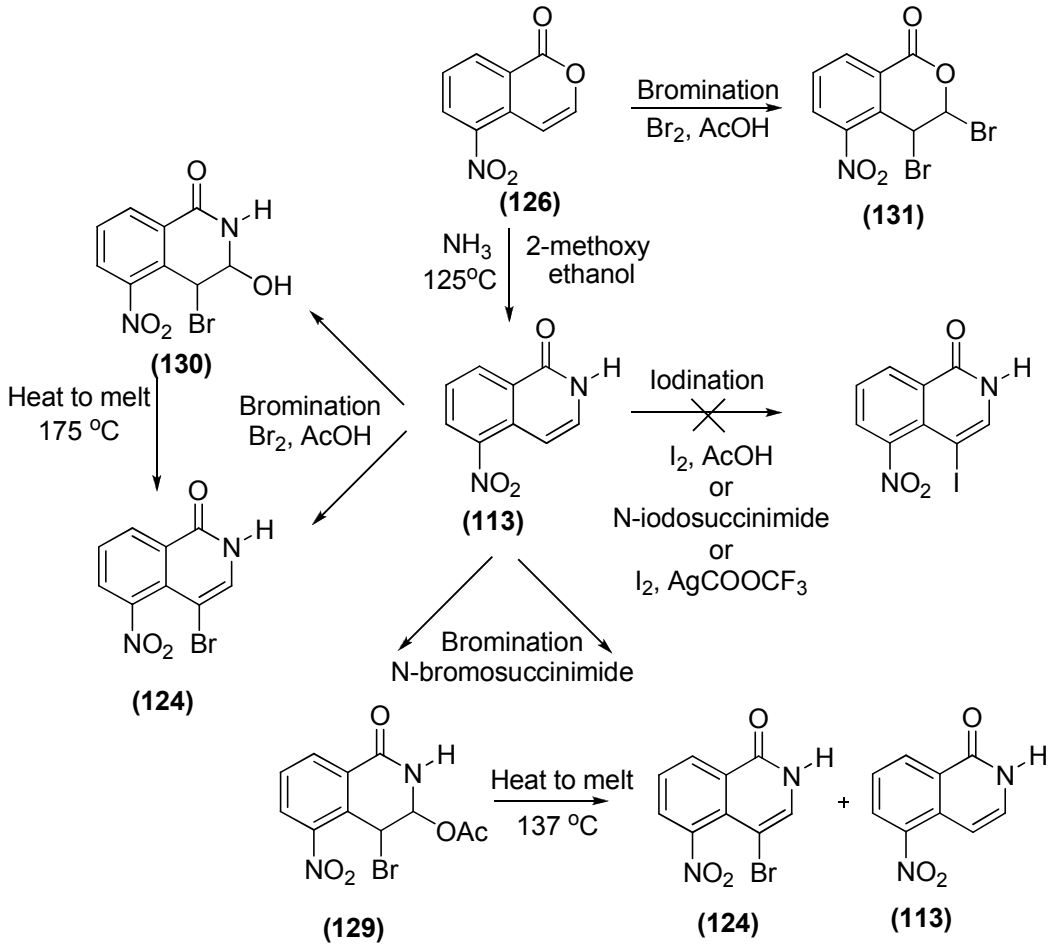

Scheme 29. Different chemical approaches for iodination / bromination at the 4-position of 5-nitroisoquinolin-1-one.

Horning *et al*[191] described various electrophilic substitutions on N-alkylated isoquinolin-1-ones and emphasised the fact that electrophilic attack of the hetero ring would be confined to one carbon atom *i.e.* to C-4. In this study, bromination of 2-methyl-5-nitroisoquinolin-1-one **(132)** was carried out with the addition of one molecular equivalent of bromine in acetic acid to a solution of **(132)** in same solvent. This reaction, on aqueous work-up, gave a 1:1 mixture of two monobromo compounds: 4-bromo-2-methyl-5-nitroisoquinolin-1-one **(133)** and 4-bromo-3-hydroxy-2-methyl-5-nitro-3,4-dihydroisoquinolin-1-one **(134)** (Scheme 30). The bromohydrin compound **(134)** was converted to **(133)** when heated to its melting point.

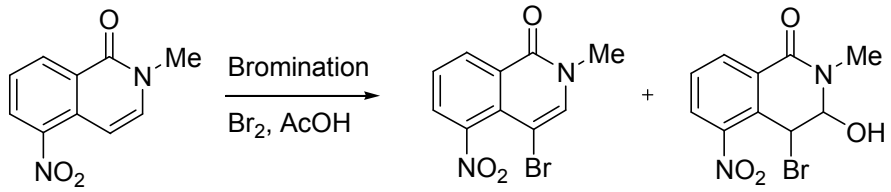

(132) **(133)** **(134)**

Scheme 30. Bromination of 2-methyl-5-nitroisoquinolin-1-one **(132)** using bromine in acetic acid.[191]

All of Horning's reactions used N-alkylated isoquinolin-1-ones. However, we decided to use isoquinolin-1-one as such as required by our project. Accordingly, we carried out bromination of 5-nitroisoquinolin-1-one **(113)** using one molecular equivalent of bromine in acetic acid, which on aqueous work-up gave a 1:1 mixture of 4-bromo-5-nitroisoquinolin-1-one **(124)** and 4-bromo-3-hydroxy-5-nitro-3,4-dihydroisoquinolin-1-one **(130)**. Analogously to the above mentioned reaction, the bromohydrin compound **(130)** was converted to the desired **(124)** when heated to its melting point (Scheme 29). The overall yield of the reaction was a moderate 53%.

Attempts to brominate 5-nitroisocoumarin **(126)** in the same way gave a dibrominated compound, 3,4-dibromo-5-nitroisocoumarin **(131)**.

3.3.3 Sonogashira, Suzuki or Stille coupling reactions

With the 4-bromo-5-nitroisoquinolin-1-one **(124)** in hand, a series of Pd(0)-catalysed cross-couplings were attempted to introduce substituents at the 4-position. The first reaction attempted was a Sonogashira coupling reaction performed between 4-bromo-5-nitroisoquinolin-1-one **(124)** and phenylacetylene **(84)**, in the presence of a catalytic amount of $(Ph_3P)_2PdCl_2$ **(78)** and copper(I) iodide in diisopropylamine (DIPA) and dry THF (standard Sonogashira conditions). The mixture was stirred at 45 ^oC under argon for 24 hours. However, the expected coupling reaction did not occur. Only the debrominated material **(113)** was isolated. Use of a sterically hindered halide such as **(124)** (with nitro and bromo group *peri* to each other) could possibly account for the inability to undergo coupling with phenylacetylene **(84)**. Buchwald *et al.*[192] performed a series of Suzuki-Miyaura coupling reactions with very hindered aryl halides using 2-(2′,6′-dimethoxybiphenyl)-dicyclohexylphosphine (SPhos) **(135)** as a ligand. Following this example, the coupling reaction of 4-bromo-5-nitroisoquinolin-1-one **(124)** was studied with phenylboronic acid in DMF using the combination of $Pd(OAc)_2$ and SPhos as catalyst system in the presence of K_3PO_4 base. The mixture was stirred at 100 ^oC

under argon for 24 h. Coupling failed to proceed and gave some unidentified complex mixture. Finally Stille cross-coupling reaction was attempted on 4-bromo-5-nitroisoquinolin-1-one **(124)** to introduce a smaller methyl substituent. Reaction of **(124)** with tetramethyltin [$(CH_3)_4Sn$] in N-methylpyrrolidin-2-one (NMP) in the presence of tetrakis(triphenylphosphine)palladium [$Pd(Ph_3P)_4$] in an inert atmosphere was carried out at 80 ^oC for 20 h.[193] The reaction failed to proceed. A switch to tetraethyltin [$(C_2H_5)_4Sn$] and refluxing at a higher temperature (100 ^oC) did not alter the outcome.

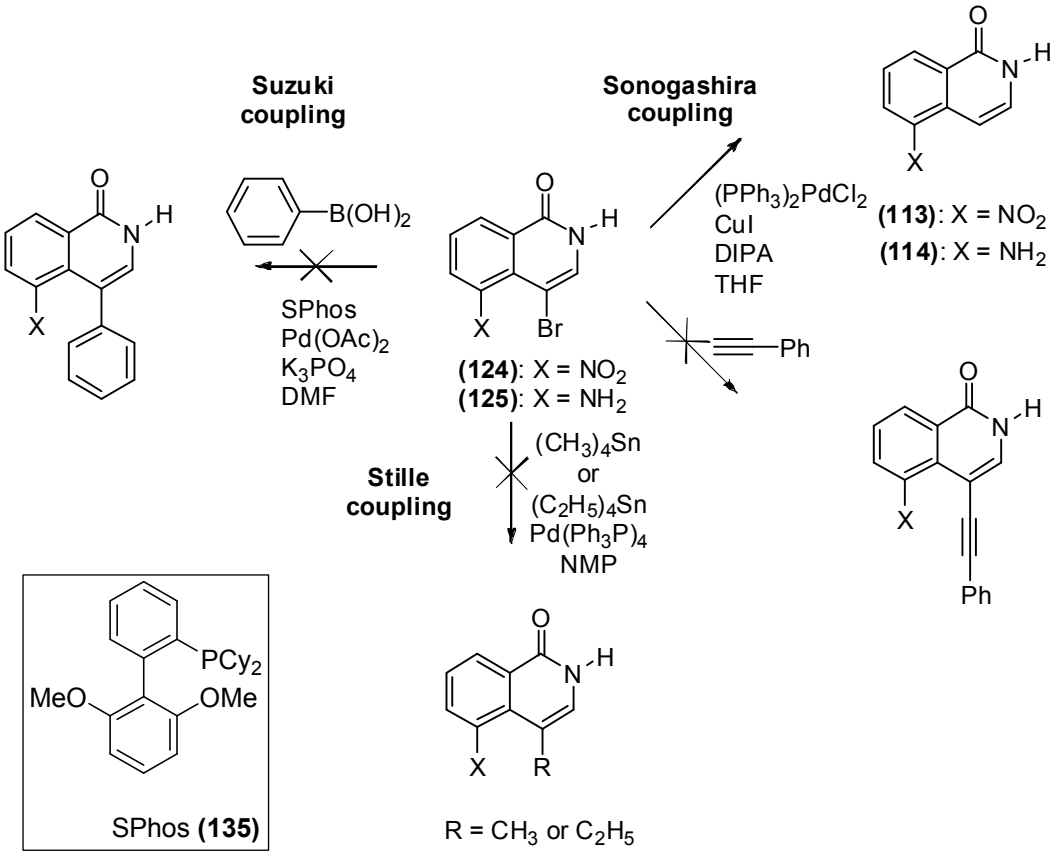

Scheme 31. Different organometallic cross-coupling reactions for introduction of substituents at the 4- position of 5-nitroisoquinolin-1-one **(124)** and 5-aminoisoquinolin-1-one **(125)**.

It was reasoned that the presence of the bulkier nitro group at the 5-position of **(124)** was hindering 4-bromo-5-nitroisoquinolin-1-one **(124)** to participate in any of the Pd(0) catalysed cross-coupling reactions. To overcome this problem, it was decided to carry out the reduction of the nitro group to the more slender amino group first and then perform the organometallic cross-coupling reactions. Thus, 4-bromo-5-nitroisoquinolin-1-one **(124)** was reduced with tin(II) chloride by heating at 70 ^oC in ethanol to give 4-bromo-5-aminoisoquinolin-1-one **(125)** in 54% yield.[150] Tin(II) chloride

was used to avoid any reductive debromination of the C-Br bond observed on treatment with Pd/C hydrogenations.

Analogously, the same set of reactions (Sonogashira and Stille) was repeated with **(125)**. Sonogashira reaction performed under standard conditions gave a mixture of unidentifiable products. Since no starting material was isolated we could speculate that product formed may not be stable under the conditions of the reaction. The Stille reaction was attempted with tetraethyltin in NMP in the presence of $Pd(PPh_3)_4$ in an inert atmosphere at 100 ^oC for 20 h. Among the products isolated were unreacted 4-bromo-5-aminoisoquinolin-1-one **(124)** and traces of debrominated compound **(114)**.

No apparent reasons could be concluded for the failure of 4-bromo-5-aminoisoquinolin-1-one **(125)** to undergo Pd(0) catalysed cross-coupling reactions. The inability to perform the organometallic cross-coupling reactions with both 4-bromo-5-nitroisoquinolin-1-one **(124)** and less hindered 4-bromo-5-aminoisoquinolin-1-one **(125)** meant that this route was no longer viable.

3.4 Route III: 4-Substituted 5-aminoisoquinolin-1(2*H*)-ones *via* intramolecular Heck coupling

3.4.1 Retrosynthesis

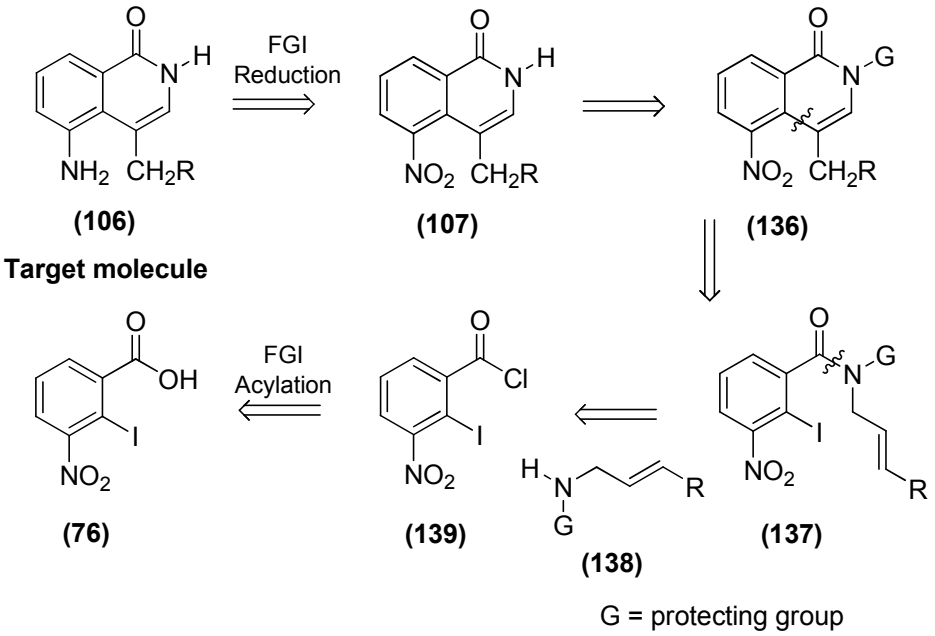

Scheme 32. Retrosynthetic analysis of the 4-substituted 5-aminoisoquinolin-1-ones.

The retrosynthetic analysis for the target molecule **(106)** is illustrated in Scheme 32. As usual, retrosynthesis began by first performing functional group interconversion (FGI) on the target molecule and this led to the corresponding 5-nitroisoquinolin-1-one **(107)**. This conversion, *i.e.* the reduction of the nitro group to amine (*via* hydrogenolysis or acid/metal reduction), is highly reliable and efficient. Formation of **(107)** involved removal of the protecting group G (allyl or benzhydryl) on nitrogen, which is introduced in order to facilitate the molecule adopting the correct reacting conformation about the amide C-N bond to allow cyclisation by intramolecular Heck coupling. Synthesis of **(136)** is achieved by an intramolecular Heck coupling / double bond migration of a 2-iodo-3-nitro-N-(alk-2-enyl)benzamide **(137)** as the key C-C bond-forming step in assembling the isoquinolinone. The C-N amide bond disconnection of **(137)** led to secondary amine **(138)**, with an N-protecting group and substitution at the alkene, and 2-iodo-3-nitrobenzoyl chloride **(139)**. The latter could be prepared from reaction of 2-iodo-3-nitrobenzoic acid **(76)** with thionyl chloride catalysed by DMF. The synthesis of **(76)** is outlined in section 3.1.2.

3.4.2 Synthesis of 2-iodo-3-nitrobenzoyl chloride

2-Iodo-3-nitrobenzoic acid **(76)** was converted into the acid chloride by treatment with thionyl chloride in the presence of catalytic DMF.

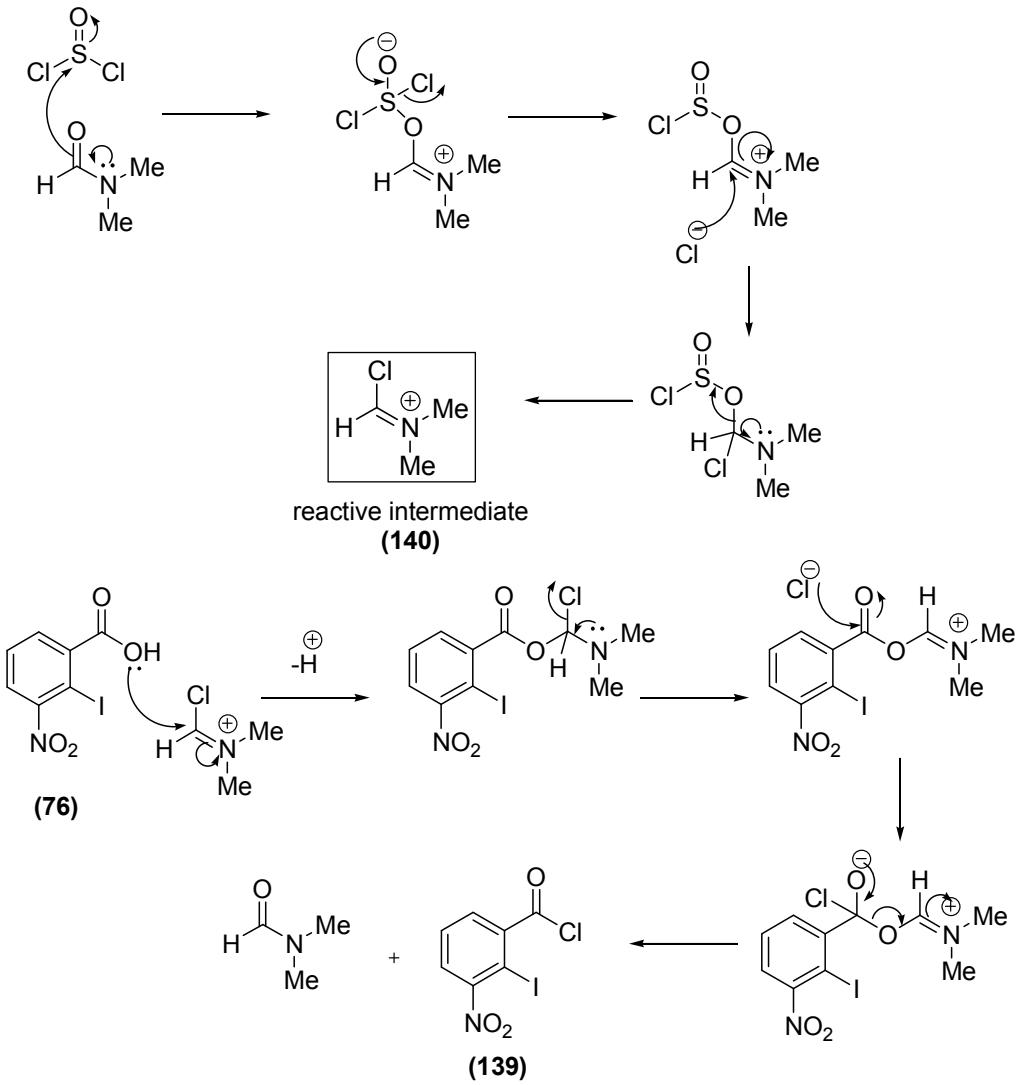

Scheme 33. Proposed mechanism for the $SOCl_2$-DMF-mediated synthesis of 2-iodo-3-nitrobenzoyl chloride **(139)**

The initial step in the mechanism is the formation of the reactive intermediate **(140)** by nucleophilic substitution of Cl^- (formed from reaction between $SOCl_2$ and DMF) at the carbonyl group (Scheme 33). The reactive intermediate is highly electrophilic and reacts rapidly with the carboxylic acid **(76)**, producing another intermediate which intercepts Cl^- to give the 2-iodo-3-nitrobenzoyl chloride **(139)** and regenerate DMF.

3.4.3 Formation of tertiary amides

In a secondary amide, the lowest energy conformation is likely to be *trans*. As shown in Figure 18, in the case of N-allyl-2-iodo-3-nitro-benzamide, the conformation required for intramolecular Heck coupling would thus be the higher energy *cis*-amide conformer **(143)**. In the tertiary amide **(141)**, with two N-allyl groups, one allyl group should always be in close proximity to the aryl ring. It was predicted that the other allyl group could be removed from the nitrogen later.

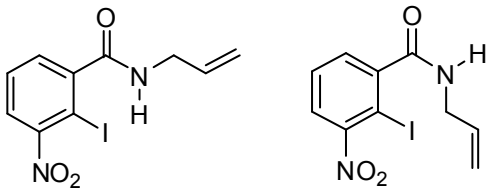

(142) **(143)**

Figure 18: Different conformations of N-allyl-2-iodo-3-nitrobenzamide **(143).**

Attempts to synthesise the tertiary amide **(141)** involved coupling reactions of 2-iodo-3-nitrobenzoyl chloride **(139)** with the appropriate amine. With N,N-diallylamine in the presence of two equivalents of triethylamine, **(139)** afforded N,N-di(prop-2-enyl)-2-iodo-3-nitrobenzamide **(141)** in good yield (75%) (Scheme 34).

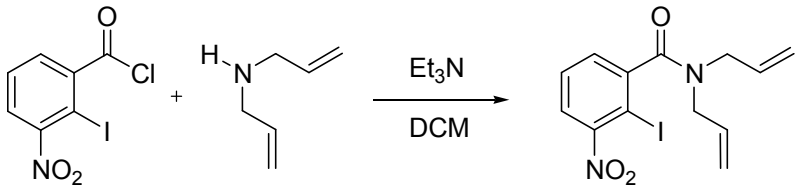

(139) **(141)**

Scheme 34. Preparation of N,N-di(prop-2-enyl)-2-iodo-3-nitrobenzamide **(141)**.

An MM2 energy minimisation for this compound **(141)**, however, suggested that the amide carbonyl should be approximately orthogonal to the benzene ring (Figure 19), owing to steric interactions with the large adjacent iodine. This would make the molecule chiral, with the asymmetric centre located in the centre of the Ar-C bond. This chirality means that not only are the two allyl groups inequivalent (owing to restricted amide C-N bond rotation) but the two aliphatic methylenes are also each in chiral environments. This was evident in the ^{1}H NMR spectrum, which showed different chemical shifts for the hydrogens of the two allyl side chains and that each CH_2 proton was diastereotopic.

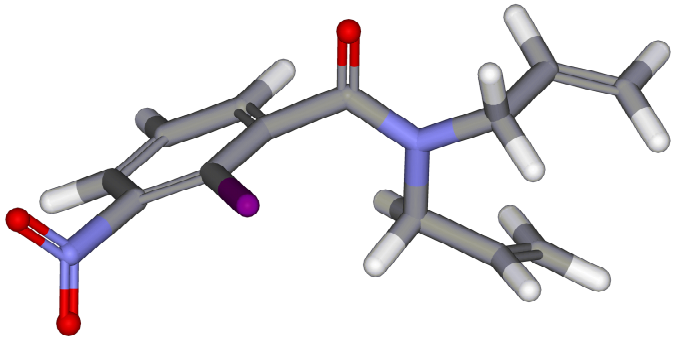

Figure 19: MM2-energy minimized model of N,N-di(prop-2-enyl)-2-iodo-3-nitrobenzamide **(141)**

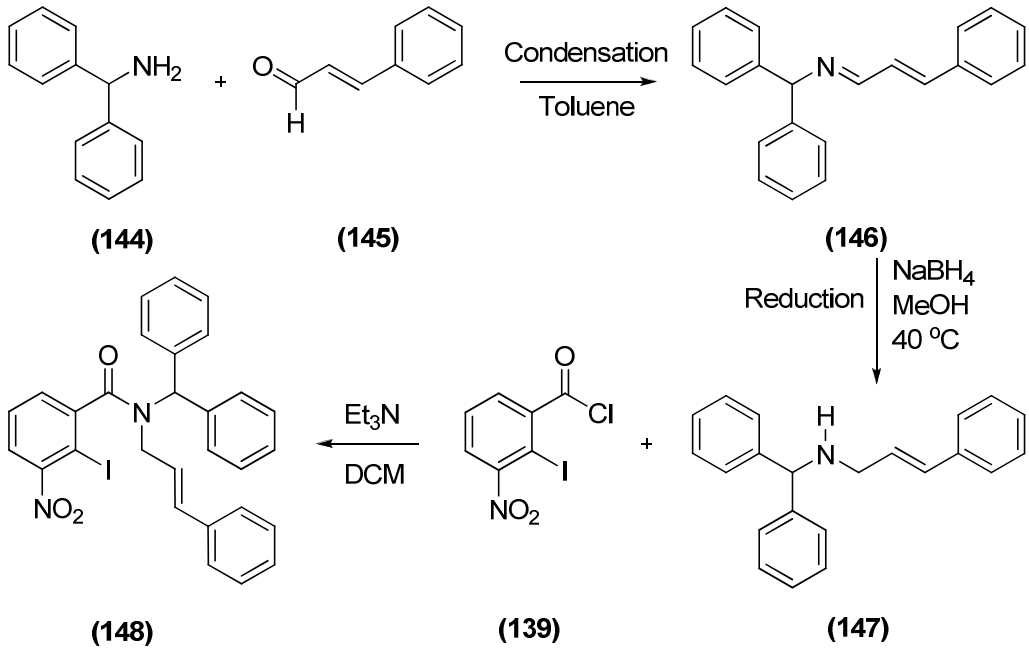

Scheme 35. Synthesis of N-diphenylmethyl-2-iodo-3-nitro-N-(3-phenylprop-2-enyl) benzamide **(148)**.

While cyclisation of N,N-di(prop-2-enyl)-2-iodo-3-nitrobenzamide **(141)** was expected to afford a 4-methyl substituent, a parallel effort was also directed to introduce a benzyl group into the 4-position of 5-aminoisoquinolin-1(*2H*)-one. For this synthesis a benzhydryl group was selected (bulkiness and predicted ease of removal) to restrict the rotation around the C-N bond, and to have a ring forming allyl group in close vicinity to the 2-position of the arene. To prepare the required secondary amine, aminodiphenylmethane **(144)** was condensed with cinnamaldehyde **(145)** in toluene in a Dean-Stark apparatus until the calculated amount of water had separated.[194] The product, (*E*)-diphenyl-N-(3-phenylprop-2-enylidene) methanamine **(146)** was formed in good yield (97%). Selective reduction of the imine of **(146)** with excess sodium

borohydride in MeOH also gave a good yield (95%) of the secondary amine (*E*)-N-diphenylmethyl-3-phenylprop-2-en-1-amine **(147)**. This, on coupling with 2-iodo-3-nitrobenzoyl chloride **(139)**, formed the Heck cyclisation precursor (*E*)-N-diphenylmethyl-2-iodo-3-nitro-N-(3-phenylprop-2-enyl)benzamide **(148)** in moderate yield (54%) (Scheme 35).

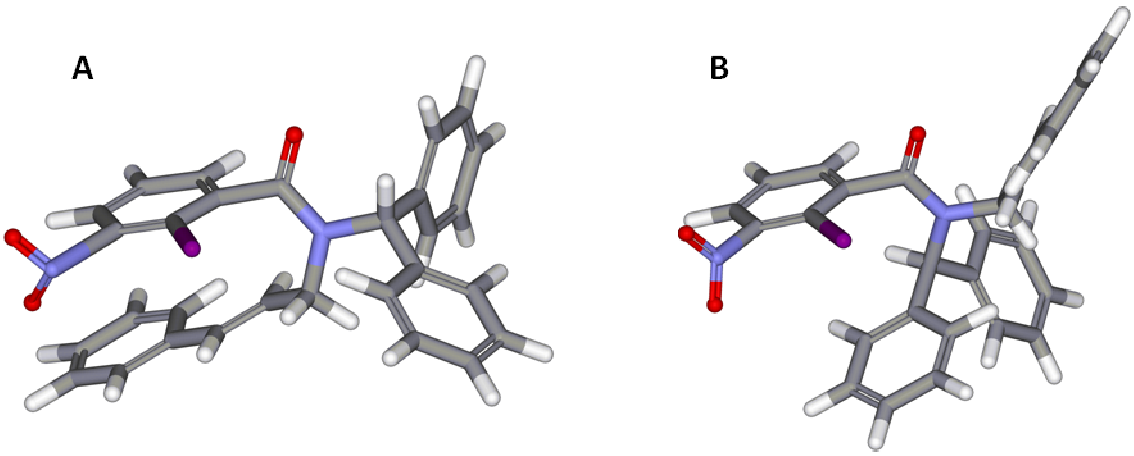

Figure 20. MM2-energy minimized models of (*E*)-N-diphenylmethyl-2-iodo-3-nitro-N-(3-phenylprop-2-enyl)benzamide **(148)**.

The structure of **(148)** was characterised by ^{1}H NMR, ^{13}C NMR, HMQC, HMBC, MS and CHN analyses. The MM2 molecular modelling studies of this compound **(148)** showed two low energy rotamers arising from rotation about C-N bond (Figure 20). Both rotamers are also chiral. Model A shows intramolecular stacking of 2-iodo-3-nitrobenzyl ring and 3-phenylprop-2-enyl rings. Model B is the result of flipping over the 3-phenylprop-2-enyl ring. The dihedral angle calculated C(15)-N(13)-C(7) was 175 Å. The ^{1}H NMR spectra of **(148)** also indicated the presence of two rotamers resulting from different conformations of side chains in space. The NMR spectrum showed a 3:4 mixture of rotamers α and β about the amide double bond and magnetic inequivalence of the diastereotopic CH_2 protons in each rotamer. Figure 21 shows assignment of ^{1}H NMR signals for N-3-phenylprop-2-enyl chain of **(148)**. It is evident that propenyl 2-H and 3-H were in *trans* configuration as shown by the coupling constant J = 16.0 Hz. Interestingly the chemical shift for CH_2 protons of α rotamer was at δ 3.91, whereas for the β rotamer the chemical shifts were different for the geminal protons (multiplet at δ 3.93 and double doublet at δ 4.81 with J value of 14.5 and 5.5). This was assigned with the help of two-dimensional HMQC (^{1}H-^{13}C COSY) spectrum (Figure 22).

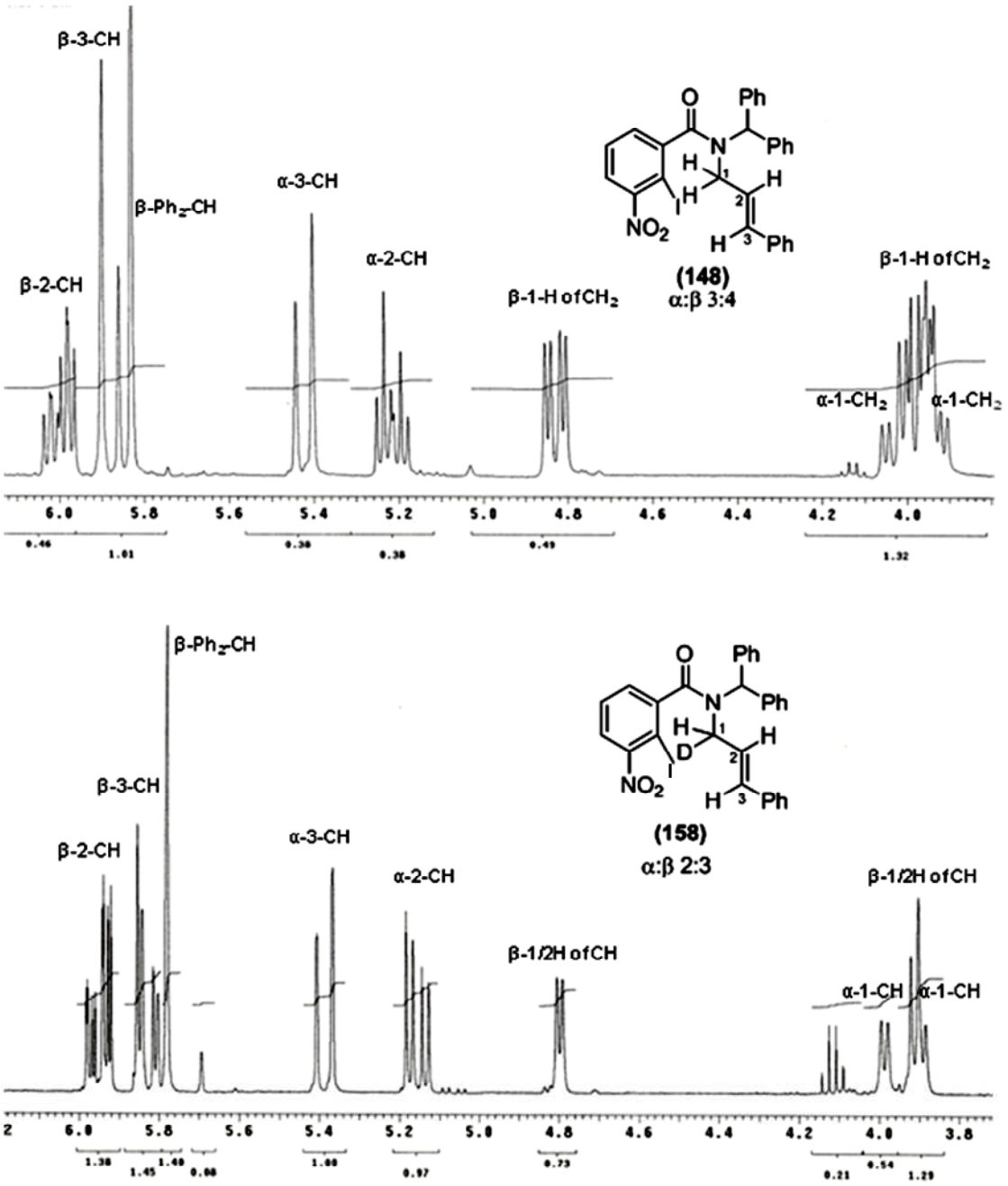

Figure 21. Assignment of ^{1}H NMR signals for N-3-phenylprop-2-enyl chain of **(148)** and its deuterated analogue **(158)**.

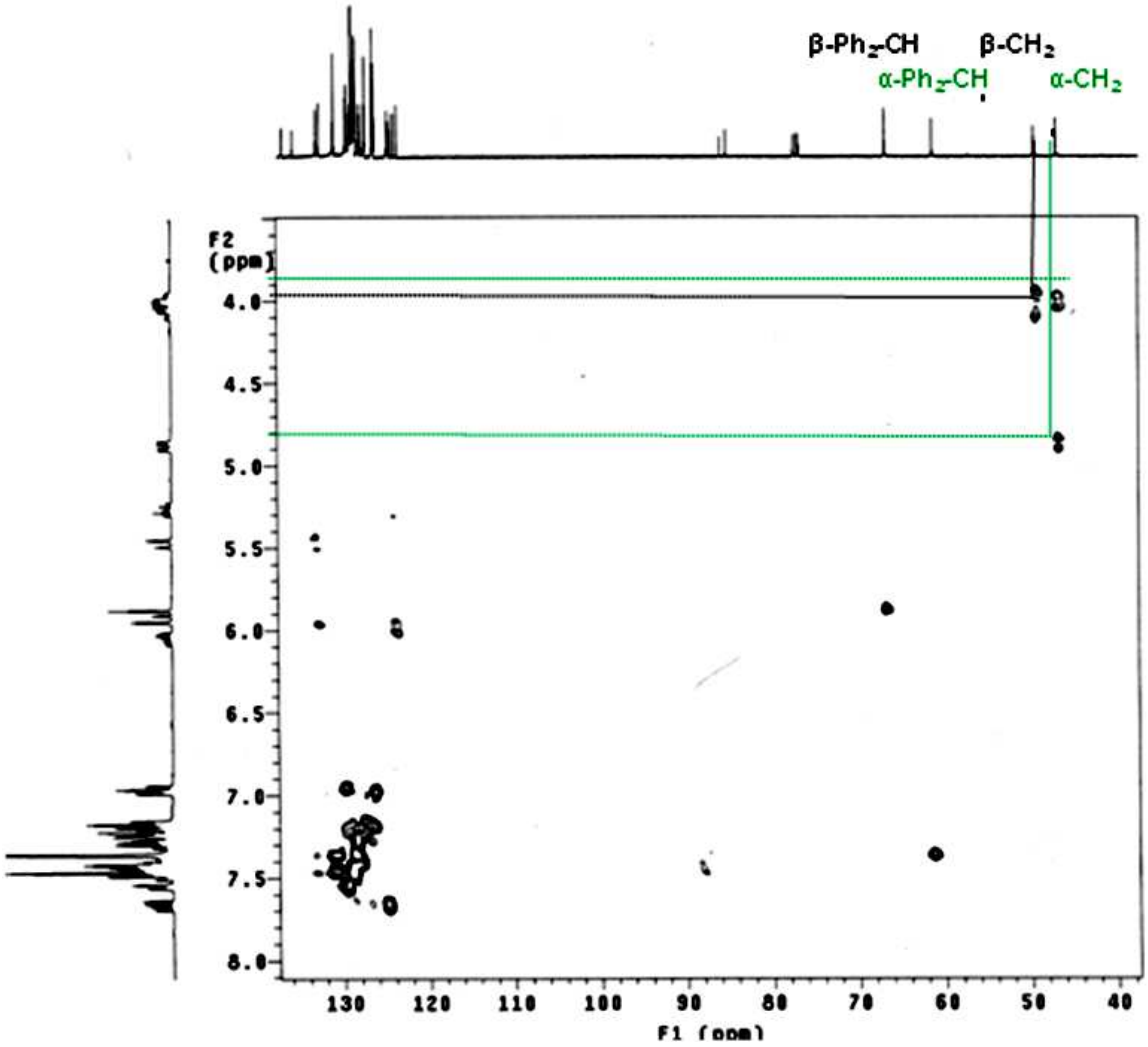

Figure 22. ^{1}H-^{13}C COSY spectrum of (*E*)-N-diphenylmethyl-2-iodo-3-nitro-N-(3-phenylprop-2-enyl)benzamide **(148)**

3.4.4 C=C Bond migration and intramolecular Heck cyclisations

The Heck reaction has shown to be very useful for the preparation of especially disubstituted olefins. This is a versatile carbon-carbon bond-forming reaction which allows desirable functionalities to be attached across alkenes. In this palladium-catalysed reaction, the carbon–carbon bond is formed from a vinyl functionality and an aryl and (or) alkyl halide or triflate. The intramolecular Heck coupling reaction is also palladium-catalysed and couples an alkene with the halide in the same molecule to form a new cyclic alkene. This reaction has been well-established as a powerful tool for the construction of polycyclic structures and quarternary carbon stereocentres. The first intramolecular Heck reaction was reported by Mori and Ban in 1977.[195] This reaction is catalysed by Pd(0) complexes of phosphines such as $Pd(PPh_3)_4$ and Pd(II) complexes like $Pd_2(dba)_3$ and $Pd(OAc)_2$. The base used could be a mild one like Et_3N, NaOAc or aqueous Na_2CO_3. Coordinating and polar solvents, such as DMF, MeCN, NMP and

DMSO are preferred.[166] Palladium complexes are also known to catalyse the migration of C=C double bonds in allyl systems (*e.g.* removal of Alloc protecting groups). Thus it was planned that reaction of the N-allyl-2-iodobenzamides (**141** and **148**) with Pd catalysts would first allow migration of the double bond into conjugation with the amide nitrogen, and then Heck cyclisation to furnish 4-substituted 5-nitroisoquinolin-1-ones.

Initial experiments used catalytic amounts (5 mol%) of $Pd(PPh_3)_4$ with Et_3N in refluxing MeCN (80 ^oC) or EtCN (100 °C) (Scheme 36). Treatment of N,N-di(prop-2-enyl)-2-iodo-3-nitro-benzamide **(141)** with $Pd(PPh_3)_4$ and Et_3N in refluxing MeCN for 48 h gave the Heck-cyclised isomers 2-(prop-2-enyl)-4-methyl-5-nitroisoquinolin-1(*2H*)-one **(149)** and 2-(prop-2-enyl)-4-methylene-5-nitro-3,4-dihydroisoquinolin-1(*2H*)-one **(150)** in good total yield (79%). The former (required) isomer results from C=C migration followed by cyclisation, whereas the latter is formed by Heck coupling without prior C=C migration. These isomers were not separable by column chromatography. The ^1H NMR spectrum of the mixture revealed that the populations of **(149)** and **(150)** were in the ratio of 1:2. The required isomer **(149)** was the minor product of this reaction and could not be isolated for further reactions (*N*-deallylation and reduction of the 5-nitro functional group) to synthesise 5-amino-4-methylisoquinolin-1(*2H*)-one. Figure 23 shows ^1H-^1H COSY spectrum of **(149)** and **(150)**. The propenyl 2-H of both compounds formed cross peaks between propenyl 1-H and propenyl 3-H, thus making assignment of protons for the propenyl side chain possible.

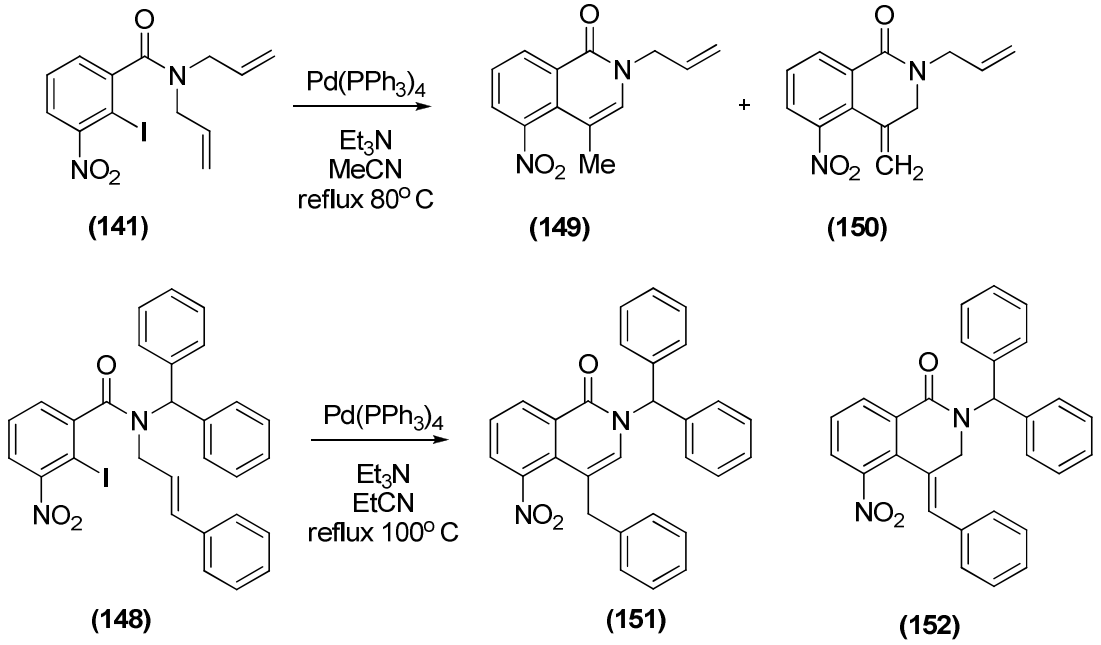

Scheme 36. Intramolecular Heck cyclisations of N,N-di(prop-2-enyl)-2-iodo-3-nitrobenzamide **(141)** and (*E*) N-diphenylmethyl-2-iodo-3-nitro-*N*-(3-phenylprop-2-enyl) benzamide **(148)**.

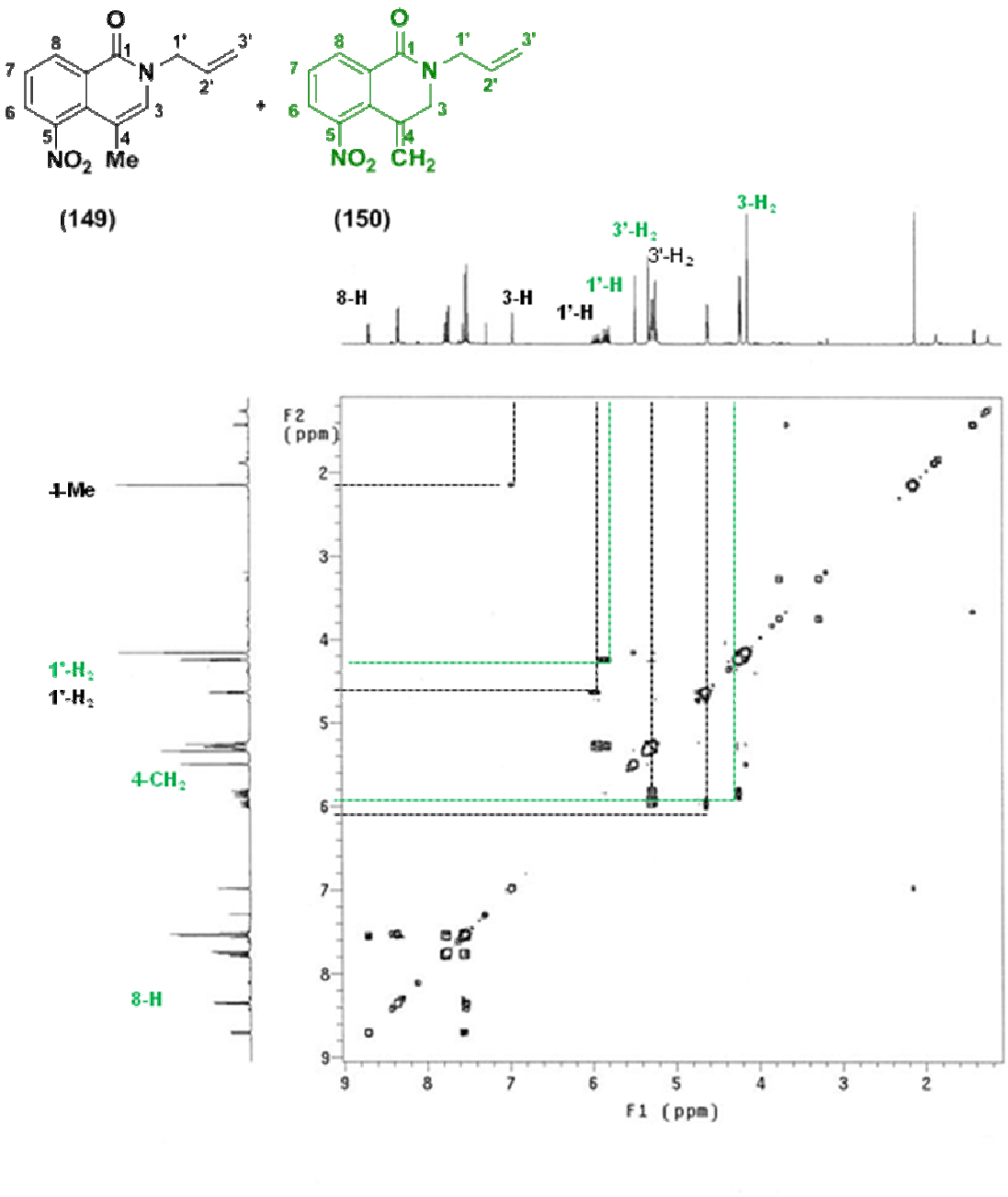

Figure 23. ^{1}H-^{1}H COSY spectrum of 1:2 mixture of 2-(prop-2-enyl)-4-methyl-5-nitroisoquinolin-1(*2H*)-one and **(149)** and 2-(prop-2-enyl)-4-methylene-5-nitro-3,4-dihydroisoquinolin-1(*2H*)-one **(150)**.

Similarly, intramolecular Heck coupling of the other iodobenzamide aryl iodide, (*E*)-N-diphenylmethyl-2-iodo-3-nitro-N-(3-phenylprop-2-enyl)benzamide **(148)** with $Pd(PPh_3)_4$ and Et_3N in refluxing EtCN for 48 h afforded the isomers 2-diphenylmethyl-5-nitro-4-phenylmethylisoquinolin-1(*2H*)-one **(151)** and (*Z*)-4-benzylidene-2-diphenylmethyl-5-nitro-3,4-dihydroisoquinolin-1(*2H*)-one **(152)** in moderate total yield (41%). Use of EtCN allows heating at higher temperature. *i.e* 100 ^{o}C. Again, these compounds could not be separated using column chromatography. A series of NMR experiments (NOESY, COSY, HMQC, HMBC) allowed the assignment of signals corresponding to each

isomer. These isomers were found to be present in the ratio of 1:3. As seen in the spectra in Figure 24, signals for protons on the two phenyl rings of benzhydryl group were overlapping and were difficult to assign. From the ^{1}H-^{1}H COSY spectrum, it was evident that there was *ortho*-coupling between 8-H and 7-H (adjacent protons on the ring) and between 6-H and 7-H in both the compounds. Cross peaks were observed due to long range coupling of 3-H and 4-CH_2 protons in **(151)** and 3-H_2 and 4-CH in **(152)**.

Surprisingly, when the cyclisations of **(148)** were repeated under the same conditions but for 2 h, the overall yield was unchanged but the ratio of isomers changed markedly as **(152)** was formed as the major product while desired **(151)** was formed only in traces. This observation suggested that Heck cyclisation may have preceded migration of the C=C in the formation of **(151)**.

The Heck reaction mechanism involves the following four steps[196] (Scheme 37).

1. oxidative addition
2. carbopalladation
3. β-hydride elimination or dehydropalladation
4. reductive elimination

Palladium (0) in $Pd(PPh_3)_4$ undergoes oxidative addition with suitable substrates such as halides resulting in the active catalytic unit, *i.e.* coordinatively unsaturated, 14-electron species PdL_2 palladium(II) complex. This would seem reasonable since PdL_2 is electron-rich and nucleophilic in character and has vacant sites so that the organic electrophile R_1X can undergo oxidative addition to give the R_1PdXL_2 **(153)** intermediate in which the R group (aryl or vinyl) is σ-bonded to the Pd(II). The resulting σ alkyl bond in such complexes is very reactive, especially towards carbon-carbon π bonds. Thus an alkene in the reacting system will lead to coordination followed by migratory insertion into the palladium-carbon σ bond. This process is called carbopalladation as carbon and palladium are attached to the ends of the alkene system. In this step, ligand dissociates to allow coordination of the alkene and associate to provide a stable product **(154)**. Dehydropalladation or β-hydride elimination from this molecule results in the product alkene and catalytically inactive $HPdXL_2$ species. A base then regenerates the palladium(0) catalyst by reductive elimination of HX.

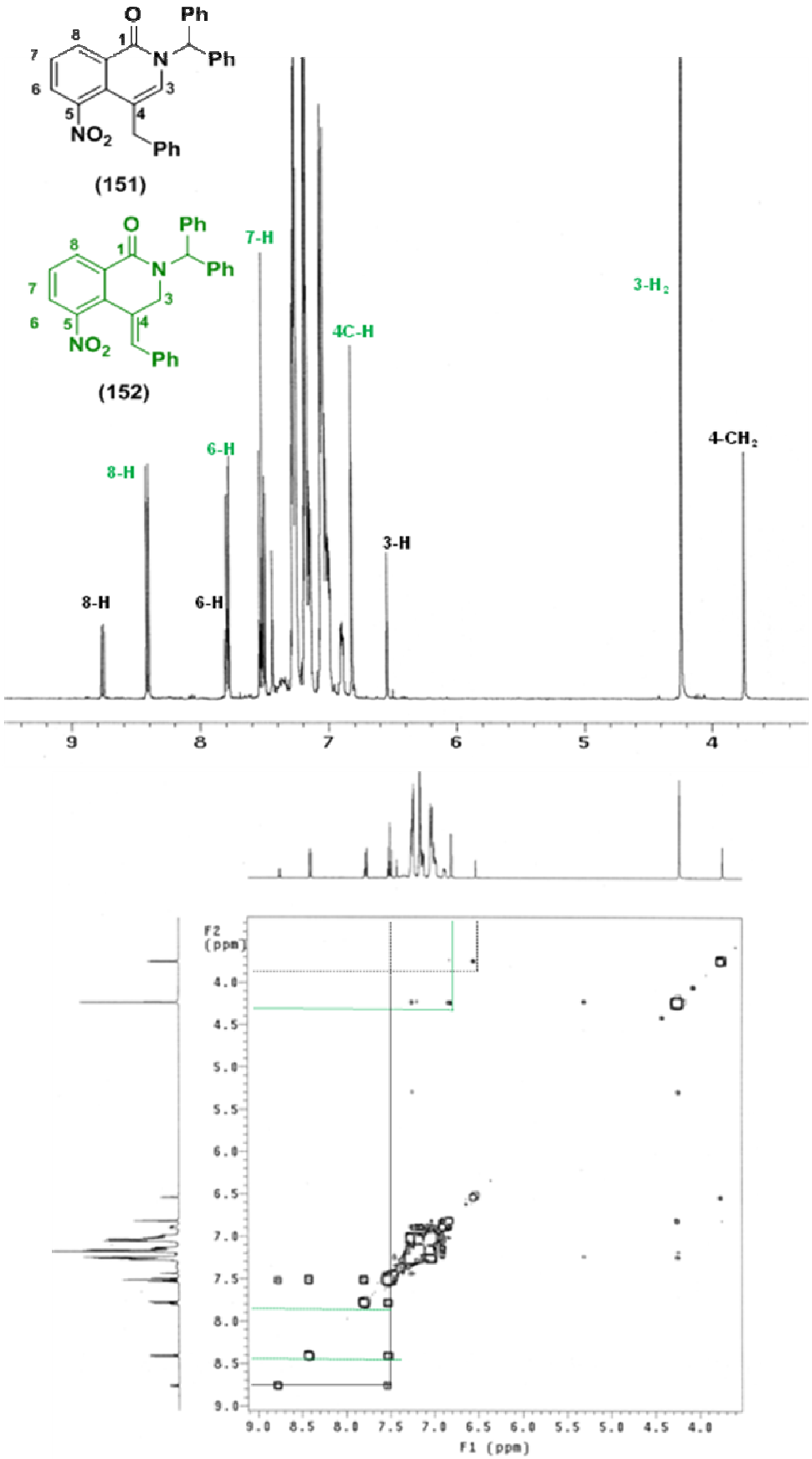

Figure 24. ^{1}HNMR and ^{1}H-^{1}H COSY spectra of 1:3 mixture of 2-diphenylmethyl-5-nitro-4-benzylisoquinolin-1(*2H*)-one **(151)** and (*Z*)-4-benzylidene-2-diphenylmethyl-5-nitro-3,4-dihydroisoquinolin-1(*2H*)-one **(152)**.

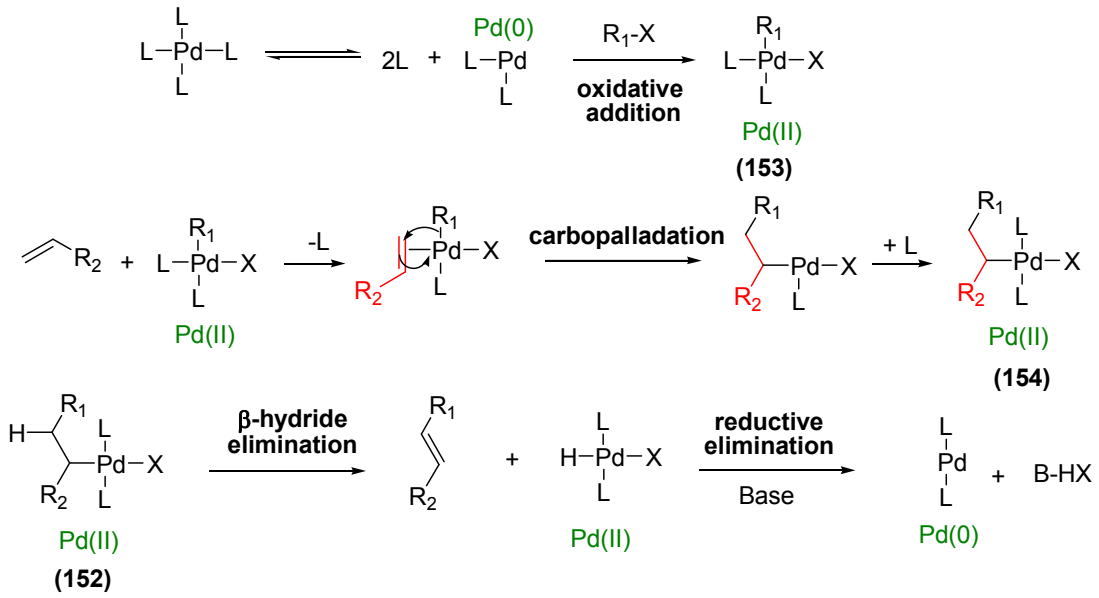

Scheme 37. Proposed general mechanism for the Heck reaction

The major problem observed in this intramolecular Heck cyclisation is the efficiency of the palladium-catalysed migration of the carbon-carbon double bond along the alkyl chain. In the mechanism proposed the order of the two steps (Heck cyclisation, C=C migration was unclear (Scheme 38). The reaction follows Route A if there is no double bond migration resulting in exocyclic 4-alkylidine-5-nitro-3,4-dihydroisoquinolin-1-one **(155)** as the product. In the case of double bond migration, the reaction proceeds according to Route B, thus forming the desired endocyclic 4-alkyl-5-nitroisoquinolin-1-one **(156)**.

However, it is known that, in many cases, further reaction of the initial products, *i.e.* isomerisation of double bonds, occurs to form thermodynamically more favoured alkenes. To check if migration of the double bond may occur after Heck cyclisation a mixture of isomers 2-(prop-2-enyl)-4-methyl-5-nitroisoquinolin-1(*2H*)-one **(149)** and 2-(prop-2-enyl)-4-methylene-5-nitro-3,4-dihydroisoquinolin-1(*2H*)-one **(150)** in the ratio (1:2) was exposed to the initial reaction conditions. Examination of the products by NMR revealed that there was no change in the ratio of isomers, suggesting either that product isomers were not interconvertible or that the 1:2 ratio of compounds with endocyclic or exocyclic C=C was the ratio at equilibrium.

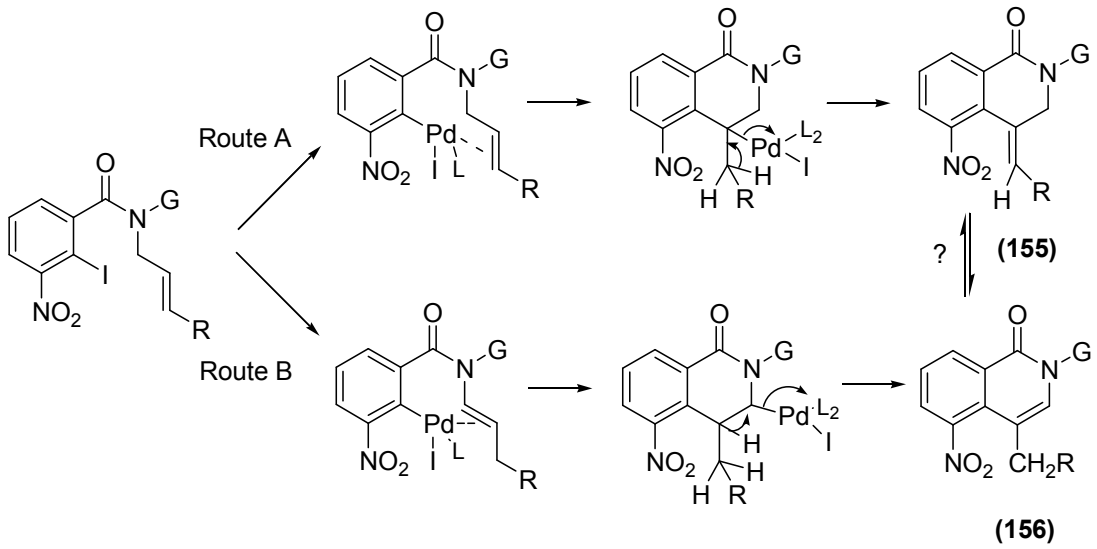

Scheme 38. Mechanism proposed for the formation of 4-alkyl-5-nitroisoquinolinones and 4-alkylidine-5-nitro-3,4-dihydroisoquinolinones by intramolecular Heck cyclisation.

3.4.5 Deuterium tracing study

These contrasting observations prompted an isotopic labelling study to study the order of the two steps (Heck coupling, C=C migration) in the reaction. Deuterium was introduced in a $NaBD_4$ reduction of **(146)** in MeOH. The resulting (*E*)-N-diphenylmethyl-1-deutero-3-phenylprop-2-en-1-amine **(157)** was coupled with 2-iodo-3-nitrobenzoyl chloride **(139)** in CH_2Cl_2 in the presence of Et_3N. (*E*)-N-Diphenylmethyl-2-iodo-3-nitro-N-(1-deutero-3-phenylprop-2-enyl)benzamide **(158)** was formed in moderate yield (61%) (Scheme 39). Analogously to **(148)**, the ^1H NMR spectrum of **(158)** indicated the presence of two rotamers about the amide C-N bond (α:β 2:3). However, **(158)** is racemic with respect to the CHD centre, which was reflected in the spectrum (Figure 21).

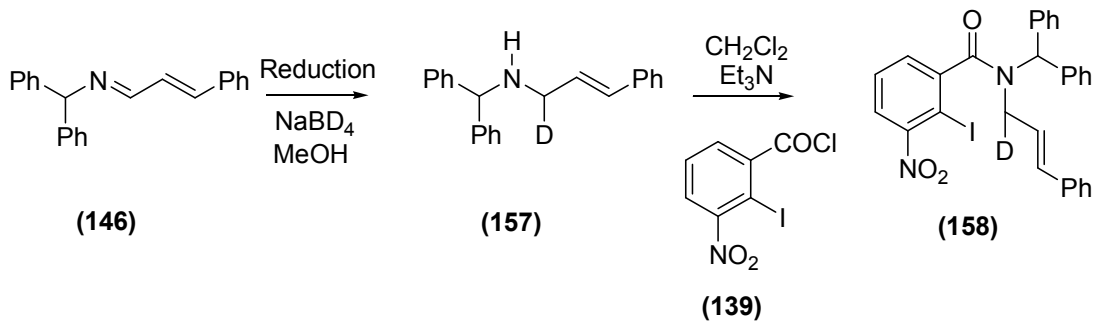

Scheme 39. Deuterium labelling reactions to give (*E*)-N-diphenylmethyl-2-iodo-3-nitro-N-(1-deutero-3-phenylprop-2-enyl)benzamide **(158)**.

Double bond migration / Heck reaction of **(158)** with $Pd(Ph_3P)_4$ and Et_3N in refluxing MeCN for 2 h gave an equimolar mixture of isotopomers **(162)** and **(151)** (minor products) and a single isotopomer **(161)** (major product).

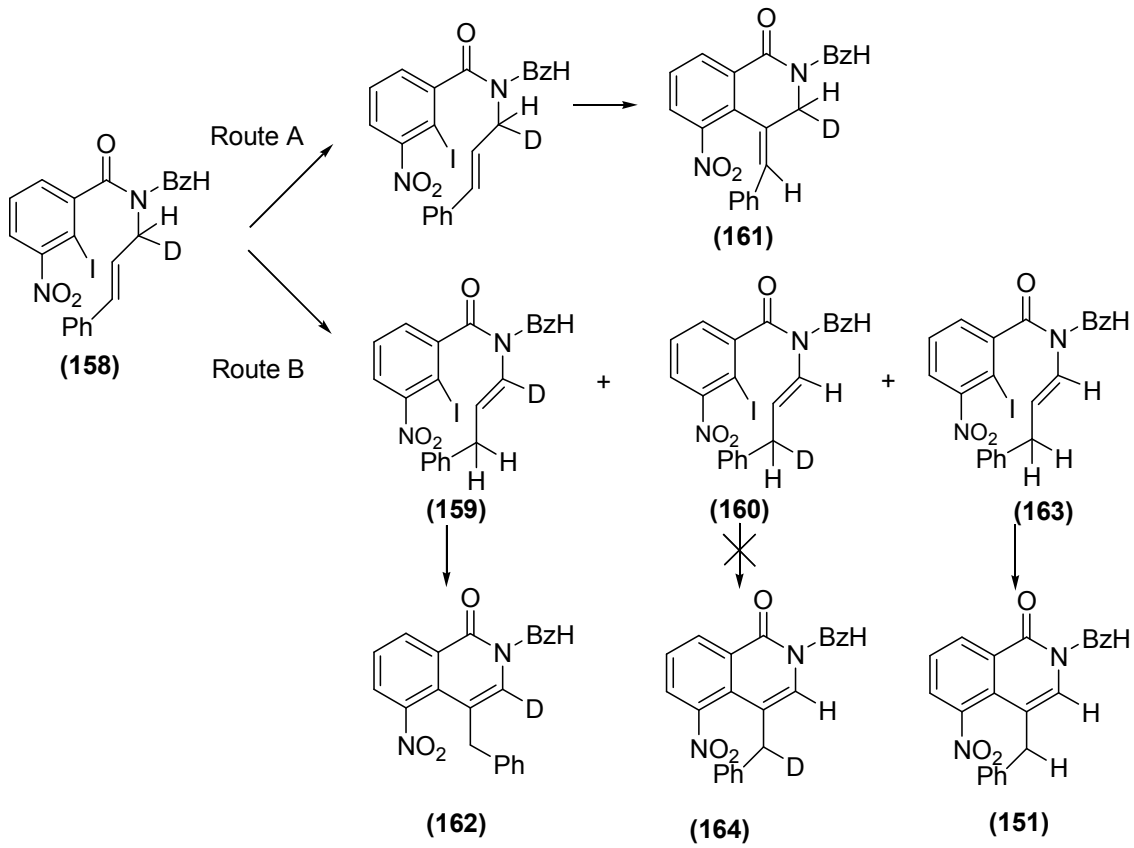

Scheme 40. Heck cyclisation of (*E*)-N-diphenylmethyl-2-iodo-3-nitro-N-(1-deutero-3-phenylprop-2-enyl)benzamide.

It was reasoned that a change of solvent to MeCN (b.p. 80 ^{o}C) might slow down the reaction and isolation of unreacted mono-D isotopomer would be possible to study probable double bond isomerisation and the isotopic composition of unreacted starting material (to help detect any kinetic deuterium isotope effect in the double bond migration). Reaction was stopped before completion and again the same trend (equimolar mixture of isotopomers **(162)** and **(151)** (minor products) and a single isotopomer **(161)** (major product)) of products was observed along with some unreacted starting material. All recovered starting material **(158)** carried one deuterium at the original position, showing that molecules were committed to cyclisation once they had reacted initially with Pd. All the 4-benzylidine-2,3-dihydroisoquinolone product contained one deuterium located at position-3 **(161)**, with no material which either contained no deuterium or had migrated (which would have been located at PhCD=). Failure to isolate any of the double-bond migrated mono-D isotopomer **(164)** suggests that C=C migration in the starting material is slow relative to ring-closure under these

conditions. In the mechanism outlined in Scheme 40, (*Z*)-4-benzylidene-2-diphenylmethyl-3-deutero-5-nitro-3,4-dihydroisoquinolin-1(*2H*)-one **(161)** was formed following route A (no double bond migration). If the C=C migration takes place and the reaction follows route B, then there are three possible intermediates: **(159)** formed by migration of H, **(160)** formed by migration of D and **(163)** formed by loss of deuterium and introduction of "migrated" H from a different source were predicted. None of the above *intermediates* were isolated.

Cyclisations of these intermediates were expected to give **(162)** **(164)** and **(151)**, respectively. However, formation of an equimolar mixture of isotopomers 2-diphenylmethyl-3-deutero-5-nitro-4-phenylmethylisoquinolin-1(*2H*)-one **(162)** and 2-diphenylmethyl-5-nitro-4-phenylmethylisoquinolin-1(*2H*)-one **(151)** suggested that reaction proceeds *via* the intermediates **(159)** and **(163)** only. Thus deuterium does not appear to migrate, possibly owing to a large kinetic deuterium isotope effect. Formation of **(151)** from **(163)** indicates loss of deuterium during the process and introduction of H from a different source. Failure to form any of **(164)** rules out the migration of deuterium.

One of the measures taken to slow down the Heck cyclisation is to replace iodine with the less reactive leaving group bromine. It was expected that replacement of iodine with bromine and use of MeCN as solvent will slow the reaction, and isolation of intermediates would be more straightforward. This approach may also allow more time for double bond migration to occur before cyclisation. The synthetic route for the preparation of the aryl bromide, (*E*)-2-bromo-N-diphenylmethyl-3-nitro-N-(1-deutero-3-phenylprop-2-enyl) benzamide is presented in Scheme 41. 2-Bromo-3-nitrobenzoic acid **(165)** was satisfactorily synthesised through mercuration (mercury(II) acetate) and bromination (sodium bromide/bromine) of 3-nitrophthalic acid and this gave a white solid in good yield (66%). 2-Bromo-3-nitrobenzoyl chloride **(166)** was prepared from **(165)** by treatment with thionyl chloride in the presence of catalytic DMF. This, on coupling with (*E*)-N-diphenylmethyl-1-deutero-3-phenylprop-2-en-1-amine **(157)** in CH_2Cl_2 in the presence of Et_3N, gave (*E*)-2-bromo-N-diphenylmethyl-3-nitro-N-(1-deutero-3-phenylprop-2-enyl) benzamide **(167)** in moderate yield (54%). Again, the NMR spectrum showed a 2:3 mixture of rotamers α and β about the amide bond.

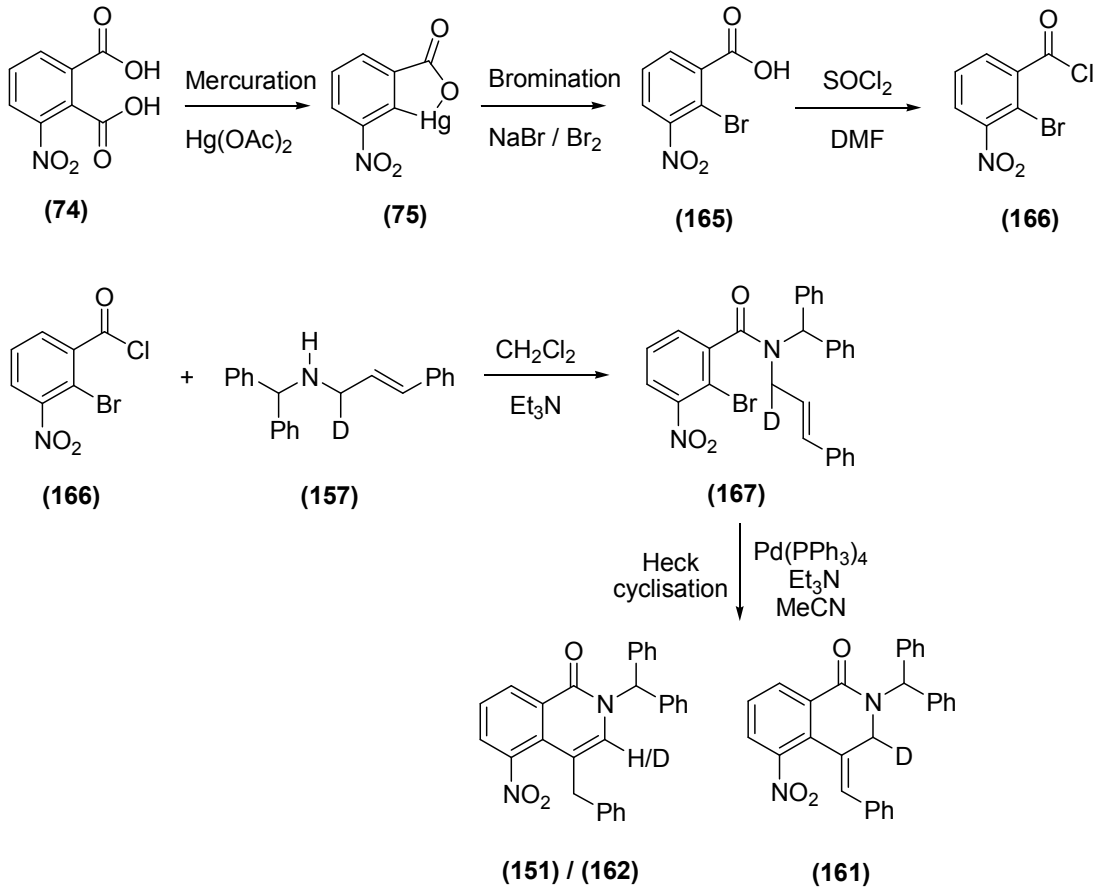

Scheme 41. Synthetic route for the preparation and double-bond migration / Heck cyclisation of (*E*)-2-bromo-N-diphenylmethyl-3-nitro-N-(1-deutero-3-phenylprop-2-enyl) benzamide **(163)**.

Intramolecular Heck reaction of **(167)** was carried out with $Pd(Ph_3P)_4$ and Et_3N in refluxing MeCN. After 48 h, along with the unreacted starting material **(167)**, an equimolar mixture of isotopomers **(162)** and **(151)** (minor products) and a single isotopomer **(161)** (major product) were isolated. The repeated failure to isolate the double-bond-migrated mono-D isotopomer intermediate despite the formation of double-bond-migrated products of cyclisation **(151)** / **(162)** was most puzzling. This observation is again consistent with the migration of the C=C after Heck cyclisation, *i.e*. the Br is not sufficiently slower in coupling to allow migration before coupling. Attempts to remove the benzhydryl group on nitrogen of (*Z*)-4-benzylidene-2-diphenylmethyl-5-nitro-3,4-dihydroisoquinolin-1(*2H*)-one **(152)** using trifluoroacetic acid were unsuccessful.

3.4.6 Synthesis of secondary amides

As explained in section 3.4.3 it was reasoned that secondary amides should be disfavoured for intramolecular Heck coupling. However, owing to the complications involved with removal of the protecting groups (allyl and benzhydryl) in tertiary amides, it was decided to investigate secondary amides instead of tertiary amides. Thus, the synthesis of secondary amides was undertaken. The first one to be synthesised was 2-iodo-3-nitro-N-(prop-2-enyl)benzamide **(143)**, which was prepared by coupling prop-2-en-1-amine with 2-iodo-3-nitrobenzoyl chloride **(139)** in the presence of two equivalents of Et_3N at room temperature for 2 h (Scheme 42). The product was isolated in good yield (71%). An interesting by-product 3-nitro-N-(prop-2-enyl)-2-(prop-2-enylamino)benzamide **(168)** was also isolated (10%) from the reaction.

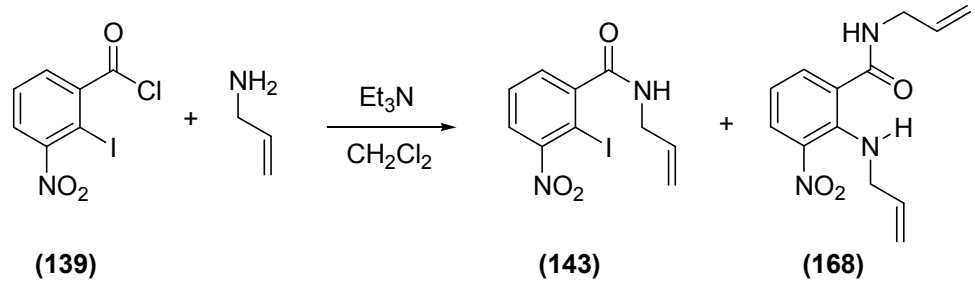

(139) **(143)** **(168)**

Scheme 42. Preparation of 2-iodo-3-nitro-N-(prop-2-enyl)benzamide **(143)**.

Compound **(168)** was formed as a result of S_NAr (nucleophilic aromatic substitution) reaction of the very activated 2-iodo-3-nitro-N-(prop-2-enyl)benzamide **(143)**. In this addition-elimination mechanism (Scheme 43), the electron-withdrawing nitro and carbonyl functional groups positioned *ortho* to the halide leaving group activate the ring towards nucleophilic attack. Prop-2-en-1-amine acts as a nucleophile and displaces iodine, a good leaving group, on the aromatic ring.

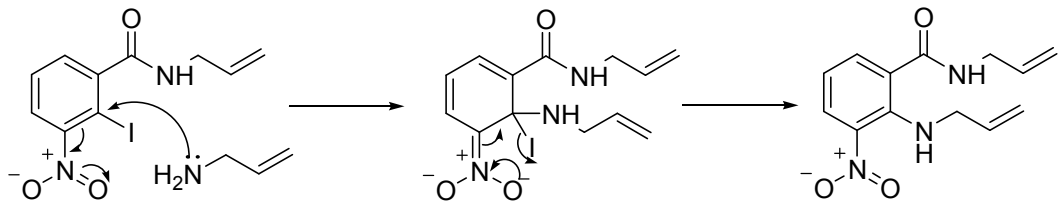

(143) **(168)**

Scheme 43. S_NAr addition-elimination mechanism proposed to form **(168)**.

The ^{1}H NMR spectrum of **(168)** showed broad singlets for each NH, one at δ 6.82 corresponding to the NH attached to the benzene ring, and another further downfield at δ 7.72 for the NH of the carboxamide. The structure of **(168)** was confirmed by X-ray crystallographic analysis (Figure 25). Interestingly, despite the presence of neighbouring nitro and secondary amide groups, no intramolecular hydrogen-bonding interactions were observed from the amine N-H in the crystal structure of **(168)**. Intermolecular hydrogen-bonding was observed between the carbonyl oxygen and carboxamide N-H of the neighbouring molecule.

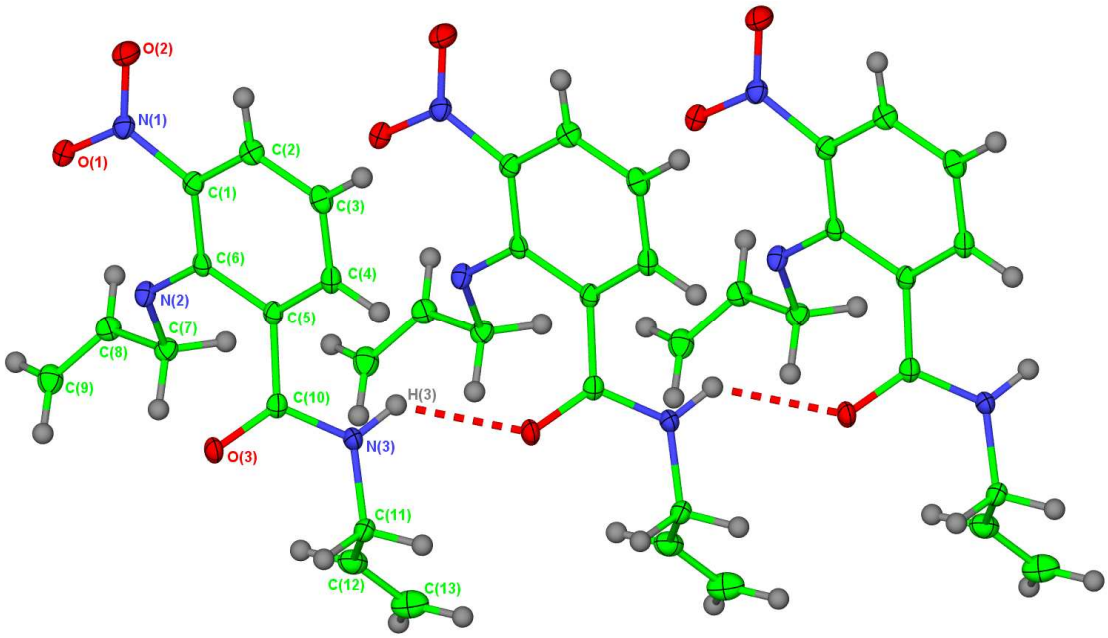

Figure 25. X-ray crystal structure of 3-nitro-N-(prop-2-enyl)-2-(prop-2-enylamino)benzamide **(168)** with crystallographic numbering.

3.4.7 Alternative approach to 4-substituted 5-aminoisoquinolin-1-ones *via* a Pinner reaction

With the secondary amide **(143)** in hand, slight modification of the synthetic approach to 4-substituted-5-aminoisoquinolin-1-ones was attempted. In this newly proposed route (Scheme 44), introduction of a methyl group on the carbonyl oxygen was attempted to avoid problems of rotation about the carboxamide bond. Once this was done, Heck cyclisation on (*E*)-methyl N-allyl-2-iodo-3-nitrobenzimidate **(169)** was expected to furnish 1-methoxy-4-methyl-5-nitroisoquinoline. Demethylation with HBr / HOAc or with trimethylsilyl iodide would give 4-substituted-5-nitro isoquinolin-1-one **(107)** which, on reduction with tin(II) chloride, would give the target **(106)**.

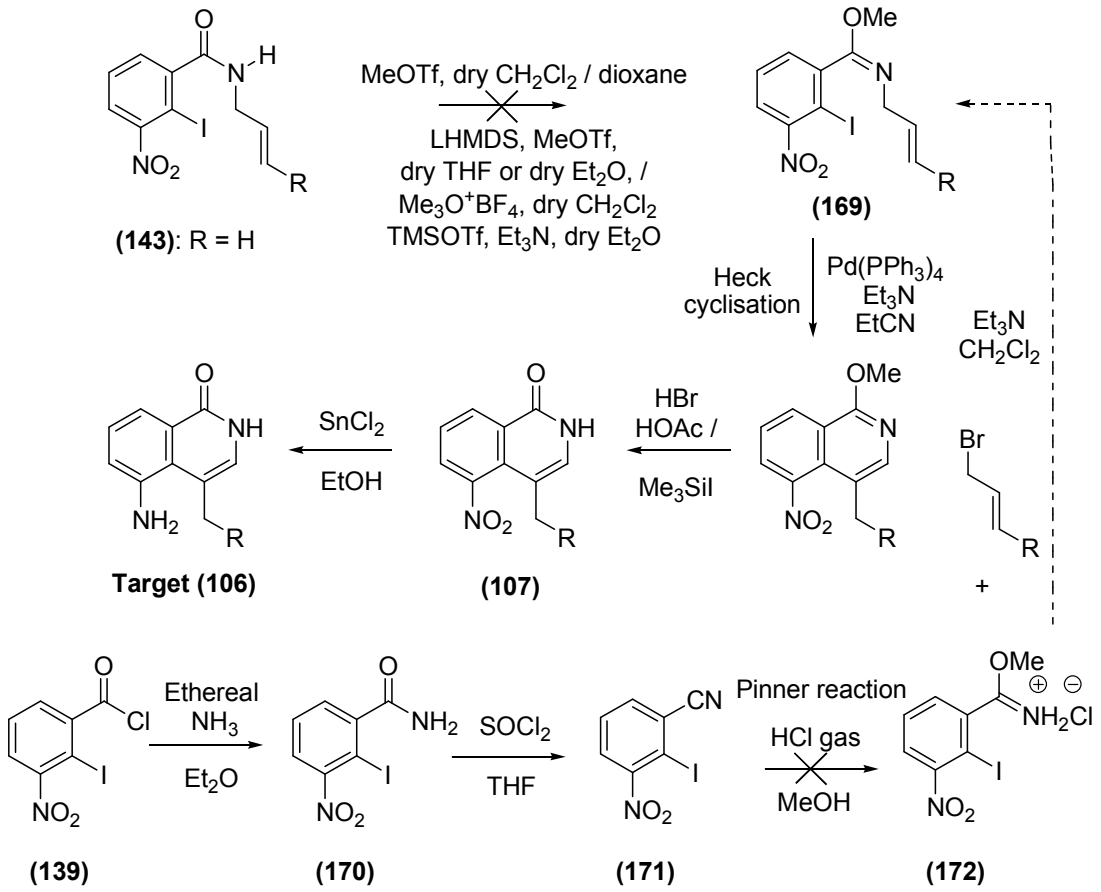

Scheme 44. Proposed alternative synthetic approach to target **(106)** *via* a Pinner reaction.

Methylation was attempted on the secondary amide **(143)** using the powerful methylating agent and hard electrophile methyl trifluoromethanesulfonate (MeOTf) in CH_2Cl_2. The reaction did not proceed as expected. Change of solvent to dioxane did not alter the outcome. In a further experiment the anion was generated with the strong non-nucleophilic base LHMDS but failed to react with the MeOTf. Attempts with trimethyloxonium tetrafluoroborate and TMSOTf followed the same outcome. The inability to synthesise (*E*)-methyl N-allyl-2-iodo-3-nitrobenzimidate **(169)** prompted us to look for alternative routes. This led us to explore the Pinner reaction where a nitrile is converted to the hydrochloric acid salt of an imino ester or an alkyl imidate, on reaction with alcohol under acid catalysis. To carry out this reaction, 2-iodo-3-nitrobenzonitrile **(171)** was needed. This was easily achieved in excellent yield from acid chloride **(139)**, *via* dehydration of its corresponding amide **(170)**, as shown in Scheme 44. The Pinner reaction is the partial solvolysis of a nitrile to yield an iminoether (Scheme 45). N-Alkylation with 3-bromoprop-1-ene should furnish (*E*)-methyl N-allyl-2-iodo-3-nitrobenzimidate **(169)**.

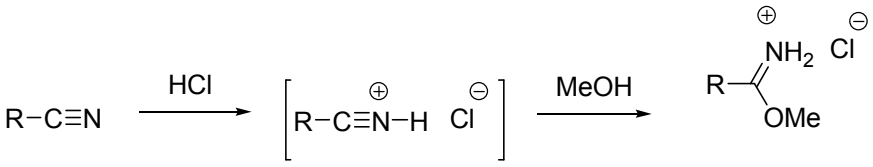

Scheme 45. General mechanism proposed for Pinner reaction

Surprisingly, treatment of the 2-iodo-3-nitrobenzonitrile **(171)** with gaseous HCl in anhydrous MeOH did not furnish the imidate salt as expected. Only the starting material was recovered from the reaction. Change of acid to stronger trifluoroacetic acid also gave the same result. Failure to synthesise (*E*)-methyl N-allyl-2-iodo-3-nitrobenzimidate **(169)** meant that the route outlined in Scheme 44 was no longer viable.

3.4.8 Synthesis and Heck cyclisations of prop-2-enyl-2-iodo-3-nitrobenzoate

In our continuing efforts to optimise the reaction conditions for Heck cyclisation we decided to synthesise the ester prop-2-enyl-2-iodo-3-nitrobenzoate **(173)** and conduct the intramolecular cyclisation on this ester, which should not suffer from conformational problems. The ester **(173)** was easily synthesised by reaction of acid chloride **(139)** with prop-2-en-1-ol in CH_2Cl_2 in good yield (64%) (Scheme 46). Intramolecular Heck cyclisation under the initial conditions ($Pd(Ph_3P)_4$, Et_3N in refluxing EtCN for 2 d gave the starting material unchanged. Change of solvent to DMF and base to N,N-diisopropylethylamine (DIPEA) and refluxing at 150 ^oC for 24 h resulted in formation of N,N-dimethyl-3-nitrobenzamide **(174)** as sole product. DMF at high temperatures (150 ^oC) for a long time (24 h) breaks down to dimethylamine and carbon monoxide. Under such strong reducing conditions deiodination takes place and the dimethylamine displaces the ester thus forming **(174)**.

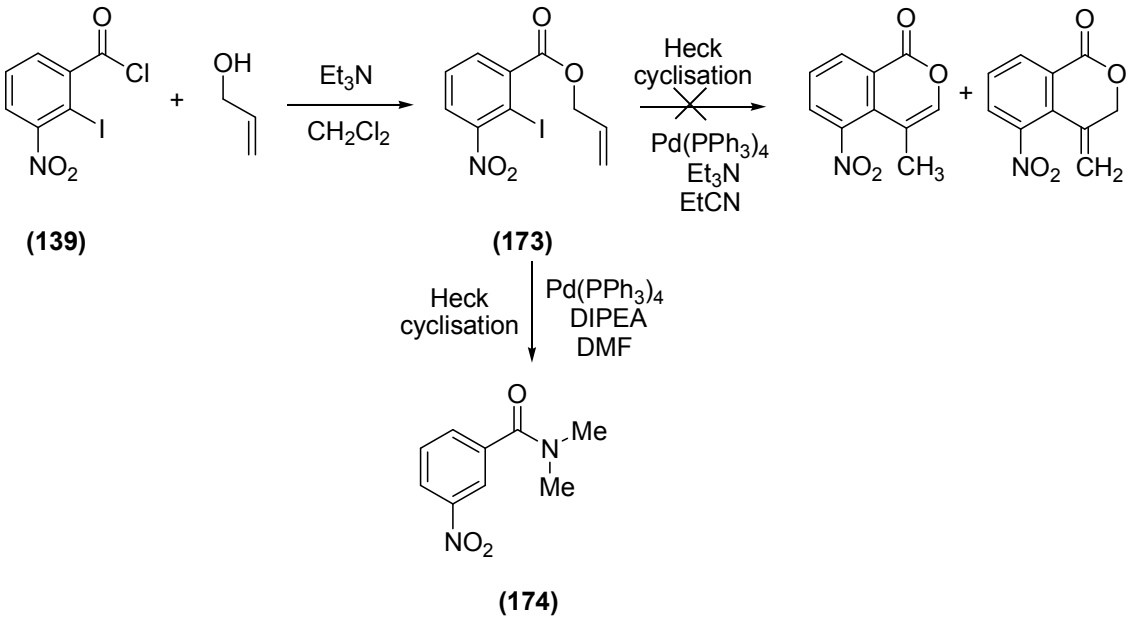

Scheme 46. Synthesis and Heck cyclisations of prop-2-enyl-2-iodo-3-nitrobenzoate **(173)**.

3.4.9 Secondary amides and improved conditions for Heck cyclisations

As discussed in section 3.4.6, synthesis of secondary amides was required to carry out the intramolecular Heck cyclisation. 2-Iodo-3-nitro-N-(prop-2-enyl)benzamide **(143)** was prepared by coupling prop-2-en-1-amine with 2-iodo-3-nitrobenzoyl chloride **(139)** in the presence of Et_3N (Scheme 42). The Heck reaction of this secondary amide **(143)** with ($Pd(Ph_3P)_4$, Et_3N, boiling EtCN, 24 h) gave the dehalogenated amide 3-nitro-N-(prop-2-enyl)benzamide **(175)**, the C=C migrated and dehalogenated amide (*E*)-3-nitro-*N*-(prop-1-enyl)benzamide **(176)** and an inseparable mixture of the target 4-methyl-5-nitroisoquinolin-1(2*H*)-one **(177)** and 4-methylene-5-nitro-3,4-dihydroisoquinolin-1(2*H*)-one **(178)** in 1:1 ratio (Scheme 47).

Larock *et al*[197] reported the synthesis of various other nitrogen heterocycles *via* palladium-catalysed intramolecular Heck cyclisation and stated that 2% $Pd(OAc)_2$ in the presence of Bu_4NCl (phase-transfer catalyst), DMF and appropriate base (Na_2CO_3, NaOAc or Et_3N) forms excellent catalytic systems. Keeping this finding in mind, in an alternative approach, $Pd(Ph_3P)_4$, Et_3N and Bu_4NCl were used in DMF at various temperatures to cyclise **(143)**.

- At 50 ^oC after 48 h, the reaction was not complete. However, **(177)** and **(178)** were formed in **1:1** ratio along with dehalogenated amide **(175)**.
- At 100 ^oC after 48 h, the ratio of **(177)** to **(178)** was the more favourable **2.5:1**. The reaction was not complete as some of the starting material was also isolated along with dehalogenated amide **(175)**.

- At 150 °C after 16 h, the reaction was complete, with target 4-methyl-5-nitroisoquinolin-1(2*H*)-one **(177)** as the sole product in 66% yield. In this reaction, $Pd(Ph_3P)_4$, Et_3N and Bu_4NCl in DMF were mixed in the flask which was placed in a preheated oil bath at 150 °C. The compound to be cyclised **(143)** was added later. This was done since these reactions indicated that C=C migration required higher temperatures and that deiodination occurs even at low temperatures.

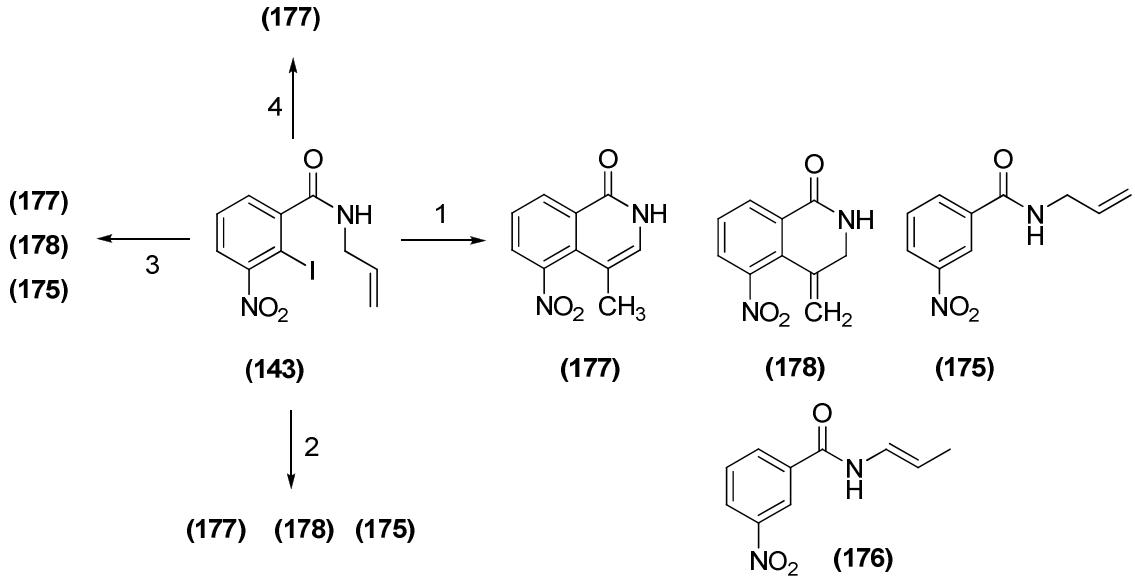

Scheme 47. Various reaction conditions attempted for the synthesis of 4-Methyl-5-nitroisoquinolin-1(2*H*)-one **(177)**. Numbers on the arrows indicate the reaction conditions and temperatures used in individual reactions as entered in table 14.

Entry	Reaction conditions	Temperature in °C	Products	Ratio of **(172)** to (**173)**
1	5 mol% $Pd(Ph_3P)_4$, EtCN, Et_3N (2 equiv.)	100	**(175), (176), (177), (178)**	1:1
2	2 mol% $Pd(Ph_3P)_4$, DMF, Bu_4NCl (1 equiv.) Et_3N (2 equiv.)	50	**(175), (177), (178)**	1:1
3	2 mol% $Pd(Ph_3P)_4$, DMF, Bu_4NCl (1 equiv.) Et_3N (2 equiv.)	100	**(175), (177), (178)**	2.5:1
4	2 mol% $Pd(Ph_3P)_4$, DMF, Bu_4NCl (1 equiv.) Et_3N (2 equiv.)	150 (fast heating)	**(177)**	

Table 14. Different reaction conditions employed for Heck cyclisation of **(143)**.

Dehalogenation to form **(175)** was a commonly observed phenomenon in Pd-catalysed couplings and is a result of decomposition of the intermediate aryl palladium, which had failed to undergo cyclisation and subsequent protonation.[198] It was observed that 2 mol% $Pd(Ph_3P)_4$, Bu_4NCl (1 equiv.) and Et_3N (2 equiv.) in DMF refluxing at 150 ^oC is the best reaction condition, and it was decided to follow the same for further intramolecular Heck cyclisations.

3.4.10 Double bond isomerisation study

Recently, some ruthenium and rhodium complexes were reported to catalyse the isomerisation of N-allylamides to the corresponding 1-propenyl derivatives.[199,200] Following this protocol, double-bond isomerisation of 2-iodo-3-nitro-N-(prop-2-enyl)benzamide **(143)** was carried out using 0.5% $RuClH(CO)(PPh_3)_3$ in benzene at 80 ^oC for 3 h. The double-bond-migrated product (*E*)-2-iodo-3-nitro-*N*-(prop-1-enyl)benzamide **(179)** was formed in excellent yield (96%) (Scheme 48). The reaction could be described as being *E*-selective as the *Z*-enamide was detected only in traces. This is the result of a specific coordination of the metal atom by the substrates and products of double-bond migration.[200]

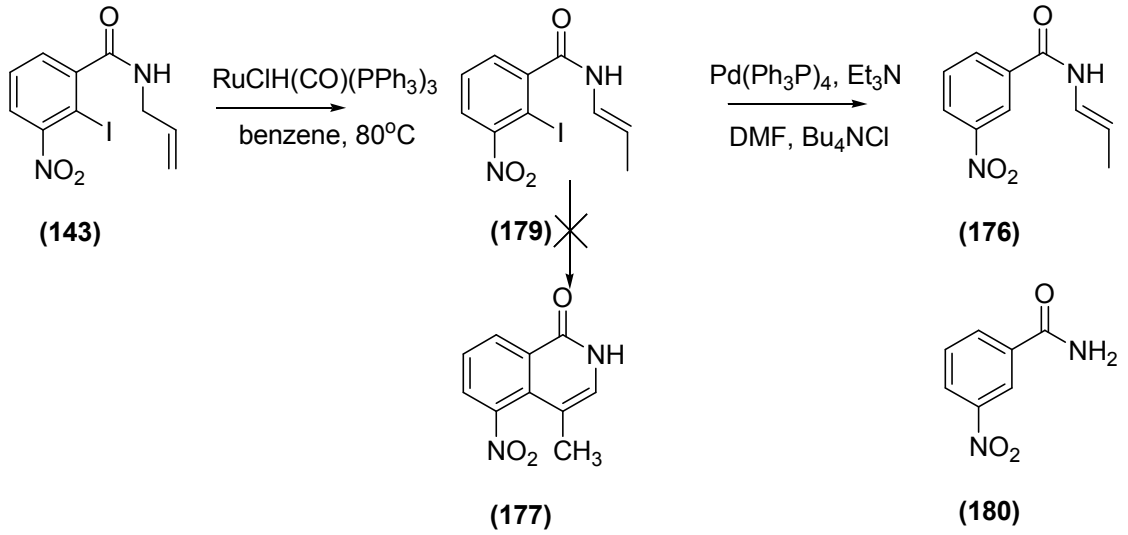

Scheme 48. Double bond isomerisation of 2-iodo-3-nitro-N-(prop-2-enyl)benzamide **(143)** to (*E*)-2-iodo-3-nitro-*N*-(prop-1-enyl)benzamide **(179)** and attempted Heck cyclisation of **(179)**.

To test whether this prior C=C bond migration might enhance the formation of 4-methyl-5-nitroisoquinolin-1(2*H*)-one **(177)**, Heck cyclisation was carried out according to the modified conditions (2 mol% $Pd(Ph_3P)_4$, Bu_4NCl (1 equiv.) and Et_3N (2 equiv.) in DMF refluxing at 150 ^oC). Curiously, **(179)** failed to cyclise under Pd-catalysis; the dehalogenated amide **(176)** and 3-nitrobenzamide **(180)** were among the products

isolated (Scheme 48). The reaction when repeated at 100 ^{o}C, resulted in isolation of unreacted starting material along with **(176)** and **(180)**. Formation of dehalogenated amide **(176)** could be explained as a result of decomposition of the intermediate aryl palladium, which had failed to undergo cyclisation and subsequent protonation. Compound 3-nitrobenzamide **(180)** might have formed by decomposition of amide **(176)**. Interestingly, the much anticipated cyclised compound **(177)** was not formed.

Now that optimum conditions for Heck cyclisation had been established, the tertiary amides **(141)** and **(148)** were investigated using the same protocol. The tertiary amides **(141)** and **(148)** also gave greater proportions of the desired 4-substituted isoquinolin-1-one isomer under the modified conditions. Compound **(141)** gave **(149)** and **(150) (8:1)** and **(148)** gave **(151)** and **(152) (3:1**).

Repetitions of Heck cyclisations of **(143)** in larger scales (0.25 g) under the modified conditions were found to give 78% of inseparable mixtures of 4-methyl-5-nitro-isoquinolin-1(2*H*)-one **(177)** isomer along with the undesired, 4-methylene-5-nitro-3,4-dihydroisoquinolin-1(2*H*)-one **(178)** in 5:1 ratio. The deiodinated amide **(175)** was formed in 19% yield. This led us to conclude that these tandem double bond migration / Heck cyclisations under the modified conditions may be scale-sensitive.

Further exploring this reaction, we decided to introduce a Boc protecting group on the amide nitrogen of **(143)**. This was done keeping in mind the bulky nature of Boc group in the tertiary imide which might direct the ring-forming allyl group to be in close vicinity to the 2-iodo group, thus increasing the rotamer population favoured for the Heck cyclisation. The Boc group should also improve solubility. This was accomplished by using $(Boc)_2O$, and DMAP in the presence of Et_3N in good yield (92%). The Heck cyclisation of *tert*-butyl N-prop-2-enyl-N-(2-iodo-3-nitrobenzoyl)carbamate **(181)** resulted in **(177)** and **(178)** in the ratio of 1:1 (Scheme 49). It was thought that thermal loss of N-Boc occurred only after cyclisation as the ratio of **(177)** and **(178)** was not 5:1 as in the previous experiment, where the Boc group was absent.

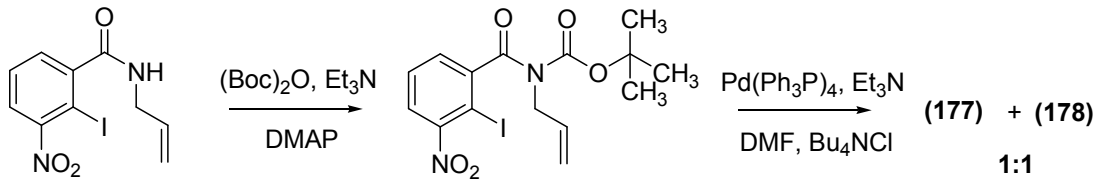

(143) **(181)**

Scheme 49. Introduction of N-Boc protection and Heck cyclisation of **(181)**.

Having successfully synthesised 4-methyl-5-nitroisoquinolin-1(2*H*)-one **(177)**, attempts were then made to reduce selectively the nitro function *via* catalytic hydrogenation with 10% palladium on charcoal (Pd/C) and hydrogen in the presence of few drops of conc. HCl in ethanol (Scheme 50). The product, 5-amino-4-methylisoquinolin-1(2*H*)-one hydrochloride **(182)** was isolated in excellent yield (70%) as buff crystals. Thus, the first 4-substituted analogue of 5-AIQ had been synthesised.

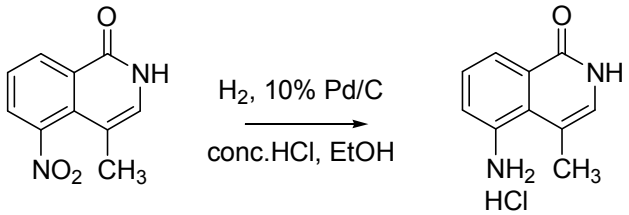

(177) **(182)**

Scheme 50. Reduction of nitro function of **(177)** to form 5-amino-4-methylisoquinolin-1(2*H*)-one hydrochloride **(182)**.

3.4.11 Synthesis of 5-amino-4-benzylisoquinolin-1*(2H)*-one

Following the successful synthesis of 5-amino-4-methylisoquinolin-1(2*H*)-one hydrochloride **(182)**, attention was now focussed towards introducing a benzyl group at the 4-position. For this, it was necessary to couple (*E*)-3-phenylprop-2-en-1-amine **(185)** with 2-iodo-3-nitrobenzoyl chloride **(139)**. Since compound **(185)** was not commercially available, the preliminary aim was to synthesise this primary amine. Nucleophilic substitution of (*E*)-(3-bromoprop-1-enyl)benzene with the potassium salt of trifluoroacetamide which was prepared *in situ* from trifluoroacetamide and potassium *t*-butoxide in dry THF, gave *(E)*-N-(3-phenylprop-2-enyl)2,2,2-trifluoroacetamide **(184)** (33%).[201] A lower yield of (7%) highly lipophilic ion-pair of *(E)*-3-phenylprop-2-enylamine trifluoroacetate salt **(183)** was also isolated. The N-trifluoroacetyl (N-TFA) group was

considered as it is easily removed by nucleophiles (ammonia, sodium carbonate) to generate the primary amines. The trifluoroacetamide **(184)** was cleaved either by ammonia in methanol or by reduction with sodium borohydride in ethanol to furnish *(E)*-3-phenylprop-2-enylamine **(185)**. This primary amine, on coupling with the acid chloride **(139)**, afforded *(E)*-2-iodo-3-nitro-N-(3-phenylprop-2-enyl)benzamide **(186)** in good yield (74%) as yellow crystals (Scheme 51).

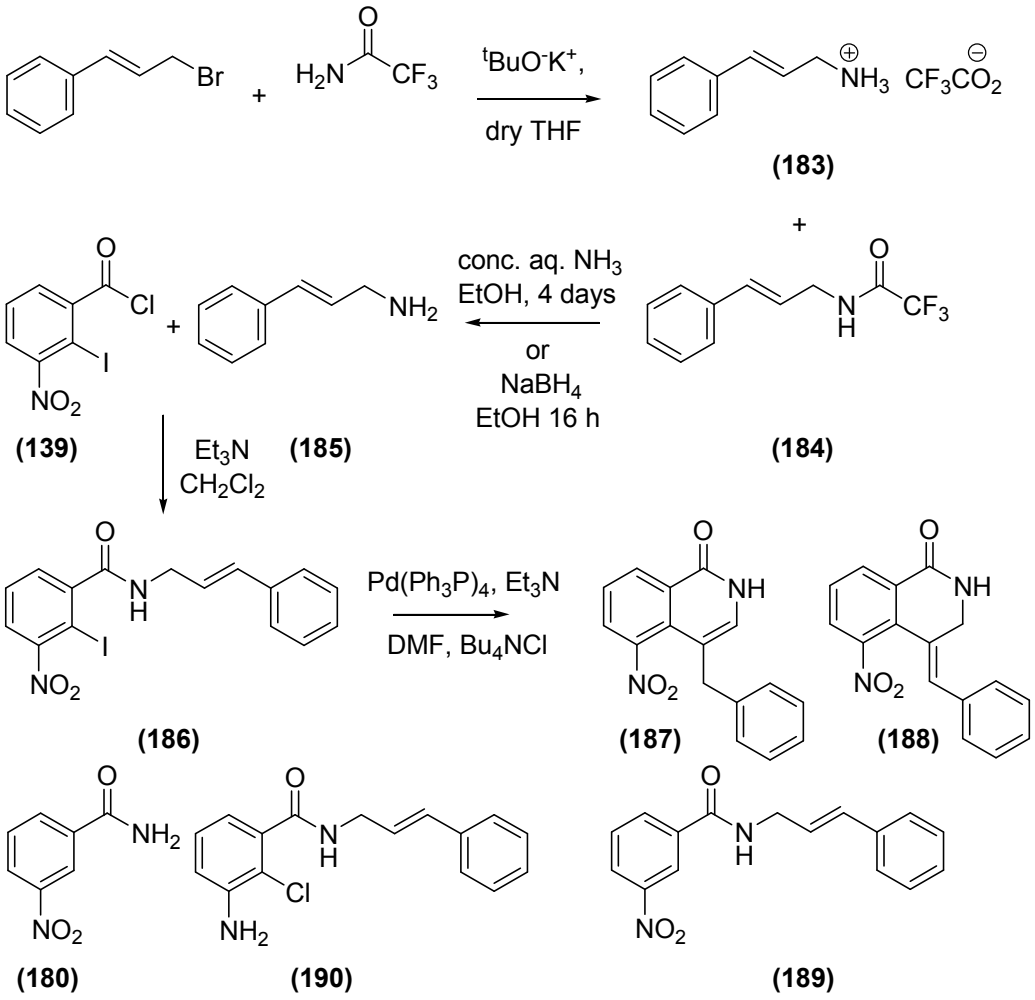

Scheme 51. Synthetic route to 4-benzyl-5-nitroisoquinolin-1(2*H*)-one **(187)**.

Double bond migration / Heck cyclisation of **(186)** was carried out under the previously optimised conditions ($Pd(Ph_3P)_4$, Et_3N, Bu_4NCl, DMF, 150 °C quick heating) for 48 h. Products isolated included a separable mixture of isomers 4-benzyl-5-nitroisoquinolin-1(2*H*)-one **(187)** (17%) and (*Z)*-4-benzylidene-5-nitro-3,4-dihydroisoquinolin-1(*2H*)-one **(188)** (14%), along with the dehalogenated products *(E)*-3-nitro-N-(3-phenylprop-2-enyl)benzamide **(189)** (11%) and traces of 3-nitro benzamide **(180)**. About 14% of *(E)*-3-amino-2-chloro-N-(3-phenylprop-2-enyl)benzamide **(190)** was also isolated as yellow crystals (Scheme 51). It appears that chloride from Bu_4NCl replaced the iodine by S_NAr

reaction (Scheme 52) and reduction of the nitro group might have occurred under Pd-catalysis.

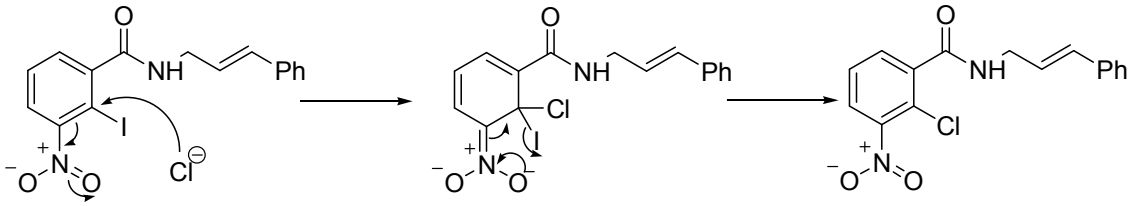

(143) **(191)**

Scheme 52. S_NAr addition-elimination mechanism proposed to form **(191)**.

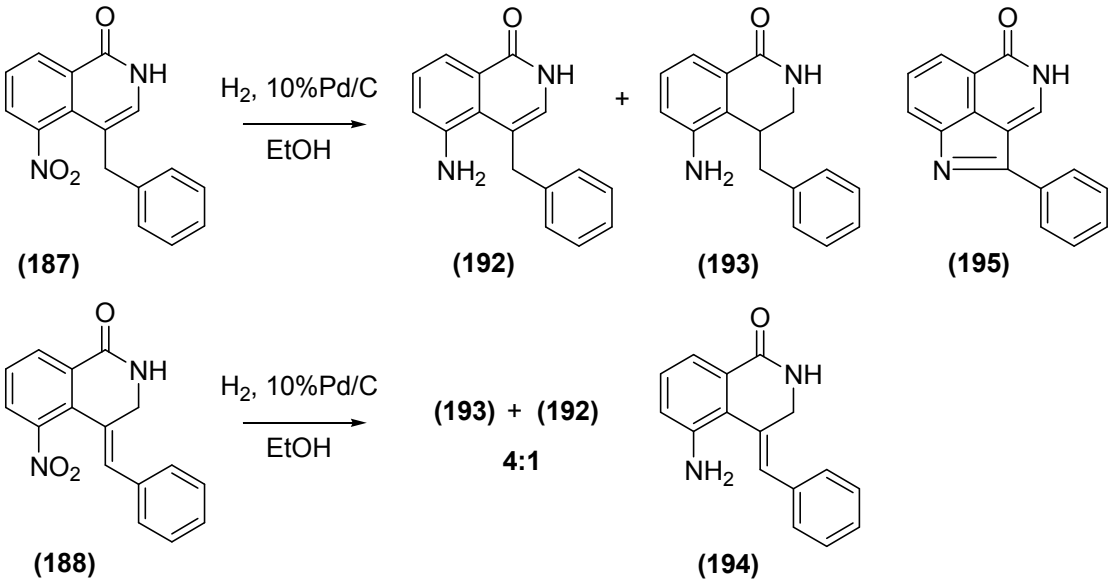

Scheme 53. Reduction of nitro functional groups of **(187)** and **(188)** using (H_2/Pd/C) catalyst.

Attempts to carry out selective reduction of the nitro group of **(187)** using 10% palladium on charcoal (Pd/C) and hydrogen in the presence of few drops of conc. HCl in EtOH gave the desired amine **(192)** with some unidentified impurities. Repeated attempts at recrystallisation (EtOH) to purify the product **(192)** failed. It was speculated that use of HCl prompts the cyclisation between the 5-amino group and the methylene group at the 4-position thus forming a compound like **(195)** which was taken to be the impurity. Hence, the reduction of **(187)** was carried out without conc. HCl and gave the desired amine **(192)** in 51% yield as a buff powder (Scheme 53). It was found that

$Pd/C/H_2$ catalytic system reduces the double bond at the 3,4 position of **(192)** along with the nitro group as traces of 5-amino-4-benzyl-3,4-dihydroisoquinolin-1(2*H*)-one **(193)** were also identified in ^1H NMR spectra of **(192)**. Interestingly, reduction of **(188)** with $Pd/C/H_2$ furnished an inseparable mixture of **(193)** and **(192)** in 4:1 ratio and none of the anticipated compound **(194)** was isolated. Formation of **(192)** from **(188)** is possible only by the migration of the exocyclic double bond into the ring. It is not clear whether the double bond migration occurs before reduction of the nitro group or after.

3.4.12 Attempted synthesis of 5-amino-4-ethylisoquinolin-1(*2H*)-one

Following the success in synthesis of **(192)** it was decided to extend the same methodology to synthesise the 5-amino-4-ethylisoquinolin-1(*2H*)-one. Since the compound but-2-en-1-amine **(200)** was not commercially available we needed to synthesise the same. At first thepotassium salt of trifluoroacetamide, which was prepared *in situ* from trifluoroacetamide and potassium *t*-butoxide in dry THF, was made to react with 1-bromobut-2-ene (available as mixture of *E*- and *Z*- isomers (5:1)). A yield of 33% of inseparable *E*- and *Z*-isomers of N-(but-2-enyl)-2,2,2-trifluoroacetamide was obtained in the ratio 3:1 and 6% of the disubstituted *E*- and *Z*-isomers of N,N-di(but-2-enyl)-2,2,2-trifluoroacetamide **(197)** and **(198)** in 4:1 ratio along with traces of *EZ*-compound **(199)**. The mixture of *E*- and *Z*-trifluoroacetamides **(195)** and **(196)** was hydrolysed using alkali (10% aq. NaOH) to give a mixture of *(E)* and *(Z)* but-2-en-1-amines **(200)** and **(201)**. This compound was not isolated for analysis as its boiling point was too low. It was used in the coupling without further purification. This, on coupling with the acid chloride **(139)** furnished an inseparable mixture of *E*- and *Z*-isomers of N-(but-2-enyl)-2-iodo-3-nitrobenzamide **(202)** and **(203)** in the ratio 5:1 (72%) as yellow crystals.

The mixture of *E*- and *Z*-isomers of **(202)** and **(203)** was subjected to Heck cyclisation under optimised conditions ($Pd(Ph_3P)_4$, Et_3N, Bu_4NCl, DMF, 150 ^oC quick heating,) for 48 h. Curiously, the above mixture failed to cyclise under Pd-catalysis as none of the anticipated product 5-nitro-4-ethylisoquinolin-1(*2H*)-one **(208)** or the isomer **(209)** were formed. However 21% of *E*- and *Z*-isomers of the dehalogenated amide **(204)** and **(205)** in 4:1 ratio and 15% of *E*- and *Z*-isomers of 3-amino-N-(but-2-enyl)-2-chlorobenzamide **(206)** and **(207)** in 4:1 ratio were the only products isolated (Scheme 52). Compound **(206)** is believed to be formed as a result of S_NAr addition-elimination reaction and reduction of nitro group under Pd-catalysis. Again the order of these two reactions was not clear. To avoid the formation of this type of compound and to

optimise the yield of desired cyclised products it was decided at this stage to use Bu_4NI as phase transfer catalyst, instead of Bu_4NCl, so that the S_NAr reaction would be futile.

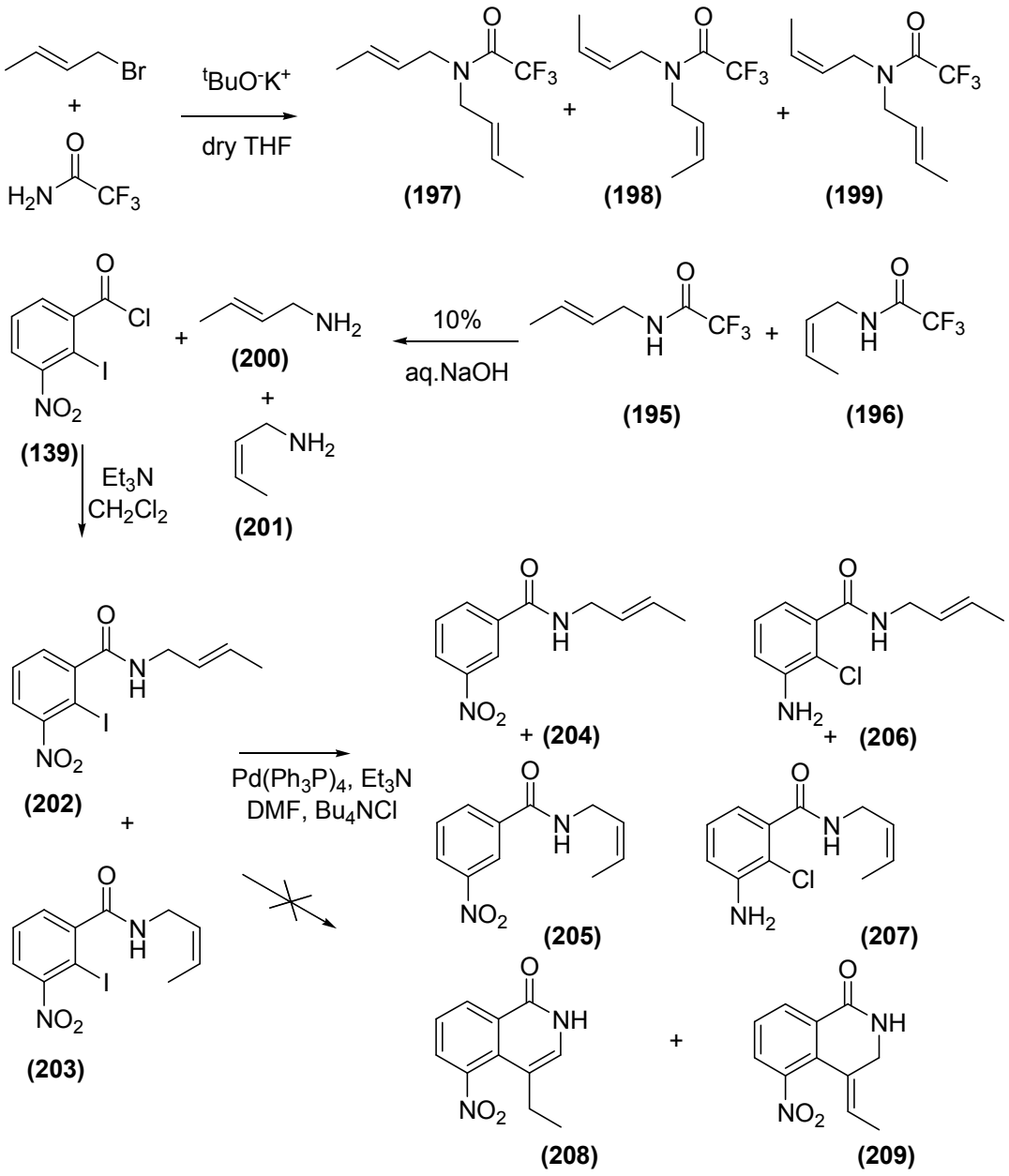

Scheme 54. Attempted synthesis of 5-nitro-4-ethylisoquinolin-1(*2H*)-one **(208)** *via* Heck cyclisation

Failure to cyclise *E*- and *Z*-isomers of **(202)** and **(203)** was puzzling since we were successful in introducing the analogous methyl and benzyl groups to the 4-position of 5-aminoisoquinolin-1-one.

3.4.13 Synthesis of 5-amino-4-(4-methylbenzyl)isoquinolin-1(*2H*)-one and 5-amino-4-(4-methoxybenzyl)isoquinolin-1(*2H*)-one

One of the main aims of the project was to introduce benzyl and substituted benzyl groups into the 4-position of 5-aminoisoquinolin-1(*2H*)-one. We were successful in synthesising 5-amino-4-benzylisoquinolin-1*(2H)*-one **(192)**. Now attention was turned towards synthesising 5-amino-4-(4-methylbenzyl)isoquinolin-1(*2H*)-one and 5-amino-4-(4-methoxybenzyl)isoquinolin-1(*2H*)-one.

To accomplish this, it was necessary to synthesise substituted cinnamylamines such as 3-(4-methylphenyl)prop-2-en-1-amine and 3-(4-methoxyphenyl)prop-2-en-1-amine. Ar-substituted 3-phenylprop-2-enylamines could be synthesised by Heck coupling of substituted aryl halides and 2-allylisoindoline-1,3-dione, and subsequent deprotection of the product with hydrazine hydrate to generate the amines.[202] Keeping in view the diversity of the aromatic residues that could be used in this coupling this method was investigated for the synthesis of 3-(4-methylphenyl)prop-2-en-1-amine and 3-(4-methoxyphenyl)prop-2-en-1-amines. In this $Pd(OAc)_2$-catalysed reaction, 2-allylisoindoline-1,3-dione was coupled to an aromatic halide in the presence of Et_3N in acetonitrile. The amines were generated by refluxing with hydrazine hydrate in ethanol.

Synthesis of the precursor 2-allylisoindoline-1,3-dione was necessary as it was not commercially unavailable. Boiling phthalic anhydride with prop-2-en-1-amine in acetic acid and aqueous work-up and recrystallisation (EtOAc) gave 87% of **(210)** as white needles. The aryl halides, 4-iodotoluene and 4-iodoanisole were used to introduce 4-methylbenzyl and 4-methoxybenzyl substituents on 5-aminoisoquinolin-1-one, respectively. The next step involved $Pd(OAc)_2$ (1 mol %)-catalysed Heck coupling of **(210)** to 4-iodotoluene and 1-iodo-4-methoxybenzene, respectively, with two equivalents of Et_3N, which also served as solvent for 16 h.. The mechanism of this reaction is as shown in section 3.4.4 (Scheme 37). In both cases, the *trans* (*E*) stereoisomer was the only product detected and isolated. The resulting (*E*)-2-(3-(4-methylphenyl)prop-2-enyl)isoindoline-1,3-dione **(211)** and (*E*)-2-(3-(4-methoxyphenyl) prop-2-enyl)isoindoline-1,3-dione **(212)** were refluxed with one equivalent of hydrazine hydrate in EtOH. Alkaline workup and extraction with Et_2O and CH_2Cl_2 afforded the amines **(213)** (65%) and **(214)** (89%), respectively as yellow oils (Scheme 55). These primary amines, on coupling with the acid chloride **(139)**, afforded **(215)** (82%) and **(216)** (75%), respectively, ready for attempts to carry out tandem double bond migration / intramolecular Heck coupling.

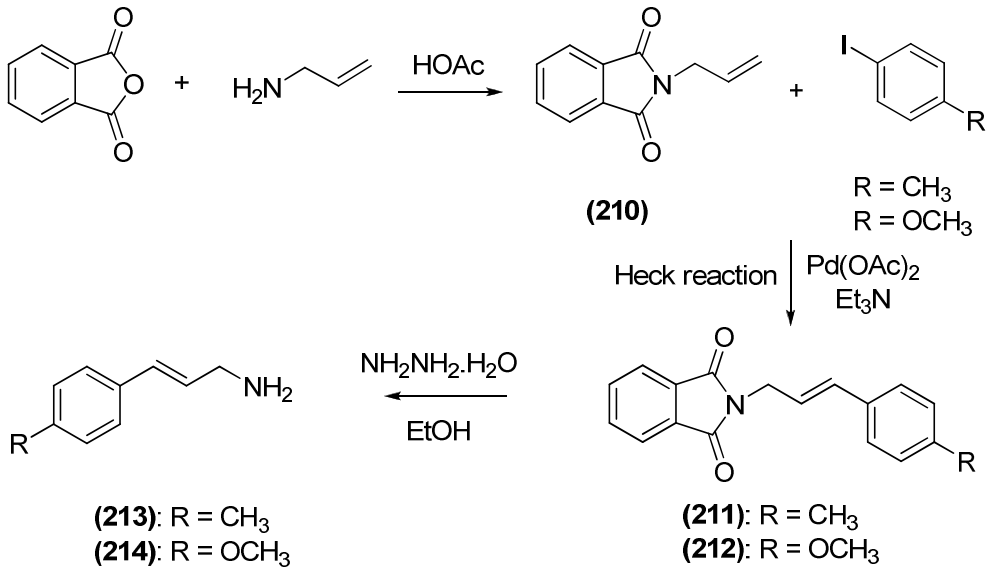

Scheme 55. Synthesis of 3-(4-methylphenyl)prop-2-en-1-amine **(213)** and 3-(4-methoxyphenyl)prop-2-en-1-amine **(214)**.

As discussed earlier in Section 3.4.12, to avoid the formation of S_NAr reaction product (chloride from Bu_4NCl replacing the iodine) and to optimise the yield of desired cyclised products, it was decided to use Bu_4NI as phase transfer-catalyst, instead of Bu_4NCl. Double bond migration / Heck cyclisation of **(215)** and **(216)** was carried out under the previously optimised conditions ($Pd(Ph_3P)_4$, Et_3N, Bu_4NI, DMF, 150 ^oC quick heating) for 48 h (Scheme 56). Products isolated from Heck cyclisation of **(215)** included an inseparable mixture of **(217)** and **(218)** in the ratio (3:1) (17 mg, 16%). Formation of dehalogenated amide (*E*)-N-(3-(4-methylphenyl)prop-2-enyl)-3-nitro benzamide **(217)** could be explained as a result of decomposition of the intermediate aryl palladium, which had failed to undergo cyclisation and subsequent protonation. However, reduction of double bond in the side chain to form N-(3-(4-methylphenyl)propyl)-3-nitrobenzamide **(218)** might have occurred under Pd-catalysis. The reaction also yielded separable mixture of isomers 4-(4-methylbenzyl)-5-nitroisoquinolin-1(2*H*)-one **(219)** (15%) and *(Z)*-4-(4-methylbenzylidene)-5-nitro-3,4-dihydroisoquinolin-1(2*H*)-one 4-benzyl-5-nitroisoquinolin-1(2*H*)-one **(220)** (13%) and traces of 3-nitrobenzamide **(180)**.

Selective reduction of the nitro group of **(219)** using 10% palladium on charcoal (Pd/C) and hydrogen in EtOH gave an inseparable mixture of the desired amine 5-amino-4-(4-methylbenzyl)isoquinolin-1(2*H*)-one **(221)** and 5-amino-4-(4-methylbenzyl)-3,4-dihydroisoquinolin-1(2*H*)-one **(222)** in the ratio 10:3 (51%). Reduction of the nitro group

of **(220)** under same conditions as above gave an inseparable mixture **(222)** and **(221)** in the ratio 11:9 (42%).

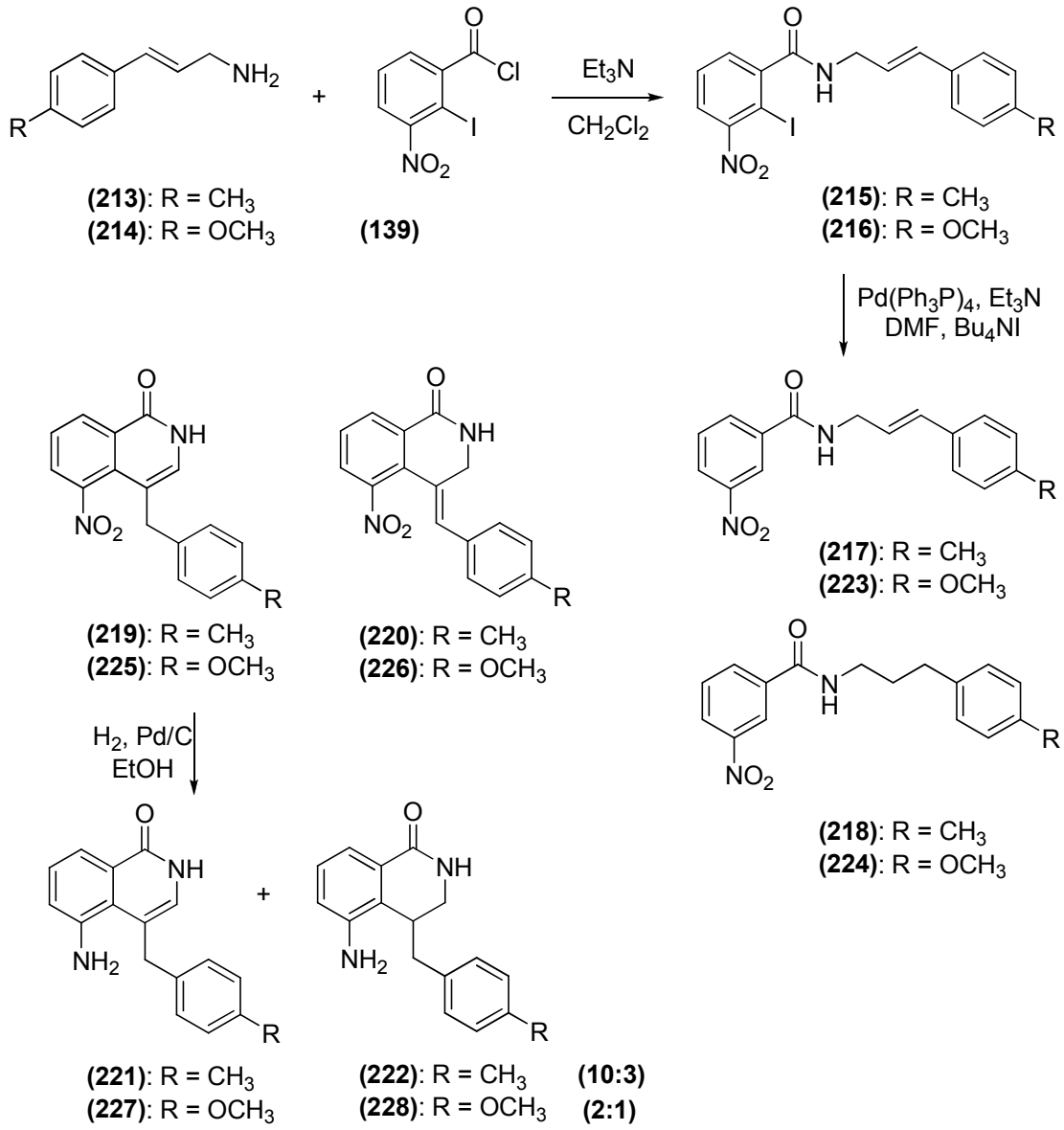

Scheme 56. Synthesis and Heck coupling of (*E*)-2-iodo-3-nitro-N-(3-(4-methylphenyl)prop-2-enyl)benzamide **(215)** and (*E*)-2-iodo-N-(3-(4-methoxyphenyl)prop-2-enyl)-3-nitrobenzamide **(216)**.

Products isolated from Heck cyclisation of (*E*)-2-iodo-N-(3-(4-methoxyphenyl)prop-2-enyl)-3-nitrobenzamide **(216)** included an inseparable mixture of dehalogenated amide **(223)** and double-bond reduced dehalogenated amide **(224)** in the ratio 2:3 (19%). Also isolated were separable mixture of cyclised isomers 4-(4-methoxybenzyl)-5-nitroisoquinolin-1(2*H*)-one **(225)** (17%) and (*Z*)-4-(4-methoxybenzylidene)-5-nitro-3,4-

dihydroisoquinolin-1(2*H*)-one **(226)** (15%). Reduction of the nitro group of **(225)** using 10% palladium on charcoal (Pd/C) and hydrogen in EtOH afforded an inseparable mixture of the desired amine 5-amino-4-(4-methoxybenzyl)isoquinolin-1(2*H*)-one **(227)** and 5-amino-4-(4-methoxybenzyl)-3,4-dihydroisoquinolin-1(2*H*)-one **(228)** in the ratio 1:2 (53%). Reduction of the nitro group of **(226)** was not attempted, owing to shortage of material.

3.4.14 Synthesis of 5-1-(3-((5-nitro-1-oxo-1,2-dihydroisoquinolin-4-yl)methyl)phenyl)pyrrolidine-2,5-dione

In the continuing quest to introduce substituted benzyl groups, it was decided to introduce the bulkier 3-succinimidobenzyl as a substituent into the 4-position of 5-aminoisoquinolin-1(*2H*)-one. Initial experiments included synthesis of 1-(3-iodophenyl)pyrrolidine-2,5-dione **(230)** from heating succinic anhydride and 3-iodoaniline at 190 ^{o}C for 6 h. Experiment was carried out with slow increase of temperature. At 150 ^{o}C formation of 4-(3-iodophenylamino)-4-oxobutanoic acid **(229)** was identified. Further increase in temperature to 190 ^{o}C afforded **(230)** (74%) as buff crystals. In the $Pd(OAc)_2$-catalysed reaction, two equivalents of Et_3N served as both base and solvent. 2-Allylisoindoline-1,3-dione was coupled to **(230)** in Et_3N for 24 h to furnish (*E*)-2-(3-(3-(2,5-dioxopyrrolidin-1-yl)phenyl)prop-2-enyl)isoindoline-1,3-dione **(231)** (86%). However, the usual method of generating amines by refluxing with hydrazine hydrate in ethanol failed to occur as none of the amine **(232)** was formed as hydrazine attacked the succinimide ring (Scheme 57).

In the process of synthesising *(E)*-1-(3-(3-aminoprop-1-enyl)phenyl)pyrrolidine-2,5-dione **(232)**, firstly *tert*-butyl N-(prop-2-enyl)carbamate **(233)** (83%) was prepared by coupling prop-2-en-1-amine with di(*tert*-butyl) dicarbonate in CH_2Cl_2 for 3 h. Heck coupling of substituted aryl halide **(230)** and **(233)** using $Pd(OAc)_2$ (1 mol %) and two equivalents of Et_3N, under nitrogen for 48 h gave an inseparable mixture of **(234)** and the undesired regioisomer **(235)** in 4:1 ratio (Scheme 58).

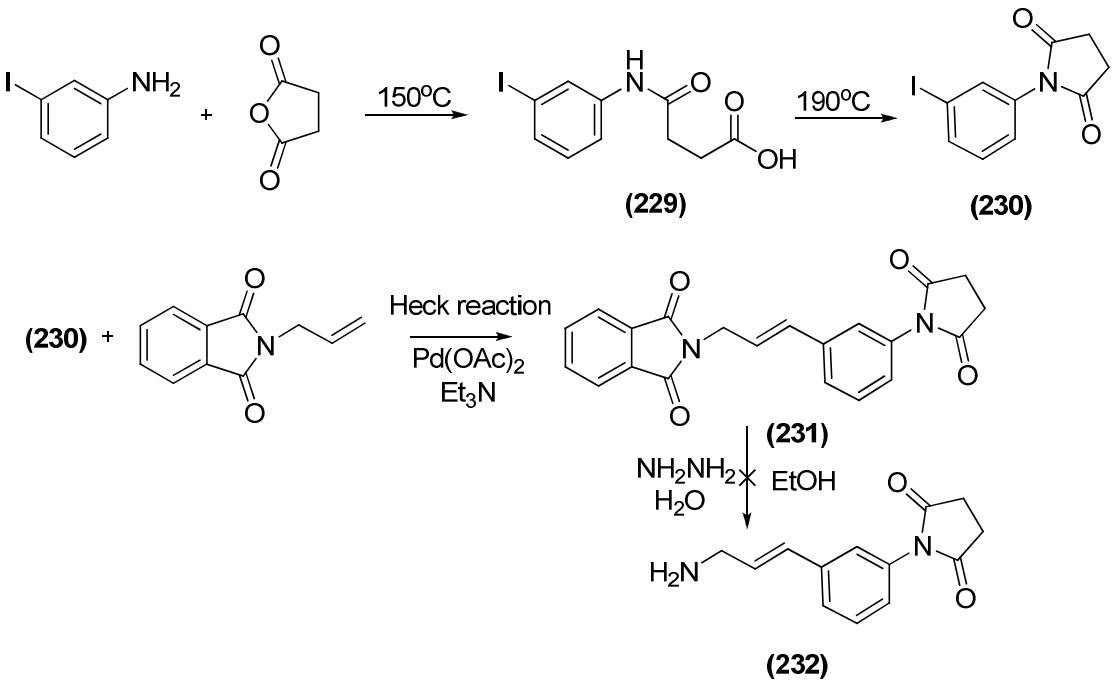

Scheme 57. Attempted synthesis of *(E)*-1-(3-(3-aminoprop-1-enyl)phenyl)pyrrolidine-2,5-dione **(232)**

Removal of the Boc group using trifluoroacetic acid in CH_2Cl_2 did not give the anticipated amine but instead gave a mixture of unidentified products. Passage of dry HCl to the solution of **(234)** and **(235)** in CH_2Cl_2 generated the mixture of amines **(236)** and **(237)** as hydrochloride salts (detected by TLC). This compound was not isolated for analysis and in its crude form was coupled with acid chloride **(139)** to furnish an inseparable mixture of (*E*)-N-(3-(3-(2,5-dioxopyrrolidin-1-yl)phenyl)prop-2-enyl)-3-nitrobenzamide **(238)** and N-(2-(3-(2,5-dioxopyrrolidin-1-yl)phenyl)prop-2-enyl)-3-nitrobenzamide **(239)** (4:1) in 32% yield.

Double bond migration / Heck cyclisation of mixture of **(238)** and **(239)** was carried out under the previously used conditions ($Pd(Ph_3P)_4$, Et_3N, Bu_4NI, DMF, 150 °C quick heating) for 48 h. Products isolated included an inseparable mixture of dehalogenated amide **(240)** and the regioisomer **(241)** (4:1) (18%) along with inseparable mixture of cyclised 1-(3-((5-nitro-1-oxo-1,2-dihydroisoquinolin-4-yl)methyl)phenyl)pyrrolidine-2,5-dione **(242)** and (*Z*)-1-(3-((5-nitro-1-oxo-2,3-dihydroisoquinolin-4(1*H*)ylidene)methyl)-phenyl) pyrrolidine-2,5-dione **(243)** in 21% yield. Reduction of the nitro groups of **(242)** and **(243)** were not attempted, owing to shortage of material.

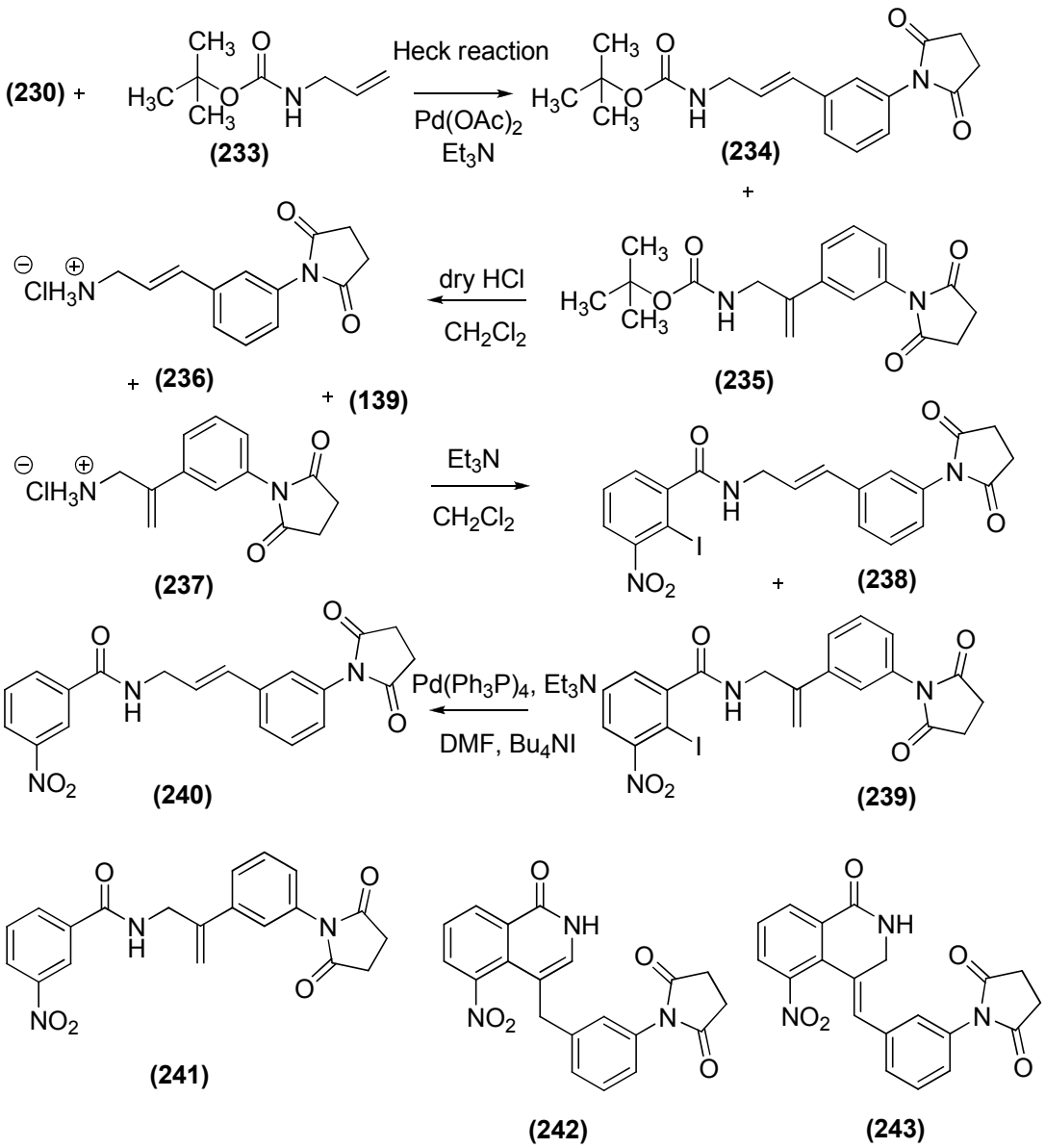

Scheme 58. Synthesis and Heck coupling of *(E)*-N-(3-(3-(2,5-dioxopyrrolidin-1-yl)phenyl)prop-2-enyl)-3-nitrobenzamide **(238)**

In conclusion, Pd-catalysed cyclisation of tertiary amides N,N-diallyl-2-iodo-3-nitrobenzamide **(141)** and N-benzhydryl-N-cinnamyl-2-iodo-3-nitrobenzamide **(148)** gave two isomeric products, the 4-alkyl-5-nitroisoquinolin-1-ones **(149)** and **(151)** and the 4-alkyl-5-nitro-3,4-dihydroisoquinolin-1-ones **(150)** and **(152)**. The corresponding secondary amide N-allyl-2-iodo-3-nitrobenzamide **(143)** cyclised efficiently to give **(177)** and **(178)**. Pd-catalysed cyclisations of a series of secondary N-cinnamyl 2-iodo-3-nitrobenzamides were also investigated. Catalytic hydrogenation was used to convert the 5-nitro groups of the 4-substituted isoquinolin-1-ones to provide the target 5-aminoisoquinolin-1-ones.

4. Biological Evaluation

4.1 PARP-1 inhibition assays

The standard assay for monitoring PARP-1 activity involves the use of radiolabeled NAD^+ (^{32}P- or ^3H).[203,204] An ELISA assay uses an antibody to ADP-ribose[205] and two recently described assays utilise[206,207] biotinylated NAD^+. The use of radioactive and/or specialized reagents (such as biotinylated NAD^+ and antibodies) in these assays can make them expensive when screening large compound collections for PARP inhibition. In addition, these assays often involve either the separation of ADP-ribose polymer product from the NAD^+ substrate or the addition of specialized streptavidin-conjugated scintillation proximity assay beads. Thus, the search for an inexpensive and convenient method for identifying PARP-1 inhibitors led us to a novel colorimetric PARP-1 assay developed by Trevigen Inc. (Gaithersburg, USA). The assay is non-radioactive and utilises 96- well plates for rapid screening for PARP inhibition. This assay is ideal for screening of PARP-1 inhibitors for *in vitro* activity.

This assay is based on the fact that PARP-1 enzyme, during the heteromodification process, catalyses poly(ADP-ribosyl)ation of histone proteins in response to damaged DNA. At first the test inhibitor is pre-incubated with the PARP-1 enzyme on a 96 strip-well plate coated with histone acceptor proteins for a brief period of time. A PARP-cocktail reagent, containing biotinylated NAD^+ (6-biotin-17-nicotinamide-adenine-dinucleotide) (Figure 26) and activated DNA, is added to the wells to initiate the reaction. Upon activation, PARP-1 cleaves biotinylated NAD^+ into nicotinamide and biotinylated (ADP-ribose) and synthesises biotinylated (ADP-ribose) polymers covalently attached to the acceptor histone proteins. The extent of biotin incorporation is measured using a conjugated streptavidin detection system. The PARP-1 inhibitory activity of the inhibitors is assessed on the basis of their inhibition of biotinyl-(ADP-ribose) incorporation. The presence of biotinylated poly(ADP-ribose) generated by PARP-1 during the ribosylation of histone proteins coated on the 96-well plate was detected using streptavidin horseradish peroxidase (Strep-HRP) and TACS Sapphire™. The TACS Sapphire™ substrate generates a soluble blue colour in the presence of Strep-HRP with a maximum absorbance of 630 nm. The development of the colourimetric reaction was terminated by addition of 0.2 M hydrochloric acid, generating a yellow colour with an absorption maximum at 450 nm.

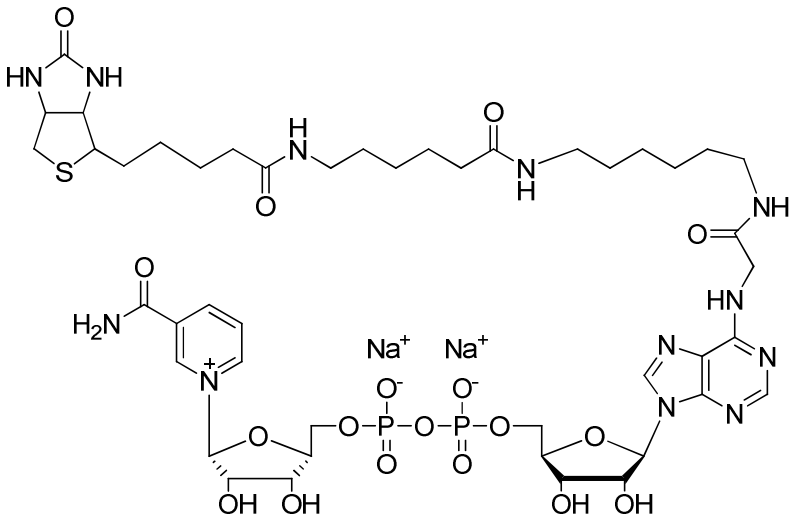

Figure 26. Structure of biotinylated NAD^+.

4.1.1 PARP-1 calibration curve

Firstly, a standard curve using different amounts of PARP-1 enzyme was prepared for the biotinylated poly(ADP-ribose) polymerisation reaction. As shown in Figure 27, a linear relationship exists between the absorbance at 450 nm and the concentration of the PARP-1 enzyme. From the standard curve, it was established that 0.8 units of PARP-1 enzyme was sufficient to give an absorbance reading in the range of 2.0-2.5 in the absence of any inhibitor. A negative control without PARP enzyme was included to determine the background absorbance.

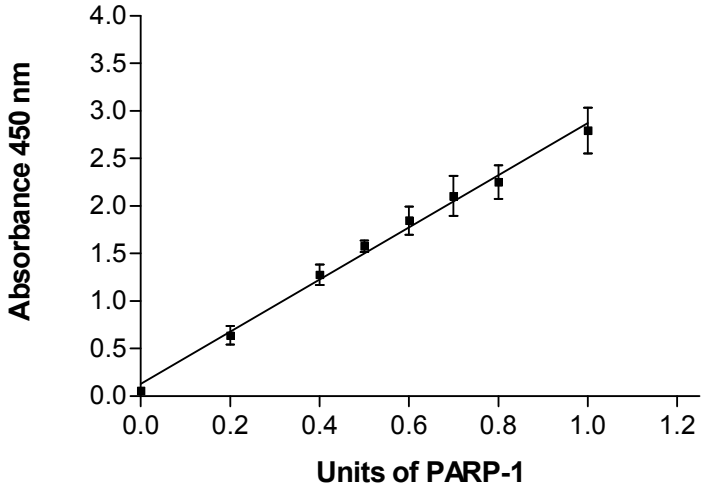

Figure 27. PARP-1 calibration curve. Data are the mean of three replicants and are reported as mean ± standard error of the mean (SEM).

4.1.2 PARP-1 inhibitory activity of 4-substituted 5-aminoisoquinolin-1-ones

Various 4-substituted 5-aminoisoquinolin-1(2*H*)-ones synthesised in this project were evaluated for *in vitro* activity using the colourimetric PARP assay system. 5-AIQ was used as the benchmark inhibitor and was evaluated in the assay for comparison purposes. In this evaluation, seven different concentrations (100, 30, 10, 3, 1, 0.3, 0.1 μM) of each inhibitor, in a range surrounding the likely IC_{50} value, were used. Figure 28 shows a colourimetric assay plate used.

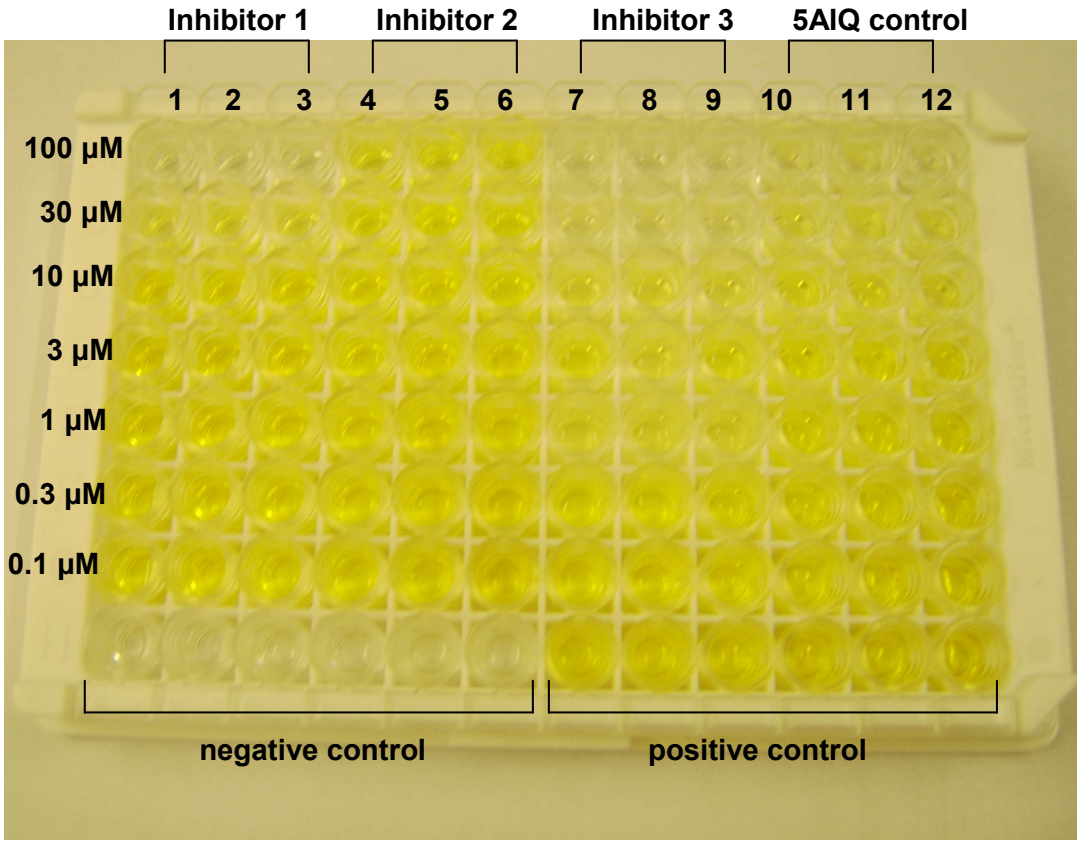

Figure 28. Colourimetric readout of PARP-1 activity assay with inhibitors 4-benzyl-5-aminoisoquinolin-1(2*H*)-one (lane 1-3), 5-amino-4-benzyl-3,4-dihydroisoquinolin-1(2*H*)-one (lane 4-6), 4-bromo-5-aminoisoquinolin-1(2*H*)-one (lane 7-9), 5-AIQ (lane 10-12). Bottom row: wells 1-6 negative control without PARP enzyme, wells 7-12 positive control without PARP inhibitor.

For each inhibitor, three determinations of activity were performed at each concentration. The IC_{50} value of the inhibitor was then estimated graphically from a plot of $\log_{10}$ [inhibitor] versus absorbance. These assays were highly sensitive and reproducible, with standard error of mean (SEM) of less than 20% for most compounds tested (Table 15). Figure 29 shows the PARP-1 inhibition curves of 4-methyl

5-aminoisoquinolin-1(*2H*)-one **(182)**. The complete results for the evaluation of 4-substituted 5-aminoisoquinolin-1(2*H*)-ones are given in the Appendices.

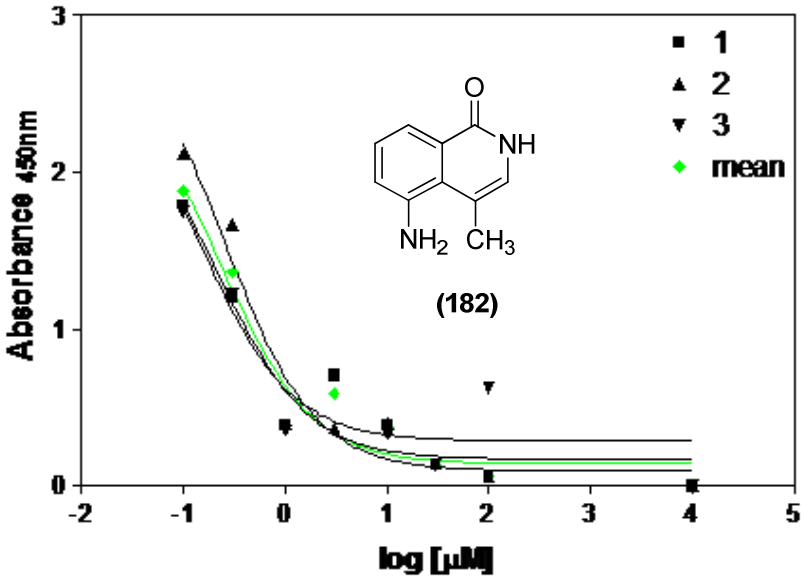

Figure 29. PARP-1 inhibition curve for 4-methyl 5-aminoisoquinolin-1(*2H*)-one **(182)**.

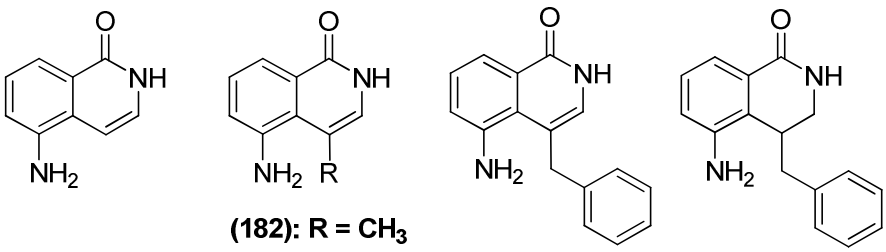

Compound number	IC_{50} (μM)	Log IC_{50} (μM)[a]
29d (5-AIQ)	1.8	0.26 ± 0.14
(182)	0.25	-0.6 ± 0.28
(125)	1.0	-0.02 ± 0.06
(192)	0.5	-0.34 ± 0.11
(193)	2.8	0.45 ± 0.08

Table 15. The IC_{50} values of the various 4-substituted 5-aminoisoquinolin-1(2H)-ones. [a]Data are the mean of three experiments and are reported as mean ± standard error of the mean (SEM).

The inhibition calculated for 4-methyl 5-aminoisoquinolin-1(*2H*)-one **(182)** was 0.25 µM. It is evident from this result that **(182)** is an excellent PARP-1 inhibitor and is 7 times more potent than 5-AIQ (IC_{50}=1.8 µM) under the colourimetric assay conditions. Similarly, 4-benzyl-5-aminoisoquinolin-1(*2H*)-one **(192)** also exhibited excellent PARP-1 inhibitory activity with IC_{50}= 0.5 µM. It is also interesting to note that 5-amino-4-benzyl-3,4-dihydroisoquinolin-1(2*H*)-one **(193)** the saturated analogue of **(192)** was less potent with respect to 5-AIQ as demonstrated by its IC_{50} 2.8 µM. 4-Bromo-5-aminoisoquinolin-1(*2H*)-one **(125)**, one of the intermediates in the synthesis also demonstrated good inhibitory properties with an IC_{50} value of 1.0 µM.

It is proposed that the 4-substituted 5-aminoisoquinolin-1-one inhibitors bind to the nicotinamide sub-site of the NAD^+-binding domain of PARP-1 (Figure 30). The carboxamide moiety of the inhibitor forms three important hydrogen bonds with the enzyme active site. The inhibitor carbonyl moiety accepts two hydrogen bonds, one from the amino-acid residue Ser904, and the other from the Gly863 N-H. The third hydrogen bond is formed between the Gly863 carbonyl oxygen and the carboxamide N-H.

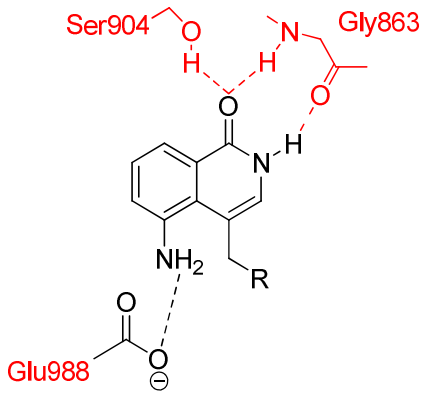

Figure 30. Proposed enzyme-inhibitor interactions between the PARP-1 active site and 4-substituted 5-AIQs.

In this study the effects of bulky aromatic substituents at the 4-position were investigated, which will interact with the hydrophobic residues in the binding pocket. The colourimetric PARP-1 assay identified four compounds with PARP-1 inhibitory activity equal or better than the lead compound 5-AIQ. In general, besides having a good water-solubility profile, most of the 4-substituted 5-aminoisoquinolin-1(2*H*)-ones exhibited excellent PARP-1 inhibitory potency with IC_{50} values in the low micromolar range. It appeared that the presence of a methyl substituent confers a slightly greater enhancement in PARP-1 inhibitory activity It is also interesting to note that the

introduction of a bromo group at the 4-position resulted in enhanced potency. This could be due to bromo being isosteric with methyl group. Bulky aryl substituents also enhanced the potency of the parent compound. Thus, compounds with bulky aromatic substituents at the 4-position were well tolerated.

5. Conclusions

Various approaches to the synthesis of novel classes of PARP-1 inhibitor, 3-substituted and 4-substituted 5-aminoisoquinolin-1(2*H*) ones were investigated, building on the pharmacophore of 5-AIQ. One approach to the 3-substituted compounds was successful and a novel and versatile synthetic route has been developed to a series of water-soluble target compounds, bearing varying substituents at the 4-position.

Initially cyclisations of methyl 2-alkynyl-3-nitrobenzoates with various electrophiles were studied. Cyclisations of methyl 3-nitro-2-phenylethynylbenzoate **(85)** with iodine monochloride and with phenylselenyl chloride followed the 6-*endo* route to give the isocoumarins **(99)** and **(105)** respectively. Similarly, cyclisation of methyl 3-nitro-2-trimethylsilylethynylbenzoate **(80)** with phenylselenyl chloride afforded the isocoumarin **(104)**. This isocoumarin is highly crowded, carrying a nitro group at the 5-position, a phenylselenyl group at the 4-position and a phenyl at the 3-position; this severe crowding was evident in an X-ray crystal structure, which showed significant out-of-plane distortion of the heterocyclic ring and extensive intramolecular and intermolecular π-stacking of the benzene rings. This demonstrates the directing influence of the electron-withdrawing nitro group on the electrophilicity of the alkyne. The observed 6-*endo* regiochemistry could be due to the 3-nitro group inducing polarisation of the alkyne, making the remote sp-carbon remote from the aryl ring more electrophilic. However, the formation of methyl 2-acetyl-3-nitrobenzoate **(95)** by treatment of **(80)** and **(82)** with Hg(II) was exceptional and suggests that a 5-*exo* cyclisation took place by the change in electron-distribution caused by the formation of an intermediate alkynylmercury σ-complex. 4-Iodo-5-nitro-3-phenylisocoumarin **(99)**, the product of iodocyclisation, could be exploited for the synthesis of 3- and 4-substituted 5-AIQs through various organometallic approaches.

In the first route to the 4-substituted 5-AIQ analogues, efforts to introduce a benzyl group into the 4-position of 5-aminoisoquinolin-1(2*H*)-one were unsuccessful, as cyclisation of methyl 2-(1-cyano-2-phenylethyl)-3-nitrobenzoate **(116)**, through selective reduction of the nitrile using DIBAL-H, failed to occur. Approach of DIBAL-H to the nitrile was sterically obstructed, leading to reduction of the ester to give 2-(2-formyl-6-nitrophenyl)-3-phenylpropanenitrile **(117)**. The second route relied on Pd-catalysed couplings of 4-bromoisoquinolin-1-one to synthesise the target molecule. Bromination of 5-nitroisoquinolin-1(*2H*)-one was achieved to give 4-bromo-5-nitroisoquinolin-1-one **(124)** but Pd-catalysed cross-couplings (Stille, Sonogashira, Suzuki-Miyaura) were

unsuccessful. Reduction of the hindering nitro group of **(124)** to amino furnished 5-amino-4-bromoisoquinolin-1-one **(125)** which also failed to participate in any of the Pd(0) catalysed cross-coupling reactions.

Much interesting chemistry was developed in the third route, which aimed at synthesising 4-substituted 5-aminoisoquinolin-1(2*H*)-ones *via* intramolecular Heck coupling of N-(alk-2-enyl)-2-iodo-3-nitrobenzamides. Pd-Catalysed cyclisation of tertiary amides N,N-diallyl-2-iodo-3-nitrobenzamide **(141)** and N-benzhydryl-N-cinnamyl-2-iodo-3-nitrobenzamide **(148)** gave two isomeric products, the 4-alkyl-5-nitroisoquinolin-1-ones **(149)** and **(151)** and the 4-alkyl-5-nitro-3,4-dihydroisoquinolin-1-ones **(150)** and **(152)**. The latter were derived from direct Heck cyclisation without prior C=C bond migration, while the former, required Pd-catalysed migration of the double bond into conjugation with the amide nitrogen before or after cyclisation. In deuterium labelling studies, failure to isolate any of the double-bond migrated mono-D isotopomer intermediate despite the formation of double-bond-migrated products of cyclisation **(151)** / **(162)** suggests that C=C migration occurs after Heck cyclisation, but the products were not interconvertable. The corresponding secondary amide N-allyl-2-iodo-3-nitrobenzamide **(143)** cyclised efficiently to give **(177)** and **(178)**. The ratios of the isomeric products varied with the reaction conditions. The optimum conditions for the reaction was found to be $Pd(Ph_3P)_4$, Et_3N, Bu_4NI, DMF with quick heating (150 ^oC). Double-bond isomerisation of **(143)** was achieved by treatment with $RuClH(CO)(PPh_3)_3$ giving the N-prop-1-enyl amide, which when subjected to the Pd-catalysed cyclisation conditions, gave only the uncyclised reductively deiodinated material (**176)**. Pd-catalysed cyclisations of a series of secondary N-cinnamyl 2-iodo-3-nitrobenzamides were also explored. The 4-unsubstituted cinnamylamine was prepared by displacement of the bromine of cinnamyl bromide with the anion derived from trifluoroacetamide, followed by cleavage of the amide by hydrolysis or reductively with sodium borohydride. The 4-substituted cinnamyl amines were synthesised by Heck coupling of a protected allylamine to the appropriate iodoarene to form the N-cinnamylphthalimides followed by hydrazinolysis. 3-Succimimidocinnamylamine **(236)** was prepared by Heck coupling of N-Boc-allylamine with N-(3-iodophenyl)succinimide **(230)**, followed by deprotection. Pd-catalysed cyclisation of **(186)** afforded a chromatographically separable mixture of 4-benzyl-5-nitroisoquinolin-1-one **(187)** and the 4-benzylidene-5-nitro-3,4-dihydroisoquinolin-1-one isomer **(188)**. N-(substituted cinnamyl)benzamides **(215), (216)** and **(238)** also gave 4-(substituted benzyl)isoquinolin-1-ones **(219), (225), (242)** and the 4-(4-substituted benzylidene)-3,4-dihydroisoquinolin-1-ones **(220), (226),**. **(243)**. Catalytic hydrogenation was used to convert the 5-nitro groups of the 4-

substituted isoquinolin-1-ones to provide the target 5-aminoisoquinolin-1-ones. 5-Amino-4-methylisoquinolin-1(2*H*)-one hydrochloride **(182)** was isolated in excellent yield. The 4-benzyl analogue **(187)**, furnished the 5-amino-4-benzylisoquinolin-1-one **(192)** contaminated with a small trace of the over-reduced 5-amino-4-benzyl-3,4-dihydroisoquinolin-1-one **(193)**. Interestingly, 4-benzylidene-3,4-dihydroisoquinolin-1-one gave **(193)** along with **(192)**, suggesting possible C=C bond migration on the Pd metal surface. Unfortunately, it was not possible to reduce the nitro groups of **(219), (220)** and **(225)** cleanly, as product mixtures always comprised inseparable mixtures of the corresponding 5-aminoisoquinolin-1-ones and over-reduced products.

Biochemical evaluation of this series of compounds showed excellent *in vitro* inhibitory activity against human recombinant PARP-1, with IC_{50} values in the low micromolar range. Most of the 4-substituents were well received by the active site and they resulted in a significant enhancement of PARP-1 inhibitory potency with respect to 5-AIQ (IC_{50}=1.8 μM). This was particularly evident for 5-amino-4-methylisoquinolin-1(2*H*)-one hydrochloride **(182)** (IC_{50} = 0.25 μM), 4-benzyl-5-aminoisoquinolin-1(*2H*)-one **(192)** (IC_{50}= 0.5 μM) and the intermediate 4-bromo-5-aminoisoquinolin-1(*2H*)-one **(125)** (IC_{50}= 1.0 μM), which were among the most potent members of this series.

Pd-catalysed cyclisation for the future preparation of a range of 4-substituted-5-nitroisoquinolin-1-ones leading to analogues of the potent water-soluble PARP-1 inhibitor, 5-AIQ was achieved. Future work would involve the synthesis of further 3- and 4-substituted 5-AIQs. Greatly encouraged by promising biological data, our main focus is to evaluate the inhibitors for their *in vivo* activity in various disease models.

6. Experimental

General Procedures

Melting points were determined using a Reichert-Jung Thermo Galen Kofler block and are uncorrected. IR spectra were recorded on a Perkin-Elmer RXI FT-IR spectrometer, either as a KBr disc (KBr) or as a liquid (film). ν_{max} values are given in cm^{-1}. Thin layer chromatography (TLC) was performed on silica gel 60 F_{254} -coated aluminium sheets (Merck) and visualised under UV light (365nm) or stained with phosphomolybdic acid or ninhydrin. Flash column chromatography was performed using silica gel 60 (0.040-0.063 mm, Merck) as the stationary phase. NMR spectra were acquired on a Jeol-Delta GX 270 (270.05 MHz ^{1}H; 67.80 MHz ^{13}C) or Varian Mercury EX 400 (399.65 MHz ^{1}H; 100.4 MHz ^{13}C; 376.05 MHz ^{19}F) or Varian Unity Inova 600 MHz spectrometers. Chemical shifts are reported in parts per million (ppm) relative to tetramethylsilane for samples in $CDCl_3$, $(CD_3)_2SO$, CD_3OD and $(CD_3)_2CO$. Multiplicities are indicated by s (singlet), d (doublet), t (triplet), q (quartet), m (multiplet) and br (broad). Where indicated, 2-D experiments were used to assign ^{13}C NMR signals. Mass spectra were obtained by either Electron Impact (EI), Electrospray (ESI) or Fast Atom Bombardment (FAB) (with 3-nitrobenzyl alcohol as the matrix) at the University of Bath Mass Spectrometry Service using a VG 7070 Mass Spectrometer, the University of Bath Department of Pharmacy and Pharmacology High Resolution Mass Spectrometry Service using a Bruker microTOF spectrometer and the EPSRC Mass Spectrometry Service, Swansea. Microanalysis was carried out at the University of Bath Microanalysis Service and School of Pharmacy, University of London, Microanalysis Service.

All reagents for chemical synthesis were purchased from Sigma-Aldrich and Alfa Aesar and were used without further purification. Experiments were conducted at ambient temperature, unless otherwise stated. Where experiments were repeated, only one description is provided. Solutions in organic solvents were dried using anhydrous $MgSO_4$ and solvents were evaporated under reduced pressure using a Büchi rotary evaporator. THF was freshly distilled under nitrogen from sodium/benzophenone and diisopropylamine, Et_3N, acetonitrile and propanenitrile were distilled from calcium hydride.

2-Hydroxymercuri-3-nitrobenzoic acid (75)

2-Iodo-3-nitrobenzoic acid (76)

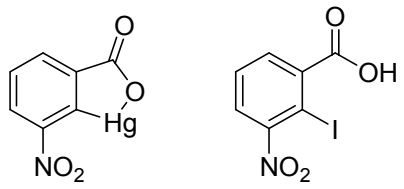

3-Nitrobenzene-1,2-dicarboxylic acid **74** (10.55 g, 50.0 mmol) in hot aq. NaOH (10%, 40 mL) was added to $Hg(OAc)_2$ (17.5 g, 55 mmol) in hot AcOH (2.5 mL) and H_2O (35 mL). The mixture was heated at 120 °C for 70 h, then filtered. The precipitate was washed (H_2O, then EtOH) and dried to give 2-hydroxymercuri-3-nitrobenzoic acid **75** (18.12 g, 99%) as a cream solid. To a refluxing solution of **75** (18.12 g, 50 mmol) in aq. NaOH (3.5%, 250 mL) was slowly added, with vigorous stirring, aq. HCl (2 M, 6 mL) and the solution was allowed to cool to room temperature. AcOH (3 mL) was then added. The precipitate dissolved upon addition of KI (9.5 g, 57 mmol) and I_2 (14.5 g, 57 mmol) in H_2O (15 mL). The solution was boiled under reflux for 24 h, cooled and neutralised with aq. NaOH before being filtered and acidified with aq. HCl (9 M). The precipitate was filtered, dried and recrystallised (EtOH) to give **76** (7.69 g, 53%) as yellow crystals: R_f = 0.61 (CH_2Cl_2:MeOH:AcOH 9:1:0.1); mp 203-204 °C (lit.[160] mp 204-205 °C); IR ν_{max} (KBr) 1375 & 1540 (NO_2), 1712 (C=O), 2520-3050 (OH) cm^{-1}; ^1H NMR $(CD_3)_2SO$ δ 7.66 (1 H, t, *J* = 7.8 Hz, 5-H), 7.79 (1 H, dd, *J* = 7.7, 1.5 Hz, 4-H), 7.92 (1 H, dd, *J* = 7.9, 1.7 Hz, 6-H).

Methyl 2-iodo-3-nitrobenzoate (71)

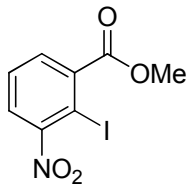

Compound **76** (4.0 g, 14 mmol) in MeOH (120 ml) and H_2SO_4 (3 ml) was boiled under reflux for 48 h, then poured into ice-H_2O (300 ml). The precipitate formed was filtered, dried and recrystallised (MeOH) gave **71** (4.0 g, 95%) as yellow crystals. R_f = 0.33 (hexane:EtOAc 4:1); mp 65-66°C (lit.[160] mp 64-66°C); IR ν_{max} (KBr) 1351 & 1533 (NO_2), 1705 (C=O); ^1H NMR ($CDCl_3$) δ 3.99 (3 H, s, CH_3), 7.54 (1 H, t, *J* = 7.8 Hz, 5-H), 7.70 (1 H, dd, *J* = 7.8, 1.7 Hz, 4-H), 7.77 (1 H, dd, *J* = 7.8, 1.7 Hz, 6-H).

Methyl 3-nitro-2-((trimethylsilyl)ethynyl)benzoate (80)

Methyl 3-nitrobenzoate (81)

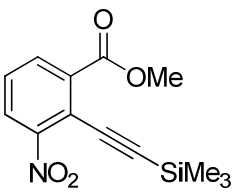

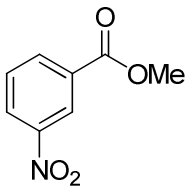

The Pd catalyst $(Ph_3P)_2PdCl_2$, used in this reaction was prepared as follows: A mixture of PPh_3 (0.375 g, 1.4 mmol) and $PdCl_2$ (0.13 g, 0.7 mmol) in DMF (20 mL) was heated at 80 °C for 24 h. Filtration and drying yielded $(Ph_3P)_2PdCl_2$ (0.4 g, 80%) as a yellow powder. Methyl 2-iodo-3-nitrobenzoate **71** (3.0 g, 9.8 mmol) in dry THF (120 mL) was added to a suspension of $(Ph_3P)_2PdCl_2$ (0.3 g, 0.4 mmol) and CuI (0.4 g, 2.1 mmol) in dry diisopropylamine (40 mL) and the mixture was stirred at 45 °C for 30 min under Ar. Trimethylsilylethyne (1.1 g, 11.0 mmol) was added during 30 min and the mixture was stirred for another 72 h at 45 °C. Filtration (Celite®), evaporation and chromatography (hexane:EtOAc 15:1) gave **80** (0.76 g, 28%) as reddish brown oil: R_f = 0.34 (hexane:EtOAc 15:1); IR ν_{max} (KBr) 1351 & 1532 (NO_2), 1738 (C=O), 2219 (C≡C) cm^{-1}; ^{1}H NMR ($CDCl_3$) δ 0.21 (9 H, s, $Si(CH_3)_3$), 3.88 (3 H, s, CH_3), 7.44 (1 H, t, *J* = 7.9 Hz, 5-H), 7.90 (1 H, dd, *J* = 8.1, 1.5 Hz, 4-H), 7.97 (1 H, dd, *J* = 7.9, 1.5 Hz, 6-H).

Also isolated by chromatography was **81** (0.24 g, 14%) as yellow crystals: R_f = 0.39 (hexane:EtOAc 15:1); mp 76-78 °C (lit.[160] mp 75-76 °C); IR ν_{max} (KBr) 1352 & 1531 (NO_2), 1720 (C=O) cm^{-1}; ^{1}H NMR ($CDCl_3$) δ 3.94 (3 H, s, CH_3), 7.62 (1 H, t, *J* = 8.0 Hz, 5-H), 8.32 (1 H, dt, *J* = 7.6, 1.5, Hz, 4-H), 8.36 (1 H, ddd, *J* = 8.2, 2.4, 1.2 Hz, 6-H), 8.79 (1 H, t, *J* = 1.7 Hz, 2-H).

Methyl 2-ethynyl-3-nitrobenzoate (82)

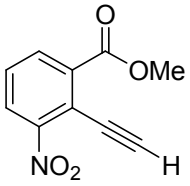

To **80** (0.25 g, 0.9 mmol) in acetone (6.5 mL), water (1.5 mL), and CH_2Cl_2 (11.5 mL) was added silver trifluoromethanesulfonate (23 mg, 0.09 mol). The mixture was stirred for 7 d. Saturated aq. NH_4Cl (2 mL) was added and the mixture was extracted thrice

with CH_2Cl_2. The combined organic layers were dried and filtered. Evaporation and chromatography (hexane:EtOAc 6:1) gave **82** (0.13 g, 72%) as pale yellow crystals: R_f = 0.4 (hexane:EtOAc 4:1); mp 78-80 °C; IR ν_{max} (KBr) 1351 & 1530 (NO_2), 1720 (C=O), 2112 (C≡C) cm^{-1}; ^1H NMR ($CDCl_3$) δ 3.72 (1 H, s, C≡CH), 3.95 (3 H, s, CH_3), 7.54 (1 H, t, *J* = 8.0 Hz, 5-H), 7.97 (1 H, dd, *J* = 8.2, 1.2 Hz, 4-H), 8.06 (1 H, dd, *J* = 7.9, 1.2 Hz, 6-H).

Methyl 3-nitro-2-(phenylethynyl)benzoate (85)
1,4-Diphenylbuta-1,3-diyne (86)
Methyl 3-nitrobenzoate (81)

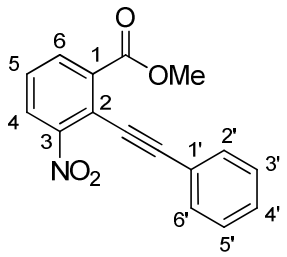

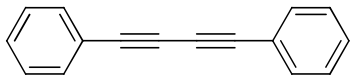

The Pd catalyst, $(Ph_3P)_2PdCl_2$, used in this reaction was prepared as above. Methyl 2-iodo-3-nitrobenzoate **71** (3.0 g, 9.8 mmol) in dry THF (120 mL) was added to a suspension of $(Ph_3P)_2PdCl_2$ (0.3 g, 0.4 mmol) and CuI (0.4 g, 2.1 mmol) in dry diisopropylamine (40 mL) and the mixture was stirred at 45 °C for 30 min under Ar. Phenylacetylene (1.5 g, 15 mmol) was then added during 30 min and the mixture was stirred for another 48 h at 45 °C. Filtration (Celite®), evaporation and chromatography (hexane:CH_2Cl_2 2:1) gave **85** (1.4 g, 51%) as reddish brown crystals: R_f = 0.78 (hexane:EtOAc 4:1); mp 58-59 °C (lit.[160] mp 59-60 °C); IR ν_{max} (KBr) 1342 & 1526 (NO_2), 1738 (C=O), 2214 (C≡C) cm^{-1}; ^1H NMR ($CDCl_3$) δ 3.99 (3 H, s, CH_3), 7.31-7.40 (3 H, m, 3',4',5'-H_3), 7.48 (1 H, t, *J* = 8.0 Hz, 5-H), 7.54-7.62 (2 H, m, 2',6'-H_2), 8.03 (1 H, dd, *J* = 8.1, 1.5 Hz, 4-H), 8.10 (1 H, dd, *J* = 7.9, 1.5 Hz, 6-H).

Compound **86** (0.5 g, 25%) was isolated by chromatography: R_f =0.9 (hexane:EtOAc 4:1); mp 85-86 °C (lit.[160] mp 83-84 °C); IR ν_{max} (KBr) 2147 (C≡C) cm^{-1}; ^1H NMR ($CDCl_3$) δ 7.32-7.41 (6 H, m, 2 x 3,4,5-H_3), 7.56-7.53 (4 H, m, 2 x 2,6-H_2).

Also isolated by chromatography was **81** (0.67 g, 38%) as pale yellow crystals with data as above.

Methyl 2-acetyl–3-nitrobenzoate (95)

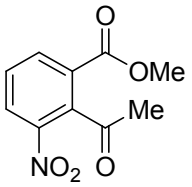

To **80** (0.11 g, 0.4 mmol) and $HgSO_4$ (0.15 g, 0.5 mmol) in acetone (10 mL) and conc. H_2SO_4 (0.1 mL) were boiled under reflux for 48 h, then evaporated to yield a brown residue. Extraction ($CHCl_3$), evaporation and chromatography (hexane:EtOAc 4:1) gave **95** (25 mg, 27%) as pale buff crystals: R_f = 0.2 (hexane:EtOAc 4:1); mp 81-82 ^oC (lit.[208] mp 81 ^oC); IR (KBr) ν_{max} 1346 & 1539 (NO_2), 1700 & 1732 (C=O) cm^{-1}; ^1H NMR ($CDCl_3$) δ 2.71 (3 H, s, $COCH_3$), 3.93 (3 H, s, OCH_3), 7.64 (1 H, t, *J* = 8.2 Hz, 5-H), 8.33 (1 H, dd, *J* = 7.9, 1.2 Hz, 4-H), 8.37 (1 H, dd, *J* = 7.9, 1.2 Hz, 6-H).

Methyl 2-acetyl-3-nitrobenzoate (95)
(±)-3-Methoxy-3-methyl-4-nitro isobenzofuran-1(*3H*)-one (96)

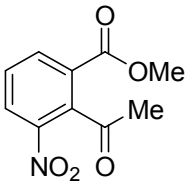

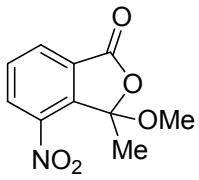

Compound **82** (0.10 g, 0.48 mmol) and $HgSO_4$ (0.17 g, 0.6 mmol) in acetone (10 mL) and conc. H_2SO_4 (0.1 mL) was boiled under reflux for 48 h, then evaporated to yield a brown residue. Extraction ($CHCl_3$) and evaporation gave **95** (27 mg, 28%) as buff crystals with properties as above. Also identified in trace amounts in the NMR spectrum was **96**: ^1H NMR ($CDCl_3$) δ 2.05 (3 H, s, CH_3), 3.22 (3 H, s, OCH_3) 7.5-8.5 (3 H, m, Ar 5,6,7-H_3).

4-Iodo-5-nitro-3-phenylisocoumarin (99)

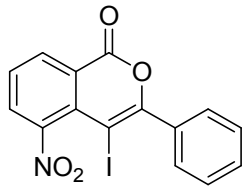

Compound **85** (0.114 g, 0.37 mmol) in dry CH_2Cl_2 (4 mL) was stirred with ICl (0.09 g, 0.55 mmol) in dry CH_2Cl_2 (1 mL) for 2 h in the dark. The mixture was diluted with Et_2O (50 mL), washed with aq. sodium thiosulfate solution and dried. Evaporation and chromatography (hexane:EtOAc 4:1) gave **99** (0.13 g, 81%) as pale yellow crystals. Recrystallisation (EtOAc:hexane) gave yellow powder: R_f = 0.6 (hexane:EtOAc 4:1); mp 154-156 °C; IR ν_{max} (KBr) 1354 & 1532 (NO_2), 1636 (C=C), 1732 (C=O) cm^{-1}; ^1H NMR ($CDCl_3$) δ 7.46-7.52 (3 H, m, Ph 3',4',5'-H_3), 7.65 (1 H, t, *J* = 7.8 Hz, 7-H), 7.70-7.74 (2 H, m, Ph 2',6'-H_2), 8.07 (1 H, dd, *J* = 7.8, 1.5 Hz, 6-H), 8.54 (1 H, dd, *J* = 7.8, 1.5 Hz, 8-H); ^{13}C NMR δ 61.58 (4-C), 123.47 (9-C), 128.35 (3',5'-C_2), 128.63 (7-C), 130.46 (2',6'-C_2), 130.92 (4'-C), 131.21 (6-C), 131.95 (10-C), 133.25 (8-C), 134.90 (1-C), 150.06 (5-C), 158.95 (3-C), 159.55 (1-C); MS (EI) *m/z* 392 (M - H), 265 (M - HI); Anal. Calcd for $C_{15}H_{18}INO_4$: C, 45.83; H, 2.05; N, 3.56; Found: C, 46.1; H, 2.15; N, 3.69.

5-Nitro-3-phenylisocoumarin (93)

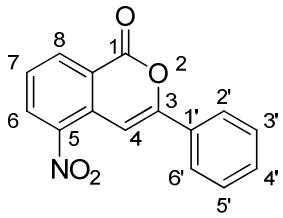

Formic acid (98%) (30 mg, 0.66 mmol) was added to a degassed mixture of **99** (0.13 g, 0.33 mol), Et_3N (0.1 g, 1.0 mmol), $Pd(OAc)_2$ (6.6 mg, 7 µmol) and Ph_3P (13.2 mg, 13 µmol) in dry DMF (10 mL). The mixture was stirred at 60 °C for 4.5 h under Ar before being poured into water (50 mL). Extraction (EtOAc), drying, evaporation and chromatography (hexane:EtOAc 9:1) gave **93** (69 mg, 78%) as bright yellow crystals: R_f = 0.43 (hexane:EtOAc 4:1); mp 141-142 °C (lit.[160] mp 142-143 °C); IR ν_{max} (KBr) 1341 & 1527 (NO_2), 1629 (C=C), 1739 (C=O) cm^{-1}; ^1H NMR ($CDCl_3$) δ 7.47-7.51 (3 H, m, Ph 3',4',5'-H_3), 7.60 (1 H, t, *J* = 7.8 Hz, 7-H), 7.86 (1 H, s, 4-H), 7.90-7.95 (2 H, m, Ph 2',6'-H_2), 8.48 (1 H, dd, *J* = 7.9,1.2 Hz, 6-H), 8.54 (1 H, dd, *J* = 7.8, 1.5 Hz, 8-H).

5-Nitro-4-(phenylselenyl)-3-(trimethylsilyl)isocoumarin (104)

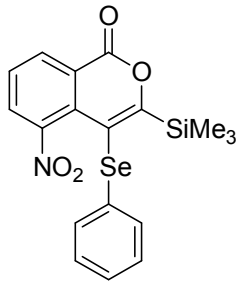

Compound **80** (0.11 g, 0.4 mmol) was stirred with phenylselenyl chloride (0.11 g, 0.6 mmol) in dry CH_2Cl_2 (3 mL) for 24 h under N_2. The mixture was washed with aq. $NaHCO_3$ and dried. Evaporation and chromatography (hexane:EtOAc 4:1) gave **104** (0.14 g, 82%) as a yellow solid. Recrystallisation (toluene) gave yellow powder: R_f = 0.62 (hexane:EtOAc 4:1); mp 105-107 ^oC; IR (KBr) ν_{max} 1370 & 1533 (NO_2), 1733 (C=O) cm^{-1}; ^1H NMR ($CDCl_3$) δ 0.34 (9 H, s, $SiMe_3$) 7.00 (2 H, m, SePh 2',6'-H_2) 7.10-7.17 (3 H, m, SePh 3',4',5'-H_3), 7.58 (1 H, t, *J* = 7.8 Hz, 7-H), 7.8 (1 H, dd, *J* = 7.9, 1.5 Hz, 6-H), 8.50 (1 H, dd, *J* = 7.8, 1.4 Hz, 8-H); ^{13}C NMR δ 0.34 ($\underline{C}H_3)_3$, 110.27 (4-C), 124.04 (9-C), 126.67 (4'-C), 127.84 (2',6'-C_2), 128.83 (7-C), 129.36 (3',5',-C_2), 130.15 (6-C), 130.33 (10-C), 132.96 (8-C), 133.73 (1'-C), 147.48 (5-C), 160.47 (1-C), 175.22 (3-C); MS (FAB^+) *m/z* 419.0095 (M) ($C_{18}H_{17}NO_4{}^{80}Se^{28}Si$ requires 419.0092), 418 (M - H); Anal. Calcd for $C_{18}H_{17}NO_4SeSi$: C, 51.67; H, 4.10; N, 3.35; Found: C, 51.8; H, 4.15; N, 3.33.

5-nitro-3-phenyl-4-(phenylselenyl)isocoumarin (105)

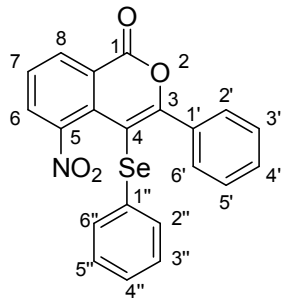

Compound **85** (0.10 g, 0.36 mmol) was stirred with phenylselenyl chloride (0.1 g, 0.53 mmol) in dry CH_2Cl_2 (5 mL) for 4 h under N_2. The mixture was washed with aq. $NaHCO_3$ and dried. Evaporation and chromatography (hexane:EtOAc 7:1) gave **105** (72 mg, 47%) as orange crystals: Recrystallisation (EtOAc) gave bright orange crystals. R_f = 0.8 (hexane:EtOAc 4:1); mp 188-190 ^oC; IR (KBr) ν_{max} 1354 & 1533 (NO_2), 1733

(C=O) cm^{-1}; ^1H NMR ($CDCl_3$) δ 6.80 (2 H, m, SePh 2",6"-H_2), 6.95 (2 H, m, SePh 3",5"-H_2) 7.06 (1 H, tt, *J* = 7.3, 1.2 Hz, SePh 4"-H), 7.32-7.37 (2 H, m, CPh 3',5'-H_2), 7.38 (1 H, tt, *J* = 7.3, 1.5 Hz, CPh 4'-H), 7.58 (2 H, m, CPh 2',6'-H_2), 7.63 (1 H, t, *J* = 8.0 Hz, 7-H), 8.14 (1 H, dd, *J* = 8.0, 1.5 Hz, 6-H), 8.55 (1 H, dd, *J* = 7.9, 1.5 Hz, 8-H); ^{13}C NMR δ 102.24 (4-C), 123.12 (9-C), 127.61 (4"-C, SePh), 127.85 (3',5'-C_2Ph), 128.04 (7-C), 128.90 (3",5"-C_2, SePh), 130.34 (2',6'-C_2Ph), 130.60 (4'-CPh), 131.05 (6-C), 131.70 (1'-C, SePh), 132.18 (2",6"-C_2, SePh), 133.26 (1'-CPh), 133.68 (8-C), 134.38 (10-C), 148.35 (5-C), 159.90 (1-C), 160.65 (3-C); MS (EI) *m/z* 422 (M), 266 (M – C_6H_5Se); Anal. Calcd for $C_{21}H_{13}NO_4Se$: C, 59.73; H, 3.10; N, 3.32; Found: C, 59.8; H, 3.06; N, 3.32.

Methyl 2-methyl-3-nitrobenzoate (111)

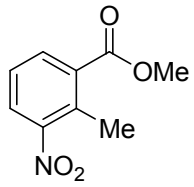

2-Methyl-3-nitrobenzoic acid **112** (10.0 g, 55.2 mmol) in MeOH (200 mL) and conc. H_2SO_4 (1 mL) was boiled under reflux for 48 h, then poured into ice-H_2O (300 mL). The precipitated ester was filtered, washed (H_2O) and recrystallised (MeOH) to give **111** (10.2 g, 94%) as yellow crystals: R_f = 0.48 (hexane:EtOAc 4:1); mp 63-64 °C (lit.[160] mp 65-66 °C); IR ν_{max} (KBr) 1363 & 1522 (NO_2), 1724 (C=O) cm^{-1}; ^1H NMR ($CDCl_3$) δ 2.63 (3 H, s, $ArCH_3$), 3.94 (3 H, s, CO_2CH_3), 7.38 (1 H, t, *J* = 8.0 Hz, 5-H), 7.85 (1 H, d, *J* = 7.9 Hz, 4-H), 7.99 (1 H, d, *J* = 7.7 Hz, 6-H).

Methyl 2-bromomethyl-3-nitrobenzoate (110)

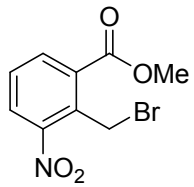

Br_2 (5.9 g, 37 mmol) in CCl_4 (15 mL) was added over 30 min to a boiling solution of **111** (5.75 g, 29.5 mmol) and dibenzoyl peroxide (0.55 g, 2.25 mmol) in CCl_4 (50 mL) under irradiation using a 150 W lamp. After 20 h, additional Br_2 (1.39 g, 8.7 mmol) and dibenzoyl peroxide (0.12 g, 0.5 mmol) in CCl_4 (5 mL) were added. Heating and

irradiation were continued for another 29 h. Evaporation and recrystallisation (MeOH) gave **110** (4.69 g, 58%) as pale brown crystals: R_f = 0.42 (hexane:EtOAc 4:1); mp 70-71 °C (lit.[160] mp 68-69 °C); IR ν_{max} (KBr) 1350 & 1528 (NO_2), 1722 (C=O) cm^{-1}; ^1H NMR ($CDCl_3$) δ 4.01 (3 H, s, CH_3), 5.17 (2 H, s, CH_2), 7.55 (1 H, t, *J* = 7.9 Hz, 5-H), 7.97 (1 H, dd, *J* = 8.1, 1.2 Hz, 4-H), 8.12 (1 H, dd, *J* = 7.9, 1.5 Hz, 6-H).

Methyl 2-cyanomethyl-3-nitrobenzoate (109)

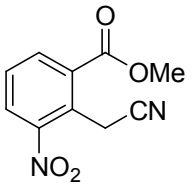

To **110** (5.00 g, 18.21 mmol) in acetonitrile (70 mL) was added Et_4N^+ ^-CN (3.4 g, 22 mmol) and the mixture was stirred for 4 h. Evaporation and chromatography (Et_2O:hexane 1:1) yielded **109** (2.77 g, 69%) as white crystals: R_f = 0.6 (hexane:EtOAc 4:1); mp 94-95 °C (lit.[160] mp 93-94 °C); IR ν_{max} (KBr) 1350 & 1531 (NO_2), 1708 (C=O), 2366 (CN) cm^{-1}; ^1H NMR ($CDCl_3$) δ 4.01 (3 H, s, CH_3), 4.35 (2 H, s, CH_2), 7.64 (1 H, t, *J* = 8.0 Hz, 5-H), 8.13 (1 H, dd, *J* = 8.1, 1.5 Hz, 4-H), 8.28 (1 H, dd, *J* = 7.9, 1.5 Hz, 6-H).

Methyl (±)-2-(1-cyano-2-phenylethyl)-3-nitrobenzoate (116)

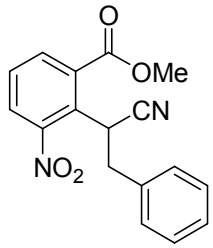

To **109** (1.00 g, 4.5 mmol) in dry THF (15 mL) was added lithium bis(trimethylsilyl)amide (5.6 mL, 5.6 mmol, 1.0 M in THF) and the mixture was stirred at –78 °C for 20 min under N_2. Benzyl bromide (1.13 g, 6.5 mmol) was added and solution was allowed to warm to room temperature and stirred for further 4 h. Extraction (CH_2Cl_2), washing (5% aq. HCl, H_2O), drying and chromatography (toluene) gave **116** (930 mg, 67%) as a pale brown oil: R_f = 0.25 (toluene); IR (film) ν_{max} 1355 & 1540 (NO_2), 1716 (C=O), 2264 (CN) cm^{-1}; ^1H NMR ($CDCl_3$) δ 3.42 (1 H, dd, *J* = 13.0, 5.4 Hz, PhCH), 3.75 (1 H, dd, *J* = 13.0, 10.2 Hz, PhCH), 4.00 (3 H, s, CH_3), 5.07 (1 H, dd, *J* = 10.2, 5.4 Hz, CH), 7.28-7.42 (5 H, m, 2',3',4',5',6'- H_5) 7.56 (1 H, t, *J* = 8.1 Hz, 5-H),

7.97 (1 H, dd, *J* = 8.1, 1.5 Hz, 4-H), 8.08 (1 H, dd, *J* = 7.9, 1.5 Hz, 6-H); ^{13}C NMR δ 34.52 (CH), 39.49 (CH_2), 53.38 (CH_3), 117.88 (CN), 127.57 (4'-C), 128.27 (4-C), 128.80(2',6'-C_2), 129.19 (2-C), 129.37 (3',5'-C_2), 133.10 (1-C), 134.93 (6-C), 136.56 (1'-C), 150.71 (3-C), 166.20 (C=O); MS (FAB$^+$) *m/z* 311.1046 (M + H) ($C_{17}H_{15}N_2O_4$ requires 311.1031).

(±)-2-(2-Formyl-6-nitrophenyl)-3-phenylpropanenitrile (117)

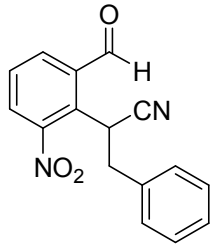

Compound **116** (100 mg, 0.322 mmol) was dissolved in dry CH_2Cl_2 (5 mL) and the solution was stirred at –78 °C for 30 min under N_2. DIBAL-H (1.0 M, 0.5 mL, 0.5 mmol) was added dropwise and the mixture was stirred for 1 h at -78 °C. The solution was then allowed to warm to room temperature. Washing (H_2O), drying and chromatography (hexane:EtOAc 4:1) gave **117** (40 mg, 44%) as buff crystals: R_f = 0.36 (hexane:EtOAc); mp 124-125 °C; IR (KBr) ν_{max} 1355 & 1530 (NO_2), 1697 (C=O), 2264 (CN) cm^{-1}; ^{1}H NMR ($CDCl_3$) δ 3.30 (1 H, dd, *J* = 13.3, 5.5 Hz, PhCH), 3.59 (1 H, dd, *J* = 10.1, 13.3 Hz, PhCH), 5.25 (1 H, dd, *J* = 9.4, 5.5 Hz, CH), 7.43-7.24 (5 H, m, 2',3',4',5',6'-H_5), 7.76 (1 H, t, *J* = 7.8, Hz, 5-H), 8.00 (1 H, dd, *J* = 8.2, 1.5 Hz, 4-H), 8.15 (1 H, dd, *J* = 7.8, 1.5 Hz, 6-H), 10.28 (1 H, s, CHO); ^{13}C NMR δ 32.70 (CH), 39.39 (CH_2), 117.65 (CN), 127.83 (4'-C), 128.92 (2',6'-C_2), 129.38 (3',5'-C_2), 129.81 (2-C), 129.85 (4-C), 130.03 (5-C), 135.03 (1-C), 135.86 (1'-C), 138.32 (6-C), 150.10 (3-C), 190.18 (C=O); MS (FAB$^+$) *m/z* 280.0850 (M) ($C_{16}H_{12}N_2O_3$ requires 280.0847).

5-Nitroisocoumarin (126)

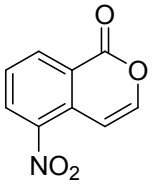

The ester **111** (5.0 g, 25.6 mmol) was heated with dimethylformamide dimethyl acetal (2.5 g, 21 mmol) in DMF (30 mL) at 150 °C for 16 h. Evaporation, chromatography

(hexane:EtOAc 10:1) gave **126** (1.9 g, 39%) as yellow crystals: mp 170-172 °C (lit.[160] mp 171-172 °C); R_f = 0.41 (hexane:EtOAc 4:1); IR (KBr) ν_{max} 1332, 1518 (NO_2), 1748 (C=O) cm^{-1}; ^1H NMR ($CDCl_3$) δ 7.35 (1 H, dd, *J* = 6.1, 0.5 Hz, 4-H), 7.43 (1 H, d, *J* = 6.0 Hz, 3-H), 7.65 (1 H, t, *J* = 7.9 Hz, 7-H), 8.48 (1 H, dd, *J* = 8.2, 1.3 Hz, 6-H), 8.64 (1 H, ddd, *J* = 7.9, 1.5, 0.5 Hz, 8-H).

5-Nitroisoquinolin-1(2*H*)-one (113)

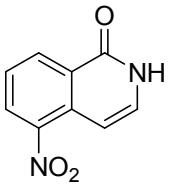

A solution of **126** (1.7 g, 8.86 mmol) in 2-methoxyethanol (30 mL) was saturated with NH_3 and boiled under reflux for 2 h. Evaporation and recrystallisation (EtOH) gave **113** (1.5 g, 89%) as yellow crystals: R_f = 0.29 (hexane:EtOAc 1:2); mp 248-249 °C (lit.[160] mp 247-249 °C); ^1H NMR ($(CD_3)_2SO$) δ 6.98 (1 H, dd, *J* = 7.7, 4-H), 7.45 (1 H, dd, *J* = 7.7, 1.5 Hz, 3-H), 7.66 (1 H, t, *J* = 7.9 Hz, 7-H), 8.47 (1 H, dd, *J* = 7.9, 1.3 Hz, 6-H), 8.59 (1 H, d, *J* = 8.0 Hz, 8-H), 11.79 (1 H, br s, NH).

4-Bromo-5-nitroisoquinolin-1-one (124)
4-Bromo-5-nitro-1-oxo-1,2,3,4-tetrahydroisoquinolin-3-yl acetate (129)

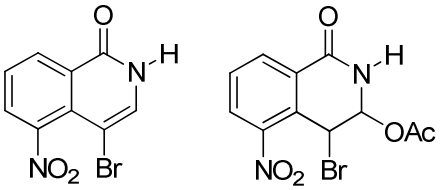

To a solution of **113** (0.1 g, 0.5 mmol) in AcOH (5 mL) was added equimolar amount of N-bromosuccinimide (0.09 g, 0.5 mmol). After 30 min the mixture was poured into ice H_2O (100 mL) stirred for 10 min. Extraction (EtOAc), washing (aq. $NaHCO_3$, H_2O) drying, evaporation and chromatography (hexane:EtOAc 4:1) yielded **129** (0.07 g, 33%) as buff solid: mp 137°C; IR (KBr) ν_{max} 1335 & 1534 (NO_2), 1675 (C=O), 3462 (NH) cm^{-1}; ^1H NMR ($(CD_3)_2CO$) δ 2.08 (3 H, s, CH_3), 5.79 (1 H, d, *J* = 4.7 Hz, 4-H), 5.95 (1 H, m, 3-H), 7.82 (1 H, t, *J* = 7.9 Hz, 7-H), 8.33 (1 H, dd, *J* = 8.2, 1.5 Hz, 6-H), 8.45 (1 H, dd, *J* = 8.0, 1.2 Hz, 8-H).

Also isolated was **124** (0.3 g, 21%) as orange crystals: mp 233-235°C; IR (KBr) ν_{max} 1368 & 1534 (NO_2), 1674 (C=O), 3467 (NH) cm^{-1}; ^1H NMR ($(CD_3)_2CO$) δ 7.73 (1 H, s, 3-H), 7.77 (1 H, t, *J* = 7.8 Hz, 7-H), 8.10 (1 H, dd, *J* = 7.8, 1.6 Hz, 6-H), 8.61 (1 H, dd, *J* = 8.6, 1.9 Hz, 8-H); ^{13}C NMR δ 90.40 (4-C), 127.98 (10-C), 128.25 (7-C), 129.46 (6-C), 129.88 (9-C), 132.05 (8-C), 135.60 (3-C), 147.25 (5-C), 159.00 (1-C); MS (ESI +ve) *m/z* 267.9478 (M) ($C_9H_5{}^{79}BrN_2O_3$ requires 267.9484), 290.9376 (M + Na) ($C_9H_5{}^{79}BrN_2O_3Na$ requires 290.9332), 292.9354 (M + Na) ($C_9H_5{}^{81}BrN_2O_3Na$ requires 292.9312), Anal. Calcd. for $C_9H_5BrN_2O_3$: C, 40.18; H, 1.87; N, 10.41; Found: C, 40.60; H, 1.61; N, 10.19.

4-Bromo-5-nitroisoquinolin-1(2*H*)-one (124)

4-Bromo-3-hydroxy-5-nitro-3,4-dihydroisoquinolin-1(2*H*)-one (130)

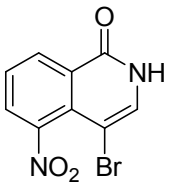

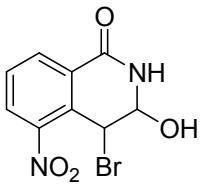

To a solution of **113** (1.5 g, 7.8 mmol) in AcOH (15 mL) was added equimolar amount of Br_2 (0.21 g, 1.31 mmol) in AcOH (7 mL). After 2 h the mixture was poured into ice H_2O (100 mL) stirred for 10 min. Extraction (CH_2Cl_2), drying, evaporation and chromatography (hexane:EtOAc 4:1) yielded **124** (0.7 g, 33%) as orange crystals with data as above.

Also isolated was **130** (0.7 g, 33%) as buff solid: mp 175-177°C; IR (KBr) ν_{max} 1338 & 1534 (NO_2), 1672 (C=O), 3460 (NH) cm^{-1}; ^1H NMR ($(CD_3)_2CO$) δ 8.55 (1 H, br s, NH), 8.30 (1 H, dd, *J* = 7.7, 1.5 Hz, 8-H), 8.0 (1 H, dd, *J* = 7.9, 1.5 Hz, 6-H), 7.82 (1 H, t, *J* = 7.9 Hz, 7-H), 6.73 (1 H, d, *J* = 5.9 Hz, 4-H), 5.52 (1 H, t, *J* = 5.7, 1.2 Hz, 6-H). ^{13}C NMR δ 85.87 (4-C), 91.21 (3-C), 128.99 (7-C), 130.21 (6-C), 130.87(9-C), 132.16 (10-C), 132.79 (8-C), 136.37 (3-C), 151.69 (5-C), 162.16 (1-C).

3,4-Dibromo-5-nitroisocoumarin (131)

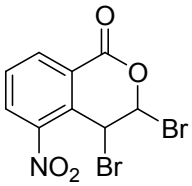

To a solution of **126** (0.25 g, 1.31 mmol) in AcOH (2.5 mL) was added equimolar amount of Br_2 (0.21 g, 1.31 mmol) in AcOH (1 mL). After 2 h the mixture was poured into ice H_2O (100 mL) stirred for 10 min. Extraction (CH_2Cl_2), drying, evaporation and chromatography (hexane:EtOAc 4:1) yielded **131** (0.24 g, 52%) as white crystals: mp 116-118 ^oC; R_f = 0.7 (hexane:EtOAc 4:1); IR (KBr) ν_{max} 1054 (C-O), 1346, 1528 (NO_2), 1761 (C=O) cm^{-1}; ^1H NMR ($CDCl_3$) δ 6.32 (1 H, d, *J* = 1.7 Hz, 4-H), 6.90 (1 H, d, *J* = 1.7 Hz, 3-H), 7.80 (1 H, t, *J* = 8.2 Hz, 7-H), 8.52 (1 H, s, 6-H), 8.64 (1 H, s, 8-H); ^{13}C NMR δ 38.41 (4-C), 78.21 (3-C), 125.07 (9-C), 130.90 (7-C), 131.31 (8-C), 133.02 (10-C), 135.65 (6-C), 145.34 (5-C), 158.28 (1-C); MS (ESI +ve) *m/z* 349.8658 (M + H) ($C_9H_6{}^{79}Br_2NO_4$ requires 349.8664), 351.8647 (M + H) ($C_9H_6{}^{79}Br^{81}BrNO_4$ requires 351.8642), 353.8621 (M + H) ($C_9H_6{}^{81}Br_2NO_4$ requires 353.8623), 373.8455 (M + Na) ($C_9H_6{}^{79}Br^{81}BrNO_4Na$ requires 373.8463).

5-Amino-4-bromoisoquinolin-1(2*H*)-one (125)

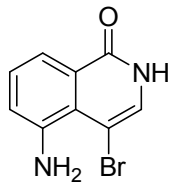

A mixture of **124** (0.54 g, 2.0 mmol) and $SnCl_2$ (1.21 g, 6.4 mmol) in EtOH (20 mL) was heated at 80°C for 4 h, then carefully poured into ice-H_2O (75 mL). The resulting suspension was made alkaline with aq. NaOH and the precipitate was filtered. Extraction of the filtrate (EtOAc), evaporation and chromatography (EtOAc:hexane 4:1) gave **125** (0.25 mg, 54%) as brown powder: R_f = 0.33 (EtOAc:hexane 1:4); mp 210-212°C; IR (KBr) ν_{max} 1661, 1624 (C=O), 3443, 3321 (NH) cm^{-1}; ^1H NMR ($(CD_3)_2SO$) δ 5.92 (2 H, br s, NH_2), 7.73 (1 H, s, 3-H), 7.02 (1 H, dd, *J* = 8.2, 1.6 Hz, 6-H), 7.22 (1 H, s, 3-H), 7.25 (1 H, t, *J* = 8.2 Hz, 7-H), 7.54 (1 H, dd, *J* = 7.8, 1.2 Hz, 8-H), 11.34 (1 H, br s, NH); ^{13}C NMR δ 93.10 (4-C), 115.83 (8-C), 119.17 (6-C), 119.42 (10-C), 128.04 (3-C), 128.44 (9-C), 128.56 (7-C), 144.72 (5-C), 160.83 (1-C); MS (ESI +ve) *m/z* 238.9815 (M + H) ($C_9H_8{}^{79}BrN_2O$ requires 238.9820).

2-Iodo-3-nitrobenzoyl chloride (139)

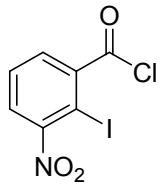

To **76** (3.0 g, 10.2 mmol) and DMF (0.2 mL) was carefully added $SOCl_2$ (30 mL) and the mixture was boiled under reflux for 24 h. Evaporation and recrystallisation (hexane) yielded **139** (3.0 g, 94%) as yellow crystals: R_f = 0.88 (EtOAc:hexane 1:4); mp 71-73 °C (lit.[160] mp 70-71 °C); IR ν_{max} (KBr) 1348 & 1530 (NO_2), 1758 (C=O) cm^{-1}; ^1H NMR ($CDCl_3$) δ 7.64 (1 H, t, *J* = 7.8 Hz, 5-H), 7.79 (1 H, dd, *J* = 7.8, 1.6 Hz, 4-H), 7.95 (1 H, dd, *J* = 7.8, 1.6 Hz, 6-H).

***N*,*N*-Di(prop-2-enyl)-2-iodo-3-nitrobenzamide (141)**

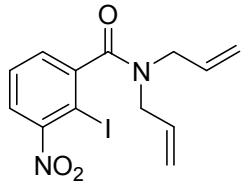

To 2-iodo-3-nitrobenzoyl chloride **139** (1.0 g, 3.2 mmol) in CH_2Cl_2 (5 mL) was added di-2-propenylamine (0.4 mL, 3.2 mmol) and Et_3N (0.64 g, 6.4 mmol) and the mixture was stirred for 30 min. Washing (5% aq. HCl, 5% aq. $NaHCO_3$), drying, evaporation and chromatography (CH_2Cl_2:EtOAc 20:1) gave **141** (0.89 g, 75%) as a buff semisolid: R_f = 0.64 (CH_2Cl_2:EtOAc 20:1); IR (film) ν_{max} 1360 & 1532 (NO_2), 1733 (C=O) cm^{-1}; ^1H NMR ($CDCl_3$) δ 3.63 (1 H, dd, *J* = 16.3, 3.9 Hz, propenyl 1-H), 3.76 (2 H, m, 2 x propenyl 1-H), 4.60 (1H, dd, *J* = 14.9, 4.3 Hz, propenyl 1-H), 5.12 (1 H, dq, *J* = 17.2, 1.6 Hz, propenyl 3-H), 5.20 (1 H, dq, *J* = 10.2, 1.2 Hz, propenyl 3-H), 5.30 (1 H, dq, *J* = 10.6, 1.2 Hz, propenyl 3-H), 5.35 (1 H, dq, *J* = 17.2, 1.2 Hz, propenyl 3-H), 5.65 (1 H, m, propenyl 2-H), 5.95 (1 H, m, propenyl 2-H), 7.34 (1 H, dd, *J* = 7.6, 1.5 Hz, 6-H), 7.49 (1 H, t, *J* = 7.8 Hz, 5-H), 7.68 (1 H, dd, *J* = 7.9, 1.5 Hz, 4-H); ^{13}C NMR δ 46.76 (CH_2), 50.16 (CH_2), 85.22 (2-C), 118.46 (=CH_2), 119.06 (=CH_2), 124.63 (4-C), 129.47 (5-C), 129.75 (6-C), 131.78 (=CH), 131.95 (=CH), 145.88 (1-C), 154.34 (3-C), 169.13 (C=O); MS (EI) *m/z* 371.9958 (M) ($C_{13}H_{13}IN_2O_3$ requires 371.9970).

***(E)*-Diphenyl-N-(*(E)*-3-phenylprop-2-enylidene)methanamine (146)**

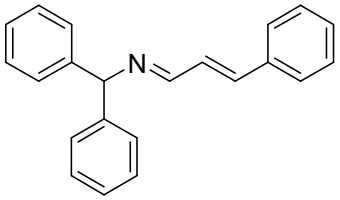

Diphenylmethylamine **144** (6.9 g, 38 mmol) and *E*-3-phenylpropenal **145** (5.0 g, 38 mmol) were boiled in toluene (50 mL) in a Dean-Stark apparatus until the calculated amount of water had separated (0.7 mL). Evaporation and recrystallisation (Et_2O) gave **146** (11.0 g, 97%) as yellow crystals: mp 115-117 °C (lit.[209] mp 116-118 °C); IR (KBr) ν_{max} 1444 & 1489 (C=C), 1598 (C=C conjugated) cm^{-1}; ^1H NMR ($CDCl_3$) δ 5.48 (1 H, s, Ph_2CH), 6.96 (1 H, d, *J* = 16.1 Hz, propene 3-H), 7.06 (1 H, dd, *J* = 16.0, 8.1 Hz, propene 2-H), 7.20-7.40 (13 H, m, 2 x Ph-H_5 + Ph 3',4',5'-H_3), 7.47 (2 H, dd, *J* = 9.4, 1.7 Hz, Ph 2',6'-H_2), 8.18 (1 H, dd, *J* = 8.2, 0.8 Hz, propene 1-H).

***(E)*-N-Diphenylmethyl-3-phenylprop-2-en-1-amine (147)**

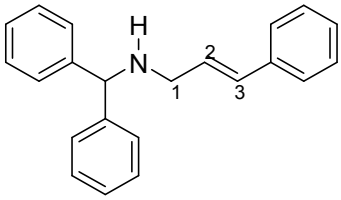

To **146** (6.0 g, 20 mmol) in MeOH (250 mL) warmed to 45 °C was slowly added $NaBH_4$ (0.77 g, 20 mmol) during 20 min. After evaporation of the solvent the residue was taken up in Et_2O, washed (5% aq. $NaHCO_3$) and dried. Evaporation gave **147** (5.8 g, 95%) as pale yellow semi-solid. IR (film) ν_{max} 1451 & 1492 (C=C), 1598 (C=C conjugated), 3332 (NH) cm^{-1}; ^1H NMR ($CDCl_3$) δ 1.94 (1 H, br s, N-H), 3.52 (2 H, dd, *J* = 6.2, 1.0 Hz, CH_2), 5.07 (1 H, s, Ph_2CH), 6.47 (1 H, dt, *J* = 15.8, 6.0 Hz, propene 2-H), 6.65 (1 H, d, *J* = 15.8 Hz, propene 3-H), 7.34-7.61 (15 H, m, 3 x Ph-H_5).

***(E)* N-Diphenylmethyl-2-iodo-3-nitro-N-(3-phenylprop-2-enyl)benzamide (148)**

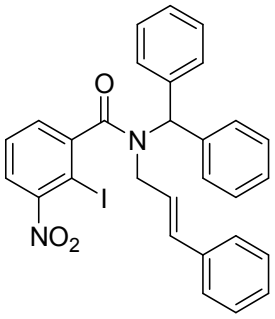

To **139** (1.5 g, 4.8 mmol) in CH_2Cl_2 (10 mL) was added **147** (1.43 g, 4.8 mmol) and Et_3N (0.97 g, 9.6 mmol) and the mixture was stirred for 30 min. Washing (5% aq. HCl, 5% aq. $NaHCO_3$) drying, evaporation and chromatography (hexane:EtOAc 4:1) gave **148** (1.49 g, 54%) as a buff solid: mp 134-136 ^oC; R_f = 0.38 (hexane:EtOAc 4:1); IR ν_{max} (KBr) 1360 & 1530 (NO_2), 1636 (C=O) cm^{-1}; The NMR spectra showed a 3:4 mixture of rotamers α & β about the amide double bond. ^1H NMR **α** ($CDCl_3$) δ 3.91-4.06 (2 H, m, CH_2), 5.20 (1 H, dt, *J* = 15.5, 6.5 Hz, =C<u>H</u>CH_2), 5.42 (1 H, d, *J* = 16.0 Hz, =CHPh), 7.31 (1 H, s, Ph_2CH), 6.9-7.65 (18 H, m, 3 x Ph-H_5 + 4,5,6-H_3); ^{13}C NMR δ 49.33 (CH_2), 61.21 (Ph_2CH), 85.89 (2-C), 123.91 (=<u>C</u>HCH_2), 124.34 (4-C), 126.03, 127.16, 127.32, 127.66, 127.76, 128.26, 128.38, 128.54, 128.84, 129.25, 130.66, 132.73 (=<u>C</u>HPh), 135.45 (q), 138.16 (q), 138.60 (q), 145.95 (1-C), 154.19 (3-C), 168.80 (C=O);

^1H NMR **β** ($CDCl_3$) δ 3.93-4.05 (1 H, m, H-CH), 4.81 (1 H, dd, *J* = 14.5, 5.5 Hz, H-CH), 5.83 (1 H, s, Ph_2CH), 5.88 (1 H, d, *J* = 16.0 Hz =CHPh), 6.0 (1 H, dt, *J* = 16.0, 6.0 Hz, =C<u>H</u>CH_2), 6.90-7.65 (18 H, m, 3 x Ph-H_5 + 4,5,6-H_3); ^{13}C NMR δ 46.72 (CH_2), 66.63 (Ph_2CH), 85.18 (2-C), 123.42 (=<u>C</u>HCH_2), 124.49 (4-C), 126.15, 127.08, 127.58, 127.68, 127.72, 128.16, 128.24, 128.35, 128.63, 128.79, 129.22, 132.36 (=<u>C</u>HPh), 136.63 (q), 137.51 (q), 139.25 (q), 145.17 (1-C), 154.26 (3-C), 169.42 (C=O); MS (EI) *m/z* 575.0821 (M + H) ($C_{29}H_{24}IN_2O_3$) requires 575.0826.

2-(prop-2-enyl)-4-methyl-5-nitroisoquinolin-1(*2H*)-one (149)
2-(prop-2-enyl)-4-methylene-5-nitro-3,4-dihydroisoquinolin-1(*2H*)-one (150)

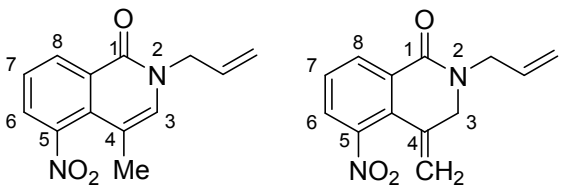

To **141** (0.31 g, 0.81 mmol) in dry MeCN (10 mL) was added $(Ph_3P)_4Pd$ (40.3 mg, 0.035 mmol) and dry Et_3N (0.175 g, 1.72 mmol) and the mixture was heated to reflux for 48 h. After evaporation of the solvent the residue was taken in EtOAc, washed (5% aq. HCl, 5% aq. $NaHCO_3$) and dried. Evaporation and chromatography (hexane:EtOAc 4:1) yielded **149** and **150** (0.15 g, 79%) (1:2) as a buff oil. R_f = 0.35 (hexane:EtOAc 4:1); IR (film) ν_{max} 1365 & 1531 (NO_2), 1658 (C=O) cm^{-1}; ^1H NMR **149** ($CDCl_3$) δ 2.10 (3 H, d, *J* = 1.2 Hz, CH_3), 4.60 (2 H, dt, *J* = 5.7, 1.5 Hz, propenyl 1-H), 5.19 (2 H, m, propenyl 3-H), 5.96 (1 H, m, propenyl 2-H), 6.93 (1 H, d, *J* =1.2 Hz, 3-H), 7.53 (1 H, t, *J* = 7.9 Hz, 7-H), 7.74 (1 H, dd, *J* = 7.8, 1.5 Hz, 6-H), 8.66 (1 H, dd, *J* = 7.8, 1.5 Hz, 8-H); ^{13}C NMR δ 15.81 (CH_3), 50.67 (NCH_2), 108.36 (4-C), 118.74 ($=CH_2$), 125.95 (7-C), 127.18 (6-C), 131.86 (8-C), 131.99 (=CH), 132.60 (10-C), 133.18 (3-C), 133.87 (9-C), 147.33 (5-C), 159.87 (1-C).

^1H NMR **150** ($CDCl_3$) δ 4.12 (2 H, s, 3-CH_2), 4.20 (2 H, dt, *J* =5.9, 1.5 Hz, propenyl 1-H), 5.26 (2 H, m, propenyl 3-H), 5.29 (1 H, s, H of 4=CH_2), 5.45 (1 H, s, H of 4=CH_2), 5.81 (1 H, m, propenyl 2-H), 7.47 (1 H, t, *J* = 7.9 Hz, 7-H), 7.70 (1 H, dd, *J* = 8.1, 1.5 Hz, 6-H), 8.31 (1 H, dd, *J* = 7.8, 1.3 Hz, 8-H); ^{13}C NMR δ 49.33 (NCH_2), 52.18 (3-C), 118.12 ($=CH_2$), 119.39 (4=CH_2),, 126.60 (6-C), 128.69 (7-C), 129.13 (10-C), 130.68 (9-C), 131.55 (4-C), 131.78 (8-C), 131.89 (=CH), 147.51 (5-C), 161.05 (1-C). MS (ESI +ve) *m/z* 245.0916 (M + H) ($C_{13}H_{13}N_2O_3$ requires 245.0926), 267.0737 (M + H) ($C_{13}H_{12}N_2NaO_3$ requires 267.0746).

2-Diphenylmethyl-5-nitro-4-phenylmethylisoquinolin-1(*2H*)-one (151)
***(Z)*-4-Benzylidene-2-diphenylmethyl-5-nitro-3,4-dihydroisoquinolin-1(*2H*)-one (152)**

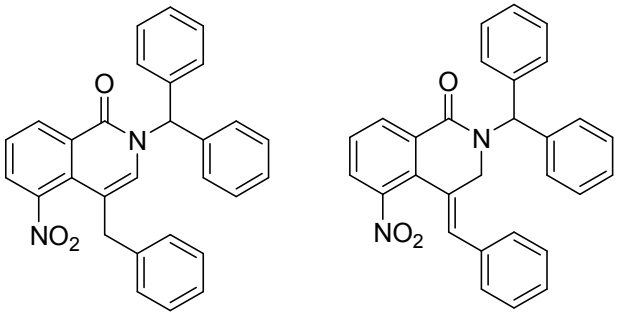

To **148** (0.5 g, 0.87 mmol) in dry propanenitrile (15 mL) was added $(Ph_3P)_4Pd$ (50.3 mg, 0.044 mmol), dry Et_3N (0.17 g, 1.7 mmol) and the mixture was boiled under reflux for 48 h. After evaporation of solvent residue was taken up in EtOAc, washed (5% aq.

HCl, 5% aq. $NaHCO_3$) and dried. Evaporation and chromatography (hexane:EtOAc 4:1) yielded an inseparable mixture of **151** and **152** (0.16 g, 41%) (1:3) as yellow crystals: IR ν_{max} (KBr) 1347 & 1524 (NO_2), 1654 (C=O) cm^{-1}; R_f = 0.35 (hexane:EtOAc 4:1); ^1H NMR **151** ($CDCl_3$) δ 3.75 (2 H, s, CH_2), 6.54 (1 H, s, 3-H), 6.86-7.30 (15 H, m, 3 x Ph-H_5), 7.44 (1 H, s, Ph_2CH), 7.52 (1 H, t, *J* = 7.8 Hz, 7-H), 7.79 (1 H, dd, *J* = 7.5, 1.4 Hz, 6-H), 8.75 (1 H, dd, *J* = 8.2, 1.7 Hz, 8-H); ^{13}C NMR δ 35.45 (CH_2), 60.72 (Ph_2CH), 112.07 (4-C), 125.96 (7-C), 126.59 (6-C), 128.16, 128.39, 128.62, 128.69, 129.05, 131.27, 132.76 (8-C), 133.47 (3-C), 133.38, 137.54 (q), 147.88 (5-C), 159.95 (1-C).

^1H NMR **152** ($CDCl_3$) δ 4.24 (2 H, d, *J* = 1.1 Hz, 3-CH_2), 6.82 (1 H, s, =CH), 7.24 (1 H, s, Ph_2CH), 6.86-7.30 (15 H, m, 3 x Ph-H_5), 7.51 (1 H, t, *J* = 8.2 Hz, 7-H), 7.78 (1 H, dd, *J* = 7.8, 1.3 Hz, 6-H), 8.41 (1 H, dd, *J* = 7.8, 1.3 Hz, 8-H); ^{13}C NMR δ 43.66 (CH_2), 60.77 (Ph_2CH), 124.93 (4-C), 127.14 (6-C), 127.48, 127.56, 128.30 (7-C), 128.38, 128.42, 128.44, 128.74, 131.15 (10-C), 131.33 (9-C), 134.63 (q), 134.75 (=CH), 137.95 (q), 147.94 (5-C), 161.52 (1-C). MS (EI) *m/z* 447.1703 (M + H) ($C_{29}H_{23}N_2O_3$ requires 447.1707.)

***(E)*-N-Diphenylmethyl-1-deutero-3-phenylprop-2-en-1-amine (157)**

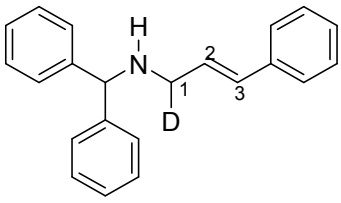

To **146** (2.0 g, 6.72 mmol) in MeOH (100 mL) warmed to 45 ^oC was slowly added $NaBD_4$ (0.28 g, 6.72 mmol) during 20 min. After evaporation of the solvent the residue was taken up in Et_2O, washed (5% aq. $NaHCO_3$) and dried. Evaporation gave **157** (2.0 g, 99%) as yellow semi-solid: IR (film) ν_{max} 1599 (C=C conjugated), 2248 (C-D), 3325 (NH) cm^{-1}; ^1H NMR ($CDCl_3$) δ 2.09 (1 H, br s, N-H), 3.61 (1 H, br d, *J* = 6.0 Hz, 1-H), 5.19 (1 H, s, Ph_2CH), 6.57 (1 H, dd, *J* = 15.8, 6.0 Hz, 2-H), 6.81 (1 H, d, *J* = 15.8 Hz, 3-H), 7.41-7.81 (15 H, m, 3 x Ph-H_5). ^{13}C NMR δ 49.61 (t, *J* = 20.70 Hz, DCH), 66.33 (Ph_2CH), 126.24, 127.04, 127.31, 128.08 (=CCHD), 128.24, 128.49, 130.04, 131.49, 132.39 (=CPh), 137.05 (q), 137.52 (q), 143.66 (q).

***(E)*-N-Diphenylmethyl-2-iodo-3-nitro-N-(1-deutero-3-phenylprop-2-enyl) benzamide (158)**

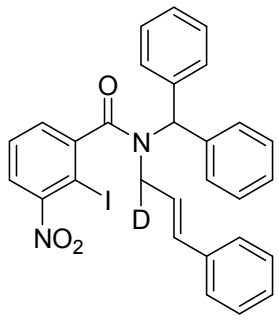

To **139** (1.5 g, 4.8 mmol) in CH_2Cl_2 (10 mL) was added **157** (1.44 g, 4.8 mmol) and Et_3N (0.97 g, 9.6 mmol) and the mixture was stirred for 30 min. Washing (5% aq. HCl, 5% aq. $NaHCO_3$) drying, evaporation and chromatography (hexane:EtOAc 6:1) gave **158** (1.69 g, 61%) as light yellow crystals: mp 135-137 ^oC; R_f = 0.43 (hexane:EtOAc 6:1); IR ν_{max} (KBr) 1339 & 1529 (NO_2), 1634 (C=O) cm^{-1}; The NMR spectra showed a 2:3 mixture of rotamers α & β about the amide double bond. ^1H NMR **α** ($CDCl_3$) δ 3.93 (1 H, m, H-CD), 5.16 (1 H, dd, *J* = 16.0, 7.0 Hz, =C<u>H</u>CHD), 5.40 (1 H, d, *J* = 16.0 Hz, =CHPh), 7.29 (1 H, s, Ph_2CH), 6.90-7.65 (18 H, m, 3 x Ph-H_5 + 4,5,6-H_3); ^{13}C NMR δ 49.25 (t, *J* = 20.7 Hz, DCH), 61.34 (Ph_2CH), 86.08 (2-C), 124.06 (=$CHCH_2$), 124.56 (4-C), 126.21, 127.24, 127.26, 127.87, 128.35, 128.46, 128.62, 128.82, 128.84, 129.47, 132.64, 132.69 (=CHPh), 135.61 (q), 138.28 (q), 138.84 (q), 146.27 (1-C), 154.30 (3-C), 168.66 (C=O);

^1H NMR **β** ($CDCl_3$) δ 3.90 (1/2 H, m, H-CD), 4.8 (1/2 H, d, *J* = 5.4 Hz, H-CD), 5.78 (1 H, s, Ph_2CH), 5.84 (1 H, dd, *J* = 16.0, 5.0 Hz, =CHPh), 5.96 (1 H, dd, *J* = 16.0, 7.5 Hz, =CHCHD), 6.9-7.65 (18 H, m, 3 x Ph-H_5 + 4,5,6-H_3); ^{13}C NMR δ 46.68 (t, *J* = 20.70 Hz, DCH), 66.84 (Ph_2CH), 85.43 (2-C), 123.44 (=$CHCH_2$), 124.69 (4-C), 126.21, 126.36, 127.37, 127.89, 128.48, 128.54, 128.74, 128.89, 129.38, 130.91, 132.95 (=CHPh), 136.83 (q), 137.68 (q), 139.53 (q), 145.45 (1-C), 154.48 (3-C), 170.03 (C=O);

2-Diphenylmethyl-3-deutero-5-nitro-4-phenylmethylisoquinolin-1(2H)-one (151)/(162)

***(Z)*-4-Benzylidene-2-diphenylmethyl-3-deutero-5-nitro-3,4-dihydroisoquinolin-1(2*H*)-one (161)**

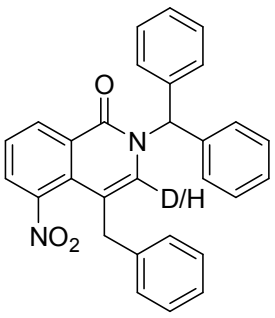

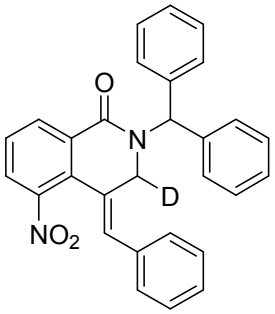

To **158** (0.5 g, 0.87 mmol) in dry propanenitrile (15 mL) was added $(Ph_3P)_4Pd$ (50.3 mg, 0.0435 mmol) and dry Et_3N (0.17 g, 1.74 mmol) and the mixture was heated to reflux for 2 h. After evaporation of the solvent the residue was taken up in EtOAc, washed (5% aq. HCl, 5% aq. $NaHCO_3$) and dried. Evaporation and chromatography (hexane:EtOAc 4:1) yielded a mixture of **151/162** and **161** (1:20) (0.33 g, 85%) as yellow crystals: R_f = 0.37 (hexane:EtOAc 4:1); IR ν_{max} (KBr) 1347 & 1523 (NO_2), 1654 (C=O) cm^{-1}; ^1H NMR **151/162** ($CDCl_3$) δ 3.73 (2 H, s, CH_2), 6.53 (1 H, s, 3-H/D), 6.86-7.30 (15 H, m, 3 x Ph-H_5), 7.42 (1 H, s, Ph_2CH), 7.53 (1 H, t, *J* = 7.9 Hz, 7-H), 7.81(1 H, dd, *J* = 7.7, 1.5 Hz, 6-H), 8.74 (1 H, dd, *J* = 7.9, 1.4 Hz, 8-H).

^1H NMR **161** ($CDCl_3$) δ 4.19 (1 H, s, 3-H/D), 6.80 (1 H, s, =CH), 7.23 (1 H, s, Ph_2CH), 6.86-7.30 (15 H, m, 3 x Ph-H_5), 7.52 (1 H, t, *J* = 8.0 Hz, 7-H), 7.77 (1 H, dd, *J* = 8.0, 1.2 Hz, 6-H), 8.39 (1 H, dd, *J* = 7.9, 1.2 Hz, 8-H); ^{13}C NMR δ 43.43 (t, *J* = 20.7 Hz, CHD), 60.73 (Ph_2CH), 124.87 (4-C), 127.11 (6-C), 127.52, 127.56, 128.28, 128.34, 128.36, 128.41, 128.43, 128.64 (q), 128.81, 129.07 (q), 132.01 (8-C), 134.61 (q), 134.74 (=CH),137.92 (q), 137.95 (q), 147.91 (5-C), 161.48 (1-C). MS (ESI +ve) *m/z* 470.1527 (M + Na) ($C_{29}H_{21}DN_2NaO_3$ requires 470.1591).

2-Hydroxymercuri-3-nitrobenzoic acid (75)

2-Bromo-3-nitrobenzoic acid (165)

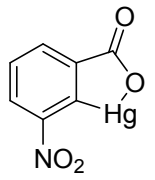

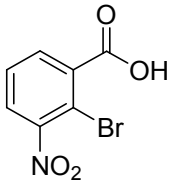

3-Nitrobenzene-1,2-dicarboxylic acid **74** (21.1 g, 100 mmol) in hot aq. NaOH (10%, 80 mL) was added to $Hg(OAc)_2$ (35.0 g, 110 mmol) in hot AcOH (5 mL) and H_2O (70 mL). The mixture was heated at 120 °C for 70 h and then filtered. The precipitate was washed (H_2O, then EtOH) and dried to give 2-hydroxymercuri-3-nitrobenzoic acid **75** (30.7 g, 84%) as a cream solid. To a refluxing solution of **75** (30.7 g, 84 mmol) in aq. NaOH (3.5%, 500 mL) was slowly added, with vigorous stirring, aq. HCl (2 M, 12 mL) and the solution was allowed to cool to room temperature. AcOH (3 mL) was then added. The precipitate dissolved upon addition of NaBr (10.0 g, 100 mmol) and Br_2 (15.98 g, 100 mmol) in H_2O (20 mL). The solution was boiled under reflux for 24 h, cooled and neutralised with aq. NaOH before being filtered and acidified with aq. HCl (9 M). The precipitate was filtered, dried and recrystallised (EtOH) to give **165** (13.7 g, 66%) as buff crystals: R_f = 0.22 (CH_2Cl_2:MeOH:AcOH 9:1:0.1); mp 185-187 °C (lit.[160] mp 186-188 °C); IR ν_{max} (KBr) 1372 & 1543 (NO_2), 1712 (C=O), 2515-3060 (OH) cm^{-1}; ^1H NMR $(CD_3)_2SO$ δ 7.70 (1 H, t, *J* = 7.9 Hz, 5-H), 7.94 (1 H, dd, *J* = 7.9, 1.5 Hz, 4-H), 8.07 (1 H, dd, *J* = 8.1, 1.7 Hz, 6-H).

2-Bromo-3-nitrobenzoyl chloride (166)

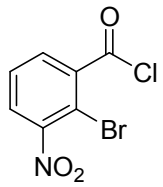

To **165** (1.0 g, 4.5 mmol) and DMF (0.1 mL) was carefully added $SOCl_2$ (10 mL) and the mixture was boiled under reflux for 24 h. Evaporation and recrystallisation (Et_2O) yielded **166** (1.02 g, 86%) as white solid: mp 65-67 °C (lit.[210] mp 66-66.5°C); R_f = 0.13 (EtOAc:hexane 1:4); IR ν_{max} (KBr) 1345 & 1534 (NO_2), 1756 (C=O) cm^{-1}; ^1H NMR $(CD_3)_2SO$ δ 7.62 (1 H, t, *J* = 7.9 Hz, 5-H), 7.87 (1 H, dd, *J* = 8.1, 1.7 Hz, 4-H), 8.03 (1 H, dd, *J* = 8.0, 1.5 Hz, 6-H).

2-Bromo*(E)*-N-Diphenylmethyl-3-nitro-N-(1-deutero-3-phenylprop-2-enyl) benzamide (167)

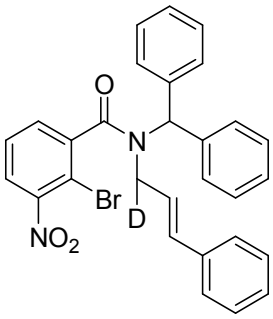

To 2-bromo-3-nitrobenzoyl chloride **166** (0.48 g, 1.8 mmol) in CH_2Cl_2 (10 mL) was added **157** (0.54 g, 1.8 mmol) and Et_3N (0.36 g, 3.6 mmol) and the mixture was stirred for 30 min. Washing (5% aq. HCl, 5% aq. $NaHCO_3$), drying, evaporation and chromatography (hexane:EtOAc 4:1) gave **167** (1.49 g, 54%) as buff crystals: mp 114-116 ^oC; R_f = 0.25 (hexane:EtOAc 4:1); IR ν_{max} (KBr) 1359 & 1532 (NO_2), 1638 (C=O) cm^{-1}; The NMR spectra showed a 2:3 mixture of rotamers α & β about the amide double bond. ^1H NMR α ($CDCl_3$) δ 3.93 (1 H, m, H-CD), 5.10 (1 H, dd, *J* = 15.87, 6.76 Hz, =CHCHD), 5.41 (1 H, d, *J* = 15.87 Hz, =CHPh), 7.29 (1 H, s, Ph_2CH), 6.80-7.46 (17 H, m, 3 x Ph-H_5 + 5,6-H_2), 7.74 (1 H, dd, *J* = 7.35, 2.1 Hz, 4-H); ^{13}C NMR δ 48.96 (t, *J* = 22.2 Hz, DCH), 61.26 (Ph_2CH), 111.79 (2-C), 124.00 (=CHCHD), 125.16 (4-C), 126.11, 128.04, 128.12, 128.17, 128.44, 128.74, 128.84, 130.14 (6-C), 131.62, 132.60 (=CHPh), 135.59 (q), 138.79 (q), 139.26 (q), 141.67 (1-C), 152.53 (3-C), 168.22 (C=O);

^1H NMR β ($CDCl_3$) δ 3.91 (1/2 H, m, H-CD), 4.75 (1/2 H, d, *J* = 4.99 Hz, H-CD), 5.81 (1 H, s, Ph_2CH), 5.81-5.88 (2 H, m, =CHPh & =CHCHD), 6.9-7.65 (18 H, m, 3 x Ph-H_5 + 4,5-H_2), 6.98 (1 H, dd, *J* = 8.2, 1.8 Hz, 4-H), 7.71 (1 H, dt, *J* = 7.9, 1.8 Hz, 6-H); ^{13}C NMR δ 46.33 (t, *J* = 22.2 Hz, DCH), 66.72 (Ph_2CH), 111.49 (2-C), 123.42 (=CHCHD), 125.29 (4-C), 126.35, 127.88, 128.30, 128.48, 128.57, 128.78, 129.16 (6-C), 130.57, 132.85 (=CHPh), 136.75 (q), 137.59 (q), 138.24 (q), 141.01 (1-C), 150.61 (3-C), 167.77 (C=O); MS (EI) *m/z* 527.0945 (M) ($C_{29}H_{22}DN_2O_3{}^{79}Br$ requires 527.0949), 528.1028 (M + H) ($C_{29}H_{23}DN_2O_3{}^{79}Br$ requires 528.1027).

2-Iodo-3-nitro-N-(prop-2-enyl)benzamide (143)

3-Nitro-N-(prop-2-enyl)-2-(prop-2-enylamino)benzamide (168)

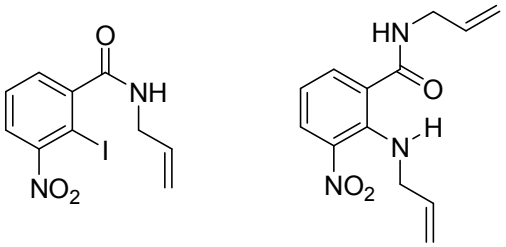

To **139** (1.65 g, 5.3 mmol) in CH_2Cl_2 (20 mL) was added prop-2-en-1-amine (0.25 mL, 5.3 mmol) and Et_3N (1.07 g, 10.6 mmol) and the mixture was stirred for 1 h. Washing (5% aq. HCl, 5% aq. $NaHCO_3$), drying, evaporation and chromatography (CH_2Cl_2:EtOAc 4:1) gave **143** (1.25 g, 71%) as yellow crystals: mp 108-110 °C; R_f = 0.20 (hexane:EtOAc 4:1); IR (KBr) ν_{max} 1349 & 1529 (NO_2), 1588 & 1643 (C=O), 3077 & 3264 (NH) cm^{-1}; ^1H NMR ($CDCl_3$) δ 3.95 (2 H, dt, *J* = 5.9, 1.5 Hz, CH_2), 5.11 (1 H, dq, *J* = 10.4, 1.3 Hz, H of $=CH_2$), 5.25 (1 H, dq, *J* = 17.1, 1.5 Hz, H of $=CH_2$), 5.77-5.91 (1 H, m, =CH), 6.28 (1 H, br s, NH), 7.41 (1 H, dd, *J* = 7.7, 1.8 Hz, 4-H), 7.49 (1 H, t, *J* = 7.5 Hz, 5-H), 7.62 (1 H, dd, *J* = 7.7, 1.8 Hz, 6-H); ^{13}C NMR δ 42.48 (CH_2), 84.86 (2-C), 117.42 ($=CH_2$), 125.00 (6-C), 129.40 (5-C), 130.30 (4-C), 132.99 (=CH), 146.03 (1-C), 154.75 (3-C), 168.24 (C=O); MS (FAB^+) *m/z* 331.9677 (M) ($C_{10}H_9IN_2O_3$ requires 371.9657); Anal. Calcd for $C_{10}H_9IN_2O_3$: C, 36.17; H, 2.73; N, 8.44; Found: C, 36.6; H, 2.85; N, 8.36.

Also isolated by chromatography was **168** (0.14 g, 10%) as bright yellow crystals: mp 54-57 °C; R_f = 0.45 (hexane:EtOAc 4:1); IR (KBr) ν_{max} 1345 & 1516 (NO_2), 1578 & 1639 (C=O), 3334 & 3468 (NH) cm^{-1}; ^1H NMR δ ($CDCl_3$) 3.75 (2 H, s, CH_2), 4.01 (2 H, tt, *J* = 6.0, 1.4 Hz, CH_2), 5.13-5.25 (4 H, m, 2 x $=CH_2$), 5.78-5.92 (2 H, m, 2 × H-C=C), 6.77 (1 H, t, *J* = 8.2 Hz, 5-H), 6.82 (1 H, br s, NH), 7.66 (1 H, dd, *J* = 7.4, 1.7 Hz, 4-H), 7.72 (1 H, br s, NH), 8.10 (1 H, dd, *J* = 8.2, 1.7 Hz, 6-H); ^{13}C NMR δ 42.41 ($O=CNCH_2$), 50.24 (NCH_2), 117.21 (5-C), 117.31 ($=CH_2$), 117.40 ($=CH_2$), 126.31 (2-C), 128.63 (6-C), 133.30 (=CH), 133.72 (=CH), 136.30 (4-C), 137.23 (1-C), 143.58 (3-C), 167.37 (C=O).

2-Iodo-3-nitrobenzamide (170)

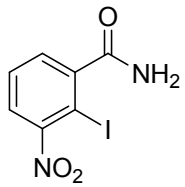

A solution of ethereal NH_3 was produced by slow addition of K_2CO_3 to mixture of Et_2O (200 mL) and conc. aq. NH_3 (20 mL). The top ethereal layer was then carefully transferred to **139** (3.0 g, 9.6 mmol) in Et_2O (10 mL). The mixture was stirred at room temperature for 1 h, then evaporated to yield **170** (2.6 g, 93%) as yellow crystals: mp 221-223 °C (lit.[160] mp 220-221 °C); R_f = 0..38 (hexane:EtOAc 1:4); IR ν_{max} (KBr) 1365 & 1524 (NO_2), 1628 & 1653 (C=O), 3178 & 3359 (NH_2) cm^{-1}; ^1H NMR ($(CD_3)_2SO$) δ 7.53 (1 H, dd, *J* = 7.9, 1.8 Hz, 6-H), 7.61 (1 H, t, *J* = 7.9 Hz, 5-H), 7.72 (1 H, br s, NH), 7.84 (1 H, dd, *J* = 7.9, 1.8 Hz, 4-H), 8.00 (1 H, br s, NH).

2-Iodo-3-nitrobenzonitrile (171)

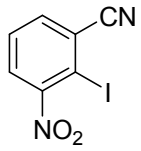

To **170** (3.0 g, 10.3 mmol) in THF (50 mL) was carefully added $SOCl_2$ (17 mL) and refluxed for 24 h. Ice H_2O (100 mL) was then added and the mixture made alkaline with cold aq. NaOH (10%, 100 mL). Extraction ($CHCl_3$), washing (saturated $NaHCO_3$, then H_2O), drying and evaporation gave **171** (1.65 g, 59%) as yellow crystals: mp 145-147 °C (lit.[160] mp 147-148 °C); R_f = 0.92 (hexane:EtOAc 1:4); IR ν_{max} (KBr) 1358 & 1530 (NO_2), 2233 (CN) cm^{-1}; ^1H NMR ($(CD_3)_2SO$) δ 7.80 (1 H, t, *J* = 8.0 Hz, 5-H), 8.12 (1 H, dd, *J* = 7.2, 1.5 Hz, 6-H), 8.18 (1 H, dd, *J* = 8.1, 1.6 Hz, 4-H).

Prop-2-enyl-2-iodo-3-nitrobenzoate (173)

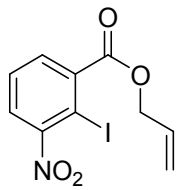

To **139** (1.51 g, 4.8 mmol) in CH_2Cl_2 (10 mL) was added prop-2-en-1-ol (0.33 mL, 4.8 mmol) and Et_3N (0.97 g, 9.6 mmol) and the mixture was stirred for 2 h. Washing (5% aq. HCl, 5% aq. $NaHCO_3$), drying, evaporation and chromatography (Petroleum ether:EtOAc 4:1) gave **173** (1.02 g, 64%) as brown liquid: R_f = 0.59 (Petroleum ether:EtOAc 4:1); IR (film) ν_{max} 1359 & 1533 (NO_2), 1588 & 1731 (C=O) cm^{-1}; ^1H NMR $CDCl_3$ δ 4.82 (2 H, dt, *J* = 6.0, 1.4 Hz, CH_2), 5.27-5.31 (1 H, dq, *J* = 10.4, 1.3 Hz, H of $=CH_2$), 5.38-5.43 (1 H, dq, *J* = 17.1, 1.4 Hz, H of $=CH_2$), 5.95-6.04 (1 H, m, H-C=C), 7.50 (1 H, t, *J* = 7.9 Hz, 5-H), 7.63 (1 H, dd, *J* = 7.9, 1.6 Hz, 4-H), 7.74 (1 H, dd, *J* = 7.9, 1.6 Hz, 6-H); ^{13}C NMR δ 66.85 (CH_2), 85.22 (2-C), 119.49 ($=CH_2$), 125.91 (5-C), 129.16 (4-C), 130.98 (=CH), 132.07 (6-C), 139.97 (1-C), 155.81 (3-C), 165.77 (C=O); MS (EI) *m/z* 332.9497 (M) ($C_{10}H_8INO_4$ requires 332.9498).

4-Methyl-5-nitroisoquinolin-1(2*H*)-one (177)

4-Methylene-5-nitro-3,4-dihydroisoquinolin-1(2*H*)-one (178)

3-Nitro-N-(prop-2-enyl)benzamide (175)

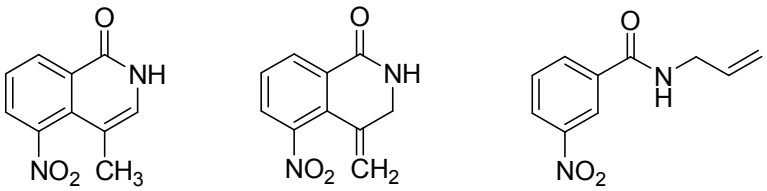

To **143** (200 mg, 0.6 mmol) in dry DMF (0.7 mL) was added $(Ph_3P)_4Pd$ (14.0 mg, 2 mol%), dry Et_3N (0.2 mL, 1.5 mmol) and tetrabutylammonium chloride (170 mg, 0.6 mmol) and the mixture was heated to 100 ^oC for 48 h. After evaporation of the solvent the residue was taken up in $CHCl_3$, washed (5% aq. HCl, 5% aq. $NaHCO_3$) and dried. Evaporation and chromatography (hexane:EtOAc 2:1) yielded **177** (40 mg, 33%) as buff powder: mp 209-211 ^oC; R_f = 0.15 (hexane:EtOAc 2:1); IR ν_{max} (KBr) 1350 & 1529 (NO_2), 1639 (C=O), 3448 & 3173 (NH) cm^{-1}; ^1H NMR ($CDCl_3$) δ 2.16 (3 H, s, CH_3), 7.05 (1 H, s, 3-H), 7.52 (1 H, t, *J* = 7.9 Hz, 7-H), 7.82 (1 H, dd, *J* = 7.8, 1.4 Hz, 6-H), 8.68 (1 H, dd, *J* = 7.8, 1.4 Hz, 8-H), 10.72 (1 H, br s, NH); ^{13}C NMR δ 15.80 ($\underline{C}H_3$), 109.03 (4-C), 126.08 (7-C), 127.79 (6-C), 127.87 (10-C), 129.47 (3-C), 129.74 (9-C), 131.37 (8-C), 147.50 (5-C), 161.83 (1-C); MS (ESI +ve) *m/z* 205.0608 (M + H) ($C_{10}H_9N_2O_3$ requires 205.0613).

Also isolated from chromatography was an inseparable mixture of **177** & **178** (2.5:1) (30 mg, 25%) as brown semi-solid: R_f = 0.14 (hexane:EtOAc 2:1); ^1H NMR **178** ($CDCl_3$) δ 4.22 (2 H, d, *J* = 1.2 Hz, CH_2), 5.34 (1 H, s, =CH), 5.50 (1 H, s, =CH), 7.06 (1 H, br s,

NH), 7.52 (1 H, t, *J* = 8.2 Hz, 7-H), 7.76 (1 H, dd, *J* = 8.2, 1.4 Hz, 6-H), 8.32 (1 H, dd, *J* = 8.2, 1.4 Hz, 8-H); ^{13}C NMR δ 47.45 (N<u>C</u>H$_2$), 119.57 (=CH$_2$), 127.19 (6-C), 128.81 (7-C), 129.77 (10-C), 129.76 (9-C), 131.46 (8-C), 131.51 (4-C), 147.92 (5-C), 163.25 (1-C).

Compound **175** was also isolated (16 mg, 13%) as yellow semi-solid: R_f = 0.44 (hexane:EtOAc 2:1); IR ν_{max} (film) 1350 & 1528 (NO_2), 1639 (C=O), 3349 & 3468 (NH) cm^{-1}; ^{1}H NMR ($CDCl_3$) δ 4.09 (2 H, t, *J* = 5.9 Hz, CH_2), 5.20 (1 H, dt, *J* = 10.1, 1.6 Hz, propenyl 3-H), 5.27 (1 H, dd, *J* = 17.2, 1.9 Hz, propenyl 3-H), 5.86-5.96 (1 H, m, propenyl 2-H), 6.73 (1 H, br s, NH), 7.62 (1 H, t, *J* = 8.2 Hz, 5-H), 8.15 (1 H, dd, *J* = 7.8, 1.6 Hz, 6-H), 8.33 (1 H, ddd, *J* = 8.2, 2.4, 1.2 Hz, 4-H), 8.60 (1 H, t, *J* = 1.9 Hz, 2-H); ^{13}C NMR δ 42.70 (NCH_2), 117.23 (=CH_2), 121.77 (2-C), 126.04 (4-C), 129.82 (5-C), 130.29 (6-C), 133.44 (=CH), 135.96 (1-C), 148.06 (3-C), 164.97 (C=O); MS (ESI +ve) *m/z* 207.077 (M + H) ($C_{10}H_{11}N_2O_3$ requires 207.0764).

Reaction was repeated with **143** (200 mg, 0.6 mmol) in dry EtCN (5 mL), $(Ph_3P)_4Pd$ (34.66 mg, 5 mol%) and dry Et_3N (0.17 mL, 1.2 mmol) at 100 ^oC for 24 h. After evaporation of the solvent the residue was taken up in $CHCl_3$, washed (5% aq. HCl, 5% aq. $NaHCO_3$) and dried. Evaporation and chromatography (hexane:EtOAc 4:1) yielded 1:1 mixture of **177** & **178** (71 mg, 58%), **175** (32 mg, 23%) and traces of **(176)**.

Same reaction was repeated with **143** (200 mg, 0.6 mmol) in dry DMF (1.0 mL), $(Ph_3P)_4Pd$ (14.0 mg, 2 mol%), dry DMF (1 mL) and tetrabutylammonium chloride (170 mg, 0.6 mmol) at 50 ^oC for 48 h. After evaporation of the solvent the residue was taken up in $CHCl_3$, washed (5% aq. HCl, 5% aq. $NaHCO_3$) and dried. Evaporation and chromatography (hexane:EtOAc 2:1) yielded 1:1 mixture of **177** & **178** (40 mg, 54%) and **175** (20 mg, 27%).

Reaction was repeated with **143** (100 mg, 0.3 mmol) in dry DMF (0.5 mL), $(Ph_3P)_4Pd$ (7.0 mg, 2 mol%), dry Et_3N (0.1 mL, 0.6 mmol) and tetrabutylammonium chloride (84 mg, 0.6 mmol) at 150 ^oC for 16h. After evaporation of the solvent the residue was taken up in $CHCl_3$, washed (5% aq. HCl, 5% aq. $NaHCO_3$) and dried. Evaporation and chromatography (hexane:EtOAc 4:1) yielded **177** (40 mg, 65%) as buff powder with data as above.

***(E)*-2-Iodo-3-nitro-*N*-(prop-1-enyl)benzamide (179)**

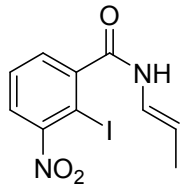

Compound **143** (0.1 g, 0.3 mmol) in 0.2 mL of anhydrous benzene and [RuClH(CO)(PPh_3)$_3$] (1.42 mg, 0.5 %mol) were heated at 80 °C for 3 h under Ar. After cooling to room temperature 25 mL of EtOAc is added and the mixture was cooled to 0 °C. The precipitated ruthenium compounds and PPh_3 were filtered off. Evaporation of the filterate and chromatography (hexane:EtOAc 4:1) gave **179** (0.96 g, 96%) as pale white coloured solid: mp 169-172 °C; IR (KBr) ν_{max} 1349 & 1528 (NO_2), 1586 & 1644 (C=O), 3067 & 3245 (NH) cm^{-1}; ^{1}H NMR δ ($CDCl_3$) 1.76 (3 H, dd, *J* = 6.76, 1.8 Hz, CH_3), 5.37 (1 H, m, =CH-CH_3), 6.83-6.92 (1 H, tq, *J* = 10.52, 1.8 Hz, =CH-NH), 7.20 (1 H, br s, NH), 7.51-7.56 (2 H, m, 5,6-H_2), 7.69 (1 H, m, 4-H); ^{13}C NMR δ 14.94 (CH_3), 84.89 (2-C), 110.99 (=C-CH_3), 122.50 (=C-NH), 125.44 (4-C), 129.55 (6-C), 130.65 (5-C), 130.83 (1-C), 154.99 (3-C), 164.91 (C=O); MS (EI) *m/z* 331.9672 (M) ($C_{10}H_9IN_2O_3$ requires 331.9658).

***(E)*-3-Nitro-*N*-(prop-1-enyl)benzamide (176)**
3-Nitrobenzamide (180)

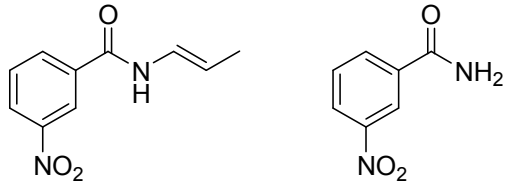

To **179** (200 mg, 0.6 mmol) in dry DMF (1 mL) was added $(Ph_3P)_4Pd$ (17.3 mg, 2 mol%), dry Et_3N (0.2 mL, 1.5 mmol) and tetrabutylammonium chloride (210 mg, 0.6 mmol) and the mixture was heated to reflux for 7 d. After evaporation of the solvent the residue was taken up in $CHCl_3$, washed (5% aq. HCl, 5% aq. $NaHCO_3$) and dried. Evaporation and chromatography (hexane:EtOAc 2:1) yielded **176** (42 mg, 52%) as a buff semi-solid: R_f = 0.87 (hexane:EtOAc 2:1); IR ν_{max} (film) 1350 & 1528 (NO_2), 1638 & 1654 (C=O), 3078 & 3306 (NH) cm^{-1}; ^{1}H NMR ($CDCl_3$) δ 1.76 (3 H, dd, *J* = 6.6, 1.6 Hz, CH_3), 5.36-5.45 (1 H, m, propenyl 2-H), 6.91-6.97 (1 H, m, propenyl 1-H), 7.66 (1 H, t, *J*

= 8.2 Hz, 5-H), 7.70 (1 H, br s, NH), 8.17 (1 H, dt, *J* = 7.8, 1.2 Hz, 6-H), 8.36 (1 H, ddd, *J* = 8.2, 2.4, 1.2 Hz, 4-H), 8.60 (1 H, t, *J* = 1.9 Hz, 2-H); ^{13}C NMR δ 14.99 (CH_3), 110.47 (C-CH_3), 121.65 (2-C), 123.04 (C-NH), 126.35 (4-C), 130.04 (5-C), 133.33 (6-C), 135.44 (1-C), 148.50 (3-C), 161.64 (C=O); MS (ESI +ve) *m/z* 229.0579 (M + Na) ($C_{10}H_{10}N_2O_3Na$ requires 229.0589).

Also identified in trace amounts in the NMR spectrum were **180**. IR ν_{max} (KBr) 1350 & 1530 (NO_2), 1624 & 1689 (C=O), 3178 & 3451 (NH_2) cm^{-1}; ^{1}H NMR ($CDCl_3$) δ, 6.07 (1 H, br s, NH), 6.34 (1 H, br s, NH), 7.68 (1 H, t, *J* = 7.9 Hz, 5-H), 8.18 (1 H, ddd, *J* = 7.9, 2.7, 1.2 Hz, 4-H), 8.39 (1 H, ddd, *J* = 8.4, 2.4, 1.2 Hz, 6-H), 8.65 (1 H, t, *J* = 2.0 Hz, 2-H).

***tert*-Butyl N-prop-2-enyl(2-iodo-3-nitrobenzoyl)carbamate (181)**

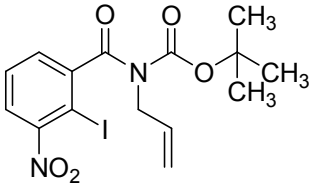

Di(*tert*-butyl)dicarbonate (0.1 g, 0.45 mmol) was slowly added to an ice-cold solution of **143** (0.1 g, 0.3 mmol). Et_3N (0.062 mL, 0.45 mmol) and 4-(dimethyl amino)pyridine (7.4 mg, 0.06 mmol) were added and the mixture was stirred for 3 h. Evaporation gave **181** (0.12 g, 92%) as yellow semi-solid: R_f = 0.77 (hexane:EtOAc 4:1); IR (film) ν_{max} 1347 & 1535 (NO_2), 1672 & 1739 (C=O), 1245 (C-O) cm^{-1}; ^{1}H NMR ($CDCl_3$) δ 1.19 (9 H, s, $(CH_3)_3$), 4.46 (2 H, d, *J* = 5.5 Hz, CH_2), 5.11-5.23 (1 H, dd, *J* = 10.2, 1.4 Hz, H of =CH_2), 5.27-5.35 (1 H, dq, *J* = 17.1, 1.4 Hz, H of =CH_2), 5.87-6.02 (1 H, m, =CH), 7.27 (1 H, dd, *J* = 7.4, 1.4 Hz, 4-H), 7.49 (1 H, t, *J* = 7.7 Hz, 5-H), 7.66 (1 H, dd, *J* = 8.0, 1.3 Hz, 6-H); ^{13}C NMR δ 27.46 $(CH_3)_3$, 46.66 (NCH_2), 83.95 (2-C), 84.45 (C-$CH_3)_3$), 117.94 (=CH_2), 124.05 (4-C), 128.86 (6-C), 129.10 (5-C), 132.05 (=CH), 148.45 (1-C), 151.04 (O-C=O), 154.16 (3-C), 169.64 (C=O); MS (ESI +ve) *m/z* 455.0048 (M+Na) ($C_{15}H_{17}IN_2NaO_5$ requires 455.0080).

5-Amino-4-methylisoquinolin-1(2*H*)-one hydrochloride (182)

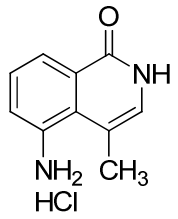

To a solution of **177** (58 mg, 0.28 mmol) in ethanol (5 mL) and conc. HCl (0.2 mL), a slurry of 10% palladium on charcoal (0.1 g) in ethanol (2 mL) was added. The mixture was stirred under H_2 for 2 h. The suspension was then flltered through Celite®. The Celite® pad and residue were suspended in water (100 mL) and heated. The hot suspension was filtered through a second Celite® pad. Concentration of the filterate and drying gave **182** (42 mg, 70%) as buff crystals: mp 227-229 °C; IR ν_{max} (KBr) 1654 (C=O), 3421 (NH) cm^{-1}; ^1H NMR (D_2O) δ 2.37 (3 H, s, CH_3), 6.94 (1 H, s, 3-H), 7.42 (1 H, t, *J* = 8.2 Hz, 7-H), 7.63 (1 H, d, *J* = 7.8 Hz, 6-H), 8.14 (1 H, d, *J* = 8.2 Hz, 8-H); ^{13}C NMR δ 18.41 (CH_3), 110.74 (4-C), 126.89 (5-C), 127.04 (9-C), 127.24 (7-C), 128.48 (8-C), 128.64 (3-C), 129.55 (6-C), 132.52 (10-C), 162.72 (1-C); MS (ESI +ve) *m/z* 175.0866 (M + H) ($C_{10}H_{11}N_2O_1$ requires 175.0871).

***(E)*-N-(3-phenylprop-2-enyl)2,2,2-trifluoroacetamide (184)**
***(E)*-3-Phenylprop-2-enylamine triflouroacetate salt (183)**

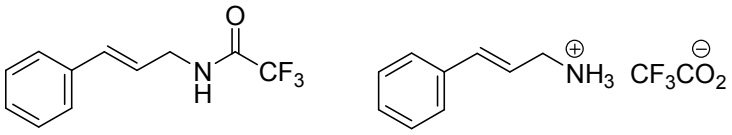

To 2,2,2-trifluoroacetamide (2.86 g, 25.4 mmol) in dry THF (25 mL), potassium *t*-butoxide (2.84 g, 25.4 mmol) was added slowly. After 30 min, *(E)*-(3-bromoprop-1-enyl)benzene (5.00g, 25.4 mmol) was added and the mixture was stirred for 2 h. After the evaporation of the solvent, the residue was taken up in CH_2Cl_2, washed (H_2O) and dried. Evaporation and chromatography (hexane:EtOAc 4:1) yielded **184** (1.89 g, 33%) as white powder: mp 101-103 °C; (lit.[212] mp 100-102 °C) R_f = 0.34 (hexane:EtOAc 4:1); IR (KBr) ν_{max} 1179 (C-F), 1556 & 1704 (C=O), 3116 & 3299 (NH) cm^{-1}; ^1H NMR ($CDCl_3$) δ 4.13 (2 H, t, *J* = 6.5 Hz, CH_2), 6.17 (1 H, dt, *J* = 15.4, 6.9 Hz, =C<u>H</u>-CH_2), 6.52 (1 H, br s, NH), 6.60 (1 H, d, *J* = 15.4 Hz, =C<u>H</u>-Ph), 7.25-7.37 (5 H, m, 2',3',4',5',6'-H_5); ^{13}C NMR δ 41.91 (CH_2), 117.22 (CF_3, q, *J* = 288.3 Hz), 122.62 (=C-CH_2), 126.48 (2,6-C_2),

128.24 (4-C), 128.68 (3,5-C_2), 134.18 (=C-Ph), 135.78 (1-C), 157.23 (C=O, q, *J* = 37.6 Hz); ^{19}F NMR ($CDCl_3$) δ -75.81 (3 F, s, CF_3).

Also isolated by chromatography was **183** (0.44 g, 7%) as yellow semisolid. R_f = 0.18 (hexane:EtOAc 4:1); IR ν_{max} (film) 1196 (C-F), 1674 & 1731 (C=O), 3197 & 3365 (NH) cm^{-1}; ^{1}H NMR ($CDCl_3$) δ 4.32 (2 H, dd, *J* = 5.7, 1.4 Hz, CH_2), 6.37 (1 H, dt, *J* = 15.9, 5.7 Hz, =C<u>H</u>-CH_2), 6.48 (3 H, br s, NH_3), 6.57 (1 H, d, *J* = 16.1 Hz, =C<u>H</u>-Ph), 7.25-7.39 (5 H, m, 2',3',4',5',6'-H_5); ^{19}F NMR ($CDCl_3$) δ -76.22 (3 F, s, CF_3).

***(E)*-3-phenylprop-2-enylamine (185)**

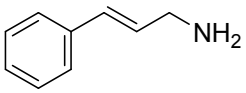

Method A:

To **184** (1.2 g, 5.2 mmol) in EtOH (15 mL), was added conc. aq. NH_3 (1 mL) and the mixture was stirred for 4 d. The evaporation residue, in CH_2Cl_2, was washed (H_2O) and dried. Evaporation and chromatography (CH_2Cl_2:MeOH 10:1) yielded **185** (0.616 g, 88%) as a pale yellow oil: R_f = 0.55 (CH_2Cl_2:MeOH 10:1); IR (film) ν_{max} 1450 & 1494 (C=C), 1598 (C=C conjugated), 3390 (NH) cm^{-1}; ^{1}H NMR ($CDCl_3$) δ 3.47 (2 H, d, *J* = 6.7 Hz, CH_2), 6.10 (1 H, dt, *J* = 15.8, 6.9 Hz, =C<u>H</u>-CH_2), 6.39 (2 H, br s, NH_2), 6.54 (1 H, d, *J* = 15.8 Hz, =C<u>H</u>-Ph), 7.20-7.31 (5 H, m, 2',3',4',5',6'-H_5);

Method B:

$NaBH_4$ (1.06 g, 28.2 mmol) was added to **184** (0.81 g, 3.52 g) in EtOH (10 mL) and the mixture was stirred for 16 h. The evaporation residue, in CH_2Cl_2, was washed (H_2O) and dried to give **185** (0.422 g, 90%) as a pale yellow oil with properties as above.

***(E)*-2-iodo-3-nitro-N-(3-phenylprop-2-enyl)benzamide (186)**

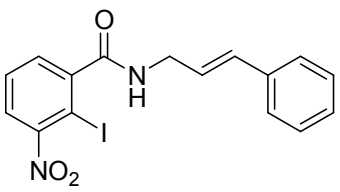

To **139** (1.55 g, 5.0 mmol) in CH_2Cl_2 (20 mL) was added **185** (0.66 g, 5.0 mmol) and Et_3N (1.4 mL, 10 mmol) and the mixture was stirred for 2 h. Washing (5% aq. HCl, 5% aq. $NaHCO_3$), drying, evaporation and chromatography (hexane:EtOAc 4:1) gave **186** (1.51 g, 74%) as yellow crystal:. mp 146-148 ^oC; R_f = 0.38 (hexane:EtOAc 2:1); IR (KBr) ν_{max} 1377 & 1537 (NO_2), 1645 (C=O), 3066 & 3263 (NH) cm^{-1}; ^1H NMR ($CDCl_3$) δ 4.22 (2 H, t, *J* = 6.3 Hz, CH_2), 6.08 (1 H, br s, NH), 6.26 (1 H, dt, *J* = 15.9, 6.3 Hz, =C<u>H</u>-CH_2), 6.64 (1 H, d, *J* = 15.6 Hz, =C<u>H</u>-Ph), 7.22-7.36 (5 H, m, 2',3',4',5',6'-H_5), 7.42-7.50 (2 H, m, 5,6-H_2), 7.63 (1 H, m, 4-H); ^{13}C NMR δ 42.24 (CH_2), 84.91 (2-C), 124.05 (=<u>C</u>-CH_2), 125.14 (4-C), 126.40 (2',6'-C_2), 127.97 (4'-C), 128.65 (3',5'-C_2), 129.46 (6-C), 130.35 (5-C), 133.23 (=<u>C</u>-Ph), 136.15 (1'-C), 146.06 (1-C), 154.85 (3-C), 168.24 (C=O); MS (ESI +ve) *m/z* 409.0035 (M + H) ($C_{16}H_{14}IN_2O_3$ requires 409.0049); Anal. Calcd for $C_{16}H_{13}IN_2O_3$: C, 47.08; H, 3.21; N, 6.86; Found: C, 47.58; H, 3.19; N, 6.93.

4-Benzyl-5-nitroisoquinolin-1(2*H*)-one (187)

***(Z)*-4-Benzylidene-5-nitro-3,4-dihydroisoquinolin-1(*2H*)-one (188)**

***(E)*-3-nitro-N-(3-phenylprop-2-enyl)benzamide (189)**

3-Amino-2-chloro-*N*-(3-phenylprop-2-enyl)benzamide (190)

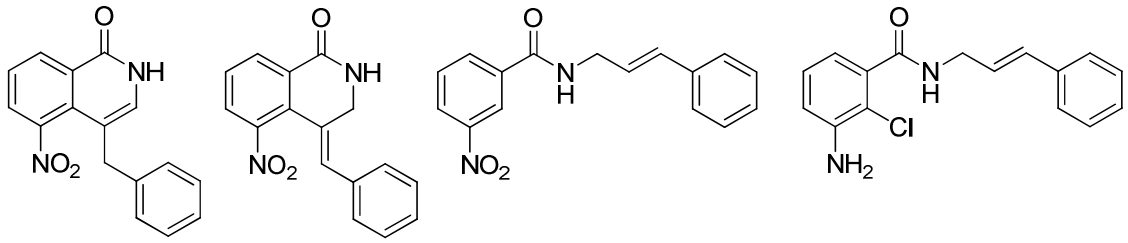

To **186** (100 mg, 0.25 mmol) in dry DMF (0.5 mL) was added $(Ph_3P)_4Pd$ (6.0 mg, 2 mol%), dry Et_3N (0.09 mL, 0.625 mmol) and tetrabutylammonium chloride (70 mg, 0.25 mmol) and the mixture was heated to reflux for 48 h. After evaporation of the solvent the residue was taken up in $CHCl_3$, washed (5% aq. HCl, 5% aq. $NaHCO_3$) and dried. Evaporation and chromatography (hexane:EtOAc 2:1) yielded **187** (12 mg, 17%) as a yellow solid. mp 108-110°C; R_f = 0.63 (hexane:EtOAc 2:1); IR (KBr) ν_{max} 1345 & 1530 (NO_2), 1638 (C=O), 3283 & 3468 (NH) cm^{-1}; ^1H NMR ($CDCl_3$) δ 4.24 (2 H, t, *J* = 6.7 Hz, CH_2), 6.25 (1 H, dt, *J* = 15.6, 6.3 Hz, =C<u>H</u>-CH_2), 6.57 (1 H, d, *J* = 16.0 Hz, =C<u>H</u>-Ph), 7.06 (1 H, t, *J* = 5.5 Hz, NH), 7.20-7.33 (5 H, m, 2',3',4',5',6'-H_5), 7.57 (1 H, t, *J* = 7.8 Hz, 5-H), 8.20 (1 H, dd, *J* = 7.8, 1.6 Hz, 6-H), 8.29 (1 H, ddd, *J* = 8.2, 2.4, 1.2 Hz, 4-H), 8.63 (1 H, t, *J* = 1.6 Hz, 2-H); ^{13}C NMR δ 42.38 (<u>C</u>H_2), 121.81 (2-C), 124.56 (=<u>C</u>-CH_2), 125.98 (4-C), 126.29 (2',6'-C_2), 127.84 (4'-C), 128.54 (3',5'-C_2), 129.73 (5-C), 132.78

(=C-Ph), 133.33 (6-C), 135.84 (1-C), 136.14 (1'-C), 147.98 (3-C), 165.00 (C=O); MS (ESI +ve) *m/z* 283.1077 (M + H) ($C_{16}H_{15}N_2O_3$ requires 283.1083).

Also isolated from chromatography was **188** (10 mg, 14%) as yellow semisolid. R_f = 0.2 (hexane:EtOAc 2:1); IR (film) ν_{max} 1644 (C=O), 3061 & 3340 (NH) cm^{-1}; ^1H NMR ($CDCl_3$) δ 4.20 (2 H, s, NH_2), 4.22-4.24 (2 H, m, CH_2), 6.11 (1 H, br s, NH), 6.26 (1 H, dt, *J* = 15.7, 6.3 Hz, =CH-CH_2), 6.58 (1 H, d, *J* = 16.0 Hz, =CH-Ph), 6.80 (1 H, dd, *J* = 8.2, 1.6 Hz, 4-H), 6.88 (1 H, dd, *J* = 7.8, 1.6 Hz, 6-H), 7.07 (1 H, t, *J* = 7.8 Hz, 5-H), 7.23-7.37 (5 H, m, 2',3',4',5',6'-H_5); ^{13}C NMR δ 41.97 (CH_2), 115.36 (2-C), 116.99 (4-C), 118.28 (6-C), 124.95 (=CH-CH_2), 126.38 (2',6'-C_2), 127.52 (4'-C), 127.76 (5-C), 128.58 (3',5'-C_2), 132.44 (=CH-Ph), 136.37 (1-C), 136.42 (1'-C), 143.64 (3-C), 167.29 (C=O); MS (ESI +ve) *m/z* 287.0946 (M + H) ($C_{16}H_{16}ClN_2O$ requires 287.0951).

Compound **189** (8 mg, 11%) was also isolated from above reaction as orange solid:. mp 210-212°C; R_f = 0.19 (hexane:EtOAc 2:1); IR (KBr) ν_{max} 1354 & 1530 (NO_2), 1636 (C=O), 3287 & 3472 (NH) cm^{-1}; ^1H NMR ($CDCl_3$) δ 3.88 (2 H, s, CH_2), 6.75 (1 H, s, 3-H), 7.11 (2 H, d, *J* = 7.0 Hz, 2',6'-H_2), 7.23-7.31 (3 H, m, 3',4',5'-H_3), 7.56 (1 H, t, *J* = 7.8 Hz, 7-H), 7.82 (1 H, dd, *J* = 7.8, 1.2 Hz, 6-H), 8.68 (1 H, dd, *J* = 7.8, 1.2 Hz, 8-H), 11.07 (1 H, br s, NH); ^{13}C NMR δ 35.45 (CH_2), 113.27 (4-C), 126.11 (7-C), 126.94 (4'-C), 127.94 (9-C), 128.71 (6-C) 128.81 (3',5'-C_2), 129.39 (2',6'-C_2), 129.59 (10-C), 130.93 (3-C), 131.85 (8-C), 137.71 (1'-C), 147.65 (5-C), 161.89 (1-C); MS (ESI +ve) *m/z* 281.0921 (M + H) ($C_{16}H_{13}N_2O_3$ requires 281.0926).

Compound **190** (10 mg, 14%) was also isolated from above reaction as yellow solid. mp 183-185°C; R_f = 0.17 (hexane:EtOAc 2:1); IR (KBr) ν_{max} 1634 (C=O), 3270 & 3458 (NH) cm^{-1}; ^1H NMR ($CDCl_3$) δ 4.50 (2 H, q, *J* = 1.37 Hz, 3-CH_2), 6.74 (1 H, br s, NH), 6.79 (1 H, s, =CH), 7.18 (2 H, d, *J* = 7.2 Hz, 2',6'-H_2), 7.30-7.41 (3 H, m, 3',4',5'-H_3), 7.50 (1 H, t, *J* = 7.9 Hz, 7-H), 7.82 (1 H, dd, *J* = 8.2, 1.4 Hz, 6-H), 8.30 (1-H, dd, *J* = 7.9, 1.4 Hz, 8-H);^{13}C NMR δ 41.99 (3-C), 124.34 (4-C), 127.65 (6-C), 128.34 (7-C), 128.58 (3',4',5'-C_3), 129.14 (2',6'-C_2), 130.31 (9-C), 131.21 (8-C), 131.66 (10-C), 134.72 (=CH), 134.80 (1'-C), 148.39 (5-C), 162.89 (1-C); Anal. Calcd for $C_{16}H_{12}N_2O_3$: C, 68.56; H, 4.32; N, 9.99; Found: C, 68.43; H, 4.07; N, 9.99. MS (ESI +ve) *m/z* 287.0946 (M + H) ($C_{16}H_{16}{}^{35}ClN_2O$ requires 287.0951).

5-Amino-4-benzylisoquinolin-1(2*H*)-one (192)

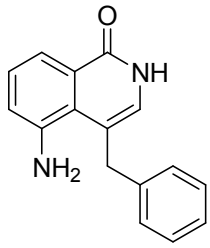

To **187** (20 mg, 0.07 mmol) in EtOH (5 mL), a slurry of 10% palladium on charcoal (50 mg) in EtOH (2 mL) was added. The mixture was stirred under H_2 for 1 h. The suspension was then flltered through Celite®. The Celite® pad and residue were suspended in ethanol (100 mL) and heated. The hot suspension was filtered through a second Celite® pad. Concentration of the filtrate and drying gave **192** (9 mg, 51%) as buff powder; mp 121-123°C; R_f = 0.3 (EtOAc:hexane 4:1); IR (KBr) ν_{max} 1623 (C=O), 3337 & 3407 (NH) cm^{-1}; ^1H NMR ($CDCl_3$) δ 4.32 (2 H, s, CH_2), 6.87 (1 H, d, *J* = 7.4 Hz, 6-H), 6.9 (1 H, s, 3-H), 7.22 (1 H, t, *J* = 7.4 Hz, 7-H), 7.25-7.35 (5 H, m, 2',3',4',5',6'-H_5), 8.02 (1 H, d, *J* = 7.8 Hz, 8-H), 11.51 (1 H, br s, NH); ^{13}C NMR δ 38.39 (CH_2), 113.34 (4-C), 119.11 (8-C), 120.92 (6-C), 126.64 (10-C), 126.93 (4'-C) 127.23 (3-C), 127.43 (7-C), 128.09 (2',6'-C_2), 128.16 (9-C), 129.16 (3',5'-C_2), 140.05 (1'-C), 143.50 (5-C), 163.99 (1-C); MS (ESI +ve) *m/z* 251.1179 (M + H) ($C_{16}H_{15}N_2O$ requires 251.1184).

(±) 5-Amino-4-benzyl-3,4-dihydroisoquinolin-1(2*H*)-one (193)

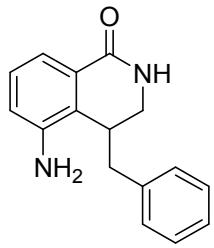

To **188** (35 mg, 0.12 mmol) in EtOH (5 mL), a slurry of 10% palladium on charcoal (50 mg) in EtOH (2 mL) was added. The mixture was stirred under H_2 for 1 h. The suspension was then flltered through Celite®. The Celite® pad and residue were suspended in ethanol (100 mL) and heated. The hot suspension was filtered through a second Celite® pad. Concentration of the filterate and drying gave **193** (24 mg, 68%) as a buff powder; mp 169-170°C; R_f = 0.6 (EtOAc:hexane 4:1); IR (film) ν_{max} 1586 & 1660 (C=O), 3238 & 3344 (NH) cm^{-1}; ^1H NMR ($CDCl_3$) δ 2.92 (2 H, d, *J* = 3.52 Hz, $PhCH_2$),

2.99 (1 H, dd, *J* = 9.4, 3.5 Hz, 4-H), 3.35 (1 H, ddd, *J* = 12.5, 5.1, 1.2 Hz, 3-H), 3.61 (1 H, dd, *J* = 12.5, 3.9 Hz, 3-H), 6.64 (1 H, br s, NH), 6.82 (1 H, dd, *J* = 7.8, 1.2 Hz, 6-H), 7.16 (2 H, d, *J* = 7.4 Hz, 2',6'-H_2), 7.18 (1 H, t, *J* = 7.8 Hz, 7-H), 7.20-7.35 (3 H, m, 3',4',5'-H_3), 7.62 (1 H, dd, *J* = 7.8, 1.2 Hz, 8-H); ^{13}C NMR δ 35.08 (4-C), 37.55 (CH_2Ph), 42.82 (3-C). 119.25 (8-C), 119.94 (6-C), 126.66 (4'-C), 127.71 (10-C), 127.61 (7-C) 128.71 (9-C), 128.75 (3',5'-C_2), 129.03 (2',6'-C_2), 139.29 (1'-C), 142.81 (5-C), 166.67 (1-C); MS (ESI +ve) *m/z* 253.1328 (M + H) ($C_{16}H_{17}N_2O$ requires 253.1335).

***(E)*-*N*-(But-2-enyl)-2,2,2-trifluoroacetamide (195)**
***(Z)*-*N*-(But-2-enyl)-2,2,2-trifluoroacetamide (196)**
***N*,*N*-Di(*(E)*-but-2-enyl)-2,2,2-trifluoroacetamide (197)**
***N*,*N*-Di(*(Z)*-but-2-enyl)-2,2,2-trifluoroacetamide (198)**

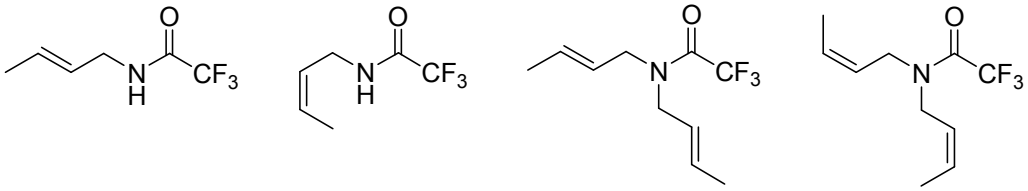

To 2,2,2-trifluoroacetamide (2.06 g, 18.2 mmol) in dry THF (10 mL), $^{t}BuO^{-}K^{+}$ (2.05 g, 18.2 mmol) was added slowly. After 30 min, 1-bromobut-2-ene (mixture of E and Z isomers (5:1)) (2.5 g, 18.34 mmol) was added and the mixture was stirred for 2 h. After the evaporation of the solvent, the residue was taken up in EtOAc and washed (H_2O) and dried. Evaporation and chromatography (hexane:EtOAc 10:1) yielded mixture of **195** & **196** (3:1) (1.02 g, 33%) as colourless oil: R_f = 0.37 (hexane:EtOAc 10:1); IR (film) ν_{max} 1179 (C-F), 1556 & 1704 (C=O), 3098 & 3306 (NH) cm^{-1}; **195** ^{1}H NMR ($CDCl_3$) δ 1.65 (3 H, dd, *J* = 6.9, 1.5 Hz, CH_3), 3.83 (2 H, m, CH_2), 5.36-5.45 (1 H, m, *J* = C<u>H</u>-CH_2), 5.62-5.70 (1 H, m, =C<u>H</u>-CH_3), 7.07 (1 H, br s, NH); ^{13}C NMR δ 17.43 (CH_3), 41.67 (CH_2), 117.24 (CF_3, q, *J* = 287.5 Hz), 124.42 (=C-CH_2), 130.24 (=C-CH_3), 157.33 (C=O, q, *J* = 36.8 Hz); ^{19}F NMR ($CDCl_3$) δ -76.15 (3 F, s, CF_3);

196 ^{1}H NMR ($CDCl_3$) δ 1.65 (3 H, dd, *J* = 6.9, 1.5 Hz, CH_2), 3.94 (2 H, t, *J* = 6.4 Hz CH_2), 5.36-5.45 (1 H, m, =C<u>H</u>-CH_2), 5.62-5.70 (1 H, m, =C<u>H</u>-CH_3), 7.07 (1 H, br s, NH); ^{13}C NMR δ 12.69 (CH_3), 36.54 (CH_2), 117.24 (CF_3, q, *J* = 287.5 Hz), 123.62 (=C-CH_2), 129.29 (=C-CH_3), 156.96 (C=O, q, *J* = 36.8 Hz); ^{19}F NMR ($CDCl_3$) δ -76.17 (3 F, s, CF_3).

Also isolated from chromatography was mixture of **197** & **198** (4:1) (0.23 g, 6%). R_f = 0.75 (hexane:EtOAc 10:1) as colourless oil: IR (film) ν_{max} 1142, 1203 (C-F), 1693 (C=O) cm^{-1}; ^1H NMR **197** ($CDCl_3$) δ 1.59-1.67 (3 H, m, CH_3), 3.81-3.85 (2 H, m, CH_2), 5.25-5.36 (1 H, m, =C<u>H</u>-CH_2), 5.55-5.68 (1 H, m, =C<u>H</u>-CH_3); ^{13}C NMR δ 17.39 (2 x CH_3), 46.89 (CH_2), 48.02 (CH_2), 117.91 (CF_3, q, *J* = 288.3 Hz), 123.66 (=C-CH_2), 124.53 (=C-CH_2), 130.54 (=C-CH_3), 130.93 (=C-CH_3), 156.03 (C=O, q, *J* = 35.27 Hz); ^{19}F NMR ($CDCl_3$) δ -68.99 (3 F, s, CF_3).

198 ($CDCl_3$) δ 1.59-1.67 (3 H, m, CH_3), 3.93-3.98 (2 H, m, CH_2), 5.25-5.36 (1 H, m, =C<u>H</u>-CH_2), 5.55-5.68 (1 H, m, =C<u>H</u>-CH_3); ^{13}C NMR δ 12.72 (2 x CH_3), 41.69 (CH_2), 42.70 (CH_2), 117.91 (CF_3, q, *J* = 288.3 Hz), 123.35 (=C-CH_2), 123.75 (=C-CH_2), 129.08 (=C-CH_3), 129.11 (=C-CH_3), 156.03 (C=O, q, *J* = 35.27 Hz); ^{19}F NMR ($CDCl_3$) δ -68.95 (3 F, s, CF_3).

***(E)*-But-2-en-1-amine (200)**
***(Z)*-But-2-en-1-amine (201)**

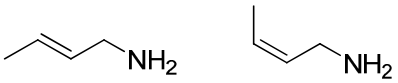

A mixture of **195** & **196** (0.83 g, 5.0 mmol) was stirred with 10% aq. NaOH (5 mL) for 3 h. Extraction (Et_2O) and drying (K_2CO_3) yielded mixture of **200** & **201** which was used in the next step without further purification.

***(E)*-*N*-(But-2-enyl)-2-iodo-3-nitrobenzamide (202)**
***(Z)*-*N*-(But-2-enyl)-2-iodo-3-nitrobenzamide (203)**

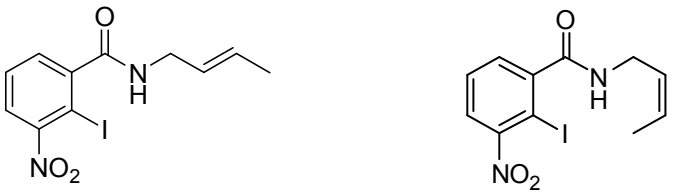

To **139** (1.55 g, 5.0 mmol) in Et_2O (20 mL) was added mixture of **200** & **201** (0.36 g, 5.0 mmol) in Et_2O and Et_3N (1.4 mL, 10 mmol) and the mixture was stirred for 2 h. Washing (5% aq. HCl, 5% aq. $NaHCO_3$), drying, evaporation and chromatography (hexane:EtOAc 3:2) gave mixture of **202** & **203** (5:1) (1.25 g, 72%) as yellow crystals:

R_f = 0.25 (hexane:EtOAc 2:1); IR (KBr) ν_{max} 1348 & 1526 (NO_2), 1589 & 1648 (C=O), 3258 & 3467 (NH) cm^{-1}; ^1H NMR ($CDCl_3$) δ 1.67 (3 H, dd, *J* = 6.5, 1.4 Hz, CH_3), 3.81 (2 H, tq, *J* = 5.64, 1.4 Hz, CH_2), 5.53 (1 H, m, =C<u>H</u>-CH_2), 5.67 (1 H, m, =C<u>H</u>-CH_3), 7.51 (1 H, dd, *J* = 7.6, 1.4 Hz, 6-H), 7.61 (1 H, t, *J* = 7.9 Hz, 5-H), 7.85 (1 H, dd, *J* = 7.9, 1.4 Hz, 4-H), 8.67(1 H, t, *J* = 5.3 Hz, NH); ^{13}C NMR δ 17.57 (CH_2), 40.84 (CH_3), 86.71 (2-C), 123.89 (4-C), 126.73 (=<u>C</u>-CH_2), 127.26 (=<u>C</u>-CH_3), 129.68 (5-C), 130.21 (6-C), 146.48 (1-C), 155.21 (3-C), 167.89 (C=O); MS (ESI +ve) *m/z* 346.9887 (M + H) ($C_{11}H_{12}IN_2O_3$ requires 346.9893). Anal. Calcd for $C_{11}H_{11}IN_2O_3$: C, 38.17; H, 3.20; N, 8.09; Found: C, 38.50; H, 3.17; N, 8.16.

^1H NMR **203** ($CDCl_3$) δ 1.67 (3 H, m, CH_3), 3.89 (2 H, t, *J* = 5.4 Hz, CH_2), 5.46-5.60 (1 H, m, =C<u>H</u>-CH_2), 5.62-5.72 (1 H, m, =C<u>H</u>-CH_3), 7.65 (1 H, t, *J* = 7.6 Hz, 5-H), 7.71 (1 H, dd, *J* = 7.6, 1.7 Hz, 6-H), 8.08 (1 H, dd, *J* = 7.9, 1.4 Hz, 4-H), 8.78 (1 H, m, NH); ^{13}C NMR δ 12.94 (CH_2), 36.19 (CH_3), 79.21 (2-C), 125.37 (4-C), 126.27 (=<u>C</u>-CH_2), 127.18 (=<u>C</u>-CH_3), 128.66 (5-C), 131.98 (6-C), 139.44 (1-C), 148.63 (3-C), 164.47 (C=O).

***(E)*-*N*-(But-2-enyl)-3-nitrobenzamide (204)**
***(Z)*-*N*-(But-2-enyl)-3-nitrobenzamide (205)**
***(E)*-3-Amino-N-(but-2-enyl)-2-chlorobenzamide (206)**
***(Z)*-3-Amino-N-(but-2-enyl)-2-chlorobenzamide (207)**

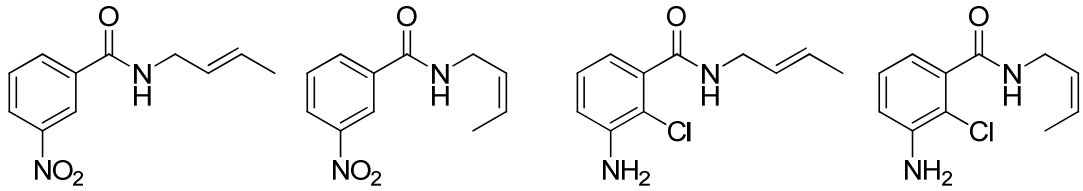

To **202** & **203** (100 mg, 0.3 mmol) in dry DMF (0.5 mL) was added $(Ph_3P)_4Pd$ (7 mg, 2 mol%), dry Et_3N (0.1 mL, 0.75 mmol) and tetrabutylammonium chloride (84 mg, 0.3 mmol) and the mixture was heated to reflux for 48 h. After evaporation of the solvent, the residue was taken up in $CHCl_3$, washed (5% aq. HCl, 5% aq. $NaHCO_3$) and dried. Evaporation and chromatography (hexane:EtOAc 2:1) yielded mixture of **204** & **205** (14 mg, 21%) as yellow semi-solid: R_f = 0.7 (hexane:EtOAc 2:1); IR ν_{max} (film) 1349 & 1529 (NO_2), 1641 (C=O), 3306 (NH) cm^{-1}; ^1H NMR **204** ($CDCl_3$) δ 1.71 (3 H, d, *J* = 6.3 Hz, CH_3), 4.01 (2 H, t, *J* = 6.7 Hz, CH_2), 5.55 (1 H, m, =C<u>H</u>-CH_2), 5.73 (1 H, m, =C<u>H</u>-CH_3), 6.28 (1 H, br s, NH), 7.63 (1 H, t, *J* = 7.8 Hz, 5-H), 8.14 (1 H, dd, *J* = 7.8, 1.4 Hz, 6-H), 8.33 (1 H, ddd, *J* = 8.2, 2.4, 1.2 Hz, 4-H), 8.57 (1 H, t, *J* = 1.6 Hz, 2-H); ^{13}C NMR δ 17.73 (CH_3), 42.29 (CH_2), 121.63 (2-C), 125.08 (=<u>C</u>-CH_3), 126.02 (4-C), 129.76 (=<u>C</u>-

CH_2), 129.86 (5-C), 133.27 (6-C), 136.14 (1-C), 148.11 (3-C), 164.72 (C=O); MS (ESI +ve) *m/z* 221.0921 (M + H) ($C_{11}H_{13}N_2O_3$ requires 221.0926).

205 ^{1}H NMR ($CDCl_3$) δ 1.71 (3 H, d, *J* = 6.3 Hz, CH_3), 4.12 (2 H, t, *J* = 6.4 Hz, CH_2), 5.55 (1 H, m, =C<u>H</u>-CH_2), 5.73 (1 H, m, =C<u>H</u>-CH_3), 6.28 (1 H, br s, NH), 7.63 (1 H, t, *J* = 7.8 Hz, 5-H), 8.14 (1 H, dd, *J* = 7.8, 1.4 Hz, 6-H), 8.33 (1 H, ddd, *J* = 8.2, 2.4, 1.2 Hz, 4-H), 8.57 (1 H, t, *J* = 1.6 Hz, 2-H); ^{13}C NMR δ 17.73 (CH_3), 36.79 (CH_2), 121.63 (2-C), 125.08 (=<u>C</u>-CH_3), 126.02 (4-C), 129.76 (=<u>C</u>-CH_2), 129.86 (5-C), 133.27 (6-C), 136.14 (1-C), 148.11 (3-C), 164.72 (C=O).

Also isolated from chromatography was mixture of **206** & **207** (10 mg, 15%) as brown powder: IR (film) ν_{max} 1628 (C=O), 3232 & 3464 (NH) cm^{-1}; R_f = 0.25 (hexane:EtOAc 2:1); ^{1}H NMR **206** ($CDCl_3$) δ 1.72 (3 H, dd, *J* = 6.3, 1.2 Hz, CH_3), 3.99 (2 H, t, *J* = 6.3 Hz, CH_2), 4.17 (2 H, br s, NH_2), 5.54 (1 H, m, =C<u>H</u>-CH_2), 5.70 (1 H, m, =C<u>H</u>-CH_3), 5.86 (1 H, br s, NH), 6.80 (1 H, dd, *J* = 8.2, 1.6 Hz, 4-H), 6.88 (1 H, dd, *J* = 7.8, 1.2 Hz, 6-H), 7.07 (1 H, t, *J* = 7.8 Hz, 5-H); ^{13}C NMR δ 17.73 (CH_3) 3 (CH_2), 115.50 (2-C), 116.85 (4-C), 118.32 (6-C), 126.36 (=<u>C</u>H-CH_2), 127.48 (5-C), 128.93 (=<u>C</u>H-CH_3), 136.63 (1-C), 143.59 (3-C), 167.07 (C=O); MS (ESI +ve) *m/z* 225.0789 (M + H) ($C_{11}H_{14}{}^{35}ClN_2O$ requires 225.0795).

207 ^{1}H NMR ($CDCl_3$) δ 1.71 (3 H, d, *J* = 6.3 Hz, CH_3), 4.09 (2 H, t, *J* = 6.3 Hz, CH_2), 5.55 (1 H, m, =C<u>H</u>-CH_2), 5.73 (1 H, m, =C<u>H</u>-CH_3), 6.28 (1 H, br s, NH), 7.63 (1 H, t, *J* = 7.8 Hz, 5-H), 8.14 (1 H, dd, *J* = 7.8, 1.4 Hz, 6-H), 8.33 (1 H, ddd, *J* = 8.2, 2.4, 1.2 Hz, 4-H), 8.57 (1 H, t, *J* = 1.6 Hz, 2-H); ^{13}C NMR δ 17.73 (CH_3), 36.80 (CH_2), 121.63 (2-C), 125.08 (=<u>C</u>-CH_3), 126.02 (4-C), 129.76 (=<u>C</u>-CH_2), 129.86 (5-C), 133.27 (6-C), 136.14 (1-C), 148.11 (3-C), 164.72 (C=O).

N-Allylphthalimide (210)

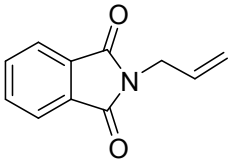

To a solution of prop-2-en-1-amine (5.70 g, 100 mmol) in acetic acid (30 mL) phthalic anhydride (14.8 g, 100 mmol) was added with stirring, then the mixture was boiled under reflux for 2 h. It was poured to water (300 mL) and the precipitate formed was filtered and dried *in vacuo* over KOH pellets. Recrystallisation (EtOAc) afforded **210**

(18.72 g, 87%) as white needles. mp 66-67 °C (lit.[213] mp 68-69 °C); IR (KBr) ν_{max} 1701 (C=O) cm^{-1}; ^1H NMR δ 4.26-4.29 (2 H, dt, *J* = 5.5, 1.4 Hz, N-CH_2), 5.15-5.19 (1 H, dq, *J* = 10.5, 1.1 Hz, H of =CH_2) 5.19-5.27 (1 H, dq, *J* = 17.6, 1.1 Hz, H of =CH_2), 5.8-5.94 (1 H, ddt, *J* = 17.1, 10.2, 1.1 Hz =CH), 7.73-7.67 (2 H, m, 3,6-H_2), 7.80-7.87 (2 H, m, 4,5-H_2);

***(E)*-2-(3-(4-methylphenyl)prop-2-enyl)isoindoline-1,3-dione (211)**

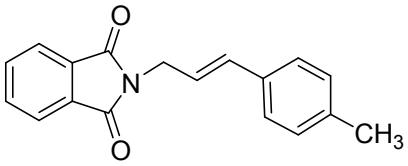

To **210** (0.2 g, 1.06 mmol), 4-iodotoluene (0.22 g, 1.06 mmol) and Et_3N (0.3 mL, 2.12 mmol) in a flask $Pd(OAc)_2$ (2.5 mg, 1 mol%) was added. Th e flask was flushed with nitrogen and the mixture was boiled under reflux at for 24 h. The solid residue was dissolved in EtOAc (20 mL). Washing (5% aq. HCl, 5% aq. $NaHCO_3$), drying, evaporation and chromatography (hexane:EtOAc 2:1) gave **211** (0.24 g, 82%) as pale buff solid. R_f = 0.4 (hexane:EtOAc 4:1); mp 164-166 °C (lit.[214] mp 165-166 °C); IR (KBr) ν_{max} 1704 (C=O) cm^{-1}; ^1H NMR δ 2.29 (3 H, s, CH_3), 4.42 (2 H, dd, *J* = 6.6, 1.1 Hz, CH_2) 6.19 (1 H, dt, *J* = 16.0, 6.3 Hz, =C<u>H</u>-CH_2), 6.64 (1 H, d, *J* = 16.0 Hz, =CH-Ph), 7.08 (2 H, d, *J* = 8.0 Hz, 2,6-H_2), 7.24 (2 H, d, *J* = 8.0 Hz, 3,5-H_2), 7.68-7.72 (2 H, m, 3,6-H_2), 7.83-7.86 (2 H, m, 4,5-H_2).

***(E)*-2-(3-(4-methoxyphenyl)prop-2-enyl)isoindoline-1,3-dione (212)**

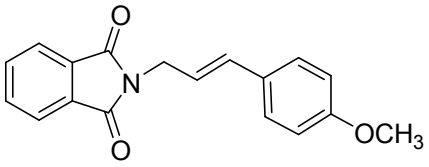

$Pd(OAc)_2$ (12.5 mg, 1 mol%) was added to **210** (1.0 g, 5.3 mmol), 1-iodo-4-methoxybenzene (1.3 g, 5.3 mmol) and Et_3N (1.5 mL, 10.6 mmol). The flask was flushed with nitrogen and the mixture was boiled under reflux for 16 h. The evaporation residue was dissolved in EtOAc (50 mL). Washing (5% aq. HCl, 5% aq. $NaHCO_3$), drying, evaporation gave **212** (1.45 g, 94%) as yellow solid: mp 137-139 °C (lit.[215] mp 139-140 °C); R_f = 0.5 (hexane:EtOAc 2:1); IR (KBr) ν_{max} 1704 (C=O) cm^{-1}; ^1H NMR ($CDCl_3$) δ 3.77 (3 H, s, CH_3), 4.39 (2 H, dd, *J* = 6.6, 1.1 Hz, CH_2) 6.13 (1 H, dt, *J* = 15.9, 6.6 Hz, =CH-CH_2), 6.56 (1 H, d, *J* = 16.0 Hz, =CH-Ph), 6.8 (2 H, d, *J* = 8.0 Hz, 3',5'-H_2),

7.28 (2 H, d, *J* = 8.0 Hz, 2',6'-H_2), 7.67-7.72 (2 H, m, 3,6-H_2), 7.80-7.87 (2 H, m, 4,5-H_2).

***(E)*-3-(4-methylphenyl)prop-2-en-1-amine (213)**

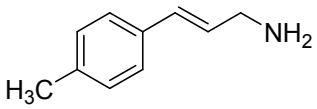

Compound **211** (0.27 g, 1.0 mmol) and hydrazine hydrate (32.0 mg, 1.0 mmol) were boiled under reflux in EtOH (10 mL) for 3 h. The solid was filtered, washed with ethanol, and then suspended in water to which 1 mL of 50% aq. NaOH solution was added. The mixture was extracted with Et_2O (2 x 10 mL) and CH_2Cl_2 (10 mL). Washing (H_2O), drying ($MgSO_4$) and evaporation yielded **213** (0.15 g, 65%) as yellow oil: R_f = 0.1 (hexane:EtOAc 1:1); IR (film) ν_{max} 3460 (NH) cm^{-1}; ^1H NMR δ 2.32 (3 H, s, CH_3), 3.43 (2 H, d, *J* = 5.8 Hz, CH_2) 6.19-6.29 (1 H, dt, *J* = 16.0, 6.0 Hz, =C<u>H</u>-CH_2), 6.48 (1 H, d, *J* = 15.9 Hz, =CH-Ph), 7.08 (2 H, d, *J* = 8.0 Hz, 2,6-H_2), 7.24 (2 H, d, *J* = 7.9 Hz, 3,5-H_2).

***(E)*-3-(4-methoxyphenyl)prop-2-en-1-amine (214)**

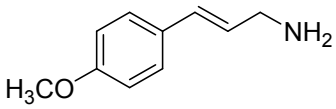

Compound **212** (3.07 g, 10.5 mmol) and hydrazine hydrate (0.34 g, 10.5 mmol) were boiled under reflux in ethanol (25 mL) for 3 h. The solid was filtered, washed with ethanol, and then suspended in water to which 1 mL of 50% aq. NaOH was added. The mixture was extracted with Et_2O (2 x 25 mL) and CH_2Cl_2 (25 mL). Washing (H_2O), drying ($MgSO_4$) and evaporation yielded **214** (1.5 g, 89%) as a yellow oil: R_f = 0.2 (EtOAc:hexane 2:1); IR (film) ν_{max} 1253, 1518 (C=C), 3460 (NH) cm^{-1}; ^1H NMR ($CDCl_3$) δ 1.35 (2 H, br s, NH_2), 3.44 (2 H, dd, *J* = 5.8, 1.4 Hz, CH_2), 3.79 (3 H, s, CH_3), 6.16 (1 H, dt, *J* = 16.0, 5.8 Hz, =C<u>H</u>-CH_2), 6.45 (1 H, d, *J* = 15.7 Hz, =CH-Ph), 6.86 (2 H, d, *J* = 8.8 Hz, 3,5-H_2), 7.31 (2 H, d, *J* = 8.8 Hz, 2,6-H_2).

***(E)*-2-iodo-3-nitro-N-(3-(4-methylphenyl)prop-2-enyl)benzamide (215)**

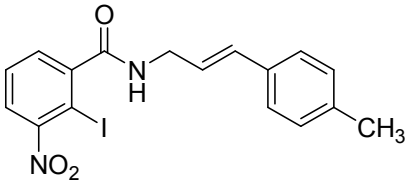

To **139** (0.55 g, 1.8 mmol) in CH_2Cl_2 (10 mL) was added **213** (0.26 g, 1.8 mmol) and Et_3N (0.5 mL, 3.6 mmol) and the mixture was stirred for 2 h. Washing (5% aq. HCl, 5% aq. $NaHCO_3$), drying, evaporation and chromatography (hexane:EtOAc 4:1) gave **215** (0.61 g, 82%) as yellow crystals: mp 159-162 °C; R_f = 0.4 (hexane:EtOAc 2:1); IR (KBr) ν_{max} 1361 & 1530 (NO_2), 1589 & 1644 (C=O), 3268 & 3468 (NH) cm^{-1}; ^1H NMR δ ($CDCl_3$) 2.34 (3 H, s, CH_3), 4.23 (2 H, t, *J* = 5.9 Hz, CH_2), 5.99 (1 H, br s, NH), 6.23 (1 H, dt, *J* = 16.0, 6.6 Hz, =C<u>H</u>-CH_2), 6.63 (1 H, d, *J* = 16.0 Hz, =C<u>H</u>-Ph), 7.14 (2 H, d, *J* = 7.8 Hz, 3',5'-H_2), 7.27 (2 H, d, *J* = 7.8 Hz, 2',6'-H_2), 7.52 (2 H, m, 5,6-H_5), 7.68 (1 H, m, 4-H); ^{13}C NMR δ 21.21 (CH_3), 42.34 (CH_2), 84.94 (2-C), 124.94 (=<u>C</u>-CH_2), 125.15 (4-C), 126.32 (2',6'-C_2), 129.35 (3',5'-C_2), 129.47 (5-C), 130.37 (6-C), 133.27 (=<u>C</u>-Ph), 133.36 (1'-C), 137.93 (4'-C), 146.13 (1-C), 154.89 (3-C), 168.19 (C=O); Anal. Calcd for $C_{17}H_{15}IN_2O_3$: C, 48.36; H, 3.58; N, 6.63; Found: C, 47.84; H, 3.37; N, 6.54.

***(E)*-2-iodo-N-(3-(4-methoxyphenyl)prop-2-enyl)-3-nitrobenzamide (216)**

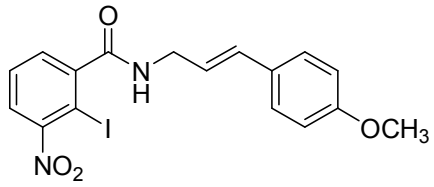

To **139** (3.12 g, 10.0 mmol) in CH_2Cl_2 (25 mL) was added **214** (1.65 g, 10.0 mmol) and Et_3N (2.8 mL, 20 mmol) and the mixture was stirred for 4 h. Washing (5% aq. HCl, 5% aq. $NaHCO_3$), drying, evaporation and chromatography (hexane:EtOAc 4:1) gave **216** (3.3 g, 75%) as yellow crystals: mp 124-127 °C; R_f = 0.35 (hexane:EtOAc 2:1); IR (KBr) ν_{max} 1348 & 1529 (NO_2), 1588 & 1640 (C=O), 3259 & 3468 (NH) cm^{-1}; ^1H NMR ($CDCl_3$) δ 3.79 (3 H, s, CH_3), 4.21 (2 H, t, *J* = 6.65 Hz, CH_2), 6.01 (1 H, br s, NH), 6.11 (1 H, dt, *J* = 16.0, 6.6 Hz, =C<u>H</u>-CH_2), 6.59 (1 H, d, *J* = 16.0 Hz, =CH-Ph), 6.83 (2 H, d, *J* = 8.6 Hz, 3',5'-H_2), 7.28 (2 H, d, *J* = 8.9 Hz, 2',6'-H_2), 7.50 (2 H, m, 5,6-H_2), 7.65 (1 H, m, 4-H); ^{13}C NMR δ 42.40 (CH_2), 55.28 (CH_3), 84.94 (C-2), 114.02 (3',5'-C_2), 121.68 (=C-CH_2), 125.13 (4-C), 127.62 (2',6'-C_2), 128.88 (1'-C), 129.45 (5-C), 130.36 (6-C), 132.91 (=C-Ph), 146.12 (1-C), 154.86 (3-C), 159.44 (4'-C), 168.19 (C=O); Anal. Calcd for $C_{17}H_{15}IN_2O_4$: C, 46.59; H, 3.45; N, 6.39; Found: C, 46.48; H, 3.33; N, 6.31.

***(E)*-N-(3-(4-methylphenyl)prop-2-enyl)-3-nitro benzamide (217)**

N-(3-(4-methylphenyl)propyl)-3-nitro-benzamide (218)

4-(4-Methylbenzyl)-5-nitroisoquinolin-1(2*H*)-one (219)

***(Z)*-4-(4-Methylbenzylidene)-5-nitro-3,4-dihydroisoquinolin-1(2*H*)-one (220)**

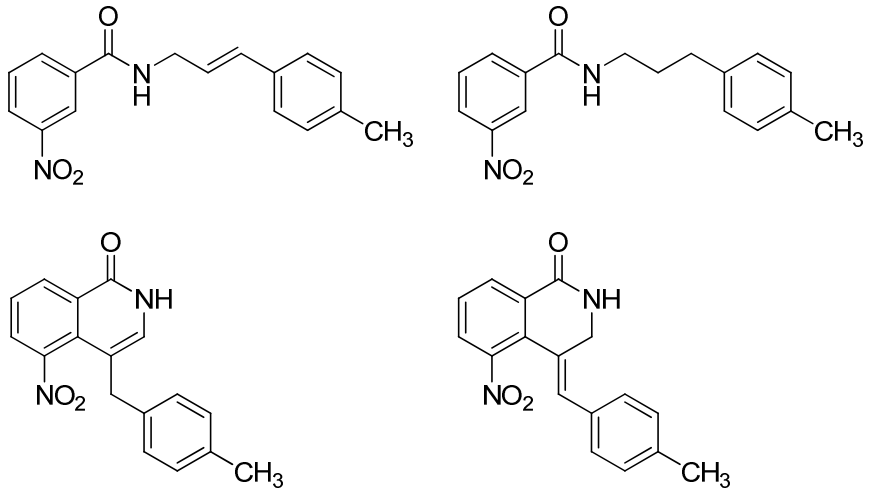

To **215** (150 mg, 0.35 mmol) in dry DMF (0.7 mL) was added $(Ph_3P)_4Pd$ (8.2 mg, 2 mol%), dry Et_3N (0.09 mL, 0.89 mmol) and tetrabutylammonium chloride (99 mg, 0.35 mmol) and the mixture was heated to reflux for 48 h. After evaporation of the solvent, the residue was taken up in $CHCl_3$, washed (5% aq. HCl, 5% aq. $NaHCO_3$) and dried. Evaporation and chromatography (hexane:EtOAc 2:1) yielded an inseparable mixture of **217** & **218** (3:1) (17 mg, 16%) as yellow semi-solid: R_f = 0.7 (hexane:EtOAc 2:1); IR (film) ν_{max} 1350 & 1524 (NO_2), 1641 (C=O), 3312 & 3467 (NH) cm^{-1}; ^1H NMR **217** ($CDCl_3$) δ 2.33 (3 H, s, CH_3), 4.23 (2 H, t, *J* = 6.3 Hz, CH_2), 6.24 (1 H, dt, *J* = 15.6, 6.6 Hz, =C<u>H</u>-CH_2), 6.55 (1 H, d, *J* = 16.0 Hz, =C<u>H</u>-Ph), 6.6 (1 H, br s, NH), 7.10 (2 H, m, 3',5'-H_2), 7.26 (2 H, d, *J* = 7.8 Hz, 2',6'-H_2), 7.64 (1 H, t, *J* = 8.2 Hz, 5-H), 8.18 (1 H, d, *J* = 8.2, 1.6 Hz, 6-H), 8.34 (1 H, ddd, *J* = 8.2, 2.4, 1.2 Hz, 4-H), 8.63 (1 H, t, *J* = 1.9 Hz, 2-H); ^{13}C NMR δ 21.18 (CH_3), 42.50 (CH_2), 121.75 (2-C), 123.38 (=C-CH_2), 126.06 (4-C), 126.28 (2',6'-C_2), 129.31 (3',5'-C_2), 129.85 (5-C), 133.11 (=C-Ph), 133.29 (6-C), 135.73 (1'-C), 135.97 (1-C), 137.85 (4'-C), 148.10 (3-C), 164.86 (C=O); MS (ESI +ve) *m/z* 297.1240 (M + H) ($C_{17}H_{17}N_2O_3$ requires 297.1239).

218 ^1H NMR ($CDCl_3$) δ 1.96 (2 H, q, *J* = 7.0 Hz, $CH_2C\underline{H}_2CH_2$), 2.29 (3 H, s, CH_3), 2.71 (2 H, t, *J* = 7.4 Hz, CH_2Ph), 3.54 (2 H, q, *J* = 6.6 Hz, NCH_2), 7.10 (2 H, m, 3',5'-H_2), 7.26 (2 H, d, *J* = 8.2 Hz, 2',6'-H_2), 7.60 (1 H, t, *J* = 7.8 Hz, 5-H), 7.98 (1 H, dt, *J* = 7.4, 1.9 Hz, 6-H), 8.30 (1 H, ddd, *J* = 8.2, 2.4, 1.2 Hz, 4-H), 8.44 (1 H, t, *J* = 1.9 Hz, 2-H), 8.54 (1 H, br s, NH); ^{13}C NMR δ 20.94 (CH_3), 30.81 ($CH_2\underline{C}H_2CH_2$), 33.19 (CH_2Ph),

40.26 (N-CH_2), 121.54 (2-C), 125.88 (4-C), 126.28 (2',6'-C_2), 129.31 (3',5'-C_2), 129.68 (5-C), 133.36 (6-C), 135.02 (1'-C), 136.11 (1-C), 138.14 (4'-C), 148.10 (3-C), 164.86 (C=O); MS (ESI +ve) *m/z* 321.1207 (M + Na) ($C_{17}H_{18}N_2NaO_3$ requires 321.1215).

Also isolated was **219** (16 mg, 15%) as an orange powder: mp 186-188 °C; R_f = 0.29 (hexane:EtOAc 2:1); IR (KBr) ν_{max} 1367 & 1526 (NO_2), 1660 (C=O), 3118 & 3392 (NH) cm^{-1}; ^1H NMR ($CDCl_3$) δ 2.33 (3 H, s, CH_3), 3.82 (2 H, s, CH_2), 6.75 (1 H, s, 3-H), 6.98 (2 H, d, *J* = 7.9 Hz, 3',5'-H_2), 7.10 (2 H, d, *J* = 7.9 Hz, 2',6'-H_2), 7.54 (1 H, t, *J* = 7.9 Hz, 7-H), 7.83 (1 H, dd, *J* = 7.9, 1.1 Hz, 6-H), 8.67 (1 H, d, *J* = 7.9, 1.1 Hz, 8-H), 11.32 (1 H, br s, NH); ^{13}C NMR δ 21.07 (CH_3), 34.98 (CH_2), 113.56 (4-C), 126.01 (7-C), 127.85 (9-C), 128.67 (6-C) 129.26 (3',5'-C_2), 129.49 (2',6'-C_2), 126.62 (10-C), 130.91 (3-C), 131.77 (8-C), 134.54 (1'-C), 136.51 (4'-C), 147.63 (5-C), 162.03 (1-C); MS (ESI +ve) *m/z* 295.1077 (M + H) ($C_{17}H_{15}N_2O_3$ requires 295.1083).

Compound **220** (14 mg, 13%) was also collected as a yellow solid: mp 152-154°C; R_f = 0.25 (hexane:EtOAc 2:1); IR (KBr) ν_{max} 1352 & 1529 (NO_2), 1662 (C=O), 3042 (NH) cm^{-1} ; ^1H NMR ($CDCl_3$) δ 2.30 (1 H, s, CH_3), 4.50 (2 H, d, *J* = 1.6 Hz, 3-CH_2), 6.75 (1 H, s, =CH), 6.84 (1 H, br s, NH), 7.09 (2 H, d, *J* = 7.8 Hz, 2',6'-H_2), 7.20 (2 H, m, 3',5'-H_2), 7.50 (1 H, t, *J* = 8.2 Hz, 7-H), 7.80 (1 H, dd, *J* = 8.1, 1.2 Hz, 6-H), 8.30 (1-H, dd, *J* = 7.8, 1.2 Hz, 8-H); ^{13}C NMR δ 21.32 (CH_3), 42.04 (CH_2), 123.51 (4-C), 127.64 (6-C), 128.15 (7-C), 129.15 (2',6'-C_2), 129.25 (3',5'-C_2), 130.24 (9-C), 131.14 (8-C), 131.85 (10-C), 132.01 (4'-C), 134.83 (=CH), 138.74 (1'-C), 148.41 (5-C), 162.96 (1-C); MS (ESI +ve) *m/z* 295.1066 (M + H) ($C_{17}H_{15}N_2O_3$ requires 295.1083).

5-Amino-4-(4-methylbenzyl)isoquinolin-1(2*H*)-one (221)
(±) 5-Amino-4-(4-methylbenzyl)-3,4-dihydroisoquinolin-1(2*H*)-one (222)

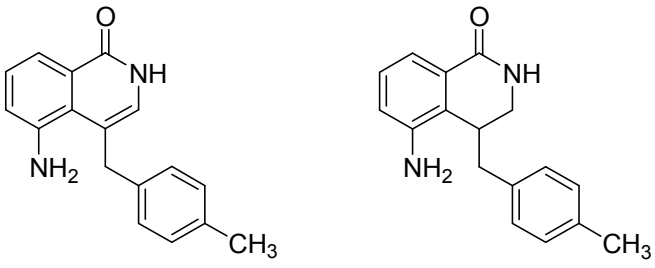

To **219** (24 mg, 0.08 mmol) in EtOH (5 mL), a slurry of 10% palladium on charcoal (50 mg) in EtOH (2 mL) was added. The mixture was stirred under H_2 for 1 h. The suspension was then filtered through Celite®. The Celite® pad and residue were

suspended in ethanol (100 mL) and heated. The hot suspension was filtered through a second Celite® pad. Concentration of the filtrate and drying gave an inseparable mixture of **221** & **222** (10:3) (11 mg, 51%) as a buff powder: R_f = 0.4 (EtOAc:hexane 2:1); IR (KBr) ν_{max} 1591 & 1654 (C=O), 3357 (NH) cm^{-1}; **221** ^{1}H NMR ($CDCl_3$) δ 2.31 (3 H, s, CH_3), 4.25 (2 H, s, CH_2), 6.82 (1 H, dd, *J* = 7.8, 1.2 Hz, 6-H), 6.86 (1 H, s, 3-H), 7.05-7.14 (4 H, m, 2',3',5',6'-H_4), 7.28 (1 H, t, *J* = 7.8 Hz, 7-H), 7.97 (1 H, d, *J* = 7.0 Hz, 8-H), 11.29 (1 H, br s, NH); ^{13}C NMR δ 20.99 (CH_3), 38.02 (CH_2), 113.57 (4-C), 119.05 (8-C), 120.83 (6-C), 126.61 (10-C), 127.02 (3-C), 127.40 (7-C), 127.96 (2',6'-C_2), 128.16 (9-C), 129.85 (3',5'-C_2), 136.58 (4'-C), 136.89 (1'-C), 143.55 (5-C), 163.91 (1-C); MS (ESI +ve) *m/z* 265.1334 (M + H) ($C_{17}H_{17}N_2O$ requires 265.1351).

222 ^{1}H NMR ($CDCl_3$) δ 2.32 (3 H, s, CH_3), 2.89 (2 H, d, *J* = 6.26 Hz, $PhCH_2$), 2.96 (1 H, m, 4-H), 3.35 (1 H, dd, *J* = 12.5, 4.3 Hz, 3-H), 3.61 (1 H, dd, *J* = 12.5, 3.9 Hz, 3-H), 6.72 (1 H, br s, NH), 6.81 (1 H, dd, *J* = 7.8, 1.2 Hz, 6-H), 7.16 (2 H, d, *J* = 8.2 Hz, 2',6'-H_2), 7.18 (1 H, t, *J* = 7.8 Hz, 7-H), 7.20-7.35 (3 H, m, 3',4',5'-H_3), 7.59 (1 H, dd, *J* = 7.8, 1.2 Hz, 8-H); ^{13}C NMR δ 21.05 (CH_3), 35.17 (4-C), 37.13 (CH_2Ph), 42.84 (3-C). 119.29 (8-C), 119.97 (6-C), 127.58 (7-C), 128.71 (10-C), 128.83 (9-C) 128.91 (2,6-C_2), 129.44 (3',5'-C_2), 136.17 (4'-C), 136.17 (1'-C), 142.81 (5-C), 167.00 (1-C); MS (ESI +ve) *m/z* 289.1311 (M + Na), 267.1491 (M + H) ($C_{17}H_{19}N_2O$ requires 265.1492).

Reaction was repeated with **220** (25 mg, 0.08 mmol) in EtOH (5 mL), gave an inseparable mixture of **222** & **221** (11:9) (10 mg, 42%) as a buff solid with properties as above.

***(E)*-*N*-(3-(4-Methoxyphenyl)prop-2-enyl)-3-nitrobenzamide (223)**
N-(3-(4-Methoxyphenyl)propyl)-3-nitrobenzamide (224)
4-(4-Methoxybenzyl)-5-nitroisoquinolin-1(2*H*)-one (225)
***(Z)*-4-(4-Methoxybenzylidene)-5-nitro-3,4-dihydroisoquinolin-1(2*H*)-one (226)**

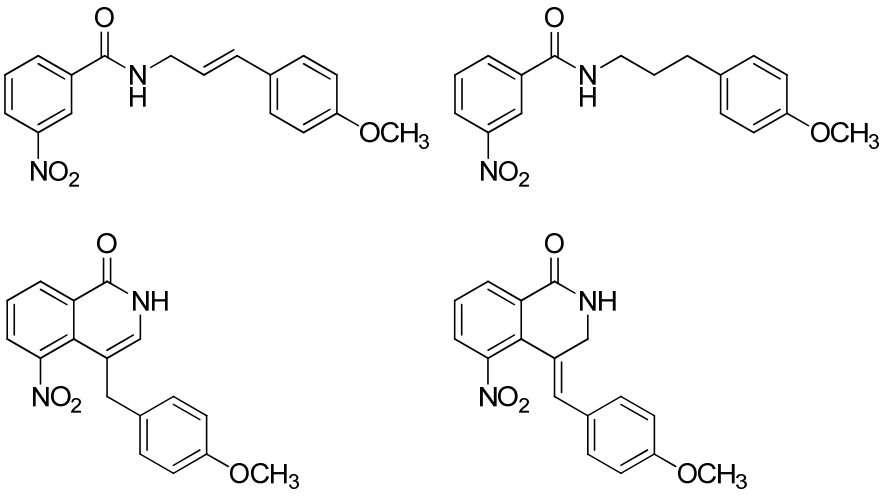

To **216** (150 mg, 0.34 mmol) in dry DMF (0.7 mL) was added $(Ph_3P)_4Pd$ (8.0 mg, 2 mol%), dry Et_3N (0.12 mL, 0.86 mmol) and tetrabutylammonium chloride (95.0 mg, 0.34 mmol) and the mixture was heated to reflux for 48 h. After evaporation of the solvent, the residue was taken up in $CHCl_3$, washed (5% aq. HCl, 5% aq. $NaHCO_3$) and dried. Evaporation and chromatography (hexane:EtOAc 2:1) yielded an inseparable mixture of **223** & **224** (2:3) (20 mg, 19%) as a yellow semi-solid: R_f = 0.4 (hexane:EtOAc 2:1); IR (film) ν_{max} 1357 & 1539 (NO_2), 1637 (C=O), 3095 & 3300 (NH) cm^{-1}; **223** ^{1}H NMR ($CDCl_3$) δ 3.76 (3 H, s, CH_3), 4.17 (2 H, t, *J* = 6.7 Hz, CH_2), 6.07 (1 H, dt, *J* = 16.0, 6.3 Hz, =C<u>H</u>-CH_2), 6.48 (1 H, d, *J* = 16.0 Hz, =CH-Ph), 6.79 (2 H, d, *J* = 8.6 Hz, 3',5'-H_2), 7.21 (2 H, d, *J* = 9.0 Hz, 2',6'-H_2), 7.33 (1 H, br s, NH), 7.56 (1 H, t, *J* = 8.2 Hz, 5-H), 8.18 (1 H, dt, *J* = 8.2, 1.6 Hz, 6-H), 8.27 (1 H, ddd, *J* = 8.2, 2.4, 1.2 Hz, 4-H), 8.64 (1 H, t, *J* = 1.9 Hz, 2-H); ^{13}C NMR δ 42.44 (CH_2), 55.14 (CH_3), 113.88 (3',5'-C_2), 121.88 (2-C), 122.24 (=<u>C</u>-CH_2), 125.84 (4-C), 127.42 (2',6'-C_2), 128.88 (1'-C), 129.61 (5-C), 132.16 (=C-Ph), 133.29 (6-C), 135.88 (1-C), 147.91 (3-C), 159.20 (4'-C), 164.99 (C=O); MS (ESI +ve) *m/z* 335.0996 (M + Na) ($C_{17}H_{16}N_2NaO_4$ requires 335.1008).

224 R_f = 0.4 (hexane:EtOAc 2:1); ^{1}H NMR ($CDCl_3$) δ 1.90 (2 H, q, *J* = 7.4 Hz, $CH_2C\underline{H}_2CH_2$), 2.63 (2 H, t, *J* = 7.4 Hz, CH_2Ph), 3.48 (2 H, m, NCH_2), 3.76 (3 H, s, CH_3), 6.90 (1 H, t, *J* = 5.4 Hz, NH), 6.79 (2 H, *J* = 8.6 Hz, 3',5'-H_2), 7.06 (2 H, d, *J* = 8.9 Hz, 2',6'-H_2), 7.50 (1 H, t, *J* = 7.8 Hz, 5-H), 8.02 (1 H, dt, *J* = 7.8, 1.2 Hz, 6-H), 8.23 (1 H, ddd, *J* = 8.2, 2.4, 1.2 Hz, 4-H), 8.48 (1 H, t, *J* = 1.9 Hz, 2-H); ^{13}C NMR δ 30.85 ($CH_2\underline{C}H_2$), 32.45 (CH_2Ph), 40.09 (N-CH_2), 55.08 (CH_3), 113.78 (3',5'-C_2), 121.64 (2-C), 125.70 (4-C), 129.10 (2',6'-C_2), 129.52 (5-C), 133.19 (1'-C), 133.11 (6-C), 136.03 (1-C), 147.83 (3-C), 157.76 (4'-C), 165.05 (C=O); MS (ESI +ve) *m/z* 315.1320 (M + H) ($C_{17}H_{19}N_2O_4$ requires 315.1345), 337.1136 (M + Na).

Also isolated was **225** (18 mg, 17%) as an orange powder: mp 121-124 °C; IR (KBr) ν_{max} 1367 & 1527 (NO_2), 1604, 1661 (C=O), 3042 & 3119 (NH) cm^{-1}; ^1H NMR ($CDCl_3$) δ 3.79 (3 H, s, CH_3), 3.81 (2 H, s, CH_2), 6.76 (1 H, s, 3-H), 6.82 (2 H, d, *J* = 8.6 Hz, 3',5'-H_2), 7.02 (2 H, d, *J* = 8.6 Hz, 2',6'-H_2), 7.52 (1 H, t, *J* = 7.8 Hz, 7-H), 7.83 (1 H, dd, *J* = 7.8, 1.2 Hz, 6-H), 8.65 (1 H, dd, *J* = 7.8, 1.6 Hz, 8-H), 11.68 (1 H, br s, NH); ^{13}C NMR δ 34.52 (CH_3), 55.23 (CH_2), 113.77 (4'-C), 114.18 (3',5'-C_2), 125.98 (7-C), 127.81 (9-C), 128.66 (6-C) 129.52 (10-C), 129.60 (4-C), 130.41(2',6'-C_2), 130.93 (3-C), 131.75 (8-C), 147.61 (5-C), 158.47 (1'-C), 162.21 (1-C); MS (ESI +ve) *m/z* 311.1026 (M + H) ($C_{17}H_{15}N_2O_4$ requires 311.1032).

Compound **226** (16 mg, 15%) was also collected as a yellow solid: mp 203-204°C; ^1H NMR ($CDCl_3$) δ 3.83 (3 H, s, CH_3), 4.52 (2 H, s, CH_2), 6.24 (1 H, br s, NH), 6.72 (1 H, s, =CH), 6.92 (2 H, d, *J* = 8.9 Hz, 3',5'-H_2), 7.12 (2 H, d, *J* = 8.2 Hz, 2',6'-H_2), 7.52 (1 H, t, *J* = 8.2 Hz, 7-H), 7.80 (1 H, dd, *J* = 8.2, 1.2 Hz, 6-H), 8.31 (1 H, dd, *J* = 7.8, 1.2 Hz, 8-H); ^{13}C NMR δ 42.14 (CH_2), 55.37 (CH_3), 114.00 (3',5'-C_2), 122.58 (4-C), 127.48 (4'-C), 127.67 (6-C), 128.02 (7-C) 130.15 (9-C), 130.73 (2',6'-C_2) 131.21 (8-C), 131.95 (10-C), 134.56 (=CH), 148.43 (5-C), 159.83 (1'-C), 162.63 (1-C); MS (ESI +ve) *m/z* 311.1001 (M + H) ($C_{17}H_{15}N_2O_4$ requires 311.1032).

5-Amino-4-(4-methoxybenzyl)isoquinolin-1(2*H*)-one (227)
(±) 5-Amino-4-(4-methoxybenzyl)-3,4-dihydroisoquinolin-1(2*H*)-one (228)

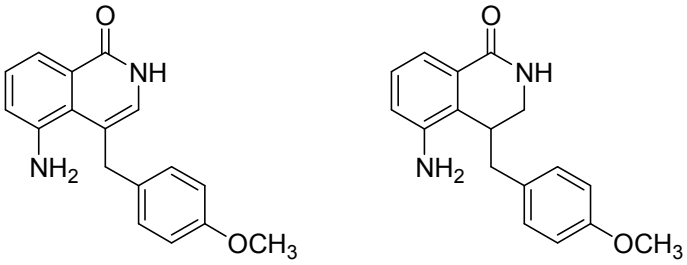

To **225** (25 mg, 0.08 mmol) in EtOH (5 mL), a slurry of 10% palladium on charcoal (50 mg) in EtOH (2 mL) was added. The mixture was stirred under H_2 for 1 h. The suspension was then flltered through Celite®. The Celite® pad and residue were suspended in ethanol (100 mL) and heated. The hot suspension was filtered through a second Celite® pad. Concentration of the filtrate and drying gave an inseparable mixture of **227** & **228** (1:2) (12 mg, 53%) as a buff powder: R_f = 0.42 (EtOAc:hexane 2:1); **227** IR (KBr) ν_{max} 1605, 1661 (C=O), 3357 (NH) cm^{-1}; ^1H NMR ($CDCl_3$) δ 3.78 (3 H, s, CH_3), 4.23 (2 H, s, CH_2), 6.79 (1 H, s, 3-H), 6.82-7.15 (5 H, m, 2',3',5',6',6-H_5),

7.30 (1 H, t, *J* = 7.8 Hz, 7-H), 8.00 (1 H, d, *J* = 7.4 Hz, 8-H), 10.6 (1 H, br s, NH); ^{13}C NMR δ 35.11 (CH_3), 36.81 (CH_2), 113.65 (4-C), 114.54 (3',5'-C_2), 119.13, 126.47, 126.47, 126.76, 127.32, 127.45, 129.11 (2',6'-C_2), 131.82, 131.82 (1'-C), 143.55 (5-C), 158.56 (1-C); MS (ESI +ve) *m/z* (M + Na) 303.1094, 281.1270 (M + H) ($C_{17}H_{17}N_2O_2$ requires 281.1290).

228 ^{1}H NMR ($CDCl_3$) δ 2.89 (2 H, m, $PhCH_2$), 2.96 (1 H, m, 4-H), 3.37 (1 H, dd, *J* = 12.5, 4.3 Hz, 3-H), 3.62 (1 H, dd, *J* = 12.5, 3.9 Hz, 3-H), 3.80 (3 H, s, CH_3), 6.23 (1 H, br s, NH), 7.20-7.35 (5 H, m, 2',3',5',6',6-H_5), 7.20 (1 H, t, *J* = 7.8 Hz, 7-H), 7.61 (1 H, d, *J* = 7.8 Hz, 8-H); ^{13}C NMR δ 35.11 (4-C), 36.81 (CH_2Ph), 42.98 (CH_2), 55.28 (CH_3), 114.14 (3',5'-C_2), 119.98, 127.32, 127.59, 128.74, 129.11, 130.00 (2',6'-C_2), 131.26, 142.85 (1'-C), 158.38 (5-C), 166.51 (1-C); MS (ESI +ve) *m/z* (M + Na) 305.1245, 283.1418 (M + H) ($C_{17}H_{19}N_2O_2$ requires 283.1447).

4-(3-Iodophenylamino)-4-oxobutanoic acid (229)

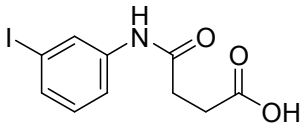

Succinic anhydride (1.0 g, 10.0 mmol) and 3-iodoaniline (2.19 g, 10 mmol) were heated slowly to 190 °C. At 150 °C **229** was identified as a buff powder: mp 154-156 °C; R_f = 0.12 (CH_2Cl_2:EtOAc 2:1); IR (KBr) ν_{max} 1656 & 1696 (C=O), 3289 (NH), 3023 (OH) cm^{-1}; ^{1}H NMR ($(CD_3)_2SO$) δ 2.48-2.64 (4 H, m, 2 × CH_2), 7.08 (1 H, t, *J* = 8.2 Hz, 5-H), 7.38 (1 H, dd, *J* = 7.8, 1.6 Hz, 4-H), 7.48 (1 H, dd, *J* = 8.2, 1.2 Hz, 6-H), 8.10 (1 H, t, *J* = 1.9 Hz, 2-H), 10.06 (1 H, s, OH), 12.15 (1 H, br s, NH); ^{13}C NMR δ 28.68 ($\underline{C}H_2CONH$), 31.05 ($\underline{C}H_2COH$), 94.67 (3-C), 118.06 (6-C), 127.07 (2-C), 130.82 (5-C), 131.48 (4-C), 140.70 (1-C), 170.45 (C=ONH), 173.83 (C=O).

1-(3-Iodophenyl)pyrrolidine-2,5-dione (230)

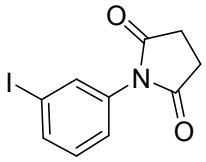

Succinic anhydride (1.0 g, 10.0 mmol) and 3-iodoaniline (2.19 g, 10 mmol) were heated at 190 °C for 6 h. Recrystallisation (EtOAc) afforded **230** (2.23 g, 74%) as buff crystals: mp 167-169 °C; R_f = 0.7 (CH_2Cl_2:EtOAc 2:1); IR (KBr) ν_{max} 1423 & 1473 (C=C), 1714 (C=O) cm^{-1}; ^1H NMR ($CDCl_3$) δ 2.82 (4 H, s, 2 × CH_2), 7.19 (1 H, t, *J* = 8.2 Hz, 5-H), 7.28 (1 H, dt, *J* = 7.8, 1.2 Hz, 6-H), 7.71 (1 H, t, *J* = 1.9 Hz, 2-H), 7.73 (1 H, dt, *J* = 7.8, 1.6 Hz, 4-H); ^{13}C NMR δ 28.35 (2 × CH_2), 93.69 (3-C), 125.79 (6-C), 130.52 (5-C), 132.84 (1-C), 135.23 (2-C), 137.65 (4-C), 175.70 (2 × C=O); MS (ESI +ve) *m/z* 301.9658 (M + H) ($C_{10}H_8NO_2$ requires 301.9678).

(E)-2-(3-(3-(2,5-Dioxopyrrolidin-1-yl)phenyl)prop-2-enyl)isoindoline-1,3-dione (231)

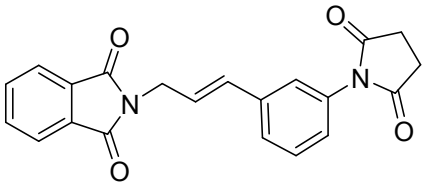

To **210** (0.20 g, 1.1 mmol), **230** (0.32 g, 1.1 mmol) and Et_3N (0.3 mL, 2.1 mmol), $Pd(OAc)_2$ (2.5 mg, 1 mol%) was added. The flask was flushed with nitrogen and the mixture was boiled under reflux at 90 °C for 24 h. The solid residue was dissolved in EtOAc (20 mL). Washing (5% aq. HCl, 5% aq. $NaHCO_3$), drying, evaporation gave **231** (0.33 g, 86%) as a buff powder: mp 210-212°C; R_f = 0.2 (hexane:EtOAc 1:1); IR (KBr) ν_{max} 1698 & 1711 (C=O) cm^{-1}; ^1H NMR ($CDCl_3$) δ 2.8 (4 H, s, 2 × CH_2), 4.44 (2 H, d, *J* = 6.3 Hz, CH_2), 6.27 (1 H, dt, *J* = 16.0, 6.3 Hz, =C<u>H</u>-CH_2), 6.66 (1 H, d, *J* = 15.7 Hz, =CH-Ph), 7.12-7.41 (4 H, m, 2,4,5,6-H_4), 7.71-7.74 (2 H, m, 3,6-H_2), 7.83-7.87 (2 H, m, 4,5-H_2); ^{13}C NMR δ 28.36 (2 x CH_2), 39.39 (CH_2), 123.30 (3,6-C_2), 124.16 (=<u>C</u>H-CH_2), 124.44 (2'-C), 125.72 (5'-C), 126.74 (6'-C), 129.31 (4'-C), 132.03 (3'-C), 132.13 (8,9-C_2), 132.48 (=CH-Ph), 133.99 (4,5-C_2), 137.52 (1'-C), 167.84 (2 × C=O of Pth), 176.06 (2 × C=O); MS (ESI +ve) *m/z* 361.1183 (M + H) ($C_{21}H_{17}N_2O_4$ requires 361.1188).

tert-Butyl N-(prop-2-enyl)carbamate (233)

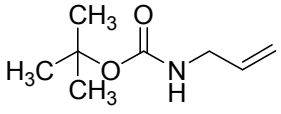

Prop-2-en-1-amine (0.75 mL, 10.0 mmol) was slowly added to an ice-cold solution of di(*tert*-butyl) dicarbonate (2.18 g, 10.0 mmol) in CH_2Cl_2 (5 mL) and the mixture was stirred for 3 h. Evaporation gave **233** (1.3 g, 83%) as colourless prisms: mp 33-35 °C (lit.[9] mp 35-36 °C); R_f = 0.8 (hexane:EtOAc 1:1); IR (KBr) ν_{max} 1169 (C-O), 1531 & 1684 (C=O), 2980 & 3354 (NH) cm^{-1}; ^1H NMR ($CDCl_3$) δ 1.42 (9 H, s, $(CH_3)_3$), 3.72 (2 H, t, *J* = 5.2 Hz, propenyl 1-H_2), 4.60 (1 H, br s, NH), 5.05 (1 H, dq, *J* = 10.2, 1.6 Hz, propenyl 3-H), 5.19 (1 H, dq, *J* = 17.1, 1.7 Hz, propenyl 3-H), 5.80 (1 H, m, propenyl 2-H).

***(E)-tert*-Butyl 3-(3-(2,5-dioxopyrrolidin-1-yl)phenyl)prop-2-enylcarbamate (234)**
***tert*-Butyl 2-(3-(2,5-dioxopyrrolidin-1-yl)phenyl)prop-2-enylcarbamate (235)**

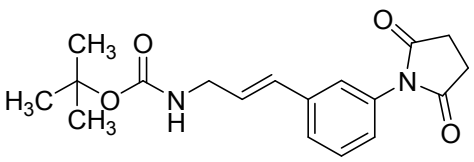
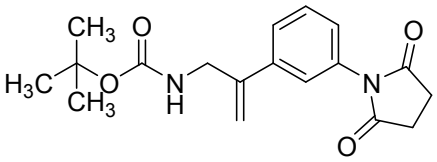

To **233** (1.57 g, 10.0 mmol), **230** (3.0 g, 10.0 mmol) and Et_3N (2.8 mL, 20 mmol), $Pd(OAc)_2$ (22.5 mg, 1 mol%) was added. The flask was flushed with nitrogen and the mixture was boiled under reflux for 48 h. The solid residue was dissolved in $CHCl_3$ (50 mL). Washing (5% aq. HCl, 5% aq. $NaHCO_3$), drying, evaporation gave an inseparable mixture of **234** & **235** (4:1) (1.2 g, 32%) as a buff semi-solid: R_f = 0.24 (CH_2Cl_2:EtOAc 3:2); IR (film) ν_{max} 1180 (C-O), 1709 (C=O), 3370, 2978 (NH) cm^{-1}; **234** ^1H NMR ($CDCl_3$) δ 1.44 (9 H, s, $(CH_3)_3$), 2.87 (4 H, s, 2 x CH_2), 3.88 (2 H, m, CH_2), 4.71 (1 H, br s, NH), 6.22 (1 H, dt, *J* = 16.0, 5.9 Hz, =C<u>H</u>-CH_2), 6.5 (1 H, d, *J* = 16.0 Hz, =CH-Ph), 7.13 (1 H, dt, *J* = 7.4, 1.6 Hz, 6-H), 7.24 (1 H, s, 2-H), 7.36 (1 H, dd, *J* = 7.8, 1.6 Hz, 4-H), 7.41 (1 H, t, *J* = 7.8 Hz, 5-H); ^{13}C NMR δ 28.34 (2 x CH_2), 28.37 $(CH_3)_3$, 42.47 (CH_2), 79.48 (C-$CH_3)_3$), 124.29 (2-C), 125.37 (4-C), 126.55 (6-C), 127.89 (=<u>C</u>HCH_2), 129.32 (5-C), 130.14 (=CHPh), 132.13 (3-C), 138.01 (1-C), 155.68 (C=O), 176.15 (2 x C=O); MS (ESI +ve) *m/z* 331.1652 (M + H) ($C_{18}H_{23}N_2O_4$ requires 331.1658).

235 ^1H NMR ($CDCl_3$) δ 1.43 (9 H, s, $(CH_3)_3$), 2.87 (4 H, s, 2 x CH_2), 4.15 (2 H, d, *J* = 5.4 Hz, CH_2), 4.5 (1 H, br s, NH), 5.26 (1 H, s, =CH), 5.43 (1 H, s, =CH), 7.13-7.41 (4 H, m, 2,4,5,6-H_4); ^{13}C NMR δ 28.16 (2 x CH_2), 28.22 $(CH_3)_3$, 44.14 (CH_2), 79.48 (C-$CH_3)_3$), 114.39 (=CH_2), 124.38 (2-C), 125.88 (4-C), 126.36 (6-C), 129.40 (5-C), 129.46 (C=CH_2), 129.87 (3-C), 132.03 (1-C), 155.68 (C=O), 176.04 (2 x C=O).

(E)-1-(3-(3-aminoprop-1-enyl)phenyl)pyrrolidine-2,5-dione (236)
1-(3-(3-aminoprop-1-en-2-yl)phenyl)pyrrolidine-2,5-dione (237)

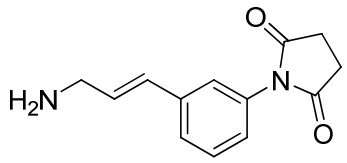
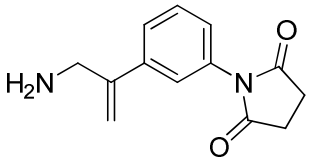

To the mixture **234** & **235** (1.2 g, 3.6 mmol) in CH_2Cl_2 (15 mL), dry HCl gas was passed for 30 min. The product mixture of **236** & **237** was used in the next step without further purification.

***(E)*-N-(3-(3-(2,5-Dioxopyrrolidin-1-yl)phenyl)prop-2-enyl)-2-iodo-3-nitrobenzamide (238)**
N-(2-(3-(2,5-dioxopyrrolidin-1-yl)phenyl)prop-2-enyl)-2-iodo-3-nitrobenzamide (239)

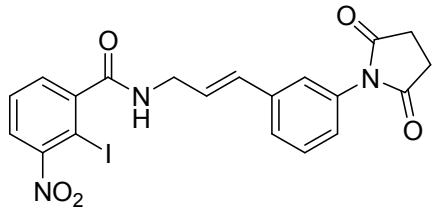
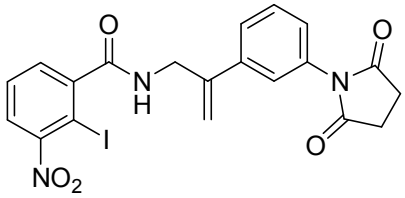

To **139** (1.5 g, 5.0 mmol) in CH_2Cl_2 (15 mL) was added mixture of **236** & **237** (1.65 g, 5.0 mmol) and Et_3N (1.5 mL, 10 mmol) and the mixture was stirred for 6 h. Washing (5% aq. HCl, 5% aq. $NaHCO_3$), drying, evaporation and chromatography (hexane:EtOAc 4:1) gave a mixture of **238** & **239** (0.8 g, 32%) as yellow crystals: IR (KBr) ν_{max} 1391, 1534 (NO_2), 1702, 1631 (C=O), 3467, 3313 (NH) cm^{-1}; **238** ^1H NMR ($(CD_3)_2SO$) δ 2.78 (4 H, s, 2 x CH_2), 4.06 (2 H, t, *J* = 5.5 Hz, CH_2), 6.38 (1 H, dt, *J* = 15.7, 5.87 Hz, =C<u>H</u>-CH_2), 6.69 (1 H, d, *J* = 16.04 Hz, =CH-Ph), 7.12 (1 H, dt, *J* = 7.43, 1.6 Hz, 6'-H), 7.33 (1 H, d, *J* = 1.6 Hz, 2'-H), 7.45 (1 H, t, *J* = 7.43 Hz, 5'-H), 7.49 (1 H, dt, *J* = 7.8, 1.6 Hz, 4'-H), 7.59 (1 H, dd, *J* = 7.8, 1.6 Hz, 4-H), 7.64 (1 H, t, *J* = 7.8 Hz, 5-H), 7.85 (1 H, dd, *J* = 7.8, 1.6 Hz, 6-H), 8.88 (1 H, t, *J* = 5.5 Hz, NH); ^{13}C NMR δ 28.55 (2 x CH_2), 40.89 (CH_2), 86.77 (2-C), 124.03 (4-C), 124.83 (2'-C), 126.09 (6'-C), 126.21 (4'-C), 127.42 (=<u>C</u>HCH_2), 129.19 (5'-C), 129.57 (=CHPh), 129.77 (6-C), 130.34 (5-C), 133.19 (1'-C), 137.44 (3'-C), 146.39 (1-C), 155.26 (3-C), 168.13 (C=O), 177.60 (2 x C=O); MS (ESI +ve) *m/z* 506.0207 (M + H) ($C_{20}H_{17}IN_3O_5$ requires 506.0213).

239 ^{1}H NMR ($(CD_3)_2SO$) δ 2.82 (4 H, s, 2 x CH_2), 4.48 (2 H, d, *J* = 5.0 Hz, CH_2), 5.38 (1 H, s, =CH_2), 5.40 (1 H, s, =CH_2), 7.01-7.73 (5 H, m, 2',4',5',6',5-H_5), 8.19 (1 H, m, 4-H), 8.28 (1 H, m, 6-H).; ^{13}C NMR δ 27.38 (2 x CH_2), 51.63 (CH_2), 121.02, 127.43, 129.47, 129.54, 129.81, 131.99, 132.04, 132.14, 132.52, 133.37, 142.66 (q),149.00 (3-C), 162.00 (C=O), 171.16 (2 x C=O).

***(E)*-N-(3-(3-(2,5-dioxopyrrolidin-1-yl)phenyl)prop-2-enyl)-3-nitrobenzamide (240)**
N-(2-(3-(2,5-dioxopyrrolidin-1-yl)phenyl)prop-2-enyl)-3-nitrobenzamide (241)
1-(3-((5-nitro-1-oxo-1,2-dihydroisoquinolin-4-yl)methyl)phenyl)pyrrolidine-2,5-dione (242)
***(Z)*-1-(3-((5-nitro-1-oxo-2,3-dihydroisoquinolin-4(1*H*)ylidene)methyl)phenyl) pyrrolidine-2,5-dione (243)**

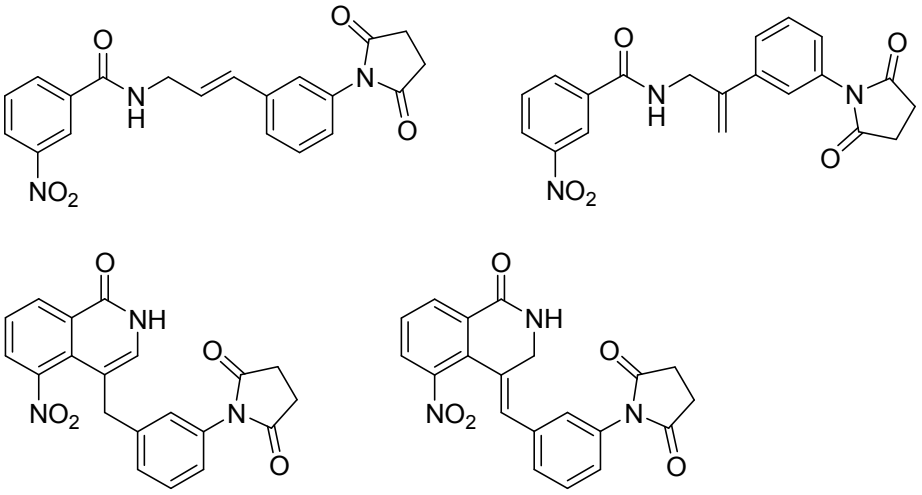

To mixture of **238** & **239** (100 mg, 0.2 mmol) in dry DMF (0.5 mL) was added $(Ph_3P)_4Pd$ (4.6 mg, 2 mol%), dry Et_3N (0.07 mL, 0.5 mmol) and tetrabutylammonium iodide (73.1 mg, 0.2 mmol) and the mixture was heated to reflux for 48 h. After evaporation of the solvent the residue was taken up in $CHCl_3$, washed (5% aq. HCl, 5% aq. $NaHCO_3$) and dried. Evaporation and chromatography (hexane:EtOAc 4:1) yielded an inseparable mixture of **240** & **241** (4:1) (14 mg, 18%) as yellow semi-solid: R_f = 0.5 (hexane:EtOAc 2:1); IR (film) ν_{max} 1350, 1528 (NO_2), 1658, 1709 (C=O), 3078, 3351 (NH) cm^{-1}; **240** ^{1}H NMR ($CDCl_3$) δ 2.87 (4 H, s, 2 x CH_2), 4.17 (2 H, t, *J* = 6.3 Hz, CH_2), 6.20 (1 H, dt, *J* = 16.0, 6.26 Hz, =C<u>H</u>-CH_2), 6.69 (1 H, d, *J* = 16.04 Hz, =CH-Ph), 7.10 (1 H, dt, *J* = 8.2, 1.6 Hz, 6'-H), 7.19 (1 H, t, *J* = 1.9 Hz, 2'-H), 7.27 (1 H, d, *J* = 8.2 Hz, 4'-H), 7.49 (1 H, dt, *J* = 7.8, 1.6 Hz, 5'-H), 7.59 (1 H, t, *J* = 7.8 Hz, 5-H), 8.20 (1 H, dt, *J* = 7.8, 1.6 Hz, 6-H), 8.29 (1 H, ddd, *J* = 8.2, 2.4, 1.2 Hz, 4-H), 8.66 (1 H, t, *J* = 1.9 Hz, 2-H); ^{13}C NMR δ 28.38 (2 x CH_2), 42.20 (CH_2), 121.92 (2'-C), 124.22 (4-C), 125.62 (2-C),

125.98 (6'-C), 126.36 (4'-C), 126.56 (=CHCH$_2$), 129.35 (5'-C), 129.67 (=CHPh), 131.37 (6-C), 131.89 (5-C), 133.51 (1'-C), 135.70 (3'-C), 137.60 (1-C), 147.99 (3-C), 164.96 (C=O), 176.36 (2 x C=O); MS (ESI +ve) *m/z* 380.1246 (M + H) ($C_{20}H_{18}N_3O_5$ requires 380.1240).

241 ^{1}H NMR ($CDCl_3$) δ 2.88 (4 H, s, 2 x CH_2), 4.48 (2 H, d, *J* = 5. Hz, CH_2), 5.36 (1 H, s, =CH_2), 5.49 (1 H, s, =CH_2), 7.08-7.63 (5 H, m, 2',4',5',6',5-H_5), 8.19 (1 H, m, 6-H), 8.28 (1 H, m, 4-H), 8.56 (1 H, s, 2-H); ^{13}C NMR δ 28.38 (2 x CH_2), 50.66 (CH_2), 122.02, 128.45, 128.57, 129.41, 129.61, 131.99, 132.04, 132.14, 132.52, 133.37, 142.66 (q),149.00 (3-C), 165.00 (C=O), 171.26 (2 x C=O).

Also isolated was an inseparable mixture of **242** & **243** (1:1) (16 mg, 21%). IR (film) ν_{max} 1350, 1528 (NO_2), 1658, 1709 (C=O), 3078, 3351 (NH) cm^{-1}; ^{1}H NMR ($CDCl_3$) δ 2.85 (4 H, s, 2 x CH_2), 4.48 (2 H, s, 4-CH_2), 7.04 (1 H, s, 3-H), 7.15-7.43 (4 H, m, 2',4',5',6',-H_4), 7.53 (1 H, t, *J* = 7.8 Hz, 7-H), 7.81 (1 H, dd, *J* = 8.2, 1.2 Hz, 6-H), 8.65 (1 H, dd, *J* = 7.8, 1.6 Hz, 8-H), 10.34 (1 H, br s, NH); ^{13}C NMR δ 28.38 (CH_3), 35.15 (CH_2), 60.39, 125.02, 126.19, 126.97, 128.64, 129.17, 129.60, 131.37, 132.22, 132.04, 139.11, 148.27, 161.20 (C=O), 176.15 (2 x C=O).

226 (16 mg, 15%) was also collected as a yellow solid: mp 203-204°C; ^{1}H NMR ($CDCl_3$) δ 2.91 (4 H, s, 2 x CH_2), 4.49 (2 H, s, 3-CH_2), 6.14 (1 H, br s, NH), 6.78 (1 H, s, 4C=CH), 7.15 (1 H, m, 2'-H), 7.22 (1 H, m, 4'-H),7.32 (1 H, m, 6'-H), 7.51 (1 H, t, *J* = 7.8 Hz, 5'-H), 7.54 (1 H, t, *J* = 7.8 Hz, 7-H), 7.83 (1 H, dd, *J* = 8.2, 1.2 Hz, 6-H), 8.33 (1 H, dd, *J* = 7.8, 1.2 Hz, 8-H); ^{13}C NMR δ 30.93 (CH_2), 41.82 (CH_3), 59.27, 125.91, 126.29, 127.65, 128.69, 129.45, 129.72, 131.037, 131.97, 133.14, 135.78, 147.51, 162.67 (C=O), 176.02 (2 x C=O).

Experimental Details for Chapter 4.0.

PARP-1 Colourimetric Assay

Materials and Method

Inhibitor constants were determined using the Universal colourimetric PARP assay kit (Trevigen). The assays were performed in 96 strip-well plates pre-coated with histones. Firstly, PARP inhibitor stock solutions (50 mM) were prepared by dissolving them in DMSO. These were diluted with 1 x PARP buffer to seven different concentrations at 5 x stock solution such that the final concentrations in the assay were 100, 30, 10, 3, 1, 0.3, and 0.1 μM. The final concentration of DMSO in the assay was less than 0.2 % (v/v). A positive control (PARP enzyme with no inhibitor) and negative control (no PARP enzyme) were included in each assay. The PARP enzyme was diluted to 0.8 units / 15 μl with 1 x PARP buffer. Diluted PARP inhibitor (40 μL) was mixed with diluted PARP enzyme (60 μL), centrifuged and incubated for 10 min at ambient temperature. Then 25 μL of each solution was distributed into wells in triplicate. To initiate the reaction 25 μL of PARP cocktail [(10 x PARP cocktail, 10 x Activated DNA, 1 x PARP buffer (1:1:8) (v/v/v)] was added to each well using a multi-channel pipettor. In all cases the final reaction volume was 50 μL. The reaction was allowed to proceed for 1 h at ambient temperature. Plates were washed four times with PBS + 0.1 % (v/v) triton X-100 (200 μL). Then 50 μL Strep-HRP (1000 fold with 1 x Strep dilutent) was added to each well with a multi-channel pipettor, and the plate was incubated for 30 min at ambient temperature. . Plates were again washed four times with PBS + 0.1 % (v/v) triton X-100 (200 μL). TACS Sapphire colourimetric substrate (50 μL / well) was added with a multi-channel pipettor and the plates were incubated in the dark for 30 min. Absorbance at 630 nm was measured using a Versamax microplate reader with SoftMax Pro 4.7.1 software. The colourimetric reaction was stopped by adding 0.2 M HCl (50 μL / well), and the absorbance was measured at 450 nm.

Data were analysed using GraphPad Prism 2.01 software. The IC_{50} values were calculated by plotting $\log_{10}$ [inhibitor] versus absorbance for the three independent determinations. Quoted IC_{50} values are mean for the three replicant curves.

7. References

1. Madhusudan, S.; Middleton, M. R. The emerging role of DNA repair proteins as predictive, prognostic and therapeutic targets in cancer. *Cancer Treat. Rev.* **2005***, 31*, 603-617.
2. Sancar, A.; Lindsey-Boltz, L. A.; Unsal-Kacmaz, K.; Linn, S. Molecular mechanisms of mammalian DNA repair and the DNA damage checkpoints. *Annu. Rev. Biochem.* **2004***, 73*, 39-85.
3. Hoeijmakers, J. H. J. Genome maintenance mechanisms for preventing cancer. *Nature* **2001***, 411*, 366-374.
4. Frosina, G. Tumor suppression by DNA base excision repair. *Mini-Reviews in Med. Chem.* **2007**, *7*, 727-743.
5. Christmann, M.; Tomicic, M. T.; Roos, W. P.; Kaina, B. Mechanisms of human DNA repair: an update. *Toxicology* **2003**, 193, 3-34.
6. Plummer, E. R. Inhibition of poly(ADP-ribose) polymerase in cancer. *Curr. Opin. Pharmacol.* **2006***, 6*, 364-368.
7. Wang, Z. DNA damage-induced mutagenesis: a novel target for cancer prevention. *Mol. Interv.* **2001***, 1*, 269-281.
8. Madhusudan, S.; Hickson, I. D. DNA repair inhibition: a selective tumour targeting strategy. *Trends in Mol. Med.* **2005***, 11*, 503-511.
9. Schreiber, V.; Dantzer, F.; Ame, J. C.; de Murcia, G. Poly(ADP-ribose): novel functions for an old molecule. *Nature Rev. Mol. Cell Biol.* **2006***, 7*, 517-528.
10. Kameshita, I.; Matsuda, Z.; Taniguchi, T.; Shizuta, Y. Poly (ADP-Ribose) synthetase. Separation and identification of three proteolytic fragments as the substrate-binding domain, the DNA-binding domain, and the automodification domain. *J. Biol. Chem.*, **1984,** *259*, 4770-4776.
11. Nguewa, P. A.; Fuertes, M. A.; Valladares, B.; Alonso, C.; Perez, J. M. Poly(ADP-ribose)polymerases: Homology, structural domains and functions. Novel therapeutical applications. *Prog. Biophys. Mol. Biol.* **2005***, 88*, 143-172.
12. Cosi, C. New inhibitors of poly(ADP-ribose) polymerase and their potential therapeutic targets. *Expert. Opin. Ther. Patents* **2002,** *12,* 1047-1071.
13. De Murcia, G.; Ménissier-de Murcia, J. Poly(ADP-ribose) polymerase: a molecular nick-sensor. *Trends Biochem. Sci.*, **1994,** *19,* 172-176.
14. Ruf, A.; Ménissier-de Murcia, J.; De Murcia, G.; Schulz, G. F. Structure of the catalytic fragment of poly(ADP-ribose) polymerase from chicken. *Proc. Natl. Acad. Sci. USA*. **1996**, *93,* 7481-7485.

15. Ame, J. C.; Rolli, V.; Schreiber, V.; Niedergang, C.; Apiou, F.; Decker, P.; Muller, S.; Hoger, T.; Menissier-de Murcia, J.; de Murcia, G. PARP-2, A novel mammalian DNA damage-dependent poly(ADP-ribose) polymerase. *J. Biol. Chem.* **1999***, 274*, 17860-17868.
16. Augustin, A.; Spenlehauer, C.; Dumond, H.; Menissier-De Murcia, J.; Piel, M.; Schmit, A. C.; Apiou, F.; Vonesch, J. L.; Kock, M.; Bornens, M.; De Murcia, G. PARP-3 localizes preferentially to the daughter centriole and interferes with the G1/S cell cycle progression. *J. Cell. Sci.* **2003***, 116*, 1551-1562.
17. Kickhoefer, V. A.; Siva, A. C.; Kedersha, N. L.; Inman, E. M.; Ruland, C.; Streuli, M.; Rome, L. H. The 193-kD vault protein, VPARP, is a novel poly(ADP-ribose) polymerase. *J. Cell. Biol.* **1999***, 146*, 917-928.
18. Smith, S.; Giriat, I.; Schmitt, A.; de Lange, T. Tankyrase, a poly(ADP-ribose) polymerase at human telomeres. *Science* **1998***, 282*, 1484-1487.
19. Chang, P.; Coughlin, M.; Mitchison, T. J. Tankyrase-1 polymerization of poly(ADP-ribose) is required for spindle structure and function. *Nature Cell Biol.* **2005,** *7*, 1133–1139.
20. Gao, G.; Guo, X.; Goff, S. P. Inhibition of retroviral RNA production by ZAP, a CCCH-type zinc finger protein. *Science*, **2002,** *297*, 1703–1706.
21. Ladurner, A. G. Inactivating chromosomes: a macro domain that minimizes transcription. *Mol. Cell.* **2003***, 12*, 1-3.
22. Karras, G. I.; Kustatscher, G.; Buhecha, H. R.; Allen, M. D.; Pugieux, C.; Sait, F.; Bycroft, M.; Ladurner, A. G. The macro domain is an ADP-ribose binding module. *Embo. J.* **2005***, 24*, 1911-1920.
23. Chou, H. Y.; Chou, H. T; Lee, S. C. Cdk-dependent activation of poly(ADP-ribose)polymerase member 10 (PARP-10). *J. Biol. Chem.* **2006**, *281*, 15201–15207.
24. Diefenbach, J.; Bürkle, A. Introduction to poly(ADP-ribose) metabolism. *Cell. Mol. Life Sci.* **2005***, 62*, 721-730.
25. Chol Ha, H.; Snyder, S. H. Poly(ADP-ribose) polymerase-1 in the nervous system. *Neurobiol. Disease* **2000**, *7*, 225-239.
26. Hassa, P. O.; Haenni, S. S.; Elser, M.; Hottiger, M. O. Nuclear ADP-ribosylation reactions in mammalian cells: where are we today and where are we going? *Microbiol. Mol. Biol. Rev.* **2006***, 70*, 789-829.
27. Shall, S. ADP-ribosylation reactions. *Biochimie* **1995,** *77*, 313-318.
28. D'Amours, D.; Desnovers, S.; D'Silva, I.; Poirier, G. G. Poly(ADP-ribosylation reactions in the regulation of nuclear functions. *Biochem. J*. **1999**, *342*, 249-268.

29. Griffin, R. J.; Curtin, N. J.; Newell, D. R.; Golding, B. T.; Durkacz, B. W.; Calvert, A. H. The role of inhibitors of poly(ADP-ribose) polymerase as resistance-modifying agents in cancer therapy. *Biochimie.* **1995,** *77,* 408-422.
30. De Murcia, G.; Huletsky, A.; Lammare, D.; Gaudreau, A.; Pouyet, J.; Daune, M.; Poirier, G. G. Modulation of chromatin superstructure induced by poly(ADP-ribose) synthesis and degradation. *J. Biol. Chem.* **1986,** *261,* 7011-7017.
31. Uchida, K.; Hanai, S.; Ishikawa, K.; Ozawa, Y.; Uchida, M.; Sugimura, T.; Miwa, M. Cloning of cDNA encoding Drosophilia poly(ADP-ribose) polymerase: leucine zipper in the auto-modification domain. *Proc. Natl. Acad. Sci. USA*, **1993**, *90*, 3481-3485.
32. Mendoza-Alvarez, H.; Alvarez-Gonzalez, R. Poly(ADP-ribose)polymerase is a catalytic dimer and the automodification reaction is intermolecular. *J. Biol. Chem.,* **1993***, 268,* 22575-22580.
33. Ratnam, K.; Low, A. J. Current development of clinical inhibitors of poly(ADP-Ribose) polymerase in oncology. *Clin. Cancer. Res.* **2007***, 13*, 1383.
34. Woon, E. C. Y.; Threadgill, M. D. Poly(ADP-ribose)polymerase inhibition – where now? *Curr. Med. Chem*. **2005**, 12, 2373-2392.
35. Davidovic, L.; Vodenicharov E.; Affar, E. B.; Poirier, G. G. Importance of poly(ADP-ribose)glycohydrolase in the control of poly(ADP-ribose) metabolism. *Exp. Cell Res.* **2001**, *268,* 7-13.
36. Oka, J.; Ueda, K.; Hayaishi, O.; Komura, H.; Nakanishi, K. ADP-ribosyl protein lyase. Purification, properties, and identification of the product. *J. Biol. Chem.* **1984***, 259*, 986-995.
37. De Murcia, J. M.; Niedergang, C.; Trucco, C.; Ricoul, M.; Dutrillaux, B.; Mark, M.; Oliver, F. J.; Masson, M.; Dierich, A.; LeMeur, M.; Walztinger, C.; Chambon, P.; De Murcia, G. Requirement of poly(ADP-ribose) polymerase in recovery from DNA damage in mice and in cells. *Proc. Natl. Acad. Sci. USA* **1997***, 94*, 7303-7307.
38. Dantzer, F.; De La Rubia, G.; Menissier-De Murcia, J.; Hostomsky, Z.; De Murcia, G.; Schreiber, V. Base excision repair is impaired in mammalian cells lacking Poly(ADP-ribose) polymerase-1. *Biochemistry* **2000***, 39*, 7559-7569.
39. Yung, T. M.; Sato, S.; Satoh, M. S. Poly(ADP-ribosyl)ation as a DNA damage-induced post-translational modification regulating poly(ADP-ribose) polymerase-1-topoisomerase I interaction. *J. Biol. Chem.* **2004***, 279*, 39686-39696.
40. Virág, L.; Szabó, C. The therapeutic potential of poly(ADP-ribose) polymerase inhibitors. *Pharmacol. Rev.* **2002,** *54,* 375-429.

41. Reale, A.; Matteis, G. D.; Galleazzi, G.; Zampieri, M.; Caiafa, P. Modulation of DNMT1 activity by ADP-ribose polymers. *Oncogene* **2005***, 24*, 13-19.

42. Hassa, P. O.; Hottiger, M. O. The functional role of poly(ADP-ribose)polymerase 1 as novel coactivator of NF-kB in inflammatory disorders. *Cell. Mol. Life Sci.* **2002***, 59*, 1534–1553.

43. Genovese, T.; Mazzon, E.; Di Paola, R.; Muia, C.; Threadgill, M. D.; Caputi, A. P.; Thiemermann, C.; Cuzzocrea, S. Inhibitors of poly(ADP-ribose) polymerase modulate signal transduction pathways and the development of bleomycin-induced lung injury. *J. Pharmacol. Exp. Ther.* **2005***, 313*, 529-538.

44. Genovese, T.; Mazzon, E.; Muià, C.; Patel, N. S. A.; Threadgill, M. D.; Bramanti, P.; De Sarro, A.; Thiemermann, C.; Cuzzocrea, S. Inhibitors of poly(ADP-ribose) polymerase modulate signal transduction pathways and secondary damage in experimental spinal cord trauma. *J. Pharmacol. Exp. Ther*. **2005**, *312*, 449-457.

45. Hao, L. X.; Wang, Y. L.; Cai, L.; Li, Y. Y. Inhibitory effect of 5-aminoisoquinolinone on PARP activity in colon carcinoma cell line HT-29. *Chinese J. Cancer Res*. **2007**, *26*, 566-571.

46. Oliver, J. F.; Menissier-De Murcia, J.; Nacci, C.; Decker, P.; Andriantsitohaina, R.; Muller, S.; De la Rubia, G.; Stoclet, C. J; De Murcia, G. Resistance to endotoxic shock as a consequence of defective NF-κB activation in poly (ADP-ribose)polymerase-1 deficient mice. *Eur. Mol. Biol. Organ. J.* **1999***, 18*, 4446-4454.

47. Carrillo, A.; Monreal, Y.; Ramirez, P.; Marin, L.; Parrilla, P.; Oliver, F. J.; Yelamos, J. Transcription regulation of TNF-alpha-early response genes by poly(ADP-ribose) polymerase-1 in murine heart endothelial cells. *Nucleic Acids Res.* **2004***, 32*, 757-766.

48. Jagtap, P.; Szabó, C. Poly(ADP-Ribose) polymerase and the therapeutic effects of its inhibitors. *Nature Rev. Drug Discovery* **2005***, 4*, 421-440.

49. Szabo, C.; Dawson, V. L. Role of poly(ADP-ribose) synthetase in inflammation and ischaemia-reperfusion. *Trends Pharmacol. Sci.* **1998***, 19*, 287-298.

50. Berger, N. A. Poly(ADP-ribose) in the cellular response to DNA damage. *Radiat. Res.* **1985***, 101*, 4-15.

51. Leist, M.; Single, B.; Castoldi, A. F.; Kuhnle, S.; Nicotera, P. Intracellular adenosine triphosphate (ATP) concentration: a switch in the decision between apoptosis and necrosis. *J. Exp. Med.* **1997***, 185*, 1481-1486.

52. Lazebnik, Y. A.; Kaufmann, S. H.; Desnoyers, S.; Poirier, G. G.; Earnshaw, W. C. Cleavage of poly(ADP-ribose) polymerase by a proteinase with properties like ICE. *Nature* **1994***, 371*, 346-347.

53. D'Amours, D.; Sallmann, F. R.; Dixit, V. M.; Poirier, G. G. Gain-of-function of poly(ADP-ribose) polymerase-1 upon cleavage by apoptotic proteases: implications for apoptosis. *J. Cell Sci.* **2001***, 114*, 3771-3778.

54. Boulton, S.; Pemberton, L. C.; Porteous, J. K.; Curtin, N. J.; Griffin, R. J.; Golding, B. T.; Durkacz, B. W. Potentiation of temozolomide-induced cytotoxicity: a comparative study of the biological effects of poly(ADP-ribose) polymerase inhibitors. *Br. J. Cancer* **1995,** *72,* 849-856.

55. Tentori, L.; Portarena, I.; Graziani, G. Potential clinical applications of poly(ADP-ribose) polymerase (PARP) inhibitors. *Pharmacol. Res*. **2002,** *45*, 73-85.

56. Calabrese, C. R.; Almassy, R.; Barton, S.; Batey, M. A.; Calvert, A. H.; Canan-Koch, S.; Durkacz, B. W.; Hostomsky, Z.; Kumpf, R. A.; Kyle, S.; Li, J.; Maegley, K.; Newell, D. R.; Notarianni, E.; Stratford, I. J.; Skalitzky, D.; Thomas, H. D.; Wang, L. Z.; Webber, S. E.; Williams, K. J.; Curtin, N. J. Anticancer chemosensitization and radiosensitization by the novel poly(ADP-ribose) polymerase-1 inhibitor AG14361. *J. Natl. Cancer Inst.* **2004***, 96*, 56-67.

57. Tentori, L.; Graziani, G. Chemopotentiation by PARP inhibitors in cancer therapy. *Pharmacol. Res.* **2005***, 52*, 25.

58. Malanga, M.; Althaus, F. R. Poly(ADP-ribose) reactivates stalled DNA topoisomerase I and Induces DNA strand break resealing. *J. Biol. Chem.* **2004***, 279*, 5244-5248.

59. Nduka, N.; Skidmore, C. J.; Shall, S. The enhancement of cytotoxicity of N-methyl-N-nitrosourea and of gamma radiation by inhibitors of poly(ADP-ribose) polymerase. *Eur. J. Biochem.*, **1980**, *105*, 525-530.

60. Pacher, P.; Liaudet, L.; Bai, P.; Virág, L.; Mabley, J. G.; Haskó G.; Szabó, C. Activation of poly(ADP-ribose) polymerase contributes to development of Doxorubicin-induced heart failure. *J. Pharmacol. Exp. Ther.* **2002**, *300,* 862-867.

61. Racz, I.; Tory, K.; Gallyas, F.; Berente, Z.; Osz, E.; Jaszlits, L.; Bernath, S.; Sumegi, B.; Rabloczky G.; Literati-Nagy, P. BGP-15 - a novel poly(ADP-ribose)polymerase inhibitor-protects against nephrotoxicity of cisplatin without compromising its antitumor activity. *Biochem. Pharmacol.* **2002**, *63,* 1099-1111.

62. Weltin, D.; Holl, V.; Hyun, J. W.; Dufour, P.; Marchal J.; Bischoff, P. effect of 6(5H)-phenanthridinone, a poly(ADP-ribose) polymerase inhibitor, and ionising

radiation on the growth of cultured lymphoma cells. *Int. J. Radiat. Biol.* **1997,** *72*, 685-692.

63. Farmer, H.; McCabe, N.; Lord, C. J.; Tutt, A. N.; Johnson, D. A.; Richardson, T. B.; Santarosa, M.; Dillon, K. J.; Hickson, I.; Knights, C.; Martin, N. M.; Jackson, S. P.; Smith, G. C.; Ashworth, A. Targeting the DNA repair defect in BRCA mutant cells as a therapeutic strategy. *Nature* **2005***, 434*, 917-921.
64. Plummer, R.; Jones, C; Middleton, M.; Wilson, R.; Evans, J.; Olsen, A.; Curtin, N. J, Boddy, A.; McHugh, P.; Newell, D.; Harris, A.; Johnson, P.; Steinfeldt, H.; Dewji, R.; Wang, D.; Robson, L.; Calvert, H. Phase I Study of the Poly(ADP-Ribose) Polymerase Inhibitor, AG014699, in combination with Temozolomide in patients with advanced solid tumors. *Clin. Cancer Res.*, **2008**, 14, 7917-7923.
65. Hearse, D. J.; Bolli, R. Reperfusion induced injury: manifestations, mechanisms, and clinical relevance. *Cardiovasc. Res.* **1992***, 26*, 101-108.
66. Szabo, C. The pathophysiological role of peroxynitrite in shock, inflammation, and ischemia-reperfusion injury. *Shock* **1996***, 6*, 79-88.
67. Schraufstätter, I.; Hyslop, P. A.; Jackson, J. H.; Cochrane, C. G. Oxidant-induced DNA damage of target cells. *J. Clin. Invest.* **1988,** *82*, 1040.
68. Pieper, A. A.; Verma, A.; Zhang, J.; Snyder, S. H. Poly (ADP-ribose) polymerase, nitric oxide and cell death. *Trends Pharmacol. Sci.* **1999***, 20*, 171-181.
69. Szabo, G.; Liaudet, L.; Hagl, S.; Szabo, C. Poly(ADP-ribose) polymerase activation in the reperfused myocardium. *Cardiovasc. Res.* **2004***, 61*, 471-480.
70. Thiemermann, C.; Bowes, J.; Myint, F. P.; Vane, J. R. Inhibition of the activity of poly(ADP-ribose) synthetase reduces ischemia-reperfusion injury in the heart and skeletal muscle. *Proc. Natl. Acad.Sci. USA* **1997,** *94*, 679-683.
71. Zingarelli, B.; Cuzzocrea, S.; Zsengeller, Z.; Salzman, A. L.; Szabo, C. Protection against myocardial ischemia and reperfusion injury by 3-aminobenzamide, an inhibitor of poly (ADP-ribose) synthetase. *Cardiovasc. Res.* **1997***, 36*, 205-215.
72. Liaudet, L.; Szabo, E.; Timashpolsky, L.; Virag, L.; Cziraki, A.; Szabo, C. Suppression of poly (ADP-ribose) polymerase activation by 3-aminobenzamide in a rat model of myocardial infarction: long-term morphological and functional consequences. *Br. J. Pharmacol.* **2001***, 133*, 1424-1430.
73. Wayman, N.; McDonald, M. C.; Thompson, A. S.; Threadgill, M. D.; Thiemermann, C. 5-aminoisoquinolinone, a potent inhibitor of poly (adenosine 5'-diphosphate ribose) polymerase, reduces myocardial infarct size. *Eur. J. Pharmacol.* **2001***, 430*, 93-100.

74. Skaper, S. D. Poly(ADP-Ribose) polymerase-1 in acute neuronal death and inflammation: a strategy for neuroprotection. *Ann. N. Y. Acad. Sci.* **2003***, 993*, 217-228; discussion 287-218.

75. Eliasson, M. J.; Sampei, K.; Mandir, A. S.; Hurn, P. D.; Traystman, R. J.; Bao, J.; Pieper, A.; Wang, Z. Q.; Dawson, T. M.; Snyder, S. H.; Dawson, V. L. Poly(ADP-ribose) polymerase gene disruption renders mice resistant to cerebral ischemia. *Nat. Med.* **1997***, 3*, 1089-1095.

76. Abdelkarim, G. E.; Gertz, K.; Harms, C.; Katchanov, J.; Dirnagl, U.; Szabo, C.; Endres, M. Protective effects of PJ34, a novel, potent inhibitor of poly(ADP-ribose) polymerase (PARP) in *in vitro* and *in vivo* models of stroke. *Int. J. Mol. Med.* **2001***, 7*, 255-260.

77. Takahashi, K.; Greenberg, J. H.; Jackson, P.; Maclin, K.; Zhang, J. Neuroprotective effects of inhibiting poly(ADP-ribose) synthetase on focal cerebral ischemia in rats. *J. Cereb. Blood Flow Metab.* **1997***, 17*, 1137-1142.

78. Cuzzocrea, S.; Zingarelli, B.; Costantino,G.; Szabó, A.; Salzman, A.; Caputi, A. P.; Szabó, C. Beneficial effects of 3-aminobenzamide, an inhibitor of poly(ADP-ribose) synthetase in a rat model of splanchnic artery occlusion and reperfusion. *Br. J. Pharmacol.* **1997**, *121*, 1065-1074.

79. Mazzon, E.; Dugo, L.; De, S. A.; Li, J. H.; Caputi, A. P.; Zhang, J.; Cuzzocrea, S. Beneficial effects of GPI 6150, an inhibitor of poly(ADP-ribose) polymerase in a rat model of splanchnic artery occlusion and reperfusion. *Shock* **2002***, 17*, 222-227.

80. Mota-Filipe, H.; Sepodes, B.; McDonald, M.; Cuzzocrea, S.; Pinto, R.; Thiemermann, C. The novel PARP inhibitor 5-aminoisoquinolinone reduces the liver injury caused by ischaemia and reperfusion in the rat. *Med. Sci. Monit*. **2002,** *8*, 444-453.

81. Khandoga, A.; Biberthaler, P.; Enders, G.; Krombach, F. 5-Aminoisoquinolinone, a novel inhibitor of poly(adenosine disphosphate-ribose) polymerase, reduces microvascular liver injury but not mortality rate after hepatic ischemia-reperfusion. *Crit. Care Med.* **2004***, 32*, 472-477.

82. Chatterjee, P. K.; Chatterjee, B. E.; Pedersen, H.; Sivarajah, A.; McDonald, M. C.; Mota-Filipe, H.; Brown, P. A. J.; Stewart, K. N.; Cuzzocrea, S.; Threadgill, M. D.; Thiemermann, C. 5-Aminoisoquinolinone reduces renal injury and dysfunction caused by experimental ischemia/reperfusion. *Kidney Int*. **2004**, *65*, 499-509.

83. Chiang, S. K. S.; Lam, T. T. Post-Treatment at 12 or 18 hours with 3-aminobenzamide ameliorates retinal ischemia–reperfusion damage. *Invest. Ophthal. Vis. Sci.* **2000***, 41*, 3210-3214.

84. Szabo, G.; Bahrle, S.; Stumpf, N.; Sonnenberg, K.; Szabo, E. E.; Pacher, P.; Csont, T.; Schulz, R.; Dengler, T. J.; Liaudet, L.; Jagtap, P. G.; Southan, G. J.; Vahl, C. F.; Hagl, S.; Szabo, C. Poly(ADP-Ribose) polymerase inhibition reduces reperfusion injury after heart transplantation. *Circ. Res.* **2002***, 90*, 100-106.

85. Liaudet, L.; Soriano, F. G.; Szabo, E.; Virag, L.; Mabley, J. G.; Salzman, A. L.; Szabo, C. Protection against hemorrhagic shock in mice genetically deficient in poly(ADP-ribose)polymerase. *Proc. Natl. Acad. Sci. USA* **2000***, 97*, 10203-10208.

86. McDonald, M. C.; Mota-Filipe, H.; Wright, J. A.; Abdelrahman, M.; Threadgill, M. D.; Thompson, A. S.; Thiemermann, C Effects of 5-aminoisoquinolinone, a water soluble, potent inhibitor of the activity of poly(ADP-ribose) polymerase on the organ injury and dysfunction caused by haemorrhagic shock. *Brit. J. Pharmacol*. **2000,** *130*, 843-850.

87. Thiemermann, C. Development of novel, water-soluble inhibitors of poly (adenosine 5'-diphosphate ribose) synthetase activity for use in shock and ischemia-reperfusion injury. *Crit. Care Med.* **2002***, 30*, 1163-1165.

88. Yamamoto, H.; Okamoto, H. Protection by picolinamide, a novel inhibitor of poly(ADP-ribose) synthetase, against both streptozotocin-induced depression of proinsulin synthesis and reduction of NAD content in pancreatic islets. *Biochem. Biophys. Res.* Commun. **1980,** *95,* 474-481.

89. Uchigata, Y.; Yamamoto, H.; Kawamura, A.; Okamoto, H. Protection by superoxide dismutase, catalase, and poly(ADP-ribose) synthetase inhibitors against alloxan- and streptozotocin-induced islet DNA strand breaks and against the inhibition of proinsulin synthesis. *J. Biol. Chem.* **1982***, 257*, 6084-6088.

90. Miesel, R.; Kurpisz, M.; Kroger, H. Modulation of inflammatory arthritis by inhibition of poly(ADP ribose) polymerase. *Inflammation* **1995***, 19*, 379-387.

91. Jijon, H. B.; Churchill, T.; Malfair, D.; Wessler, A.; Jewell, L. D.; Parsons, H. G.; Madsen, K. L. Inhibition of poly(ADP-ribose) polymerase attenuates inflammation in a model of chronic colitis. *Am. J. Physiol. Gastrointest. Liver Physiol.* **2000***, 279*, G641-651.

92. Cuzzocrea, S.; Mazzon, E.; Paola, R. D.; Genovese, T.; Patel, N. S.; Threadgill, M. D.; Bramanti, P.; De Sarro, A.; Thiemermann, C. 5-Aminoisoquinolinone

reduces colon injury by experimental colitis. *Naunyn Schmiedebergs Arch. Pharmacol*. **2004,** *370*, 464-473.

93. Boulares, A. H.; Zoltoski, A. J.; Sherif, Z. A.; Jolly, P.; Massaro, D.; Smulson, M. E. Gene knockout or pharmacological inhibition of poly(ADP-ribose) polymerase-1 prevents lung inflammation in a murine model of asthma. *Am. J. Respir. Cell Mol. Biol.* **2003***, 28*, 322-329.
94. Liaudet, L.; Pacher, P.; Mabley, J. G.; Virag, L.; Soriano, F. G.; Hasko, G.; Szabo, C. Activation of poly(ADP-Ribose) polymerase-1 is a central mechanism of lipopolysaccharide-induced acute lung inflammation. *Am. J. Respir. Crit. Care Med.* **2002***, 165*, 372-377.
95. Cuzzocrea, S.; McDonald, M. C.; Mazzon, E.; Dugo, L.; Serraino, I.; Threadgill, M. D.; Caputi, A. P.; Thiemermann, C. Effects of 5-aminoisoquinolinone, a water soluble, potent inhibitor of the activity of poly(ADP-ribose) polymerase, in a rodent model of lung injury. *Biochem. Pharmacol*. **2002**, *63,* 293-304.
96. Soriano, F. G.; Virag, L.; Jagtap, P.; Szabo, E.; Mabley, J. G.; Liaudet, L.; Marton, A.; Hoyt, D. G.; Murthy, K. G.; Salzman, A. L.; Southan, G. J.; Szabo, C. Diabetic endothelial dysfunction: the role of poly(ADP-ribose) polymerase activation. *Nat. Med.* **2001***, 7*, 108-113.
97. Szabo, C.; Pacher, P.; Zsengeller, Z.; Vaslin, A.; Komjati, K.; Benko, R.; Chen, M.; Mabley, J. G.; Kollai, M. Angiotensin II-mediated endothelial dysfunction: role of poly(ADP-ribose) polymerase activation. *Mol. Med.* **2004***, 10*, 28-35.
98. Pacher, P.; Mabley, J. G.; Soriano, F. G.; Liaudet, L.; Szabo, C. Activation of poly(ADP-ribose) polymerase contributes to the endothelial dysfunction associated with hypertension and aging. *Int. J. Mol. Med.* **2002***, 9*, 659-664.
99. Obrosova, I. G.; Li, F.; Abatan, O. I.; Forsell, M. A.; Komjati, K.; Pacher, P.; Szabo, C.; Stevens, M. J. Role of poly(ADP-ribose) polymerase activation in diabetic neuropathy. *Diabetes* **2004***, 53*, 711-720.
100. Zheng, L.; Szabo, C.; Kern, T. S. Poly(ADP-ribose) polymerase is involved in the development of diabetic retinopathy via regulation of nuclear factor-kappaB. *Diabetes* **2004***, 53*, 2960-2967.
101. Gäken. J. A.; Tavassoli, M.; Gan, S-U.; Vallian, S.; Giddings, I.; Darling, D. C.; Galea-Lauri, J.; Thomas, M. G.; Abedi, H.; Schreiber, V.; Ménissier-de Murcia, J.; Collins, M. K. L.; Shall, S.; Farzaneh, F. Efficient retroviral infection of mammalian cells is blocked by inhibition of poly(ADP-ribose) activity. *J. Virol.* **1996**, 70, 3992-4000.
102. Cole, G. A.; Bauer, G.; Kirsten, E.; Mendeleyev, J.; Bauer, P. I.; Buki, K. G.; Hakam, A.; Kun, E. Inhibition of HIV-1 IIIb replication in AA-2 and MT-2 cells in

culture by two ligands of poly (ADP-ribose) polymerase: 6-amino-1,2-benzopyrone and 5-iodo-6-amino-1,2-benzopyrone. *Biochem. Biophys. Res. Commun.*, **1991,** *180,* 504-514.

103. Cosi, C.; Colpaert, F.; Koek, W.; Degryse, A.; Marien, M. Poly(ADP-ribose) polymerase inhibitors protect against MPTP-induced depletions of striatal dopamine and cortical noradrenaline in C57B1/6 mice. *Brain Res.* **1996***, 729*, 264-269.
104. Love, S.; Barber, R.; Wilcock, G. K. Increased poly(ADP-ribosyl)ation of nuclear proteins in Alzheimer's disease. *Brain* **1999***, 122*, 247-253.
105. Kroger, H.; Dietrich, A.; Ohde, M.; Lange, R.; Ehrlich, W.; Kurpisz, M. Protection from acetaminophen-induced liver damage by the synergistic action of low doses of the poly(ADP-ribose) polymerase-inhibitor nicotinamide and the antioxidant N-acetylcysteine or the amino acid L-methionine. *Gen. Pharmacol.* **1997***, 28*, 257-263.
106. Farkas, B.; Magyarlaki, M.; Csete, B.; Nemeth, J.; Rabloczky, G.; Bernath, S.; Literati Nagy, P.; Sumegi, B. Reduction of acute photodamage in skin by topical application of a novel PARP inhibitor. *Biochem. Pharmacol.* **2002***, 63*, 921-932.
107. Suzuki, Y.; Masini, E.; Mazzocca, C.; Cuzzocrea, S.; Ciampa, A.; Suzuki, H.; Bani, D. Inhibition of poly(ADP-ribose) polymerase prevents allergen-induced asthma-like reaction in sensitized Guinea pigs. *J. Pharmacol. Exp. Ther.* **2004***, 311*, 1241-1248.
108. Scott, G. S.; Kean, R. B.; Mikheeva, T.; Fabis, M. J.; Mabley, J. G.; Szabo, C.; Hooper, D. C. The therapeutic effects of PJ34 [N-(6-oxo-5,6-dihydrophenanthridin-2-yl)-N,N-dimethylacetamide.HCl], a selective inhibitor of poly(ADP-ribose) polymerase, in experimental allergic encephalomyelitis are associated with immunomodulation. *J. Pharmacol. Exp. Ther.* **2004***, 310*, 1053-1061.
109. Drazen, D. L.; Bilu, D.; Edwards, N.; Nelson, R. J. Disruption of poly (ADP-ribose) polymerase (PARP) protects against stress-evoked immunocompromise. *Mol. Med.* **2001***, 7*, 761-766.
110. Clark, J. B.; Ferris, G. M.; Pinder, S. Inhibition of nuclear NAD nucleosidase and poly ADP-ribose polymerase activity from rat liver by nicotinamide and 5'-methyl nicotinamide. *Biochim. Biophys. Acta.* **1971***, 238*, 82-85.
111. Shall, S. Experimental manipulation of the specific activity of poly(ADP-ribose) polymerase. *Biochem. (Tokyo),* **1975,** *77*, 2.
112. Purnell, M.R.; Whish, W. J. D. Novel inhibitors of poly(ADP-ribose) synthetase. *Biochem. J*. **1980,** *185*, 775-777.

113. Sims, J. L.; Sikorski, G. W.; Catino, D. M.; Berger, S. J.; Berger, N. A. Poly(adenosinediphosphoribose) polymerase inhibitors stimulate unscheduled deoxyribonucleic acid synthesis in normal human lymphocytes. *Biochemistry* **1982***, 21*, 1813-1821.

114. Sestili, P.; Balsamini, C.; Spadoni, G.; Cattabeni, F.; Cantoni, O. Analogues of benzamide as poly(ADP-ribose)transferase inhibitors: a study on structure activity relationships. *Pharmacol. Res. Commun.* **1988***, 20*, 613-614.

115. Sestili, P.; Spadoni, G.; Balsamini, C.; Scovassi, I.; Cattabeni, F.; Duranti, E.; Cantoni, O.; Higgins, D.; Thomson, C. Structural requirements for inhibitors of poly(ADP-ribose) polymerase. *J. Cancer Res. Clin. Oncol.* **1990***, 116*, 615-622.

116. Shinkin, A. E.; Whish, W. J. D.; Threadgill, M. D.; Synthesis of thiophene carboxamides, thieno[3,4-c]pyrimidin-4(*3H*)-ones and preliminary evaluation as inhibitors of poly(ADP-ribose) polymerase (PARP). *Bioorg. Med. Chem*. **1999**, *7*, 297-308.

117. Banasik, M.; Komura, M.; Shimoyama, M.; Ueda, K. Specific inhibitors of poly(ADP-ribose) synthetase and mono(ADP-ribosyl) transferase. *J. Biol. Chem.* **1992**, *267*, 1569-1575.

118. Suto, M. J.; Turner, W. R.; Arundel-Suto, C. M.; Werbel, L. M.; Sebolt-Leopold, J. S. Dihydroisoquinolinones: the design and synthesis of a new series of potent inhibitors of poly(ADP-ribose) polymerase. *AntiCancer Drug Des.* **1991**, *7,* 107-117.

119. Griffin, R.J.; Pemberton, L. C.; Rhodes, D.; Bleasdale, C.; Bowman, K.; Calvert, A. H.; Curtin, N. J.; Durkacz, B. W.; Newell, D. R.; Porteous, J. K.; Golding, B. T. Novel potent inhibitors of the DNA repair enzyme poly(ADP-ribose)polymerase(PARP). *Anticancer Drug Des.* **1995,** *10*, 507-514.

120. Ruf, A.; de Murcia, G.; Schulz, G. E. Inhibitor and NAD^+ binding to poly(ADP-ribose)polymerase as derived from crystal structures and homology modeling. *Biochemistry* **1998***, 37*, 3893-3900.

121. Costantino, G.; Macchiarulo, A.; Camaioni, E.; Pellicciari, R. Modeling of poly(ADP-ribose)polymerase (PARP) inhibitors. Docking of ligands and quantitative structure-activity relationship analysis. *J. Med. Chem.* **2001***, 44*, 3786-3794.

122. Kinoshita, T.; Nakanishi, I.; Warizaya, M.; Iwashita, A.; Kido, Y.; Hattori, K.; Fujii, T. Inhibitor-induced structural change of the active site of human poly(ADP-ribose) polymerase. *FEBS Lett.* **2004***, 556*, 43-46.

123. Hattori, K.; Kido, Y.; Yamamoto, H.; Ishida, J.; Kamijo, K.; Murano, K.; Ohkubo, M.; Kinoshita, T.; Iwashita, A.; Mihara, K.; Yamazaki, S.; Matsuoka, N.;

Teramura, Y.; Miyake, H. Rational approaches to discovery of orally active and brain-penetrable quinazolinone inhibitors of poly(ADP-ribose)polymerase. *J. Med. Chem.* **2004***, 47*, 4151-4154.

124. Zhang, J.; Dawson, V. L.; Dawson, T. M.; Snyder, S. H. Nitric oxide activation of poly(ADP-ribose)synthetase in neurotoxicity. *Science* **1994***, 263*, 687-689.
125. Arundel-Suto, C. M.; Scavone, S. V.; Turner, W. R.; Suto, M. J.; Sebolt-Leopold, J. S. Effect of PD 128763, a new potent inhibitor of poly(ADP-ribose) polymerase, on X-ray-induced cellular recovery processes in Chinese hamster V79 cells. *Radiat. Res.* **1991***, 126*, 367-371.
126. Mazzon, E.; Serraino, I.; Li, J. H.; Dugo, L.; Caputi, A. P.; Zhang, J.; Cuzzocrea, S. GPI 6150, a poly (ADP-ribose) polymerase inhibitor, exhibits an anti-inflammatory effect in rat models of inflammation. *Eur. J. Pharmacol.* **2001***, 415*, 85-94.
127. Li, J. H.; Serdyuk, L.; Ferraris, D. V.; Xiao, G.; Tays, K. L.; Kletzly, P. W.; Li, W.; Lautar, S.; Zhang, J.; Kalish, V. J. Synthesis of substituted 5[H]phenanthridin-6-ones as potent poly(ADP-ribose)polymerase-1 (PARP1) inhibitors. *Bioorg. Med. Chem. Lett.* **2001***, 11*, 1687-1690.
128. Jagtap, P.; Soriano, F. G.; Virag, L.; Liaudet, L.; Mabley, J.; Szabo, E.; Hasko, G.; Marton, A.; Lorigados, C. B.; Gallyas, F., Jr.; Sumegi, B.; Hoyt, D. G.; Baloglu, E.; VanDuzer, J.; Salzman, A. L.; Southan, G. J.; Szabo, C. Novel phenanthridinone inhibitors of poly (adenosine 5'-diphosphate-ribose) synthetase: potent cytoprotective and antishock agents. *Crit. Care Med.* **2002***, 30*, 1071-1082.
129. Ferraris, D.; Ficco, R. P.; Pahutski, T.; Lautar, S.; Huang, S.; Zhang, J.; Kalish, V. Design and synthesis of poly(ADP-ribose)polymerase-1 (PARP-1) inhibitors. Part 3: In vitro evaluation of 1,3,4,5-tetrahydro-benzo[c][1,6]- and [c][1,7]-naphthyridin-6-ones. *Bioorg. Med. Chem. Lett.* **2003***, 13*, 2513-2518.
130. Ferraris, D.; Ko, Y. S.; Pahutski, T.; Ficco, R. P.; Serdyuk, L.; Alemu, C.; Bradford, C.; Chiou, T.; Hoover, R.; Huang, S.; Lautar, S.; Liang, S.; Lin, Q.; Lu, M. X.; Mooney, M.; Morgan, L.; Qian, Y.; Tran, S.; Williams, L. R.; Wu, Q. Y.; Zhang, J.; Zou, Y.; Kalish, V. Design and synthesis of poly ADP-ribose polymerase-1 inhibitors. 2. Biological evaluation of aza-5[H]-phenanthridin-6-ones as potent, aqueous-soluble compounds for the treatment of ischemic injuries. *J. Med. Chem.* **2003***, 46*, 3138-3151.
131. Pellicciari, R.; Camaioni, E.; Costantino, G.; Marinozzi, M.; Macchiarulo, A.; Moroni, F.; Natalini, B. Towards new neuroprotective agents: design and

synthesis of 4H-thieno[2,3-c] isoquinolin-5-one derivatives as potent PARP-1 inhibitors. *Farmaco* **2003***, 58*, 851-858.

132. Chiarugi, A.; Meli, E.; Calvani, M.; Picca, R.; Baronti, R.; Camaioni, E.; Costantino, G.; Marinozzi, M.; Pellegrini-Giampietro, D. E.; Pellicciari, R.; Moroni, F. Novel isoquinolinone-derived inhibitors of poly(ADP-ribose) polymerase-1: pharmacological characterization and neuroprotective effects in an in vitro model of cerebral ischemia. *J. Pharmacol. Exp. Ther.* **2003***, 305*, 943-949.
133. White A. W.; Almassy, R.; Calvert, A. H.; Curtin, N. J.; Griffin, R. J.; Hostomsky, Z.; Maegley, K.; Newell, D. R.; Srinivasan, S.; Golding, B. T. Resistance-modifying agents. Synthesis and biological properties of benzimidazole inhibitors of the DNA repair enzyme poly(ADP-ribose) polymerase. *J. Med. Chem*., **2000**, *43,* 4084-4097.
134. Skalitzky, D. J.; Marakovits, J. T.; Maegley, K. A.; Ekker, A.; Yu, X. H.; Hostomsky, Z.; Webber, S. E.; Eastman, B. W.; Almassy, R.; Li, J.; Curtin, N. J.; Newell, D. R.; Calvert, A. H.; Griffin, R. J.; Golding, B. T. Tricyclic benzimidazoles as potent poly(ADP-ribose) polymerase-1 inhibitors. *J. Med. Chem.* **2003***, 46*, 210-213.
135. Canan Koch, S. S.; Thoresen, L. H.; Tikhe, J. G.; Maegley, K. A.; Almassy, R. J.; Li, J.; Yu, X. H.; Zook, S. E.; Kumpf, R. A.; Zhang, C.; Boritzki, T. J.; Mansour, R. N.; Zhang, K. E.; Ekker, A.; Calabrese, C. R.; Curtin, N. J.; Kyle, S.; Thomas, H. D.; Wang, L. Z.; Calvert, A. H.; Golding, B. T.; Griffin, R. J.; Newell, D. R.; Webber, S. E.; Hostomsky, Z. Novel tricyclic poly(ADP-ribose) polymerase-1 inhibitors with potent anticancer chemopotentiating activity: design, synthesis, and X-ray cocrystal structure. *J. Med. Chem.* **2002***, 45*, 4961-4974.
136. Griffin, R. J.; Srinivasan, S.; Bowman, K.; Calvert, A. H.; Curtin, N. J.; Newell, D. R.; Pemberton, L. C.; Golding, B. T. Resistance-modifying agents. 5. Synthesis and biological properties of quinazolinone inhibitors of the DNA repair enzyme poly(ADP-ribose) polymerase (PARP). *J. Med. Chem.* **1998***, 41*, 5247-5256.
137. Hattori, K.; Kido, Y.; Yamamoto, H.; Ishida, J.; Kamijo, K.; Murano, K.; Ohkubo, M.; Kinoshita, T.; Iwashita, A.; Mihara, K.; Yamazaki, S.; Matsuoka, N.; Teramura, Y.; Miyake, H. Rational approaches to discovery of orally active and brain-penetrable quinazolinone inhibitors of poly(ADP-ribose)polymerase. *J. Med. Chem.* **2004***, 47*, 4151-4154.

138. Iwashita, A.; Hattori, K.; Yamamoto, H.; Ishida, J.; Kido, Y.; Kamijo, K.; Murano, K.; Miyake, H.; Kinoshita, T.; Warizaya, M.; Ohkubo, M.; Matsuoka, N.; Mutoh, S. Discovery of quinazolinone and quinoxaline derivatives as potent and selective poly(ADP-ribose) polymerase-1/2 inhibitors. *FEBS Lett.* **2005***, 579*, 1389-1393.

139. Iwashita, A.; Tojo, N.; Matsuura, S.; Yamazaki, S.; Kamijo, K.; Ishida, J.; Yamamoto, H.; Hattori, K.; Matsuoka, N.; Mutoh, S. A novel and potent poly(ADP-ribose) polymerase-1 inhibitor, FR247304 (5-chloro-2-[3-(4-phenyl-3,6-dihydro-1(2H)-pyridinyl)propyl]-4(3H)-quinazolinone), attenuates neuronal damage in in vitro and in vivo models of cerebral ischemia. *J. Pharmacol. Exp. Ther.* **2004***, 310*, 425-436.

140. Iwashita, A.; Mihara, K.; Yamazaki, S.; Matsuura, S.; Ishida, J.; Yamamoto, H.; Hattori, K.; Matsuoka, N.; Mutoh, S. A new poly(ADP-ribose)polymerase inhibitor, FR261529 [2-(4-chlorophenyl)-5-quinoxalinecarboxamide], ameliorates methamphetamine-induced dopaminergic neurotoxicity in mice. *J. Pharmacol. Exp. Ther*. **2004,** *310*, 1114-1124.

141. Nakajima, H.; Kakui, N.; Ohkuma, K.; Ishikawa, M.; Hasegawa, T. A newly synthesized poly(ADP-ribose) polymerase inhibitor, DR2313 [2-methyl-3,5,7,8-tetrahydrothiopyrano[4,3-d]-pyrimidine-4-one]: pharmacological profiles, neuroprotective effects, and therapeutic time window in cerebral ischemia in rats. *J. Pharmacol. Exp. Ther.* **2005***, 312*, 472-481.

142. Southan, G. J.; Szabó, C. Poly(ADP-ribose) polymerase inhibitors. *Curr. Med. Chem.* **2003**, *10*, 321-340.

143. Loh, V. M., Jr.; Cockcroft, X. L.; Dillon, K. J.; Dixon, L.; Drzewiecki, J.; Eversley, P. J.; Gomez, S.; Hoare, J.; Kerrigan, F.; Matthews, I. T.; Menear, K. A.; Martin, N. M.; Newton, R. F.; Paul, J.; Smith, G. C.; Vile, J.; Whittle, A. J. Phthalazinones. Part 1: The design and synthesis of a novel series of potent inhibitors of poly(ADP-ribose)polymerase. *Bioorg. Med. Chem. Lett.* **2005***, 15*, 2235-2238.

144. Cockcroft, X. L.; Dillon, K. J.; Dixon, L.; Drzewiecki, J.; Kerrigan, F.; Loh, V. M., Jr.; Martin, N. M.; Menear, K. A.; Smith, G. C. Phthalazinones 2: Optimisation and synthesis of novel potent inhibitors of poly(ADP-ribose)polymerase. *Bioorg. Med. Chem. Lett.* **2006***, 16*, 1040-1044.

145. Kamanaka, Y.; Kondo, K.; Ikeda, Y.; Kamoshima, W.; Kitajima, T.; Suzuki, Y.; Nakamura, Y.; Umemura, K. Neuroprotective effects of ONO-1924H, an inhibitor of poly ADP-ribose polymerase (PARP), on cytotoxicity of PC12 cells and ischemic cerebral damage. *Life. Sci.* **2004***, 76*, 151-162.

146. Tao, M.; Park, C. H.; Bihovsky, R.; Wells, G. J.; Husten, J.; Ator, M. A.; Hudkins, R. L. Synthesis and structure-activity relationships of novel poly(ADP-ribose) polymerase-1 inhibitors. *Bioorg. Med. Chem. Lett.* **2006***, 16*, 938-942.

147. Wells, G. J.; Bihovsky, R.; Hudkins, R. L.; Ator, M. A.; Husten, J. Synthesis and structure-activity relationships of novel pyrrolocarbazole lactam analogs as potent and cell-permeable inhibitors of poly(ADP-ribose)polymerase-1 (PARP-1). *Bioorg. Med. Chem. Lett.* **2006***, 16*, 1151-1155.

148. Miknyoczki, S. J.; Jones-Bolin, S.; Pritchard, S.; Hunter, K.; Zhao, H.; Wan, W.; Ator, M.; Bihovsky, R.; Hudkins, R.; Chatterjee, S.; Klein-Szanto, A.; Dionne, C.; Ruggeri, B. Chemopotentiation of temozolomide, irinotecan, and cisplatin activity by CEP-6800, a poly(ADP-ribose) polymerase inhibitor. *Mol. Cancer Ther.* **2003***, 2*, 371-382.

149. Buki, K. G.; Bauer, P. I.; Mendeleyev, J.; Hakam, A.; Kun, E. Destabilization of Zn2+ coordination in ADP-ribose transferase (polymerizing) by 6-nitroso-1,2-benzopyrone coincidental with inactivation of the polymerase but not the DNA binding function. *FEBS Lett.* **1991***, 290*, 181-185.

150. Parveen, I.; Naughton, D. P.; Whish, W. J.; Threadgill, M. D. 2-nitroimidazol-5-ylmethyl as a potential bioreductively activated prodrug system: reductively triggered release of the PARP inhibitor 5-bromoisoquinolinone. *Bioorg. Med. Chem. Lett.* **1999***, 9*, 2031-2036.

151. Ferrer, S.; Naughton, D. P.; Threadgill, M. D. Studies on the reductively triggered release of heterocyclic and steroid drugs from 5-nitrothien-2-ylmethyl prodrugs. *Tetrahedron* **2003***, 59*, 3437-3444.

152. Ferrer, S.; Naughton, D. P.; Threadgill, M. D. ^{1}H NMR studies on the reductively triggered release of heterocyclic and steroid drugs from 4,7-dioxoindole-3-methyl prodrugs. *Tetrahedron* **2003***, 59*, 3445-3454.

153. Denny, W. A. Prodrug strategies in cancer therapy. *Eur. J. Med. Chem.* **2001***, 36*, 577-595.

154. Watson, C. Y.; Whish, W. J. D.; Threadgill, M. D. Synthesis of 3-substituted benzamides and 5-substituted isoquinolin-1(*2H*)-ones and preliminary evaluation as inhibitors of poly(ADP-ribose)polymerase (PARP). *Bioorg. Med. Chem.* **1998**, *6*, 721-734.

155. Ferrer, S.; Naughton, D. P.; Parveen, I.; Threadgill, M. D. N- and O-Alkylation of isoquinolin-1-ones in the Mitsunobu reaction: development of potential drug delivery systems. *J. Chem. Soc. Perkin Trans. 1* **2002**, 335-340.

156. Bauer, P. I.; Mendeleyeva, J.; Kirsten, E.; Comstock, J. A.; Hakam, A.; Buki, K. G.; Kun, E. Anti-cancer action of 4-iodo-3-nitrobenzamide in combination with

buthionine sulfoximine: inactivation of poly(ADP-ribose) polymerase and tumor glycolysis and the appearance of a poly(ADP-ribose) polymerase protease. *Biochem. Pharmacol.* **2002***, 63*, 455-462.

157. Sheridan, C. Genentech raises stakes on PARP inhibitors. *Nat. Biotechnol.* **2006***, 24*, 1179-1180.
158. Ashwood-Smith, M. J. Radioprotective and cryoprotective properties of dimethyl sulfoxide in cellular systems. *Ann. N Y Acad. Sci.* **1967***, 141*, 45-62.
159. Banasik, M.; Stedeford, T.; Strosznajder, R. P.; Persad, A. S.; Tanaka, S.; Ueda, K. The effects of organic solvents on poly(ADP-ribose) polymerase-1 activity: implications for neurotoxicity. *Acta Neurobiol. Exp. (Wars)* **2004***, 64*, 467-473.
160. Woon, E. C. Y. PhD thesis, University of Bath, **2004.**
161. Stephens, R. D.; Castro, C. E. The substitution of aryl iodides with cuprous acetylides. A synthesis of tolanes and heterocyclics. *J. Org. Chem.* **1963***, 28*, 3313-3315.
162. Cassar, L. Synthesis of aryl-substituted and vinyl-substituted acetylene derivatives by use of nickel and palladium complexes. *J. Organomet. Chem.* **1975***, 93*, 253-257.
163. Dieck, H. A.; Heck, F. R. Palladium catalyzed synthesis of aryl, heterocyclic and vinylic acetylene derivatives. *J. Organomet. Chem.* **1975***, 93*, 259-263.
164. Sonogashira, K.; Tohda, Y.; Hagihara, N. Convenient synthesis of acetylenes - catalytic substitutions of acetylenic hydrogen with bromoalkenes, iodoarenes, and bromopyridines. *Tetrahedron Lett.* **1975**, 4467-4470.
165. Takahashi, S.; Kuroyama, Y.; Sonogashira, K.; Hagihara, N. A Convenient synthesis of ethynylarenes and diethynylarenes. *Synthesis* **1980**, 627-630.
166. Tsuji, J. Palladium reagents and catalysts, eds. F. Diederich and P. J. Stang, Wiley-VCH, Weinheim, 2004. **ISBN:** 9780470850329.
167. Culhane, P. J. *Organic Syntheses* **1967**, Coll. Vol. 1, 125.
168. Johnson, W. S.; Yarnell, T. M.; Myers, R. F.; Morton, D. R.; Boots, S. G. Biomimetic polyene cyclizations - participation of the (trimethylsilyl)acetylenic group and the total synthesis of the d-homosteroid system. *J. Org. Chem.* **1980***, 45*, 1254-1259.
169. Jackson, W. P.; Ley, S. V. Synthesis of substituted cis-decalins as potential insect antifeedants. *J. Chem. Soc.-Perkin Transactions 1* **1981**, 1516-1519.
170. Orsini, A.; Viterisi, A.; Bodlenner, A.; Weibel, J. M.; Pale, P. A chemoselective deprotection of trimethylsilyl acetylenes catalyzed by silver salts. *Tetrahedron Lett.* **2005***, 46*, 2259-2262.

171. Viterisi, A.; Orsini, A.; Weibel, J. M.; Pale, P. A mild access to silver acetylides from trimethylsilyl acetylenes. *Tetrahedron Lett.* **2006***, 47*, 2779-2781.

172. Baldwin, J. E. Rules for ring-closure. *J. Chem. Soc.-Chem. Commn.* **1976**, 734-736.

173. Nagarajan, A.; Balasubramanian, T. R. Organomercury mediated synthesis of isocoumarins. *Indian J. Chem., Sect. B* **1987***, 26*, 917-919.

174. Larock, R. C.; Harrison, L. W. Mercury in organic-chemistry.26. Synthesis of heterocycles *via* intramolecular solvomercuration of aryl acetylenes. *J. Am. Chem. Soc.* **1984***, 106*, 4218-4227.

175. Yao, T. L.; Larock, R. C. Synthesis of isocoumarins and alpha-pyrones via electrophilic cyclization. *J. Org. Chem.* **2003***, 68*, 5936-5942.

176. Oliver, M. A.; Gandour, R. D. The identity of 4-bromo-3-phenylisocoumarin - a facile preparation by bromolactonization of alkyl 2-(2-phenylethynyl)benzoates. *J. Org. Chem.* **1984***, 49*, 558-559.

177. Biagetti, M.; Bellina, F.; Carpita, A.; Stabile, P.; Rossi, R. New procedures for the selective synthesis of 2(*2H*)-pyranone derivatives and 3-aryl-4-iodoisocoumarins. *Tetrahedron* **2002***, 58*, 5023-5038.

178. Rossi, R.; Carpita, A.; Bellina, F.; Stabile, P.; Mannina, L. Synthesis of 3-arylisocoumarins, including thunberginols a and b, unsymmetrical 3,4-disubstituted isocoumarins, and 3-ylidenephthalides via iodolactonization of methyl 2-ynylbenzoates or the corresponding carboxylic acids. *Tetrahedron* **2003***, 59*, 2067-2081.

179. Hesse, S.; Kirsch, G. Synthesis of new furocoumarin analogues via cross-coupling reaction of triflate. *Tetrahedron Lett.* **2003***, 44*, 97-99.

180. Ogawa, Y.; Maruno, M.; Wakamatsu, T. Silver catalyzed cyclization of alkynoic acids efficient synthesis of 3-alkylidenephthalides, gamma-alkylidene butenolides, and gamma-alkylidenebutyrolactones. *Heterocycles* **1995***, 41*, 2587-2599.

181. Bellina, F.; Ciucci, D.; Vergamini, P.; Rossi, R. Regioselective synthesis of natural and unnatural (z)-3-(1-alkylidene)phthalides and 3-substituted isocoumarins starting from methyl 2-hydroxybenzoates. *Tetrahedron* **2000***, 56*, 2533-2545.

182. Cherry, K.; Parrain, J. L.; Thibonnet, J.; Duchene, A.; Abarbri, M. Synthesis of isocoumarins and alpha-pyrones via tandem stille reaction/heterocyclization. *J. Org. Chem.* **2005**, *70*, 6669-6675.

183. Castro, C. E.; Gaughan, E. J.; Owsley, D. C. Indoles, benzofurans, phthalides, and tolanes *via* copper(I) acetylides. *J. Org. Chem*. **1966**, *31*, 4071-4078.

184. Jones, P. R.; Desio, P. J. Ring-chain tautomerism in *o*-acylbenzoic acids. A comparison of experimental methods and a study of substituent effects *J. Org. Chem*. **1965,** *30*, 4293-4298.

185. Watanabe, K.; Kuroda, S.; Yokoi, A.; Ito, K.; Itsuno, S. Enantioselective synthesis of optically active homoallylamines by allylboration of n-diisobutylaluminum imines. *J. Organomet. Chem.* **1999***, 581*, 103-107.

186. Wiklund, P.; Bergman, J. Ring forming reactions of imines of 2-aminobenzaldehyde and related compounds. *Org. Biomol. Chem.* **2003***, 1*, 367-372.

187. Woon, E. C. Y.; Dhami, A.; Sunderland, P. T.; Chalkley, D. A.; Threadgill, M. D. Reductive cyclisation of 2-cyanomethyl-3-nitrobenzoates. *Lett. Org. Chem.* **2006***, 3*, 619-621.

188. Wong, S. M.; Shah, B.; Shah, P.; Butt, I. C.; Woon, E. C. Y.; Wright, J. A.; Thompson, A. S.; Upton, C.; Threadgill, M. D. A new synthesis of 'push-pull' naphthalenes by condensation of nitro-2-methylbenzoate esters with dimethylacetamide dimethyl acetal. *Tetrahedron Lett.* **2002***, 43*, 2299-2302.

189. Henry, R. A.; Heller, C. A.; Moore, D. W. Preparation and fluorescence of substituted 2-methyl-1-isoquinolones. *J. Org. Chem.* **1975***, 40*, 1760-1766.

190. Matthews, S. E.; Felix, V.; Drew, M. G. B.; Beer, P. D. Halo-derivatised calix[4]tubes. *Org. Biomol. Chem.* **2003***, 1*, 1232-1239.

191. Horning, D. E.; Lacasse, G.; Muchowski, J. M. Isocarbostyrils. I. Electrophilic substitution reactions. *Can. J. Chem.* **1971***, 49*, 2785-2796.

192. Barder, T. E.; Walker, S. D.; Martinelli, J. R.; Buchwald, S. L. Catalysts for Suzuki-Miyaura coupling processes: Scope and studies of the effect of ligand structure. *J. Am. Chem. Soc.* **2005***, 127*, 4685-4696.

193. Vanaerschot, A. A.; Mamos, P.; Weyns, N. J.; Ikeda, S.; Declercq, E.; Herdewijn, P. A. Antiviral activity of C-alkylated purine nucleosides obtained by cross-coupling with tetraalkyltin reagents. *J. Med. Chem.* **1993***, 36*, 2938-2942.

194. Stűtz, A.; Georgopoulos, A.; Granitzer, W.; Petranyi, G.; Berney, D. Synthesis and structure-activity relationships of Naftifine-related allylamine antimycotics. *J. Med. Chem*. **1986**, *29*, 112-125.

195. Mori, M.; Chiba, K.; Ban, Y. Reactions and syntheses with organometallic compounds .5. New synthesis of indoles and isoquinolines by intramolecular palladium-catalyzed reactions of aryl halides with olefinic bonds. *Tetrahedron Lett.* **1977**, 1037-1040.

196. Crisp, G. T. Variations on a theme - recent developments on the mechanism of the Heck reaction and their implications for synthesis. *Chem. Soc. Rev.* **1998***, 27*, 427-436.

197. Larock, R. C.; Babu, S. Synthesis of nitrogen-heterocycles via palladium-catalyzed intramolecular cyclization. *Tetrahedron Lett.* **1987***, 28*, 5291-5294.

198. Chen, J.; Zhang, Y.; Yang, L.; Zhang, X.; Liu, J.; Li, L.; Zhang, H. A practical palladium catalyzed dehalogenation of aryl halides and alpha-haloketones. *Tetrahedron* **2007***, 63*, 4266-4270.

199. Krompiec, S.; Pigulla, M.; Szczepankiewicz, W.; Bieg, T.; Kuznik, N.; Leszczynska-Sejda, K.; Kubicki, M.; Borowiak, T. Highly selective synthesis of (*E*)-N-aryl-N-(1-propenyl) ethanamides via isomerization of N-allyl ethanamides catalyzed by ruthenium complexes. *Tetrahedron Lett.* **2001***, 42*, 7095-7098.

200. Krompiec, S.; Pigulla, M.; Krompiec, M.; Baj, S.; Mrowiec-Bialon, J.; Kasperezyk, J. Highly selective isomerization of N-allylamides and N-allylamines. *Tetrahedron Lett.* **2004***, 45*, 5257-5261.

201. Harland, P. A.; Hodge, P.; Maughan, W.; Wildsmith, E. Synthesis of primary amines via alkylation of the sodium-salt of trifluoroacetamide - an alternative to the Gabriel synthesis. *Synthesis-Stuttgart* **1984**, 941-943.

202. Malek, N. J.; Moorman, A. E. Palladium-catalyzed synthesis of cinnamylamines. *J. Org. Chem.* **1982**, 47, 5397-5398.

203. Schraufstatter, I. U.; Hyslop, P. A.; Hinshaw, D. B.; Spragg, R. G.; Sklar, L. A.; Cochrane, C. G. Hydrogen peroxide-induced injury of cells and its prevention by inhibitors of poly(ADP-ribose) polymerase. *Proc. Natl. Acad. Sci. USA* **1986**, *83*, 4908-4912.

204. Dillon, K. J.; Smith, G. C.; Martin, N. M. A flash plate assay for the identification of PARP-1 inhibitors. *J. Biomol. Screen.* **2003**, *8*, 347-352.

205. Decker, P.; Miranda, E. A.; de Murcia, G.; Muller, S. An improved nonisotopic test to screen a large series of new inhibitor molecules of poly(ADP-ribose) polymerase activity for therapeutic applications. *Clin. Cancer Res.* **1999**, *5*, 1169-1172.

206. Brown, J. A.; Marala, R. B. Developement of a high-throughput screening amenable assay for human poly(ADP-ribose) polymerase inhibitors. *J. Pharmacol. Toxicol. Methods* **2002**, *47*, 137-141.

207. Cheung, A.; Zhang, J. A scintillation proximity assay for poly(ADP-ribose) polymerase. *Anal. Biochem*. **2000**, 282, 24-28.

208. Tirouflet, J. *Bull. Soc. Sci. Bretagne* **1951**, *S26*, 7.

209. Stűtz, A.; Georgopoulos, A.; Granitzer, W.; Petranyi, G.; Berney, D. Synthesis and structure-activity relationships of Naftifine-related allylamine antimycotics. *J. Med. Chem*. **1986**, *29*, 112-125.

210. Burger, A.; Schmalz, C. A. Some derivatives of phenothiazine II. *J. Org. Chem.* **1954**, *19*, 1841-1846.

211. Albanese, D.; Benaglia, M.; Landini, D.; Maia, A.; Lupi, V.; Penso, M. Use of a quaternary ammonium salt supported on a liposoluble poly(ethylene glycol) matrix for laboratory and industrial synthetic applications of phase-transfer catalysis. *Ind. Eng. Chem. Res.* **2002**, *41*, 4928-4935.

212. Abulikemu, A.; Halász, G.; Csámpai, A.; Gömöry, Á.; Rábai J. Improved synthesiss of perfluorooctylpropyl amine. *J. Fluor. Chem.* **2004**, 125, 1143-1146.

213. Brewbaker, J.; Hart. H. The cyclization of 3-diazoalkenes to pyrazoles. *J. Am. Chem. Soc.* **1969**, 91, 711-715.

214. Meyers, A. I.; Lawson, P.J.; Carver, D. R. Highly stereoselective route to *(E)*-allyl amines via vinyltri-n-butylphosphonium salts (Schweizer reaction). *J. Org. Chem.* **1981**, 46, 3119 – 3123.

215. De Amici, M.; De Micheli C.; Misani V. Nitrile oxides in medicinal chemistry - 2. synthesis of the two enantiomers of dihydromuscimol. *Tetrahedron*, **1990**, 46, 1975-1986.

Appendices

Appendix 1. Raw data for PARP-1 colourimetric activity assay

5-Aminoisoquinolin-1(*2H*)-one (29d)

Log [μM]	Absorbance reading (450nm)			
	Data Set A	Data Set B	Data Set C	Mean
2.0	0.1410	0.1620	0.0900	0.131000
1.5	0.3290	0.3060	0.2970	0.3106667
1.0	0.5720	0.5490	0.4340	0.5183334
0.5	1.0620	0.9940	1.0060	1.020667
0.0	1.3340	1.3150	1.1480	1.265667
-0.5	2.0220	2.0330	2.0100	2.021667
-1.0	2.3310	1.9850	2.1020	2.139333

4-Methyl 5-aminoisoquinolin-1(*2H*)-one (182)

Log [μM]	Absorbance reading (450nm)			
	Data Set A	Data Set B	Data Set C	Mean
2.0	0.066	0.063	0.062	0.063667
1.5	0.134	0.138	0.137	0.136333
1.0	0.381	0.396	0.331	0.369333
0.5	0.699	0.367	0.705	0.590333
0.0	0.39	0.389	0.356	0.378333
-0.5	1.196	1.665	1.217	1.359333
-1.0	1.79	2.11	1.745	1.881667

4-Benzyl-5-aminoisoquinolin-1(*2H*)-one (192)

Log [μM]	Absorbance reading (450nm)			
	Data Set A	Data Set B	Data Set C	Mean
2.0	0.1209	0.0886	0.112	0.107167
1.5	0.159	0.1556	0.1487	0.154433
1.0	0.3051	0.292	0.2789	0.292
0.5	0.3207	0.4409	0.4444	0.402
0.0	1.1391	0.7631	0.7179	0.873367
-0.5	1.6657	1.2028	1.0851	1.317867
-1.0	2.4658	2.2033	1.2307	1.9666

5-Amino-4-benzyl-3,4-dihydroisoquinolin-1(2*H*)-one (193)

Log [μM]	Absorbance reading (450nm)			
	Data Set A	**Data Set B**	**Data Set C**	**Mean**
2.0	0.1901	0.1843	0.1836	0.186
1.5	0.455	0.2923	0.2938	0.347033
1.0	0.5728	0.5934	0.4829	0.5497
0.5	0.8076	0.9385	1.0543	0.933467
0.0	1.2561	1.3833	1.5834	1.4076
-0.5	1.6334	1.48	1.8916	1.668333
-1.0	2.6138	1.4332	1.6171	1.888033

4-Bromo-5-aminoisoquinolin-1(*2H*)-one (125)

Log [μM]	Absorbance reading (450nm)			
	Data Set A	**Data Set B**	**Data Set C**	**Mean**
2.0	0.1189	0.0852	0.0775	0.093867
1.5	0.145	0.1611	0.1321	0.146067
1.0	0.2206	0.1255	0.2134	0.1865
0.5	0.3898	0.3184	0.3472	0.3518
0.0	0.7252	0.7401	0.6362	0.7005
-0.5	0.7256	1.3807	0.9798	1.0287
-1.0	1.2314	1.2406	1.2098	1.227267

Appendix 2. IC_{50} Data analysis for PARP-1 inhibitors

5-Aminoisoquinolin-1(*2H*)-one (29d)

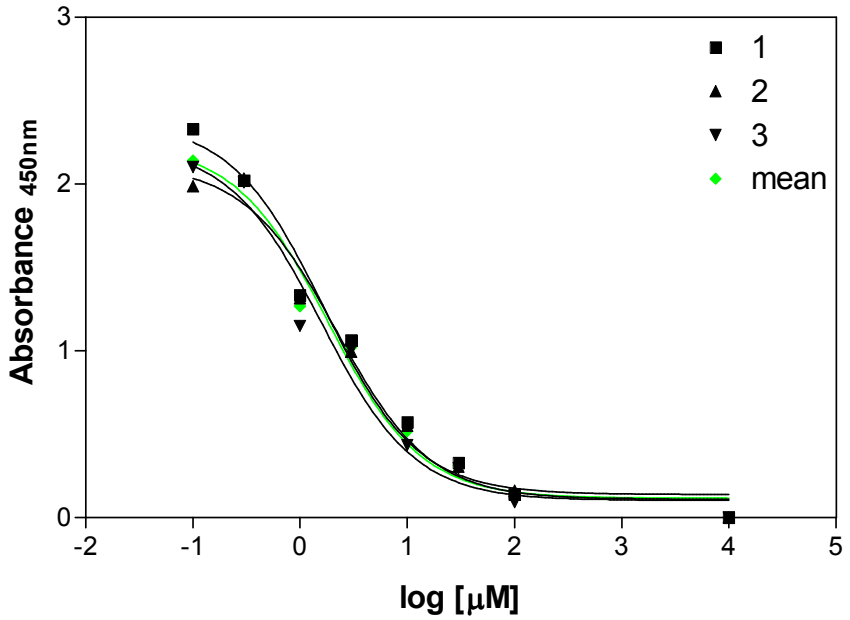

	Data Set-A	Data Set-B	Data Set-C	Data Set-D
Best-fit values				
BOTTOM	0.1381	0.1090	0.1023	0.1159
TOP	2.377	2.121	2.235	2.240
LOGEC50	0.2225	0.3419	0.1977	0.2564
EC50	1.669	2.198	1.577	1.805
Std. Error				
BOTTOM	0.08561	0.07864	0.09635	0.08178
TOP	0.1465	0.1186	0.1695	0.1349
LOGEC50	0.1257	0.1204	0.1506	0.1242
95% Confidence Intervals				
BOTTOM	-0.08204 to 0.3582	-0.09317 to 0.3112	-0.1454 to 0.3500	-0.09439 to 0.3261
TOP	2.000 to 2.754	1.816 to 2.426	1.800 to 2.671	1.893 to 2.586
LOGEC50	-0.1007 to 0.5457	0.03231 to 0.6516	-0.1896 to 0.5850	-0.06298 to 0.5758
EC50	0.7931 to 3.514	1.077 to 4.483	0.6462 to 3.846	0.8650 to 3.765
Goodness of Fit				
Degrees of Freedom	5	5	5	5
R^2	0.9807	0.9821	0.9726	0.9811
Absolute Sum of Squares	0.1022	0.08003	0.1313	0.09135
Sy.x	0.1430	0.1265	0.1621	0.1352
Data				
Number of X values	8	8	8	8
Number of Y replicates	1	1	1	1
Total number of values	8	8	8	8
Number of missing values	0	0	0	0

4-Methyl 5-aminoisoquinolin-1(*2H*)-one (182)

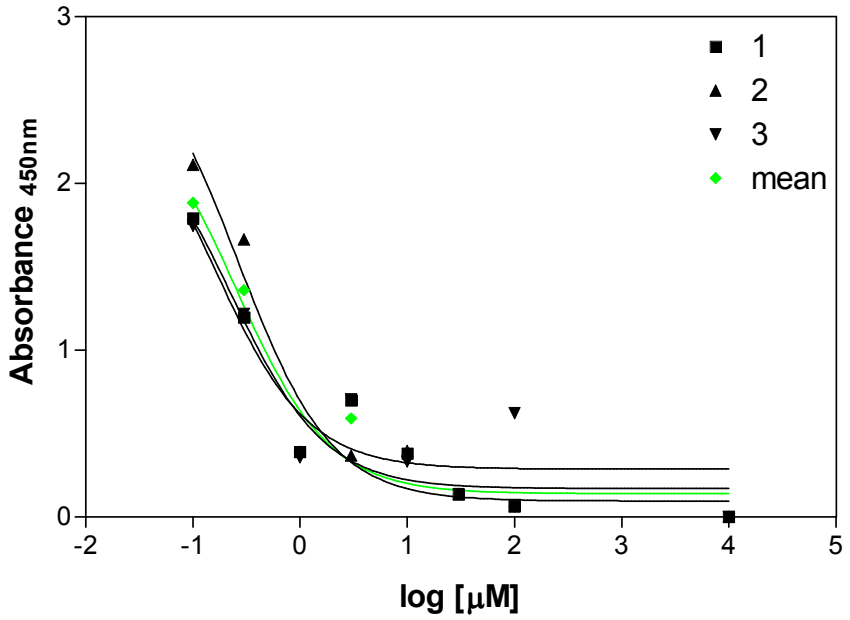

	Data Set-A	Data Set-B	Data Set-C	Data Set-D
Best-fit values				
BOTTOM	0.1698	0.09447	0.2863	0.1394
TOP	2.488	2.965	2.688	2.602
LOGEC50	-0.6375	-0.5766	-0.7958	-0.5979
EC50	0.2304	0.2651	0.1600	0.2524
Std. Error				
BOTTOM	0.1096	0.1027	0.1334	0.09881
TOP	0.7646	0.6220	1.405	0.6278
LOGEC50	0.3544	0.2449	0.5484	0.2832
95% Confidence Intervals				
BOTTOM	-0.1120 to 0.4516	-0.1697 to 0.3586	-0.05670 to 0.6292	-0.1146 to 0.3935
TOP	0.5218 to 4.453	1.366 to 4.564	-0.9236 to 6.300	0.9877 to 4.216
LOGEC50	-1.549 to 0.2736	-1.206 to 0.05315	-2.206 to 0.6142	-1.326 to 0.1302
EC50	0.02827 to 1.878	0.06218 to 1.130	0.006225 to 4.113	0.04721 to 1.350
Goodness of Fit				
Degrees of Freedom	5	5	5	5
R^2	0.9095	0.9516	0.8401	0.9376
Absolute Sum of Squares	0.2474	0.2132	0.3832	0.1986
Sy.x	0.2225	0.2065	0.2769	0.1993
Data				
Number of X values	8	8	8	8
Number of Y replicates	1	1	1	1
Total number of values	8	8	8	8
Number of missing values	0	0	0	0

4-Benzyl-5-aminoisoquinolin-1(*2H*)-one (192)

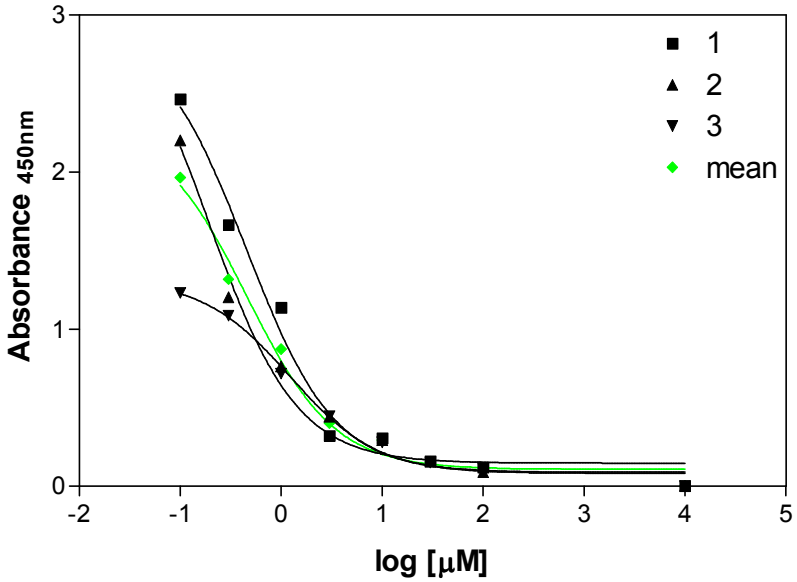

	Data Set-A	Data Set-B	Data Set-C	Data Set-D
Best-fit values				
BOTTOM	0.08791	0.1464	0.08048	0.1070
TOP	2.930	3.209	1.319	2.309
LOGEC50	-0.3444	-0.7154	0.08510	-0.3400
EC50	0.4525	0.1926	1.216	0.4571
Std. Error				
BOTTOM	0.06763	0.06231	0.02967	0.04783
TOP	0.2557	0.5274	0.05945	0.1794
LOGEC50	0.1222	0.1733	0.08562	0.1110
95% Confidence Intervals				
BOTTOM	-0.08597 to 0.2618	-0.01383 to 0.3066	0.004204 to 0.1568	-0.01602 to 0.2299
TOP	2.273 to 3.588	1.853 to 4.564	1.167 to 1.472	1.848 to 2.770
LOGEC50	-0.6586 to -0.03024	-1.161 to -0.2699	-0.1350 to 0.3052	-0.6254 to -0.05455
EC50	0.2195 to 0.9327	0.06905 to 0.5371	0.7328 to 2.019	0.2369 to 0.8820
Goodness of Fit				
Degrees of Freedom	5	5	5	5
R^2	0.9849	0.9789	0.9911	0.9875
Absolute Sum of Squares	0.08460	0.08183	0.01328	0.04224
Sy.x	0.1301	0.1279	0.05153	0.09191
Data				
Number of X values	8	8	8	8
Number of Y replicates	1	1	1	1
Total number of values	8	8	8	8
Number of missing values	0	0	0	0

5-Amino-4-benzyl-3,4-dihydroisoquinolin-1(2*H*)-one (193)

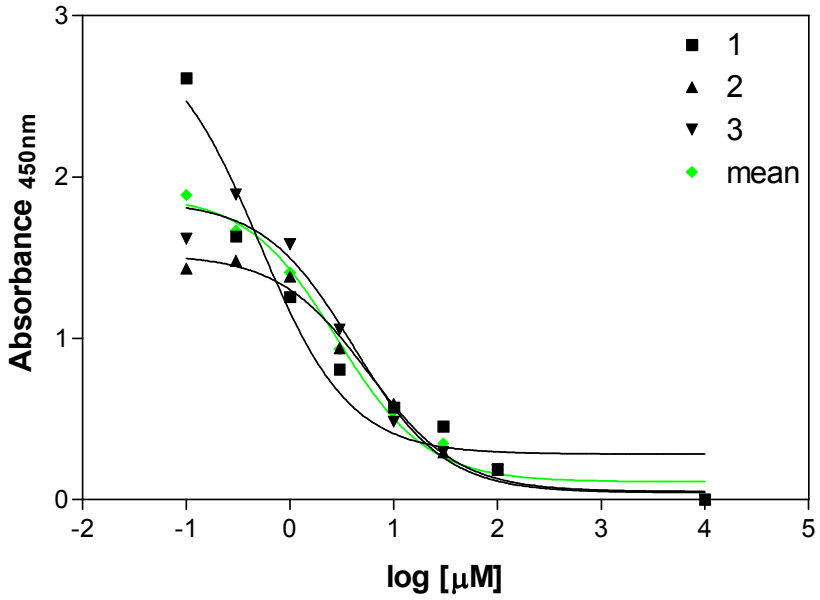

	Data Set-A	Data Set-B	Data Set-C	Data Set-D
Best-fit values				
BOTTOM	0.2827	0.05018	0.04334	0.1108
TOP	2.903	1.520	1.850	1.889
LOGEC50	-0.2972	0.7562	0.6132	0.4508
EC50	0.5044	5.705	4.104	2.824
Std. Error				
BOTTOM	0.1224	0.04907	0.09029	0.05008
TOP	0.4268	0.04994	0.1046	0.06775
LOGEC50	0.2286	0.08426	0.1349	0.08216
95% Confidence Intervals				
BOTTOM	-0.03211 to 0.5974	-0.07599 to 0.1763	-0.1888 to 0.2755	-0.01793 to 0.2396
TOP	1.805 to 4.000	1.392 to 1.648	1.581 to 2.119	1.715 to 2.063
LOGEC50	-0.8850 to 0.2905	0.5396 to 0.9729	0.2664 to 0.9599	0.2396 to 0.6621
EC50	0.1303 to 1.952	3.464 to 9.395	1.847 to 9.118	1.736 to 4.593
Goodness of Fit				
Degrees of Freedom	5	5	5	5
R^2	0.9479	0.9909	0.9774	0.9915
Absolute Sum of Squares	0.2719	0.02307	0.08712	0.03016
Sy.x	0.2332	0.06792	0.1320	0.07766
Data				
Number of X values	8	8	8	8
Number of Y replicates	1	1	1	1
Total number of values	8	8	8	8
Number of missing values	0	0	0	0

4-Bromo-5-aminoisoquinolin-1(*2H*)-one (125)

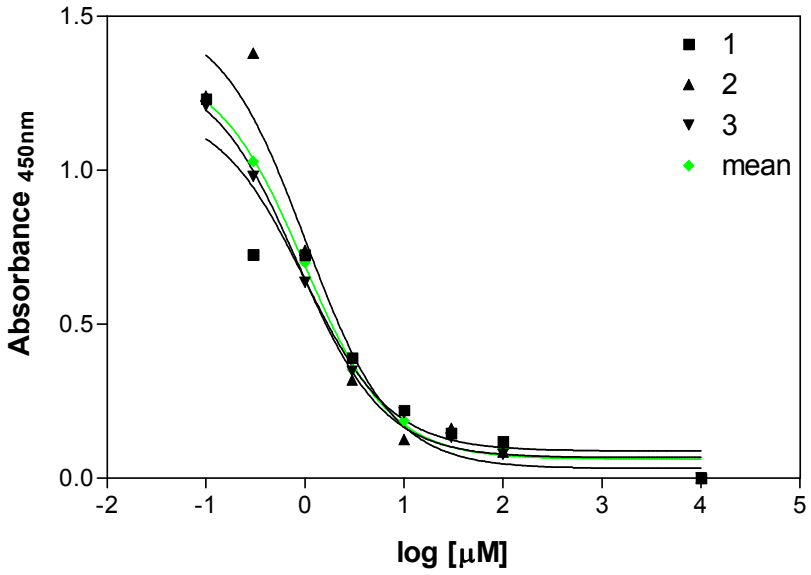

	Data Set-A	Data Set-B	Data Set-C	Data Set-D
Best-fit values				
BOTTOM	0.08838	0.03138	0.06685	0.06174
TOP	1.204	1.505	1.328	1.343
LOGEC50	-0.003503	0.009086	-0.07098	-0.01689
EC50	0.9920	1.021	0.8492	0.9618
Std. Error				
BOTTOM	0.07189	0.07211	0.02264	0.02102
TOP	0.1612	0.1591	0.05551	0.04790
LOGEC50	0.2451	0.1843	0.07177	0.06295
95% Confidence Intervals				
BOTTOM	-0.09644 to 0.2732	-0.1540 to 0.2168	0.008644 to 0.1250	0.007709 to 0.1158
TOP	0.7891 to 1.618	1.096 to 1.914	1.185 to 1.470	1.220 to 1.466
LOGEC50	-0.6336 to 0.6266	-0.4648 to 0.4830	-0.2555 to 0.1136	-0.1787 to 0.1450
EC50	0.2325 to 4.232	0.3429 to 3.041	0.5553 to 1.299	0.6626 to 1.396
Goodness of Fit				
Degrees of Freedom	5	5	5	5
R^2	0.9332	0.9609	0.9940	0.9953
Absolute Sum of Squares	0.08174	0.08170	0.008379	0.007030
Sy.x	0.1279	0.1278	0.04094	0.03750
Data				
Number of X values	8	8	8	8
Number of Y replicates	1	1	1	1
Total number of values	8	8	8	8
Number of missing values	0	0	0	0

Appendix 3. X-ray crystallography data for compound 105

Table 1. Crystal data and structure refinement for **105**

Identification code	Compound **105**
Empirical formula	$C_{21}H_{13}NO_4Se$
Formula weight	422.28
Temperature	150(2) K
Wavelength	0.71073 Å
Crystal system	Monoclinic
Space group	$P2_1/n$
Unit cell dimensions	a = 11.8050(1)Å α = 90°
	b = 11.8550(1)Å β = 113.969(1)°
	c = 13.3860(1)Å γ = 90°
Volume	1711.80(2) $Å^3$
Z	4
Density (calculated)	1.639 Mg/m^3
Absorption coefficient	2.222 mm^{-1}
F(000)	848
Crystal size	0.50 x 0.30 x 0.10 mm
Theta range for data collection	3.54 to 27.54 °.
Index ranges	-15<=h<=15; -15<=k<=15; -17<=l<=17
Reflections collected	28103
Independent reflections	3928 [R(int) = 0.0549]
Reflections observed (>2σ)	3671
Data Completeness	0.993
Absorption correction	Semi-empirical from equivalents
Max. and min. transmission	0.65 and 0.40
Refinement method	Full-matrix least-squares on F^2
Data / restraints / parameters	3928 / 0 / 245
Goodness-of-fit on F^2	1.031
Final R indices [I>2σ(I)]	R^1 = 0.0248 wR_2 = 0.0627
R indices (all data)	R^1 = 0.0275 wR_2 = 0.0643
Largest diff. peak and hole	0.380 and -0.568 $eÅ^{-3}$

Table 2. Atomic coordinates (x 10^4) and equivalent isotropic displacement parameters ($Å^2$ x 10^3) for **105**.

Atom	x	y	z	U(eq)
Se(1)	8295(1)	-649(1)	8838(1)	18(1)
O(1)	6563(1)	1337(1)	6090(1)	19(1)
O(2)	4653(1)	1413(1)	4823(1)	27(1)
O(3)	6883(1)	308(1)	9881(1)	23(1)
O(4)	5754(1)	-1127(1)	9900(1)	32(1)
N(1)	6041(1)	-373(1)	9420(1)	20(1)
C(1)	7099(1)	301(1)	7752(1)	16(1)
C(2)	7433(1)	916(1)	7064(1)	17(1)
C(3)	5325(2)	1116(1)	5737(1)	19(1)
C(4)	4914(2)	569(1)	6513(1)	16(1)
C(5)	3641(2)	417(1)	6193(1)	22(1)
C(6)	3194(2)	-79(2)	6890(1)	25(1)
C(7)	4023(2)	-376(1)	7938(1)	23(1)
C(8)	5280(2)	-207(1)	8252(1)	18(1)
C(10)	5792(1)	220(1)	7541(1)	16(1)
C(11)	9071(1)	-1265(1)	7943(1)	17(1)
C(12)	8385(2)	-1708(1)	6908(1)	21(1)
C(13)	9012(2)	-2144(1)	6309(1)	26(1)
C(14)	10295(2)	-2163(1)	6740(2)	28(1)
C(15)	10966(2)	-1738(2)	7778(2)	27(1)
C(16)	10360(2)	-1276(1)	8381(1)	21(1)
C(17)	8695(2)	1214(1)	7180(1)	18(1)
C(18)	9017(2)	1128(1)	6289(1)	23(1)
C(19)	10212(2)	1381(2)	6412(2)	29(1)
C(20)	11086(2)	1742(2)	7414(2)	30(1)
C(21)	10759(2)	1872(2)	8294(2)	28(1)
C(22)	9568(2)	1608(1)	8178(1)	23(1)

Table 3. Bond lengths [Å] and angles [°] for **105**.

Se(1)-C(11)	1.9233(15)	Se(1)-C(1)	1.9256(15)
O(1)-C(3)	1.3663(19)	O(1)-C(2)	1.3843(18)
O(2)-C(3)	1.209(2)	O(3)-N(1)	1.2333(19)
O(4)-N(1)	1.2265(18)	N(1)-C(8)	1.466(2)
C(1)-C(2)	1.353(2)	C(1)-C(10)	1.454(2)
C(2)-C(17)	1.476(2)	C(3)-C(4)	1.464(2)
C(4)-C(5)	1.397(2)	C(4)-C(10)	1.407(2)
C(5)-C(6)	1.376(2)	C(6)-C(7)	1.391(2)
C(7)-C(8)	1.383(2)	C(8)-C(10)	1.412(2)
C(11)-C(16)	1.390(2)	C(11)-C(12)	1.393(2)
C(12)-C(13)	1.393(2)	C(13)-C(14)	1.385(3)
C(14)-C(15)	1.384(3)	C(15)-C(16)	1.391(2)
C(17)-C(18)	1.395(2)	C(17)-C(22)	1.395(2)
C(18)-C(19)	1.385(2)	C(19)-C(20)	1.387(3)
C(20)-C(21)	1.389(3)	C(21)-C(22)	1.387(2)
C(11)-Se(1)-C(1)	98.12(6)	C(3)-O(1)-C(2)	122.51(12)
O(4)-N(1)-O(3)	123.54(14)	O(4)-N(1)-C(8)	118.48(14)
O(3)-N(1)-C(8)	117.77(13)	C(2)-C(1)-C(10)	118.90(14)
C(2)-C(1)-Se(1)	120.10(12)	C(10)-C(1)-Se(1)	120.17(11)
C(1)-C(2)-O(1)	121.67(14)	C(1)-C(2)-C(17)	128.22(14)
O(1)-C(2)-C(17)	110.09(13)	O(2)-C(3)-O(1)	117.62(14)
O(2)-C(3)-C(4)	125.28(16)	O(1)-C(3)-C(4)	117.07(13)
C(5)-C(4)-C(10)	122.36(15)	C(5)-C(4)-C(3)	117.67(15)
C(10)-C(4)-C(3)	119.97(14)	C(6)-C(5)-C(4)	120.55(16)
C(5)-C(6)-C(7)	119.00(15)	C(8)-C(7)-C(6)	119.92(15)
C(7)-C(8)-C(10)	123.17(15)	C(7)-C(8)-N(1)	114.93(14)
C(10)-C(8)-N(1)	121.49(14)	C(4)-C(10)-C(8)	114.69(14)
C(4)-C(10)-C(1)	118.19(14)	C(8)-C(10)-C(1)	127.10(14)
C(16)-C(11)-C(12)	120.73(14)	C(16)-C(11)-Se(1)	117.21(12)
C(12)-C(11)-Se(1)	122.04(12)	C(13)-C(12)-C(11)	118.83(16)
C(14)-C(13)-C(12)	120.87(16)	C(15)-C(14)-C(13)	119.69(16)
C(14)-C(15)-C(16)	120.44(17)	C(11)-C(16)-C(15)	119.42(15)
C(18)-C(17)-C(22)	119.41(15)	C(18)-C(17)-C(2)	120.47(15)
C(22)-C(17)-C(2)	120.10(14)	C(19)-C(18)-C(17)	120.04(16)
C(18)-C(19)-C(20)	120.30(16)	C(19)-C(20)-C(21)	119.99(16)
C(22)-C(21)-C(20)	119.94(17)	C(21)-C(22)-C(17)	120.25(16)

Table 4. Anisotropic displacement parameters ($Å^2$ x 10^3) for **105**.

Atom	U11	U22	U33	U23	U13	U12
Se(1)	17(1)	23(1)	16(1)	4(1)	9(1)	5(1)
O(1)	20(1)	19(1)	18(1)	4(1)	8(1)	2(1)
O(2)	24(1)	32(1)	21(1)	8(1)	6(1)	5(1)
O(3)	20(1)	31(1)	20(1)	-4(1)	9(1)	-3(1)
O(4)	42(1)	33(1)	27(1)	7(1)	19(1)	-6(1)
N(1)	22(1)	23(1)	20(1)	0(1)	13(1)	0(1)
C(1)	16(1)	16(1)	15(1)	0(1)	7(1)	2(1)
C(2)	18(1)	16(1)	17(1)	-1(1)	8(1)	2(1)
C(3)	20(1)	18(1)	19(1)	0(1)	9(1)	3(1)
C(4)	18(1)	16(1)	17(1)	-1(1)	9(1)	2(1)
C(5)	19(1)	23(1)	22(1)	-2(1)	6(1)	2(1)
C(6)	16(1)	28(1)	30(1)	-5(1)	10(1)	-2(1)
C(7)	23(1)	25(1)	26(1)	-4(1)	16(1)	-5(1)
C(8)	19(1)	18(1)	18(1)	-2(1)	9(1)	-1(1)
C(10)	18(1)	14(1)	17(1)	-2(1)	9(1)	0(1)
C(11)	18(1)	15(1)	19(1)	2(1)	10(1)	2(1)
C(12)	21(1)	18(1)	22(1)	1(1)	6(1)	0(1)
C(13)	38(1)	19(1)	22(1)	-2(1)	12(1)	0(1)
C(14)	37(1)	22(1)	35(1)	-2(1)	25(1)	3(1)
C(15)	21(1)	26(1)	38(1)	-2(1)	17(1)	1(1)
C(16)	19(1)	22(1)	24(1)	-3(1)	10(1)	-1(1)
C(17)	18(1)	15(1)	23(1)	2(1)	11(1)	0(1)
C(18)	25(1)	26(1)	22(1)	1(1)	13(1)	-1(1)
C(19)	31(1)	32(1)	34(1)	4(1)	23(1)	0(1)
C(20)	23(1)	28(1)	45(1)	4(1)	19(1)	-4(1)
C(21)	23(1)	25(1)	33(1)	-2(1)	9(1)	-7(1)
C(22)	24(1)	22(1)	24(1)	-2(1)	12(1)	-2(1)

Table 5. Hydrogen coordinates (x 10^4) and isotropic displacement parameters ($Å^2$ x 10^3) for **105**.

Atom	x	y	z	U(eq)
H(5)	3079	659	5489	27
H(6)	2332	-217	6658	29
H(7)	3727	-695	8437	27
H(12)	7504	-1713	6615	25
H(13)	8553	-2433	5595	31
H(14)	10713	-2466	6325	33
H(15)	11846	-1763	8079	32
H(16)	10822	-972	9087	26
H(18)	8416	897	5597	28
H(19)	10433	1306	5808	35
H(20)	11909	1901	7499	36
H(21)	11350	2142	8974	33
H(22)	9345	1696	8780	27

Appendix 4. X-ray crystallography data for compound 168

Table 1. Crystal data and structure refinement for **168**.

Identification code	Compound **168**
Empirical formula	$C_{13}H_{14}N_3O_3$
Formula weight	260.27
Temperature	150(2) K
Wavelength	0.71073 Å
Crystal system	Monoclinic
Space group	P21
Unit cell dimensions	a = 11.1000(5)Å α = 90°
	b = 5.0730(2)Å β = 101.651(2)°
	c = 11.9100(6)Å γ = 90°
Volume	656.84(5) Å^3
Z	2
Density (calculated)	1.316 Mg/m^3
Absorption coefficient	0.096 mm^{-1}
F(000)	274
Crystal size	0.50 x 0.10 x 0.10 mm
Theta range for data collection	3.62 to 27.54°
Index ranges	-14<=h<=14; -6<=k<=6; -15<=l<=15
Reflections collected	11607
Independent reflections	2887 [R(int) = 0.0555]
Reflections observed (>2σ)	2417
Data Completeness	0.996
Absorption correction	Semi-empirical from equivalents
Max. and min. transmission	0.99 and 0.90
Refinement method	Full-matrix least-squares on F^2
Data / restraints / parameters	2887 / 1 / 173
Goodness-of-fit on F^2	1.059
Final R indices [I>2σ(I)]	R1 = 0.0457 wR2 = 0.1019
R indices (all data)	R1 = 0.0603 wR2 = 0.1092
Absolute structure parameter	-1.1(13)
Largest diff. peak and hole	0.534 and -0.169 eÅ^{-3}

Table 2. Atomic coordinates (x 10^4) and equivalent isotropic displacement parameters ($Å^2$ x 10^3) for **168**.

Atom	x	y	z	U(eq)
O(1)	5803(1)	-4149(3)	5147(1)	33(1)
N(1)	6298(2)	-2443(3)	5838(2)	31(1)
C(1)	7100(2)	-482(4)	5484(2)	27(1)
O(2)	6130(2)	-2361(4)	6829(1)	49(1)
N(2)	6550(2)	-1728(3)	3462(1)	29(1)
C(2)	7737(2)	1114(4)	6353(2)	32(1)
O(3)	8761(1)	-225(3)	2569(1)	34(1)
N(3)	8638(2)	4209(3)	2535(2)	31(1)
C(3)	8496(2)	3073(4)	6109(2)	34(1)
C(4)	8639(2)	3395(4)	4984(2)	31(1)
C(5)	8036(2)	1805(4)	4101(2)	26(1)
C(6)	7199(2)	-182(4)	4316(2)	26(1)
C(7)	6101(2)	-867(4)	2268(2)	31(1)
C(8)	4924(2)	-2297(4)	1816(2)	34(1)
C(9)	4793(2)	-4060(5)	997(2)	41(1)
C(10)	8480(2)	1842(4)	2994(2)	28(1)
C(11)	9218(2)	4443(5)	1544(2)	33(1)
C(12)	8309(2)	4418(6)	432(2)	43(1)
C(13)	8211(3)	6297(6)	-333(2)	56(1)

Table 3. Bond lengths [Å] and angles [°] for **168**.

O(1)-N(1)	1.243(2)	N(1)-O(2)	1.232(2)
N(1)-C(1)	1.453(3)	C(1)-C(2)	1.390(3)
C(1)-C(6)	1.426(3)	N(2)-C(6)	1.368(3)
N(2)-C(7)	1.475(3)	C(2)-C(3)	1.371(3)
O(3)-C(10)	1.232(2)	N(3)-C(10)	1.346(3)
N(3)-C(11)	1.459(3)	C(3)-C(4)	1.391(3)
C(4)-C(5)	1.385(3)	C(5)-C(6)	1.429(3)
C(5)-C(10)	1.497(3)	C(7)-C(8)	1.496(3)
C(8)-C(9)	1.309(3)	C(11)-C(12)	1.494(3)
C(12)-C(13)	1.308(4)		
O(2)-N(1)-O(1)	121.73(17)	O(2)-N(1)-C(1)	118.35(18)
O(1)-N(1)-C(1)	119.92(17)	C(2)-C(1)-C(6)	122.43(19)
C(2)-C(1)-N(1)	115.63(18)	C(6)-C(1)-N(1)	121.92(17)
C(6)-N(2)-C(7)	124.86(17)	C(3)-C(2)-C(1)	120.5(2)
C(10)-N(3)-C(11)	121.10(16)	C(2)-C(3)-C(4)	118.9(2)
C(5)-C(4)-C(3)	122.14(19)	C(4)-C(5)-C(6)	120.41(18)
C(4)-C(5)-C(10)	117.83(17)	C(6)-C(5)-C(10)	120.54(17)
N(2)-C(6)-C(5)	122.34(18)	N(2)-C(6)-C(1)	122.09(18)
C(5)-C(6)-C(1)	115.56(17)	N(2)-C(7)-C(8)	107.70(17)
C(9)-C(8)-C(7)	123.9(2)	O(3)-C(10)-N(3)	121.85(18)
O(3)-C(10)-C(5)	120.46(18)	N(3)-C(10)-C(5)	117.52(17)
N(3)-C(11)-C(12)	112.76(18)	C(13)-C(12)-C(11)	123.9(2)

Table 4. Anisotropic displacement parameters ($Å^2$ x 10^3) for **168**.

Atom	U11	U22	U33	U23	U13	U12
O(1)	33(1)	28(1)	39(1)	3(1)	7(1)	-4(1)
N(1)	34(1)	26(1)	35(1)	5(1)	9(1)	3(1)
C(1)	26(1)	24(1)	32(1)	4(1)	5(1)	4(1)
O(2)	70(1)	46(1)	38(1)	-2(1)	24(1)	-14(1)
N(2)	32(1)	25(1)	29(1)	3(1)	1(1)	-2(1)
C(2)	30(1)	33(1)	32(1)	1(1)	2(1)	3(1)
O(3)	33(1)	19(1)	52(1)	-3(1)	16(1)	1(1)
N(3)	37(1)	20(1)	41(1)	-2(1)	18(1)	2(1)
C(3)	32(1)	30(1)	37(1)	-4(1)	-1(1)	2(1)
C(4)	26(1)	23(1)	43(1)	-1(1)	4(1)	0(1)
C(5)	24(1)	20(1)	35(1)	2(1)	5(1)	4(1)
C(6)	26(1)	18(1)	33(1)	0(1)	5(1)	4(1)
C(7)	32(1)	30(1)	31(1)	3(1)	6(1)	1(1)
C(8)	32(1)	36(1)	35(1)	0(1)	6(1)	0(1)
C(9)	46(1)	37(1)	38(1)	-2(1)	1(1)	-5(1)
C(10)	21(1)	24(1)	39(1)	0(1)	6(1)	0(1)
C(11)	36(1)	25(1)	40(1)	2(1)	15(1)	-1(1)
C(12)	38(1)	51(2)	41(1)	-10(1)	14(1)	-7(1)
C(13)	49(2)	74(2)	45(1)	8(1)	13(1)	7(1)

Table 5. Hydrogen coordinates (x 10^4) and isotropic displacement parameters ($Å^2$ x 10^3) for **168**.

Atom	x	y	z	U(eq)
H(2)	7646	846	7121	39
H(3)	8388	5640	2838	38
H(3A)	8918	4191	6700	41
H(4)	9166	4749	4815	37
H(7A)	6716	-1285	1798	37
H(7B)	5958	1060	2241	37
H(8)	4232	-1902	2142	41
H(9A)	5469	-4496	655	50
H(9B)	4021	-4903	746	50
H(11A)	9803	2966	1552	39
H(11B)	9694	6106	1605	39
H(12)	7770	2951	272	51
H(13A)	8737	7790	-197	67
H(13B)	7613	6168	-1025	67

Publications

Woon, E. C. Y.; Dhami, A.; Mahon, M. F.; Threadgill, M. D. Isocoumarins from tandem Castro-Stephens coupling – 6-*endo*-dig cyclisation of 2-iodo-3-nitrobenzoic acid and arylethynes and ring-closure of methyl 2-alkynyl-3-nitrobenzoates with electrophiles. *Tetrahedron* **2006**, *62*, 4829-4837.

Woon, E. C. Y.; Dhami, A.; Sunderland, P. T.; Chalkley, D. A.; Threadgill, M. D. Reductive cyclisation of 2-cyanomethyl-3-nitrobenzoates. *Lett. Org. Chem*. **2006**, *3*, 619-621.